Earth-Science Reviews 113 (2012) 212–270

Contents lists available at SciVerse ScienceDirect

Earth-Science Reviews

journal homepage: www.elsevier.com/locate/earscirev

Global continental and ocean basin reconstructions since 200 Ma

M. Seton [a,*], R.D. Müller [a], S. Zahirovic [a], C. Gaina [b,1], T. Torsvik [b,c,d,e], G. Shephard [a], A. Talsma [a], M. Gurnis [f], M. Turner [f], S. Maus [h], M. Chandler [g]

[a] EarthByte Group, School of Geosciences, Madsen Building F09, University of Sydney, NSW, 2006, Australia
[b] Centre for Geodynamics, Geological Survey of Norway, Leiv Eirikssons vei 39, N-7491 Trondheim, Norway
[c] Physics of Geological Processes/School of Geosciences, University of Oslo, 0316 Oslo, Norway
[d] Center for Advanced Study, Norwegian Academy of Science and Letters, Drammensveien 78, 0271 Oslo, Norway
[e] School of Geosciences, University of the Witwatersrand, Wits 2050, South Africa
[f] Seismological Laboratory, California Institute of Technology, Pasadena, CA, USA
[g] School of Ocean and Earth Science and Technology (SOEST), University of Hawai'i at Manoa, 1680 East–west Rd., POST # 806, Honolulu, HI 96822, USA
[h] National Geophysical Data Center, NOAA, 325 Broadway, Boulder, CO 80305-3328, USA

ARTICLE INFO

Article history:
Received 16 March 2011
Accepted 2 March 2012
Available online 15 March 2012

Keywords:
Plate reconstructions
Plate motion model
Panthalassa
Laurasia
Tethys
Gondwana

ABSTRACT

Global plate motion models provide a spatial and temporal framework for geological data and have been effective tools for exploring processes occurring at the earth's surface. However, published models either have insufficient temporal coverage or fail to treat tectonic plates in a self-consistent manner. They usually consider the motions of selected features attached to tectonic plates, such as continents, but generally do not explicitly account for the continuous evolution of plate boundaries through time. In order to explore the coupling between the surface and mantle, plate models are required that extend over at least a few hundred million years and treat plates as dynamic features with dynamically evolving plate boundaries. We have constructed a new type of global plate motion model consisting of a set of continuously-closing topological plate polygons with associated plate boundaries and plate velocities since the break-up of the supercontinent Pangea. Our model is underpinned by plate motions derived from reconstructing the seafloor-spreading history of the ocean basins and motions of the continents and utilizes a hybrid absolute reference frame, based on a moving hotspot model for the last 100 Ma, and a true-polar wander corrected paleomagnetic model for 200 to 100 Ma. Detailed regional geological and geophysical observations constrain plate boundary inception or cessation, and time-dependent geometry. Although our plate model is primarily designed as a reference model for a new generation of geodynamic studies by providing the surface boundary conditions for the deep earth, it is also useful for studies in disparate fields when a framework is needed for analyzing and interpreting spatio-temporal data.

Contents

* Corresponding author. Tel.: +61 2 9351 4255.
E-mail address: maria.seton@sydney.edu.au (M. Seton).
[1] Now at Physics of Geological Processes/School of Geosciences, University of Oslo, 0316 Oslo, Norway.

0012-8252/$ – see front matter © 2012 Elsevier B.V. All rights reserved.
doi:10.1016/j.earscirev.2012.03.002

1. Introduction

Plate tectonic reconstructions are essential for providing a spatio-temporal context to geological and geophysical data and help uncover the driving forces of supercontinent break-up, separation and accretion, linkages between surface processes and the deep earth, modes of intra-plate deformation and the mechanisms behind geological processes. Currently, plate reconstructions fall into three main categories: (1) "Geologically current" models based on present day plate motions from GPS measurements (Argus and Heflin, 1995), space geodesy e.g. GEODVEL (Argus et al., 2010) or a combination of spreading rates, fault azimuths and GPS measurements e.g. NUVEL-1 (DeMets et al., 1990, 2010) and MORVEL (DeMets et al., 2010); (2) Traditional plate tectonic models based on the interpretation of the seafloor spreading record and/or paleomagnetic data to reconstruct the ocean basins, continents and terranes within an absolute reference framework (Scotese et al., 1988; Scotese, 1991; Golonka and Ford, 2000; Schettino and Scotese, 2005; Golonka, 2007; Müller et al., 2008b); (3) Coupled geodynamic–plate models, which model plate boundary locations and mantle density heterogeneity to predict past and/or present plate motions (Hager and O'Connell, 1981; Lithgow-Bertelloni and Richards, 1998; Conrad and Lithgow-Bertelloni, 2002; Stadler et al., 2010).

"Geologically current" plate models provide the most accurate representation of global plate motions, are available in several global reference frameworks and can be independently verified with present day observations. However, they are limited from the Pliocene to present. Traditional plate tectonic reconstructions have good temporal coverage, which may extend as far back as the Paleozoic, but are often instantaneous snapshots rather than dynamically evolving models. For example, rather than representing plates in terms of their evolving shape, these models are generally built on rotating selected objects that form part of plates, such as continents, back through time, without addressing the implied evolution of the surrounding mid-ocean ridges, transform faults and subduction zones in a self-consistent manner. This limits the adaptability of traditional plate motion models, as they cannot easily be used as boundary conditions for geodynamic models. This is particularly acute for tracking the evolution of subduction since static plate reconstructions cannot simultaneously trace the continuous rollback of subduction zones while having slabs coupled to the subducting plate. Coupled geodynamic-plate models, which use numerical calculations to predict past and present plate motions, are sensitive to initial boundary conditions, as well as physical mantle properties, all subject to uncertainties and often work only for selected or interpolated timesteps. In addition, these published plate models are usually available in a form that does not easily lend itself to an exploration of the plate kinematic parameter space, in terms of testing alternative models in a geodynamic sense.

The rapid improvement in computational capability and efficiency (in terms of algorithms and hardware) with the simultaneous advancement in geodynamic modeling tools capable of addressing a range of applications, has created a need within the earth sciences community for a "deep-time" (i.e. time scales of a few hundred million years) reference plate motion model provided in digital form in such a way that it can be easily used, modified, and updated to address a variety of geological problems on a global scale. To ensure self-consistency, tectonic plates and plate boundaries should be explicitly modeled as dynamically evolving features rather than the previous paradigm, which modeled the motion of discrete tectonic blocks, without much thought to the shape, size and boundaries between tectonic plates.

We have developed a "deep-time" reference plate motion model consisting of a set of dynamic topological plate polygons using the approach described in Gurnis et al. (2012) with associated plate boundaries and plate velocities since the break-up of Pangea (~200 Ma). Our model is underpinned by plate motions derived from reconstructing

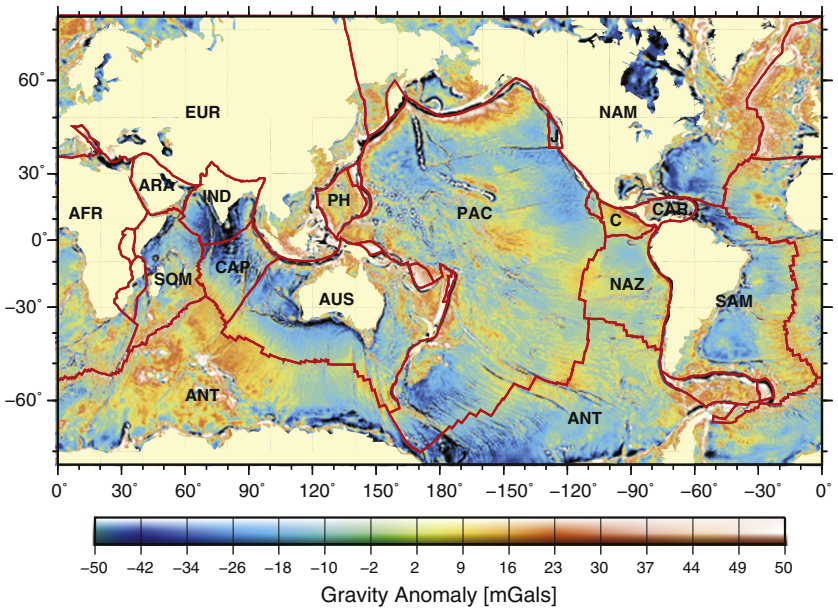

Fig. 1. Global gravity anomalies from satellite altimetry (Sandwell and Smith 2009). Red lines denote present day plate boundaries from the plate boundary set presented in this study. AFR = Africa, ANT = Antarctica, ARA = Arabia, AUS = Australia, C = Cocos, CAP = Capricorn, CAR = Caribbean, EUR = Eurasia, IND = India, NAM = North America, NAZ = Nazca, PAC = Pacific, PH = Philippine, SAM = South America, SOM = Somalia. (For interpretation of the references to color in this figure legend, the reader is referred to the web version of this article.)

the seafloor-spreading history of the ocean basins and motions of the continents and built around a hybrid absolute reference frame. In reconstructing the ocean floor, we use satellite-derived gravity anomalies (Sandwell and Smith, 2009) (Fig. 1) and an updated set of magnetic anomaly identifications to construct seafloor spreading isochrons for all the major oceanic plates. We use a combination of public and in-house magnetic anomaly data, which were line leveled and then gridded, to produce global magnetic anomaly grids and compare with our seafloor spreading isochrons (Figs. 2, 3, 5–7, 9, 11, 13, 14). We derive a global set of finite rotations for relative motions between all the major plates. In addition, we restore now-subducted oceanic crust for the major plates following the methodology in Müller et al. (2008b), by using evidence of subduction, slab windows and anomalous volcanism from onshore geology and the rules of plate tectonics. We create a set of dynamically closed plate polygons in one million year time intervals, which evolve from a series of dynamically evolving plate boundaries (Figs. 18–28).

In building a topological closed plate polygon network, we have deliberately excluded many of the smaller tectonic plates and micro-plates in order to produce a self-consistent global dataset for the community. However, the method of Gurnis et al. (2012) allows for construction of more detailed topological plate polygon networks. The data involved in reproducing our models are being made publicly available enabling researchers to either use our model as a framework in which to build upon for their particular area of expertise, input into geodynamic simulations as surface boundary conditions or to understand the context of regional tectonics. We hope that this paper and the accompanying data will help those researchers from disparate fields critically evaluate plate reconstructions, determine areas in need of further analysis, use as a basis to further refine models and explore the limitations and sources of error inherent in plate motion models.

2. Methodology

There are four main components that comprise our plate motion model: an absolute reference frame, the relative motions between tectonic plates linked via a plate circuit, the geomagnetic polarity timescale and a collection of plate boundaries that combine to form a network of continuously closed plate polygons. The continuously closed plate polygons were created using *GPlates* software (www.gplates.org).

2.1. Absolute reference frames

The anchor for any global plate motion model is an absolute reference frame (i.e. how the plates move relative to a fixed reference system, such as the spin axis). A comprehensive discussion of absolute reference frames and the merits of each can be found in Torsvik et al. (2008). Our model uses a hybrid reference frame, which merges a moving Indian/Atlantic hotspot reference frame (O'Neill et al., 2005) back to 100 Ma with a paleomagnetically-derived true polar wander corrected reference frame (Steinberger and Torsvik, 2008) back to 200 Ma. This reference frame links to the global plate circuit through Africa, as Africa has been surrounded by mid-ocean ridges for at least the last 170 Ma and, according to Torsvik et al. (2008), Africa has moved less than 500 km over the past 100 Ma.

All the major tectonic plates are linked to Africa via the seafloor spreading or rifting back to 200 Ma, except the Pacific and associated plates, such as the Farallon, Izanagi, Phoenix and Kula. The Pacific plate can only be linked to the plate circuit for times younger than 83.5 Ma, after the establishment of seafloor spreading between the Pacific and West Antarctic plates. Prior to this time we switch to a fixed Pacific hotspot reference frame for the Pacific plate, using a combination of Wessel and Kroenke (2008) and Wessel et al. (2006). We assume that the Pacific reference frame is fixed relative to other hotspots as we have no reliable model for whether the Pacific mantle plumes moved relative to each other or relative to the Earth's spin axis before 83.5 Ma, although some authors have invoked motion between some hotspots in the Pacific to account for paleo-latitude estimates from paleomagnetic data for the Ontong-Java Plateau (Riisager et al., 2003).

2.2. Relative plate motions

In building our relative plate motion model, we combine published and new magnetic anomaly identifications (magnetic anomaly picks) and their associated rotations to construct a global set of

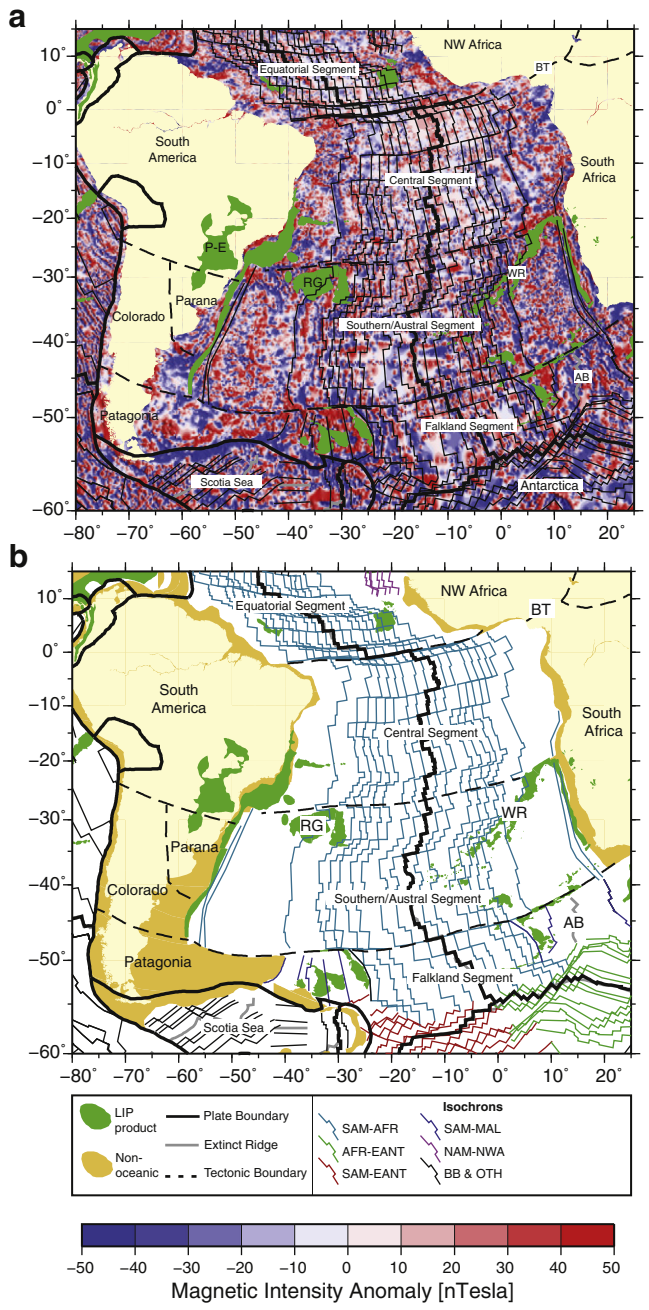

Fig. 2. (a) Gridded magnetic anomalies for the South Atlantic. Seafloor spreading isochrons used in this study plotted as thin black lines. Due to poor data coverage, correlations between the gridded data and isochrons are difficult. AB = Agulhas Basin, BT = Benue Trough, P-E = Parana Flood Basalts, RG = Rio-Grande Rise, WR = Walvis Ridge. (b) Seafloor spreading isochron map colored by spreading system or plate pair. Map abbreviations are same as a. Legend abbreviations are: AFR = South Africa, BB = Back-arc Basins, EANT = East Antarctica/Antarctica, MAL = Malvinas, NWA = Northwest Africa, OTH = Other spreading systems outside area of interest, SAM = South America.

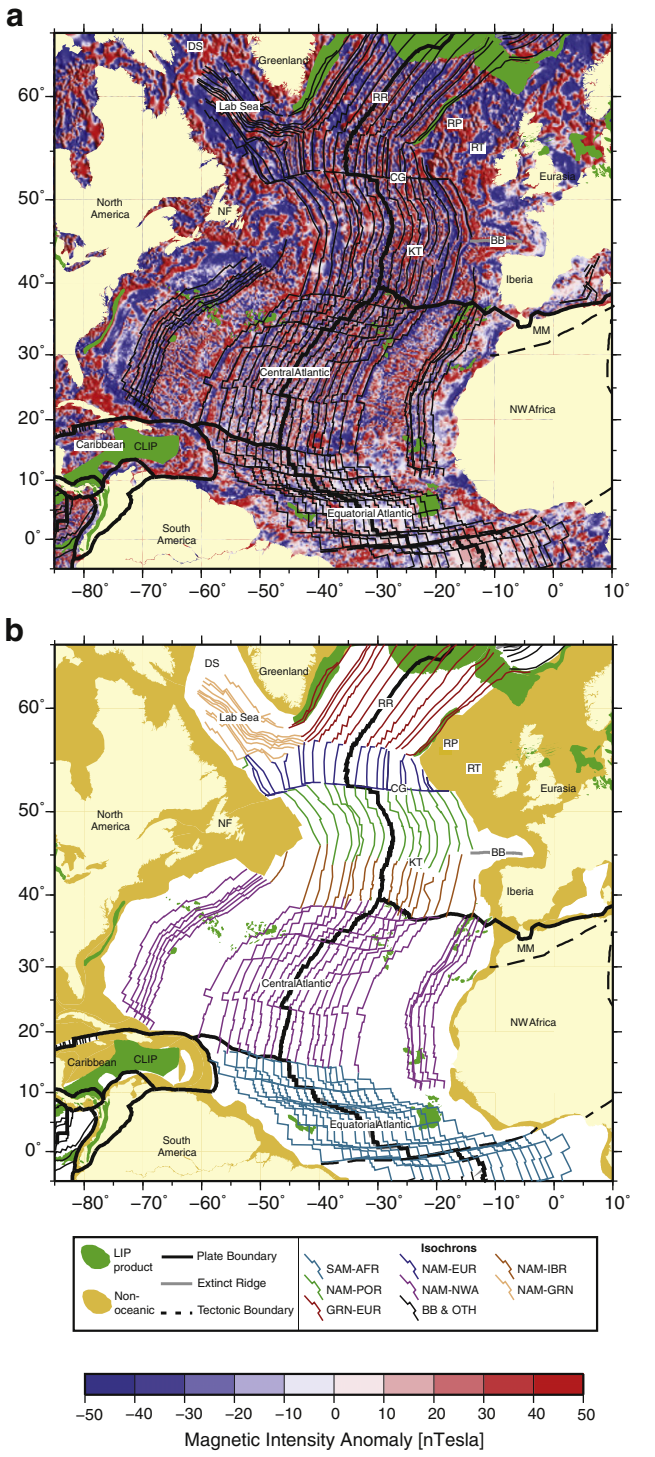

Fig. 3. (a) Gridded magnetic anomalies for the Central and North Atlantic. Seafloor spreading isochrons used in this study plotted as thin black lines. BB = Bay of Biscay, CG = Charlie-Gibbs Fracture Zone, CLIP = Caribbean Large Igneous Province, DS = Davis Strait, JFZ = Jacksonville Fracture Zone, KT = Kings Trough, MM = Morocco Meseta, NF = Newfoundland, RR = Rekyjanes Ridge, RP = Rockall Plateau, RT = Rockall Trough. (b) Seafloor spreading isochron map colored by spreading system or plate pair. Map abbreviations are same as a. Legend abbreviations are: AFR = Africa, BB = Back-arc Basins, EUR = Eurasia, GRN = Greenland, IBR = Iberia, NAM = North America, NWA = Northwest Africa, OTH = Other spreading systems outside area of interest, POR = Porcupine, SAM = South America.

seafloor spreading isochrons (see Section 3: Regional continental and ocean floor reconstructions for details). This is largely based on the global plate model presented in Müller et al. (2008a), which builds upon the present day seafloor agegrid work of Müller et al. (1997) and includes a database consisting of over 70,000 magnetic anomaly identifications, extinct and active spreading ridge locations and boundary locations defining the transition from continental to oceanic crust. Seafloor spreading isochrons were constructed at Chrons 5o (10.9 Ma), 6o (20.1 Ma), 13y (33.1 Ma), 18o (40.1 Ma), 21o (47.9 Ma), 25y (55.9 Ma), 31y (67.7 Ma), 34y (83.5 Ma), M0 (120.4 Ma), M4 (126.7 Ma), M10 (131.9 Ma), M16 (139.6 Ma), M21 (147.7 Ma), and M25 (154.3 Ma) with more detailed timesteps during major tectonic

events. A finer set of seafloor spreading isochrons was drawn in back-arc and marginal basins. Quoted ages use Cande and Kent (1995) for times after 83.5 Ma and Gradstein et al. (1994) for times prior to 83.5 Ma. The letter "y" stands for young end of chron and "o" for old end of chron. We verify our isochron interpretation by correlating with the magnetic lineations in the World Digital Magnetic Anomaly Map (WDMAM) (Maus et al., 2007), the Earth Magnetic Anomaly Grid (EMAG2) (Maus et al., 2009) and our own preferred magnetic anomaly compilation (Fig. 2). EMAG2 includes a compilation of both ship-track and long-wavelength satellite magnetic anomaly data with trend-gridding based on the Müller et al. (2008a) isochrons in most areas, hence WDMAM and our own compilation are preferred for correlation. We constrain fracture zone locations using global gravity from satellite altimetry (Sandwell and Smith, 1997, 2005) (Fig. 1). The boundary between oceanic and continental lithosphere was taken from Müller et al. (2008a), except where otherwise stated in the text.

The computation of finite rotations and construction of seafloor spreading isochrons are relatively straightforward for areas where both flanks of a spreading system are preserved (e.g. Atlantic, SE Indian Ridge, Pacific–Antarctic Ridge), but becomes more problematic in other settings. When only one flank of a spreading system is preserved (e.g. Pacific–Farallon, Pacific–Kula, Pacific–Izanagi, Pacific–Phoenix), we compute half-stage rotations (stage rotation between adjacent isochrons on one flank) and double the half-stage angle (i.e. assume that spreading was symmetrical) to create a full stage rotation, following the methodology of Stock and Molnar (1988). This assumption of spreading symmetry is reasonable as the maximum cumulative spreading asymmetry globally is only 10%, on average (Müller et al., 1998b). In instances where crust from both flanks has been subducted, we rely on the onshore geological record (e.g. mapping of major sutures, terrane boundaries and active and ancient magmatic arcs) to help define the locations of paleo-plate boundaries and use inferences from younger, preserved crust to estimate earlier spreading directions and rates. Where continental terranes have crossed ocean basins we use the implied history of mid-ocean ridge evolution and subduction to create synthetic ocean floor by constructing isochrons based on assuming spreading symmetry and ensuring triple junction closure. The location of mid-ocean ridges as they intersect continents can be further constrained by tracking slab window formation along continental margins (Thorkelson, 1996) and their correlation to anomalous geochemistry and volcanism (Bradley et al., 1993; Sisson and Pavlis, 1993; Breitsprecher et al., 2003; Madsen et al., 2006), elevated geothermal gradients (Bradley et al., 1993; Thorkelson, 1996; Lewis et al., 2000) and the eruption of massive sulfides (Haeussler et al., 1995; Rosenbaum et al., 2005). We do not use arguments for the location subduction based on mantle tomography as our model is solely underpinned by surface constraints.

Triple junction closure follows the rules set out in McKenzie and Morgan (1969) where we assume that the ridge axes are perpendicular to the spreading direction, transform faults are purely strike-slip features, plates are rigid and spreading is symmetrical. We use the finite difference method to compute spreading along the third arm of a triple junction. In addition, we assume that ridge–ridge–ridge triple junctions are stable features, but note that there is evidence that fast seafloor spreading rates cause triple junction instability and complexities in spreading (Bird and Naar, 1994).

2.3. Geomagnetic polarity timescales

Geomagnetic polarity timescales (GPTS) correlate the reversals of the Earth's geomagnetic field, most often the sequence of magnetic anomalies recorded on the ocean floor, to those based on biostratigraphy, cyclostratigraphy (which includes Earth's orbital variations), absolute ages from radiometric studies and average spreading rates for interpolation.

The early GPTS for the Cenozoic (Heirtzler et al., 1968) and Mesozoic (Larson and Pitman, 1972) have been superseded by a range of updated timescales. Cande and Kent (1995) (CK95) developed a timescale for the Cenozoic (0–83.5 Ma) based on a model of smoothly varying spreading rates in the South Atlantic (Cande and Kent, 1992) with the inclusion of astronomical information for the past 5.23 Ma. Gradstein et al. (1994) (G94) presented an integrated geomagnetic and stratigraphic Mesozoic timescale, which is commonly merged with the CK95 timescale to create a hybrid timescale through to the Mesozoic (e.g. (Müller et al., 2008b)). The GTS2004 timescale (Gradstein et al., 2004) recalibrated CK95 using alternative tie-points from updated radiometric ages and astronomical tuning for the Cenozoic and updated the Mesozoic timescale using the methodology of Cande and Kent (1992) and additional radiometric age constraints. The most recent GPTS (Gee and Kent, 2007) is a hybrid model, which uses CK95 for the Cenozoic and CENT94 (Channell, 1995) for the Mesozoic and includes sub-chrons from Lowrie and Kent (2004). The choice of GPTS (i.e. the ages assigned to each magnetic anomaly chron) has major implications for the timing of geological events and the significance of geological processes. For example, the inferred mid-Cretaceous seafloor spreading pulse (Larson, 1995) is apparent if using the CK94G95 timescale but diminished if using GTS2004 due to a ~4 million year difference in the age assigned to M0 (~120 Ma) (Seton et al., 2009) (Table 1).

The occurrence of magnetic reversals in the so-called Jurassic Quiet Zone is not a widely accepted explanation for magnetic anomalies of ages 157 Ma and older, which are rather modeled as geomagnetic intensity variations (Gee and Kent, 2007). Despite this, geomagnetic timescales based on detailed magnetic anomalies collected closer to the seafloor (using a deep towed magnetometer) in regions of high seafloor spreading rates (in the Pacific ocean) suggest the existence of a range of short reversals spanning from M29 to M40 (Sager et al., 1998) or M29 to M44 (Tivey et al., 2006) (T06). Dating of Jurassic Quiet Zone based on the timescale of Sager et al. (1998) has been also attempted in the Central Atlantic Ocean by Roeser et al. (2002) and Bird et al. (2007).

We ensure that our data, including magnetic anomaly identifications, finite rotations and seafloor spreading isochrons are calibrated to one timescale. We choose the CK95 geomagnetic reversal timescale for the Cenozoic (to Chron 34y; 0–83.5 Ma), G94 for the Mesozoic (Chrons M0–M33; 120.4–158.1 Ma) and T06 for the Jurassic (Chrons M34–M44; 160.3–169.7 Ma), as our standard. Our continuously closed plate polygons can be combined using either timescale.

2.4. Continuously closed plate polygons

A network of tectonic plates, bounded by a series of plate boundaries, combines to cover the surface of the Earth. Most plate tectonic models reconstruct features on the surface of the Earth without regard to the plate margins and are created in time intervals that are too sparse for current needs. These models are insufficient for studies that couple motions of the plates to other dynamic earth processes, for example mantle convection and oceanic and atmospheric circulation. This prompted Gurnis et al. (2012) to develop a novel methodology to create a set of dynamically closed plate polygons back in time. The continuously closing plate (CCP) methodology works by assigning a different Euler pole for each plate boundary that constitutes a plate polygon, ensuring that the polygon remains topologically closed as a function of time (Gurnis et al., 2012). The feature is built into the plate reconstruction software *GPlates* (Boyden et al., 2011).

We use the CCP method and the base set of plate polygons in Gurnis et al. (2012) to create a new set of dynamically closed plate polygons based on the plate motion model presented in this study for the last 200 Ma. The plate polygons are built using a series of plate boundaries, the location and timing of which have been determined by using present day plate boundaries (Bird, 2003), geological evidence for locations of island arcs, magmatic arcs, sutures and

Table 1
Summary table of magnetic chrons used in this study and referred to in text with ages based on alternative timescales. CK94, G94, T06 refers to a merged Cande and Kent (1995) (Chrons 0–34), Gradstein et al. (1994) (Chrons M0–M33) and Tivey et al. (2006) (M34–M44) timescale. GTS2004 from Gradstein et al. (2004). GK07 refers to the timescale presented in Gee and Kent (2007).

Chron	Abbreviation	Age—CK95, G94, T06		Age—GST 2004		Age—GK07	
		Young	Old	Young	Old	Young	Old
C1n	1	0.0	0.8	0.0	0.8	0.0	0.8
C2An.1n	2	2.6	3.0	2.5	3.0	2.6	3.0
C3An.1n	3	5.9	6.1	6.0	6.3	5.9	6.1
C4An	4	8.7	9.0	8.8	9.1	8.7	9.0
C5n.2n	5	9.9	10.9	10.0	11.0	9.9	10.9
C5Dn	5D	17.3	17.6	17.2	17.5	17.3	17.6
C6n	6	19.0	20.1	18.7	19.7	19.0	20.1
C7n.2n	7	24.8	25.2	24.2	24.6	24.8	25.2
C8n.2n	8	26.0	26.6	25.5	26.2	26.0	26.6
C9n	9	27.0	28.0	26.7	27.8	27.0	28.0
C10n.1n	10	28.3	28.5	28.2	28.5	28.3	28.5
C11n.2n	11	29.8	30.1	29.9	30.2	29.8	30.1
C12n	12	30.5	30.9	30.6	31.1	30.5	30.9
C13n	13	33.1	33.5	33.3	33.7	33.1	33.5
C15n	15	34.7	34.9	34.8	35.0	34.7	34.9
C16n.2n	16	35.7	36.3	35.7	36.3	35.7	36.3
C17n.1n	17	36.6	37.5	36.5	37.2	36.6	37.5
C18n.2n	18	39.6	40.1	39.0	39.5	39.6	40.1
C19n	19	41.3	41.5	40.4	40.7	41.3	41.5
C20n	20	42.5	43.8	41.6	42.8	42.5	43.8
C21n	21	46.3	47.9	45.3	47.2	46.3	47.9
C22n	22	49.0	49.7	48.6	49.4	49.0	49.7
C23n.2n	23	51.0	51.7	51.1	51.9	51.0	51.7
C24n.3n	24	52.9	53.3	53.3	53.8	52.9	53.3
C25n	25	55.9	56.4	56.7	57.2	55.9	56.4
C26n	26	57.6	57.9	58.4	58.7	57.6	57.9
C27n	27	60.9	61.3	61.7	62.0	60.9	61.3
C28n	28	62.5	63.6	63.1	64.1	62.5	63.6
C29n	29	64.0	64.7	64.4	65.1	64.0	64.7
C30n	30	65.6	67.6	65.9	67.7	65.6	67.6
C31n	31	67.7	68.7	67.8	68.7	67.7	68.7
C32n.1n	32	71.1	71.3	71.0	71.2	71.1	71.3
C33n	33	73.6	79.1	73.6	79.5	73.6	79.1
C34n	34	83.5	120.4	84.0	125.0	83.0	120.6
M0r	M0	120.4	121.0	124.6	125.0	120.6	121.0
M1n	M1	121.0	123.7	125.0	127.6	121.0	123.2
M3n	M3	124.1	124.7	127.6	128.1	123.6	124.1
M5n/M4	M4	126.7	127.7	129.8	130.8	125.7	126.6
M6n	M6	128.2	128.3	131.2	131.4	126.9	127.1
M7n	M7	128.4	128.6	131.6	131.9	127.2	127.5
M8n	M8	129.0	129.3	132.2	132.5	127.8	128.1
M9n	M9	129.5	129.8	132.8	133.1	128.3	128.6
M10n	M10	130.2	130.6	133.5	133.9	128.9	129.3
M10Nn.3n	M10N	131.6	131.9	135.0	135.3	130.2	130.5
M11n	M11	132.1	132.7	135.7	136.4	130.8	131.5
M12n	M12	134.0	134.2	137.6	137.8	132.6	132.8
M13n	M13	135.3	135.5	139.1	139.3	134.1	134.3
M14n	M14	135.8	136.0	139.5	139.8	134.5	134.8
M15n	M15	136.2	137.2	140.4	140.7	135.6	136.0
M16n	M16	137.9	139.6	141.1	142.1	136.5	137.9
M17n	M17	140.3	140.8	142.6	142.8	138.5	138.9
M18n	M18	142.4	143.0	144.0	144.6	140.5	141.2
M19n	M19	143.7	144.7	145.1	146.0	141.9	143.1
M20n.2n	M20	145.4	146.0	146.5	147.2	143.8	144.7
M21n	M21	146.8	147.7	147.8	148.5	145.5	146.6
M22n.1n	M22	148.1	149.5	148.9	150.1	147.1	148.6
M23n.1n	M23	150.7	151.1	151.0	151.3	150.0	150.7
M24n.1n	M24	152.1	152.5	152.3	152.5	151.4	151.7
M25n	M25	154.1	154.3	154.1	154.4	153.4	154.0
M26.1n	M26	155.0	155.1	155.1	155.1	154.3	155.3
M27n	M27	155.4	155.5	155.7	155.9	155.6	155.8
M28n	M28	155.7	155.8	156.0	156.3	156.1	156.2
M29.1n	M29	156.0	156.1	157.3	157.4	156.5	157.3
M30.1n	M30	156.8	157.2	N/A	N/A	N/A	N/A
M31n	M31	157.4	157.6	N/A	N/A	N/A	N/A
M32n	M32	157.7	157.9	N/A	N/A	N/A	N/A
M33n	M33	158.0	158.1	N/A	N/A	N/A	N/A
M34	M34	160.3	160.9	N/A	N/A	N/A	N/A
M35	M35	161.0	161.1	N/A	N/A	N/A	N/A
M36	M36	161.3	161.8	N/A	N/A	N/A	N/A
M37	M37	162.0	162.4	N/A	N/A	N/A	N/A
M38	M38	162.5	163.5	N/A	N/A	N/A	N/A
M39	M39	163.7	165.4	N/A	N/A	N/A	N/A
M40	M40	165.5	166.2	N/A	N/A	N/A	N/A
M41	M41	166.3	167.0	N/A	N/A	N/A	N/A
M42	M42	167.1	168.2	N/A	N/A	N/A	N/A
M43	M43	168.2	168.9	N/A	N/A	N/A	N/A
M44	M44	168.9	169.7	N/A	N/A	N/A	N/A

major faults through time as well as an analysis of plate motion vectors based on our kinematic model. The Euler poles describing the motion of each plate margin are derived from the plate tectonic model presented in this study. Each plate boundary feature within the dataset has a set of feature-specific attributes assigned. For example, mid-ocean ridge features include information on the plate to the left and right of the spreading ridge and whether it is an active or extinct feature; subduction zones contain information regarding the polarity of subduction, dip angle (when known) and the duration of activity; transform faults track the sense and direction of motion.

Our set of continuously closed plate polygons covers the entire surface of the Earth with no gaps in one million year time intervals. These can be used as input into geodynamic modeling software, to extract plate velocity data for each tectonic plate through time, to reconstruct raster data and to "cookie-cut" geological data based on tectonic plate. Using the CCP algorithm code in GPlates, the time interval between closed polygons can be made arbitrarily small and is only limited to how the underlying start and end ages of both margins and polygons has been encoded. For ease of use, the polygons are presented as static polygons at 1 million year time intervals. All data are available in digital format and can be downloaded from the following location: ftp://ftp.earthbyte.org/papers/Seton_etal_Global_ESR/Seton_etal_Data.zip.

3. Regional continental and ocean floor reconstructions

In the following section, we will describe the plate kinematic models we used for each region of the world. We separate the globe into four main regions: the Atlantic and Arctic; the Pacific and Panthalassa; the Tethys and Indian/Southern Ocean; and marginal and back-arc basins. We suggest that the accompanying data with this paper be loaded in order to most easily follow the plate boundaries and configurations mentioned in the text.

3.1. Atlantic and Arctic

3.1.1. South Atlantic

Over the recent decades there has been considerable debate on the exact timing and kinematics of the opening of the South Atlantic Ocean. It is commonly accepted that rifting in the South Atlantic occurred progressively from south to north along reactivated older tectonic lineaments dating from the late Triassic–early Jurassic (Daly et al., 1989) and was associated with substantial intra-continental deformation within Africa and South America (Unternehr et al., 1988; Nürnberg and Müller, 1991; Eagles, 2007; Torsvik et al., 2009; Moulin et al., 2010). To account for these motions, South America and Africa are subdivided using Jurassic–Cretaceous sedimentary basins, which document the various rift phases related to the dispersal of west Gondwana. South America is commonly subdivided into the Patagonia, Colorado and Parana subplates and Africa into South, Northwest and Northeast Africa (Nürnberg and Müller, 1991; Torsvik et al., 2009) (Fig. 2). Internal deformation within both continents is required to minimize gaps/overlaps in full-fit

reconstructions (see discussions in Eagles, 2007, Torsvik et al., 2009, and Moulin et al., 2010).

Rifting prior to seafloor spreading in the southernmost Atlantic ("Falkland segment") is believed to have occurred in the early Jurassic (190 Ma) and involved dextral movement between Patagonia and the Colorado sub-plate until the early Cretaceous (126.7 Ma) (Torsvik et al., 2009) (Fig. 2). Opening propagated northward into the "Southern/Austral segment" adjacent to the Colorado sub-plate in the late Jurassic (around 150 Ma) based on late Jurassic–early Cretaceous sediment fill and activation (Nürnberg and Müller, 1991) and the onset of deformation for a "fit" reconstruction using spreading rate interpolation (Eagles, 2007) or early Cretaceous (140 Ma) according to Schettino and Scotese (2005). The model of Torsvik et al. (2009) suggests that rifting was accommodated between the Colorado and Parana subplates, Colorado and Africa, and Parana and Africa from 150 Ma and was associated with dextral strike-slip motion between Patagonia/Colorado subplate and Parana (Nürnberg and Müller, 1991; Torsvik et al., 2009). Further north, rifting adjacent to the Parana subplate and south of the Walvis Ridge/Rio Grande Rise is believed to have occurred by about 130 Ma (Nürnberg and Müller, 1991), 132 Ma corresponding to the Parana–Etendeka magmatic event peak (Torsvik et al., 2009), 134 Ma based on the presence of Anomaly M10 and the GTS2004 timescale (Moulin et al., 2010) or 135 Ma based on dating of the continent–ocean transition (Bradley, 2008). The oldest magnetic anomaly that has been identified is M4 (~127 Ma) (Nürnberg and Müller, 1991; Torsvik et al., 2009) adjacent to Falkland and Parana/Chacos basin. Coincident with opening along the South Atlantic rift was the activation of the West and Central African Rift systems and the Central African Shear Zone (Binks and Fairhead, 1992; Genik, 1992; Guiraud and Maurin, 1992; Torsvik et al., 2009).

The "Central" segment of the South Atlantic margin (Fig. 2) is characterized by widespread Aptian salt basin formation. Rifting continued propagating northward and extended into the African interior, active in the Benue Trough by at least 118 Ma (Nürnberg and Müller, 1991), although earlier extension in the Benue Trough is possible (Torsvik et al., 2009). The onset of seafloor spreading in the "Central" segment is difficult to ascertain because the oceanic crust adjacent to the margin formed during the Cretaceous Normal Superchron (CNS), however Anomaly M0 has been identified extending to latitude 22°S (Cande et al., 1988; Nürnberg and Müller, 1991; Müller et al., 1999). Torsvik et al. (2009) used the shape and age of the Aptian salt basins to further refine the opening history in this section of the margin and suggested that seafloor spreading only reached north of the Walvis Ridge–Rio Grande Rise at ~112 Ma, much later than 120.4 Ma suggested by previous models.

The "Equatorial" segment of the South Atlantic margin (Fig. 2) was the youngest region of plate break-up. Magnetic anomalies cannot be interpreted due to equatorial formation of the oceanic crust relative to spreading direction. However, Anomaly 33 and fracture zone segments are well defined. Seafloor spreading is believed to have propagated into this area after Anomaly M0 (120.4 Ma) (Nürnberg and Müller, 1991), ~100 Ma (Torsvik et al., 2009), 105 Ma (Moulin et al., 2010) or 102–96 Ma (Eagles, 2007), corresponding to a subtle bend in the fracture zones in the South Atlantic. Either coincident or subsequent to the opening of the equatorial segment, the areas undergoing continental extension in the African interior ceased but only after a short-lived compressional phase in the late Cretaceous (around 85–80 Ma) observed in folding and faulting across seismic sections (Nürnberg and Müller, 1991; Binks and Fairhead, 1992; Schettino and Scotese, 2005).

The spreading history along the entire length of the South Atlantic from Anomaly 34 (83.5 Ma) onwards is relatively uncomplicated with most studies in agreement that largely symmetrical spreading occurred after Anomaly 34 to the present day (LaBrecque and Rabinowitz, 1977; Shaw and Cande, 1990; Nürnberg and Müller, 1991; Torsvik et al., 2009; Moulin et al., 2010). The stability and symmetry of this spreading system during the Cenozoic led to this region being used as a type example for calibrating the geomagnetic reversal timescale (Cande and Kent, 1992).

Recent models have been developed to refine rifting and minimize misfits in the South Atlantic. Although no model accurately restores all continental margins without gaps or overlaps, we find that the model of Torsvik et al. (2009) agrees well with continental stretching rates and conjugate margin rifting episodes. We therefore implement the model of Torsvik et al. (2009) for the early rifting phase of the South Atlantic, including intra-continental deformation in South America and Africa but adjust their rotations to be consistent with the Gradstein et al. (1994) timescale for the Mesozoic. In the early Jurassic (190 Ma), we follow a plate boundary between Patagonia and South Africa connected to the Permian–Triassic to Jurassic rifting in the Karoo Basin (Banks et al., 1995; Catuneanu et al., 2005) and along the Agulhas-Falkland Fracture Zone to the Panthalassic subduction zone to the west. The South Atlantic central rift propagated northward, with extension between Colorado, Parana and Africa from 150 Ma. Rifting reached the African continental interior through the West and Central African Rift Zones, along the Central African Shear Zone at 131.7 Ma, connecting with the West and Central African Rift Zones. These continental rift zones encompass the major hydrocarbon-producing Cretaceous basins of the Central and West African rift system from East Niger to Sudan. We cease rifting in the interior of Africa at about 85 Ma.

We use the model of Nürnberg and Müller (1991) for the seafloor spreading record but refine the timing of the onset of seafloor spreading to 132 Ma to correspond to the peak of magmatism (Torsvik et al., 2009). In addition, we switch to the updated Cenozoic rotations of Müller et al. (1999) from Anomaly 34 to the present day. The poles presented in Müller et al. (1999) are similar to those of Shaw and Cande (1990) but reflect finer scale changes in spreading direction due to the inversion method used for fracture zone interpretation (Müller et al., 1999). Our seafloor spreading isochrons match well with the magnetic lineations observed in our magnetic anomaly grid (Fig. 2), although poor data coverage hinders broad scale correlation.

We also incorporate spreading in the Agulhas Basin (southernmost South Atlantic) between South America and the Malvinas Plate (LaBrecque and Hayes, 1979; Marks and Stock, 2001) from Anomaly 34 (83.5 Ma) to Anomaly 30 (~66 Ma) according to the rotations of Nürnberg and Müller (1991). The extinct spreading ridge associated with this spreading system as well as distinct fracture zone trends are clearly observed in satellite gravity data (Marks and Stock, 2001) (Fig. 1).

3.1.2. Central Atlantic

The Central Atlantic contains the region between North America conjugate to Northwest Africa bounded by Pico and Gloria Fracture Zones to the north and the 15° 20′N and Guinean Fracture Zones to the south (Fig. 3). Break-up marked the beginning of Pangea separation and involved at least a three-plate system between North America, Northwest Africa and the Moroccan Meseta (Fig. 3). Rifting was controlled by pre-existing structures leading to the formation of a series of rift basins during late Triassic–early Jurassic between North America and Northwest Africa (Lemoine, 1983; Klitgord and Schouten, 1986), which subsequently filled with salt and became inactive during plate separation. In addition, transtensional rifting between Northwest Africa and the Moroccan Meseta formed rift basins along the Atlas rift (Labails et al. 2010). The first stage of Atlas Mountain uplift occurred during the opening of the Central Atlantic (Beauchamp, 1998). Incorporating motion along the Atlas rift has implications for full-fit reconstructions of the Central Atlantic.

The establishment of seafloor spreading in the Central Atlantic is debated, with ages ranging from 175 Ma marked by the West African Coast Magnetic Anomaly and East Coast Magnetic Anomaly and an extrapolation of spreading rates (Klitgord and Schouten, 1986;

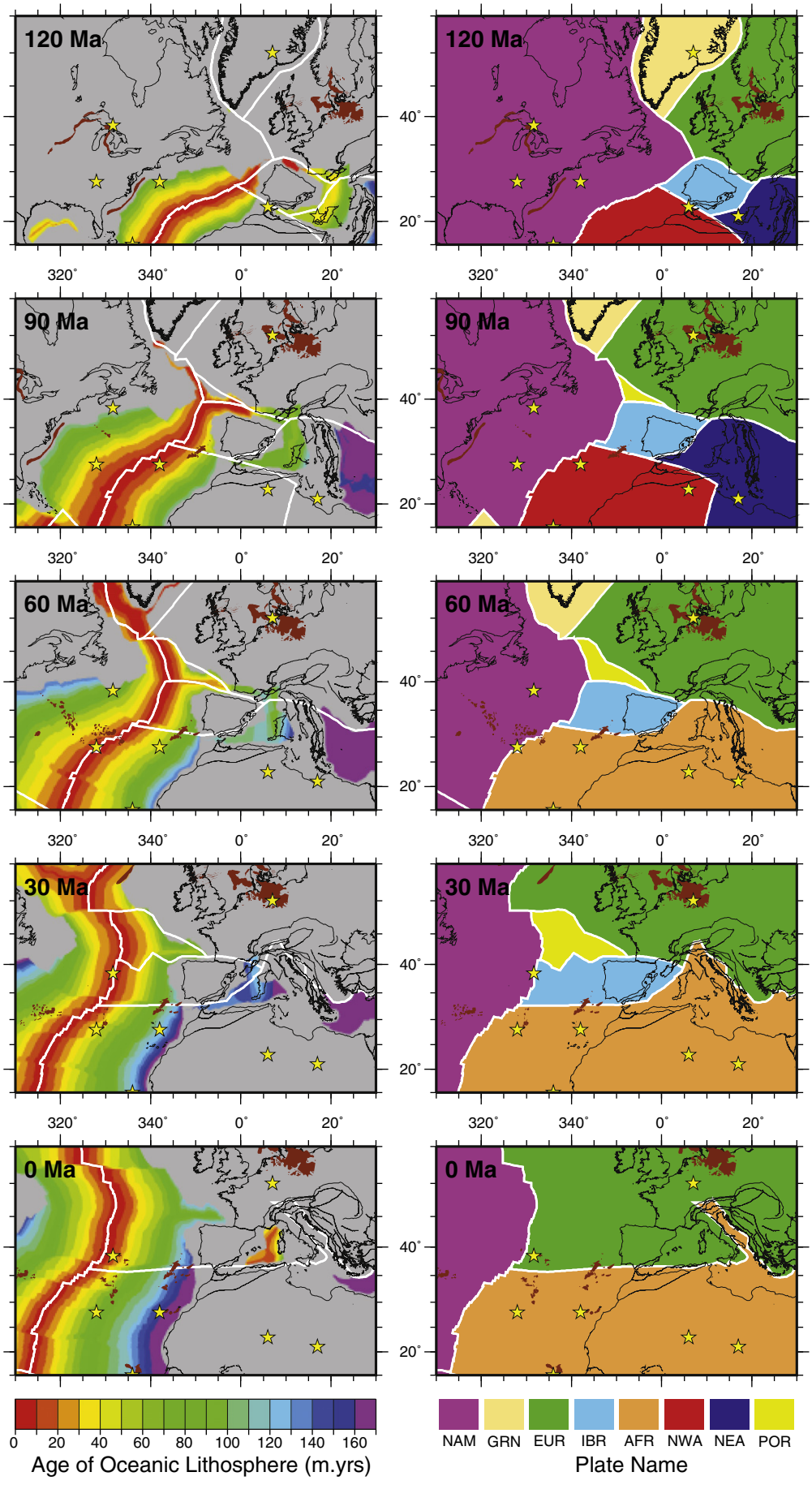
120 Ma
90 Ma
60 Ma
30 Ma
0 Ma
320°
340°
0°
20°
40°
0 20 40 60 80 100 120 140 160
Age of Oceanic Lithosphere (m.yrs)
NAM GRN EUR IBR AFR NWA NEA POR
Plate Name

Müller and Roest, 1992; Müller et al., 1999), 170–171 Ma based on a review of global passive margins (Bradley, 2008), diachronous opening with 200 Ma in the south progressing to 185 Ma in the north based on dating of post-rift sediment deposition (Withjack et al., 1998) and 200 Ma according to model of Schettino and Turco (2009). A recent re-evaluation of the Central Atlantic opening (Labails et al., 2010) suggests that the earliest seafloor spreading occurred at 190 Ma (maximum at 203 Ma) based on an updated magnetic anomaly grid and interpretation of salt basins offshore Morocco and North America (Sahabi et al., 2004). In this model, spreading was initially very slow at half-spreading rates of ~8 mm/yr with an increase in spreading rate and direction at 170 Ma to ~17 mm/yr and spreading asymmetry until Anomaly M0 (120.4 Ma). This is in contrast to previous models (Klitgord and Schouten, 1986; Bird et al., 2007) that invoke an early ridge jump at 170 Ma rather than significant spreading asymmetry to account for increased crustal accretion onto the North American plate.

Anomalies M25–M0 (~154–120 Ma) and 34–30 (~84–65 Ma) are well established primarily due to the density of data on the western flank (Klitgord and Schouten, 1986; Müller and Roest, 1992; Müller et al., 1999). The spreading rates in the Central Atlantic in the Cenozoic are quite slow making identification of magnetic anomalies more difficult than for the Mesozoic (Klitgord and Schouten, 1986). Anomalies from 25 (~56 Ma) onwards have been identified quite consistently between studies (Klitgord and Schouten, 1986; Müller and Roest, 1992; Müller et al., 1999) with the main difference occurring between Anomalies 8 and 5 (~26–10 Ma) due to finer constraints on fracture zone trends using the models by Müller and Roest (1992) and Müller et al. (1999).

We have implemented the early break-up history of Labails et al. (2010) to define the Jurassic–early Cretaceous history of the Central Atlantic as a highly asymmetric, slow spreading system. We initiate the Central Atlantic rift prior to 200 Ma together with a transtensional plate boundary between Northwest Africa and Morocco along the Atlas rift using rotations derived from Labails et al. (2010). The Central Atlantic rift connects to a major transform fault along the Jacksonville Fracture Zone to the south linking with Mesozoic rift basins in the Caribbean (see Section 3.4.1: Caribbean). To the north, the Central Atlantic rift extends into the northern Atlantic, where Triassic/Jurassic rifts are observed (see Section 3.1.3: North Atlantic). Immediately following the initiation of seafloor spreading in the Central Atlantic was the cessation of transtensional motion along the Atlas rift and the first stage of uplift of the Atlas Mountains (Beauchamp, 1998).

We initiate seafloor spreading at 190 Ma (Labails et al. 2010) and subsequently use the magnetic anomaly picks from Klitgord and Schouten (1986) and rotations from Müller et al. (1997) for M25–M0 (~154–120 Ma). Spreading propagated northward between the Iberia–Newfoundland margin during Anomaly M20 (~146 Ma) (Müller et al., 1997) (Fig. 4). To the south, spreading in the Central Atlantic connected with the Equatorial Atlantic in the late Cretaceous. We incorporate the Cenozoic rotations from Müller et al. (1999), which have been updated from those of Müller and Roest (1992) and use the isochrons from Müller et al. (2008a). The isochrons match well with the gridded magnetic anomalies (Fig. 3) and fracture zone identifications from global satellite gravity (Sandwell and Smith, 2009) (Fig. 1).

3.1.3. Northern Atlantic

The Northern Atlantic encompasses the area between Newfoundland–Iberia and the Eurasian Basin in the Arctic Ocean (Figs. 3 and 5). It includes active and extinct spreading systems, ridge–hotspot interactions related to the Iceland plume, volcanic and magma-poor margins and microcontinent formation (e.g. Jan Mayen). The Northern Atlantic underwent episodic continental extension in the Permo-Triassic, late Jurassic, early and mid Cretaceous, with reactivation and basin formation largely following pre-existing structures from the closure of the Iapetus Ocean and subsequent Baltica–Laurentia collision (400–450 Ma) (Dore et al., 1999; Silva et al., 2000; Skogseid et al., 2000; Kimbell et al., 2005). Seafloor spreading propagated from the Central Atlantic starting in the late Cretaceous in six distinct phases: Iberia–Newfoundland, Porcupine–North America, Eurasia–Greenland (conjugate to Rockall), North America–Greenland (Labrador Sea), Eurasia–Greenland (Greenland and Norwegian Sea and Jan Mayen), North America–Eurasia (Eurasian Basin, Arctic Ocean) (Figs. 3–5).

3.1.3.1. Iberia–Newfoundland. The Iberia–Newfoundland margin is a type example of a highly extended, magma-poor, rifted continental margin (Boillot et al., 1988; Srivastava et al., 2000; Hopper et al., 2004; Peron-Pinvidic et al., 2007) with two main phases of extension. Extension during the late Triassic to early Jurassic formed large rift basins within the continental lithosphere of both margins (Tucholke and Whitmarsh, 2006) and was followed by a period of quiescence in the early–mid Jurassic marked by subsidence and the accumulation of shallow-water carbonates (Tankard and Welsink, 1987). The second phase of deformation, from late Jurassic to early Cretaceous, formed a wide zone of layered basalts, gabbros and serpentinized mantle ("transitional" crust) indicative of seafloor spreading and mantle exhumation (Srivastava et al., 1990; Tucholke and Whitmarsh, 2006; Peron-Pinvidic et al., 2007; Sibuet et al., 2007).

The onset and location of normal seafloor spreading are widely debated. The interpretation of low amplitude magnetic anomalies as old as Anomaly M21 (~147 Ma) related to ultraslow seafloor spreading within the southern part of the transition zone (Srivastava et al., 2000; Sibuet et al., 2007) is the oldest seafloor spreading age assigned to the margin. Other studies have instead suggested younger ages for the onset of seafloor spreading: Anomalies M3–M5 (~124–128 Ma) based on deep sea drilling and seismic refraction (Whitmarsh and Miles, 1995; Russell and Whitmarsh, 2003) and late Aptian (~112–118 Ma) based on stratigraphic studies (Tucholke et al., 2007). Although the earliest timing of seafloor spreading remains controversial, reconstructions between the Iberia and Newfoundland margin from Anomaly M0 (~120 Ma) onwards are well established with changes in spreading rates occurring at Anomaly 25 (~56 Ma) coincident with the initiation of spreading further north in the Norwegian–Greenland Sea (Srivastava and Tapscott, 1986; Srivastava et al., 2000).

Related to the development of the Iberia–Newfoundland margin is the opening of the Bay of Biscay north of Iberia and the motion of the Iberia block itself. The Bay of Biscay formed at a ridge–ridge–ridge triple junction (Klitgord and Schouten, 1986) commonly believed to have opened in the late Cretaceous (110–83.5 Ma) according to Müller et al. (1997). However, Anomalies M0 to 33 (~120–79 Ma) have been identified (Sibuet et al., 2004) suggesting that seafloor spreading initiated in the Bay of Biscay at the same time as an increase in spreading rate and cessation of mantle exhumation along the Iberia–Newfoundland margin (Sibuet et al., 2007). The end of seafloor spreading occurred at Anomaly 33 (~79 Ma) (Roest and Srivastava, 1991; Sibuet et al., 2004).

Most models agree that the Iberian continental block was fixed relative to Africa since the start of rifting along the Iberia–Newfoundland

Fig. 4. (a) Agegrid reconstructions of the Central and North Atlantic at 120, 90, 60, 30, 0 Ma highlighting the age–area distribution of oceanic lithosphere at the time of formation and the extent of continental crust (gray polygons). Plate boundaries from our continuously closing plate polygon dataset are denoted as thick white lines, hotspot locations as yellow stars, large igneous provinces and flood basalts as brown polygons and coastlines as thin black lines. (b) Reconstructions showing the outlines of the plates in the Central and North Atlantic for each reconstruction time listed above. Feature descriptions as in panel (a). Abbreviations are: NAM = North American plate, GRN = Greenland plate, EUR = Eurasian plate, IBR = Iberian plate, AFR = African plate, NWA = Northwest African plate, NEA = Northeast African plate, POR = Porcupine plate. (For interpretation of the references to color in this figure legend, the reader is referred to the web version of this article.)

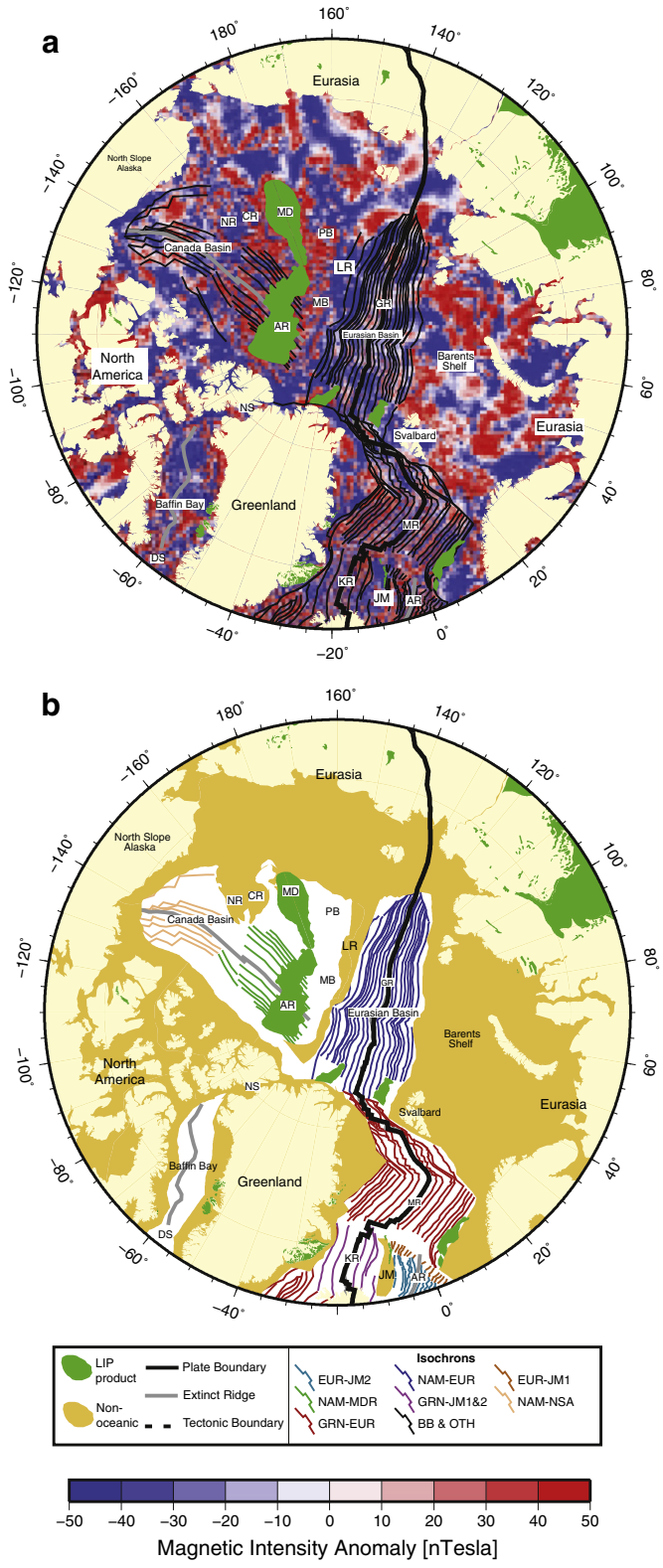

Fig. 5. (a) Gridded magnetic anomalies for the Arctic. Seafloor spreading isochrons used in this study plotted as thin black lines. AL = Alpha Ridge, AR = Aegir Ridge, CR = Chukchi Ridge, DS = Davis Strait, GR = Gakkel Ridge, JM = Jan Mayen, KR = Kolbeinsey Ridge, LR = Lomonosov Ridge, MB = Makarov Basin, MD = Mendeleev Ridge, MR = Mohns Ridge, NR = Northwind Ridge, NS = Nares Strait, PB = Podvodnikov Basin. (b) Seafloor spreading isochron map colored by spreading system or plate pair. Map abbreviations are same as a. Legend abbreviations are: BB = Back-arc Basins, EUR = Eurasia, GRN = Greenland, JAM = Jan Mayen, MDR = Mendeleev, NAM = North America, NOR = Norway, NSA = North Slope Alaska, OTH = Other spreading systems outside area of interest.

margin until Anomaly 10 (~28 Ma) (Srivastava and Tapscott, 1986) based on geological evidence from the Pyrenees and geophysical data from the Northern Atlantic (Roest and Srivastava, 1991; Sibuet et al., 2004). The location of the plate boundary is proposed to have been located north of the Kings Trough from M0 (~120 Ma) to the Eocene (Srivastava et al., 1990), extended along the Kings Trough into the Bay of Biscay and along the Pyrenees from the Eocene to Anomaly 10 (~28 Ma) (Klitgord and Schouten, 1986; Roest and Srivastava, 1991; Whitmarsh and Miles, 1995) and was followed by southward ridge jump along the Azores transform fault and Straits of Gibraltar (Klitgord and Schouten, 1986; Roest and Srivastava, 1991).

In our plate kinematic model, we use the boundary between continental and oceanic crust interpretation of Todd et al. (1988) for the Newfoundland margin and Boillot and Winterer (1988) and Srivastava et al. (2000) for the Iberia margin. We take the age given by Srivastava et al. (2000) for the initiation of ultra-slow seafloor spreading based on their interpretation of magnetic anomalies back to M20 (~146 Ma) as we believe that this corresponds to the boundary between true continental crust and oceanic/transitional crust. Our seafloor spreading isochrons are based on Müller et al. (1997) and correlate well with magnetic anomaly grids (Fig. 3).

In our plate model, we fix Iberia to Africa from the initiation of seafloor spreading in the Eocene and use the rotations of Srivastava and Tapscott (1986) for seafloor spreading between the Iberia–Newfoundland margin (~146 Ma) to Anomaly 10 (~28 Ma) (Fig. 4). We define the plate boundary between Iberia and Eurasia along the Kings Trough through the Pyrenees, connecting with the northern Tethyan subduction zone (Fig. 4). In addition, we incorporate spreading in the Bay of Biscay between Iberia and Eurasia based on timing of Sibuet et al. (2004) (~120 Ma) and the finite difference method for the rate and direction of spreading. After Anomaly 10 (~28 Ma), we incorporate a southern jump of the plate boundary to the Azores transform fault and along the Straits of Gibraltar leading to the capture of Iberia by the Eurasian plate (Fig. 4).

3.1.3.2. Porcupine–North America. The Porcupine Abyssal Plain is bounded by the Kings Trough, Labrador Sea and Charlie Gibbs Fracture Zone (Figs. 3 and 4). The existence of the Porcupine Plate as an independent plate during the Eocene–Oligocene was first hypothesized by Srivastava and Tapscott (1986) in order to account for overlapping reconstructed anomalies in the Porcupine Abyssal Plain when using a single pole of rotation for North Atlantic opening and to explain Eocene deformation recorded along the north Biscay and Porcupine margins. The need for a separate Porcupine Plate was challenged by Gerstell and Stock (1994) when they computed new rotations for Eurasia–North America without overlaps between the magnetic anomalies. However, these reconstructions were themselves challenged as they could not account for the observed intra-plate deformation recorded both onshore and offshore in the Porcupine Abyssal Plain (Srivastava and Roest, 1996).

A major phase of rifting occurred from the late Jurassic to early Cretaceous, marked by the formation of extensional basins along both margins (Rowley and Lottes, 1988) and the deposition of syn-rift sediments in the Barremian/late Hauterivian 130–125 Ma (De Graciansky et al., 1985). Seafloor spreading began by at least the mid–late Albian (110–105 Ma) based on the dating of the sediments above tholeiitic basalt from DSDP sites 550 and 551 and an Aptian regional unconformity (De Graciansky et al., 1985) and supported by the interpretation of Anomaly 34 (~84 Ma) seaward of this location (Srivastava and Tapscott, 1986; Müller and Roest, 1992). Further refinement based on magnetic anomalies is not possible as the early part of this crust was formed during the CNS.

Magnetic anomalies from 34 (~84 Ma) are well identified in the Porcupine Abyssal Plain and initially formed as a continuous spreading ridge to the north and south (i.e. between North America and Eurasia) (Fig. 4). Magnetic anomalies between 25 and 13 (~56-33 Ma)

record the motion of the independent Porcupine plate relative to Eurasia (Srivastava and Tapscott, 1986; Srivastava and Roest, 1989; Müller and Roest, 1992). Spreading in the Porcupine Abyssal Plain was coincident with spreading in the Labrador Sea between Anomalies 34–13 (~84–33 Ma). After Anomaly 13 (~33 Ma), the Porcupine plate ceased its independent motion and spreading continued via North America–Eurasia motion.

We use the rotations of Srivastava and Roest (1989) for the initial rift phase between the Porcupine and North American Plate and incorporate the onset of break-up and seafloor spreading at 110 Ma (Müller et al., 1997), marked by a regional unconformity and dating of sediments at DSDP 550 (De Graciansky et al., 1985). We use our preferred rotations from Srivastava and Roest (1989) for the early spreading phase and the initiation of independent motion of the Porcupine Plate between Anomalies 25 and 13 (~56–33 Ma) (Fig. 4). This results in a small clockwise rotation of Eurasia and counterclockwise rotation of Iberia relative to the Porcupine Plate. The cessation of independent Porcupine motion coincides with the cessation of seafloor spreading in the neighboring Labrador Sea and the establishment of a simple two-plate system (North America and Eurasia) to describe the plate motions in the North Atlantic (Fig. 4). From Anomaly 13 (~33 Ma) onwards, we use the rotations of Lawver et al. (1990). A comparison with fracture zone traces and satellite gravity data reveals a slight mismatch due to the compression inferred from our model that is supported by the seafloor spreading fabric (Srivastava and Roest, 1996).

3.1.3.3. Rockall–North America/Greenland. The Rockall region in the North Atlantic encompasses spreading between the Rockall Plateau conjugate to North America along its southern arm and conjugate to Greenland along its northern arm (Fig. 3). A failed rift basin in the Rockall Trough exists adjacent to the Eurasian margin. Previous authors have determined that Rockall behaved as an independent plate throughout part of its history (Srivastava and Roest, 1989; Müller and Roest, 1992) but recent re-analysis of the magnetic anomalies and satellite gravity data can be explained by Eurasia–North America and Eurasia–Greenland motion (Gaina et al., 2002).

The Rockall Plateau underwent periods of extension in the early Triassic, early and mid-Jurassic and early, mid and late Cretaceous (Knott et al., 1993). The majority of rifting in the Rockall Trough occurred in the mid–late Cretaceous, continuing into the Eocene after an earlier Triassic–Jurassic rift phase (Cole and Peachey, 1999). Simultaneous rifting in the Porcupine Abyssal Plain occurred in the Cretaceous (Srivastava and Tapscott, 1986). Spreading between the Rockall Plateau and North America was established at ~83 Ma independent of the Eurasian plate according to the models of Srivastava and Roest (1989) and Müller and Roest (1992) or as part of the Eurasian plate from Anomaly 33 (~79 Ma) based on a reinterpretation of magnetic anomalies and fracture zone locations from satellite gravity data (Gaina et al., 2002) or 83 Ma according to Cole and Peachey (1999). Spreading propagated to the northwest into the Labrador Sea (Srivastava and Tapscott, 1986; Rowley and Lottes, 1988; Müller and Roest, 1992; Gaina et al., 2002).

The establishment of a three-plate system between North America, Eurasia/Rockall and Greenland occurred after Anomaly 25 (~56 Ma) (Srivastava and Tapscott, 1986; Rowley and Lottes, 1988; Gaina et al., 2002). After the cessation of spreading in the Labrador Sea, the system reorganized into a two-plate configuration with spreading between Rockall/Eurasia and Greenland along the Reykjanes Ridge (Srivastava and Tapscott, 1986) after Anomaly 13 (~33 Ma) to the present day (Fig. 3).

In constructing our model for spreading in the Rockall region, we separate the margin into two segments: Rockall Plateau/Eurasia relative to North America and Rockall Plateau/Eurasia relative to Greenland. Preceding the opening of the ocean basin between Rockall and North America, rifting occurred in the Rockall Trough (landward of the Rockall Plateau) in the mid–late Cretaceous, coincident with rifting in the Porcupine Basin to the south (Fig. 4). The main rift phase then jumped westward between the Rockall Plateau (fixed to Greenland) and North America at ~85 Ma (Gaina et al., 2002), similar to previous studies (Rowley and Lottes, 1988). We follow the plate boundaries in this area from Srivastava and Tapscott (1986) for the earliest part of its history. Rifting progressed to seafloor spreading by Chron 33o (~79 Ma) (Gaina et al., 2002) and propagated into the Labrador Sea (Gaina et al., 2002) (Fig. 4). We follow the plate reconstructions of Gaina et al. (2002) whereby spreading initiated between the Rockall Plateau and Greenland after Chron 25 forming a triple junction between the North American, Greenland and Eurasian plates (Fig. 4). As the pole of rotation describing Eurasia–North America motion accounts for the magnetic anomalies in the area, we do not incorporate motion between the Rockall Plateau and Eurasia, as proposed by other authors (Srivastava and Roest, 1989; Müller and Roest, 1992).

Seafloor spreading isochrons were constructed based on the magnetic anomaly identification and finite rotations of Gaina et al. (2002) and compared to the several magnetic anomaly datasets (Fig. 3). We find that there is generally good agreement between the gridded magnetic anomaly data and our seafloor spreading isochrons but find interpretation difficult proximal to the spreading axis. This may be due to the thermal influence of the Iceland hotspot on the mid-ocean ridge together with slow seafloor spreading rates. We find very good agreement between our fracture zone trends and those expressed in the satellite gravity data (Fig. 1).

3.1.3.4. Labrador Sea and Baffin Bay. The Labrador Sea is located between North America and Greenland south of Baffin Bay in the Canadian Arctic (Fig. 3). Continental stretching in the Labrador Sea produced a narrow and symmetrical margin with less than 100 km of extension (Dunbar and Sawyer, 1989) at around 130 Ma (Umpleby, 1979) based on the dating of pre to early syn-rift sediments. Rifting in the Labrador Sea is believed to have begun only after the initiation of seafloor spreading in the Rockall Trough (Srivastava and Tapscott, 1986).

The onset of seafloor spreading in the Labrador Sea is quite controversial. The oldest magnetic anomaly identified in the area is Anomaly 33 (~79 Ma) but spreading is believed to have initiated earlier during the CNS around 90–92 Ma (Rowley and Lottes, 1988; Roest and Srivastava, 1989; Gaina et al., 2002). An analysis of reprocessed seismic data (Chalmers, 1991; Chalmers and Laursen, 1995) suggests that seafloor spreading began much later at Anomaly 27 (~61 Ma) with thin continental crust extending into the region where older magnetic anomalies have been interpreted. However, this young age is inconsistent with the sedimentary–tectonic history of the basins around the Labrador Sea which record post-rift deposition and a phase of thermal subsidence around 100–62 Ma and fault block rotation between 80 and 63 Ma. Other estimates for the onset of seafloor spreading come from an analysis of global passive margins (Bradley, 2008), invoking an age of between 109 Ma and 68 Ma for the initiation of spreading.

An interpretation of seafloor spreading anomalies by Roest and Srivastava (1989) produced similar results to Srivastava and Tapscott (1986) except for a re-identification of Anomaly 25 (~56 Ma), which yielded a more symmetrical spreading system implying a significant change in spreading direction in the Labrador Sea. The change in spreading direction was linked to the initiation of the Greenland–Eurasia plate boundary and a change in spreading direction experienced in the Central and South Atlantic (Rowley and Lottes, 1988). Spreading is believed to have continued to Chron 7 (~25 Ma) (Rowley and Lottes, 1988) or just after Chron 13 (~33 Ma) (Roest and Srivastava, 1989; Gaina et al., 2002).

Northward propagation of the Labrador Sea rift into Baffin Bay through the Davis Strait (Fig. 3) has been dated to the late Aptian–

early Cenomanian (110–100 Ma) by the deposition of fluvial sediments during active rifting and occurred at least 20 Ma after the initiation of rifting in the Labrador Sea. Although there are no identifiable magnetic anomalies in Baffin Bay, seismic refraction profiles indicate that the area is floored by oceanic crust (Chalmers and Pulvertaft, 2001) and is predicted by the Labrador Sea opening model of Roest and Srivastava (1989). The cessation of seafloor spreading in Baffin Bay may have been coincident with the termination of spreading in the Labrador Sea.

For the Labrador Sea and Baffin Bay, we use a set of rotations that are based on the model presented in Roest and Srivastava (1989) and Gaina et al. (2002). We model continental extension starting at 135 Ma by extrapolation to match the Mesozoic basins on the North American and conjugate Greenland margin. We invoke seafloor spreading at Chron 33 (~79 Ma) and incorporate a major change in spreading direction between Chrons 31–25 (68–56 Ma), which was subsequently followed by oblique spreading and eventually cessation of spreading after Anomaly 13 (33 Ma) (Roest and Srivastava, 1989; Gaina et al., 2002) (Fig. 4). The extinct ridge matches well with a negative gravity anomaly observed in the satellite gravity data (Sandwell and Smith, 2009). We infer that the spreading axis in the Labrador Sea and Baffin Bay was joined across the Davis Strait via left-lateral transform faults (Rowley and Lottes, 1988; Roest and Srivastava, 1989) from 63 Ma. We model the cessation of spreading in Baffin Bay to be coincident with the Labrador Sea at 33 Ma (Fig. 4).

We use the magnetic anomaly identifications of Gaina et al. (2002) to construct seafloor spreading isochrons in the Labrador Sea. The magnetic lineations in this area are not well resolved (Fig. 3) and may be due to a combination of high sedimentation rates, spreading obliquity and data resolution. However, a continuation of magnetic lineations from the Rockall segment into the southern Labrador Sea (i.e. the expression of the triple junction) is clearly observed. Although we agree that oceanic crust floors Baffin Bay, no magnetic lineations can be resolved from the global gridded magnetic anomaly data (Figs. 3 and 5).

3.1.3.5. Greenland–Eurasia and Jan Mayen microcontinent. The separation of Greenland and Eurasia is occurring along the Reykjanes Ridge adjacent to the Rockall Plateau, through Iceland and along the Kolbeinsey and Mohns Ridge in the Norwegian and Greenland Seas (Figs. 3 and 5). The margin has undergone several rift phases since the Triassic primarily during the mid Jurassic–early Cretaceous and late Cretaceous–early Cenozoic (Brekke, 2000). The late Jurassic–early Cretaceous rift phase created most of the basin structures in the hydrocarbon-bearing MØre and VØring Basins, offshore Norway (Skogseid et al., 2000). The final rift phase at the Campanian–Maastrichtian boundary (~70 Ma) (Skogseid et al., 2000) was followed by volcanism (mid Paleocene to early Eocene) and finally to break-up and volcanism prior to Chron 25 (~56 Ma).

Traditionally, spreading between Greenland and Eurasia is modeled as a two-plate system with seafloor spreading initiating around 55–56 Ma, near the Paleocene–Eocene boundary (Talwani and Eldholm, 1977; Srivastava and Tapscott, 1986; Rowley and Lottes, 1988; Peron-Pinvidic et al., 2007). An updated interpretation including new geophysical data suggests that the system underwent several plate boundary changes since the inception of seafloor spreading around Anomaly 25 (~56 Ma) (Gaina et al., 2009). Fracture zone trends mark changes in spreading direction at Chron 21 (~47 Ma) and Chron 18 (~40 Ma) (Gaina et al., 2009). A major reorganization of the system occurred at Anomaly 13 (~33 Ma) with relative motion between Greenland and Eurasia migrating from NW–SE to NE–SW, leading to the cessation of spreading in the Labrador Sea, the amalgamation of Greenland with North America and the cessation of spreading in the Norway Basin.

Spreading in the Norway Basin (part of the Norwegian Sea) was initiated at 56 Ma isolating the Jan Mayen microcontinent (which was still fixed to Greenland) from the MØre and VØring Basin margins. Spreading along the extinct Aegir Ridge formed magnetic lineations (fan-shaped from Chron 21) in the Norway Basin until about Anomaly 13 (33–30 Ma) when the spreading ridge jumped westward, likely as a result of ridge–hotspot interactions and initiated spreading along the Kolbeinsey Ridge (Gaina et al., 2009). This is in contrast to a model of simultaneous spreading east and west of Jan Mayen at Anomaly 13 (~33 Ma), initiation of spreading along the Kolbeinsey Ridge at Anomaly 7 (~25 Ma) and cessation of spreading in the Norway basin at Anomaly 7 (~25 Ma) (Talwani and Eldholm, 1977; Nunns, 1983). Using new marine geophysical data, Gaina et al. (2009) suggest further complications in the rifting and spreading history of the Jan Mayen microcontinent and Faeroe Islands with numerous triple junctions and ridge propagators leading to significant continental stretching and the formation of rift-related basins. The Mohns Ridge was connected to the Aegir Ridge from the initiation of spreading at ~55–56 Ma until 30 Ma and the cessation of spreading in the Norway Basin. After the seaward ridge jump, the Mohns Ridge linked to the Kolbeinsey Ridge defining the boundary between Greenland and Eurasia.

We use a combination of magnetic anomaly picks and rotations from Gaina et al. (2002) and Gaina et al. (2009) to reconstruct the entire Greenland–Eurasia margin. We do not incorporate the complex spreading (triple junctions and ridge propagators) around the Jan Mayen microcontinent implied by the model of Gaina et al. (2009), but envisage that these will be incorporated in a further release. In our model, spreading initiates along the entire Greenland–Eurasia margin at 56 Ma, initially connecting up to the spreading in the Eurasian Basin to the north and the Greenland–Eurasia–North America triple junction in the south (Fig. 5). At 33 Ma, spreading between North America and Greenland in the Labrador Sea ceased fusing the two plates together, shutting down the Greenland–Eurasia–North America triple junction and leading to a change in spreading rate and direction along the Greenland–Eurasia spreading system. The Jan Mayen microcontinent rifted off the Norwegian margin at 56 Ma forming the fan-shaped Norway Basin along the Aegir Ridge between 56 and 33–30 Ma (Fig. 5). The Aegir Ridge connected to the Mohns Ridge in the north and Reykjanes Ridge in the south via a series of transform faults. Spreading then jumped to the Kolbeinsey Ridge at 30 Ma, connecting with the Mohns Ridge further north and forming the present day plate configuration (Fig. 5). A comparison between our resultant seafloor spreading isochrons and the magnetic anomaly grids reveals that our trends match quite well with the magnetic lineations from the gridded dataset.

3.1.3.6. Lomonosov Ridge–Eurasia (Eurasian Basin). The Eurasian Basin is the youngest ocean basin within the Arctic Ocean and was formed by spreading between the Lomonosov Ridge and the Barents Shelf along the Gakkel and Nansen Ridges (Fig. 5). The continental nature of the Lomonosov Ridge has been confirmed through seismic reflection imaging (Jokat et al., 1992) and ACEX drilling (Moran et al., 2006). The broad scale early rift phase mimics those of the North Atlantic margin but is less well constrained due to the remoteness of the region, data quality and persistent ice-coverage. Although the Barents Shelf is agreed to have formed part of the Eurasian margin, there is debate in the literature as to whether the Lomonosov Ridge has been fixed to the North American plate since at least 80 Ma (Srivastava and Tapscott, 1986; Rowley and Lottes, 1988) or whether it operated as an independent plate until at least Anomaly 13 (~33 Ma) (Jackson and Gunnarsson, 1990; Brozena et al., 2003). The lack of evidence for contemporaneous seafloor spreading in other parts of the Arctic Ocean and the good fit of the magnetic anomalies in the Eurasian Basin are cited as reasons for the Lomonosov Ridge being part of the North American Plate. However, a recent compilation of marine geophysical data identified a feature that resembles an extinct spreading ridge near the Lomonosov Ridge, which possibly connected spreading in the Eurasian Basin with spreading in the

Labrador Sea (Brozena et al., 2003), thus requiring independent motion of the Lomonosov Ridge.

The last rifting phase (late Cretaceous) led to break-up and seafloor spreading at 68 Ma (Rowley and Lottes, 1988) or around Anomaly 25 (~56 Ma) (Srivastava, 1985; Gaina et al., 2002) in the south around Svalbard and at 50 Ma in the Laptev Sea (Rowley and Lottes, 1988). There appears to be a consensus in early studies that the oldest magnetic anomaly that can be confidently identified is Anomaly 25–24 (~56–53 Ma) (Srivastava, 1985; Srivastava and Tapscott, 1986; Rowley and Lottes, 1988; Gaina et al., 2002), yet there is space landward of Anomalies 25–24 (~56–53 Ma) to suggest that seafloor spreading initiated earlier. The early spreading phase was the result of transtensional opening (Rowley and Lottes, 1988) producing slow seafloor spreading rates, strike-slip motion between Svalbard and Greenland (Srivastava and Tapscott, 1986) and displacement along the Nares Strait (Srivastava, 1985). After Chron 13 (33 Ma), true seafloor spreading was established coincident with the major reorganization of the Greenland–Eurasia system and cessation of Labrador Sea spreading. Currently, the Eurasian Basin is undergoing the slowest observed seafloor spreading rates, with a full rate of ~10–13 mm/yr.

We have used the magnetic anomaly picks and finite rotations of Gaina et al. (2002) to describe the opening of the Eurasian Basin from Anomaly 24 (~53 Ma) to the present day. The rotations used are the same as for North America–Eurasia. We incorporate the plate boundary model of Rowley and Lottes (1988) whereby the Gakkel and Nansen Ridges connect to the Baffin Bay ridge axis through the Nares Strait and Mohns Ridge via a major strike-slip fault with minor compression between Greenland and Svalbard (Fig. 5). In our interpretation, we couple the Lomonosov Ridge with North America as the rotations of Gaina et al. (2002) to describe North America–Eurasia motion do not result in overlap of the magnetic anomalies. The seafloor spreading isochrons we implement are digitized from Gaina et al. (2002) and match well with the magnetic anomaly grid (Fig. 5).

3.1.4. Arctic Basins

The Arctic Ocean encompasses the Eurasian and Amerasia Basins (divided into the Canada, Makarov and Podvodnikov Basins) as well as numerous continental blocks such as the Lomonosov, Mendeleev, Alpha, Northwind and Chukchi Ridges (Fig. 5). The Cenozoic Eurasian Basin (see Section 3.1.3.6: Eurasian Basin) has a distinct spreading history from the late Jurassic–Cretaceous Amerasia Basin. The early Mesozoic evolution of the Arctic region involves the closure of the South Anyui Basin along the North Siberian subduction zone, marked by the South Anyui suture (Nokleberg et al., 2001; Sokolov et al., 2002; Kuzmichev, 2009). This resulted in pre-breakup rifting in the earliest Jurassic, forming the Dinkum and Banks graben systems in Alaska and North America, respectively and the subsequent isolation of the Northwind and Chukchi Ridge by the earliest late Cretaceous (Grantz et al., 1998).

Rifting and opening of the Canada Basin is believed to have resulted from anticlockwise rotation of the North Slope Alaska–Chukotka Block away from the Canadian Arctic Islands, with a possible early strike-slip component, sometime from the late Jurassic to mid Cretaceous (Carey, 1955; Rowley and Lottes, 1988; Grantz et al., 1998; Alvey et al., 2008). Although the rotation model is supported by paleomagnetic data (Halgedahl and Jarrard, 1987), the fan-shaped nature of the magnetic lineations (Taylor et al., 1981) and crustal thickness mapping (Alvey et al., 2008), the exact timing of the rotation of Alaska and formation of the Canada Basin is debated. The dating of the magnetic anomalies in the Canada Basin is difficult due to extensive volcanic overprinting, low amplitude signature of the magnetic anomalies and high sedimentation rates. Anomalies M25–M11 (~154–132 Ma) have been tentatively identified (Taylor et al., 1981; Srivastava and Tapscott, 1986), but other magnetic anomaly interpretations are possible. An analysis of rift-related structures and stratigraphy (Grantz et al., 1998) reveals that the opening of the Canada Basin could have occurred as early as the late Jurassic–earliest Cretaceous. Less well-accepted models exist to explain the opening of the Canada Basin such as a non-rotational, step-wise late Jurassic–late Cretaceous opening model (Lane, 1997) and a model involving trapped crust from Kula–Pacific spreading (Churkin and Trexler, 1980).

Following the opening of the Canada Basin, Alvey et al. (2008) postulated that the Mendeleev and Alpha Ridges in the central Arctic formed either: (1) During continental rifting from the Canadian margin in the late Jurassic trapping Jurassic ocean floor in the Marakov/Podvodnikov Basin (Grantz et al., 1998); (2) During continental rifting from the Lomonosov Ridge forming the Marakov/Podvodnikov Basins during the late Cretaceous–mid Eocene (Alvey et al., 2008); (3) A hybrid model which includes an element of Jurassic ocean floor in the Podvodnikov Basin and a Cenozoic Marakov Basin (Alvey et al., 2008) or (4) The ridges formed purely via LIP emplacement related to the Iceland plume in the late Cretaceous (Forsyth et al., 1986; Lawver and Müller, 1994; Lawver et al., 2002; Jokat et al., 2003; Dove et al., 2010) overprinting old oceanic crust. Interpretations suggesting a Cenozoic age for the Marakov Basin match well with the identification of Anomalies 34–21 (~84–46 Ma; late Cretaceous–mid Eocene) (Taylor et al., 1981) as well as crustal thickness estimates (Alvey et al., 2008) in the Marakov Basin, but crustal thickness estimates postulate that the Podvodnikov Basin must be floored by older oceanic floor (Alvey et al., 2008). The volcanic nature of the Mendeleev and Alpha Ridges has been confirmed from recovered basalt samples of late Cretaceous age (Jokat et al., 2003), an age slightly younger than the predicted location of the Iceland plume around 130 Ma (Hauterivian/Berremian) (Lawver and Müller, 1994). However, this does not preclude a continental nature for the Mendeleev and Alpha Ridges. Subsequent to the opening of the Marakov/Podvodnikov Basins, the locus of spreading jumped to the Eurasian Basin at ~56 Ma, forming the youngest piece of ocean floor in the Arctic domain.

We have incorporated a model whereby initial rifting occurred between the North American and Alaskan margins in the early Jurassic (~210–200 Ma) followed by the isolation of the Northwind and Chukchi Ridges by the earliest late Cretaceous, triggered by the subduction of the Anyui Ocean. We invoke a simple counterclockwise rotational model for the opening of the Canada Basin whereby the North Slope of Alaska starts to rotate at 145 Ma (latest Jurassic) with seafloor spreading initiating at 142 Ma (Berriasian), with a much lower spreading rate in the south due to its proximity to the pole of rotation, creating fan-shaped anomalies. The timing is consistent with paleomagnetic data from Alaska but is inconsistent with previous magnetic anomaly interpretations (Taylor et al., 1981; Srivastava and Tapscott, 1986). Cessation of spreading in the Canada Basin and rotation of North Slope occurred at 118 Ma, coincident with a change in the southern North Slope margin from largely strike-slip to convergence due to a change in spreading direction in Panthalassa. We use the finite rotations and seafloor spreading isochrons from Model 1 presented in Alvey et al. (2008), however we modify the isochrons to extend the interpretation of the Canada Basin over the Alpha Ridge and into the Marakov Basin. The isochrons are not constrained by magnetic anomaly identifications but rather are a synthetic interpretation of the timing and orientation of spreading based on the rotation of the North Slope of Alaska. Hence, we do not expect an exact correlation with the magnetic anomaly grid.

The preferred model presented in Alvey et al. (2008) based on crustal thickness estimates, invokes Cenozoic spreading in the Marakov Basin. We do not incorporate a younger Marakov Basin as this would require either a short-lived subduction zone along either the Lomonosov or Mendeleev Ridge during the opening of this basin for which there is no geological evidence. Instead, we suggest that the Alpha and Mendeleev Ridges are predominately LIP-related features associated with the Iceland plume that overprinted the Canada

Basin in the early Cretaceous (Lawver and Müller, 1994) and not part of a rifted Cenozoic continental margin. In our model the Makarov and parts of the Podvodnikov Basin form the northern extent of the Canada Basin. We do agree with Alvey et al. (2008) that there may be a trapped piece of Jurassic ocean floor from the Anyui Basin in the Podvodnikov Basin, which would explain the anomalous crustal thickness and would provide a mechanism for the Mendeleev Ridge having some continental affinities as continental material may have been isolated during Jurassic rifting.

3.2. Pacific Ocean and Panthalassa

Present day seafloor spreading in the Pacific basin involves nine oceanic plates: the Pacific, Antarctic, Nazca, Cocos and Juan De Fuca plates and the smaller Rivera, Galapagos, Easter and Juan Fernandez microplates along the East Pacific Rise (Bird, 2003) (Fig. 1). Additionally, the Pacific basin seafloor spreading record preserves clear evidence that several now extinct plates (e.g. Farallon, Phoenix, Izanagi, Kula, Aluk and Bauer plates) existed within the Pacific and proto-Pacific basin (Panthalassa) since at least the Jurassic/Cretaceous. In addition, the onshore geological record from the Pacific margins provides evidence for the opening and closure of several marginal basins, particularly along the western North American margin.

Previous plate tectonic models of the Pacific have largely focused on identifying magnetic lineations and deriving relative plate motions between presently active plates where both sides of the spreading ridge are preserved (e.g. Juan De Fuca–Pacific spreading (Atwater, 1970, 1990; Engebretson et al., 1985; Caress et al., 1988; Stock and Molnar, 1988; Wilson, 1988; Atwater and Severinghaus, 1990), Pacific–Antarctic spreading (Stock and Molnar, 1987; Cande et al., 1998; Larter et al., 2002), the east Pacific Rise (Cande et al., 1982; Tebbens and Cande, 1997) and Cocos and Nazca spreading (Wilson, 1996)). Other plate tectonic models have focused on identifying magnetic lineations in the older parts of the Pacific, particularly the north and western Pacific, where conjugate magnetic lineations no longer exist as they have been subducted (e.g. Kula–Pacific (Rea and Dixon, 1983; Engebretson et al., 1985; Lonsdale, 1988; Mammerickx and Sharman, 1988; Atwater, 1990), Izanagi–Pacific (Larson et al., 1972; Woods and Davies, 1982; Sager and Pringle, 1987; Handschumacher et al., 1988; Sager et al., 1988; Nakanishi et al., 1992; Nakanishi and Winterer, 1998), Farallon–Pacific (Atwater, 1970, 1990; Engebretson et al., 1985; Caress et al., 1988; Stock and Molnar, 1988; Wilson, 1988; Atwater and Severinghaus, 1989), Phoenix–Pacific spreading (Stock and Molnar, 1987; Cande et al., 1998; Sutherland and Hollis, 2001; Larson et al., 2002; Larter et al., 2002; Viso et al., 2005) and the plates related to the break-up of the Ontong Java–Hikurangi–Manihiki Plateaus (Taylor, 2006)). Beyond this, few studies have attempted to derive relative plate rotation models of these now vanished plates (e.g. Engebretson et al., 1985; Stock and Molnar, 1988) to establish a longer tectonic history of the Pacific plate where minimal or no information about the seafloor spreading record exists.

Another common approach to constrain plate tectonic models of the Pacific has been through the interpretation of the onshore geology, in particular examining anomalous volcanism and geochemistry associated with ridge subduction, crustal shortening rates and events, accretion of exotic terranes, ophiolite emplacement, large-scale crustal deformation and massive sulfide and other subduction related ore-deposit formation (e.g. Bradley et al., 1993; Haeussler et al., 1995; Madsen et al., 2006; Sun et al., 2007). This information is sometimes translated into a schematic representation of past plate configurations based purely on the onshore record but these plate reconstruction schematics are often only snapshots in time rather than evolving and are not quantitatively derived through the seafloor spreading record. Nevertheless, they are helpful in developing conceptual models for the evolution of now vanished ocean crust.

Engebretson et al. (1985) presented a quantitative plate kinematic model of the seafloor spreading record focused on the northern Pacific basin for the past 180 Ma and is currently the most comprehensive and often cited study on Pacific plate reconstructions. This study enabled subsequent authors to place their regional tectonic reconstructions and geological observations into a Pacific-wide tectonic framework. The model of Engebretson et al. (1985) is based on an absolute reference frame using fixed Atlantic and fixed Pacific hotspots (Morgan, 1972) with relative plate motions for the Pacific, Farallon, Izanagi, Kula and Phoenix plates determined by computing the displacements of each plate relative to the absolute reference frame rather than via plate circuit closure as is commonly used. Since the publication of Engebretson et al. (1985), additional data acquisition, updated interpretations and more accurate magnetic anomaly timescales have been published, providing improved constraints on the Izanagi–Pacific, Phoenix–Pacific, Farallon–Phoenix and Pacific–Antarctic ridges.

The Pacific triangle is an area of the western Pacific where three Mesozoic magnetic lineation sets (Japanese, Hawaiian and Phoenix lineations) intersect (Fig. 6), recording the birth of the Pacific plate from three "parents": the Farallon, Izanagi and Phoenix plates. The evolution of the three parent plates has influenced the development of subsequent seafloor spreading systems in the Pacific. The northwestern (Japanese) lineations represent spreading between the Pacific and Izanagi plates and young towards the west–northwest, the easternmost (Hawaiian) lineations represent spreading between the Pacific and Farallon plates and young towards the east and the southernmost (Phoenix) lineations represent spreading between the Pacific and Phoenix plates and young towards the south (Atwater, 1990; Nakanishi et al., 1992) (Fig. 6). These three plates radiated out from the emerging Pacific plate during the Mesozoic and existed prior to the establishment of the Pacific plate in a simple ridge–ridge–ridge configuration. We will present an assessment of the Pacific and Panthalassa by describing each parent plate with their associated children.

3.2.1. Izanagi plate

The M-sequence Japanese magnetic lineation set found in the westernmost Pacific represents the last preserved fragments of a westward-younging Jurassic–Cretaceous spreading system (Fig. 6). Early reconstructions of the area linked the Japanese lineation set to the younger, Cenozoic seafloor spreading history of the Pacific–Kula ridge (Larson et al., 1972). To reconcile the geometry of the preserved NE–SW trending Japanese lineations with the E–W trending Cenozoic lineations formed by Pacific–Kula spreading, Woods and Davies (1982) introduced the idea of an independent Izanagi plate, although some models still prefer a single Kula plate (Norton, 2007). Due to progressive subduction since the Mesozoic, the entire crust that floored the Izanagi plate as well as the portion of the Pacific plate recording the death of the Izanagi has been lost, leaving behind only the Mesozoic fragment of the Pacific plate. This complicates reconstructions as few present day constraints exist to tie down tectonic parameters for the evolution of the area. Additionally, there are no constraints on the history of the Izanagi plate prior to the birth of the Pacific plate.

Magnetic anomalies M33–M0 (~158–120 Ma) of the Japanese lineation set have been confidently identified in the northwest Pacific (Sager and Pringle, 1988; Handschumacher et al., 1988; Sager et al., 1988; Atwater, 1989; Nakanishi et al., 1992; Nakanishi and Winterer, 1998). A recent deep-tow magnetometer survey over the Pigafetta Basin in the vicinity of ODP drill site 801C revealed a low amplitude magnetic anomaly sequence extending to M44 (~170 Ma), within the Jurassic Quiet Zone (Tivey et al., 2006) with Anomaly M42 (~168 Ma) corresponding to the location of ODP drill site 801C (Tominaga et al., 2008). Previous interpretations infer the oldest crust in the Pacific to be 175 Ma (Engebretson et al., 1985; Müller et al., 1997) based on

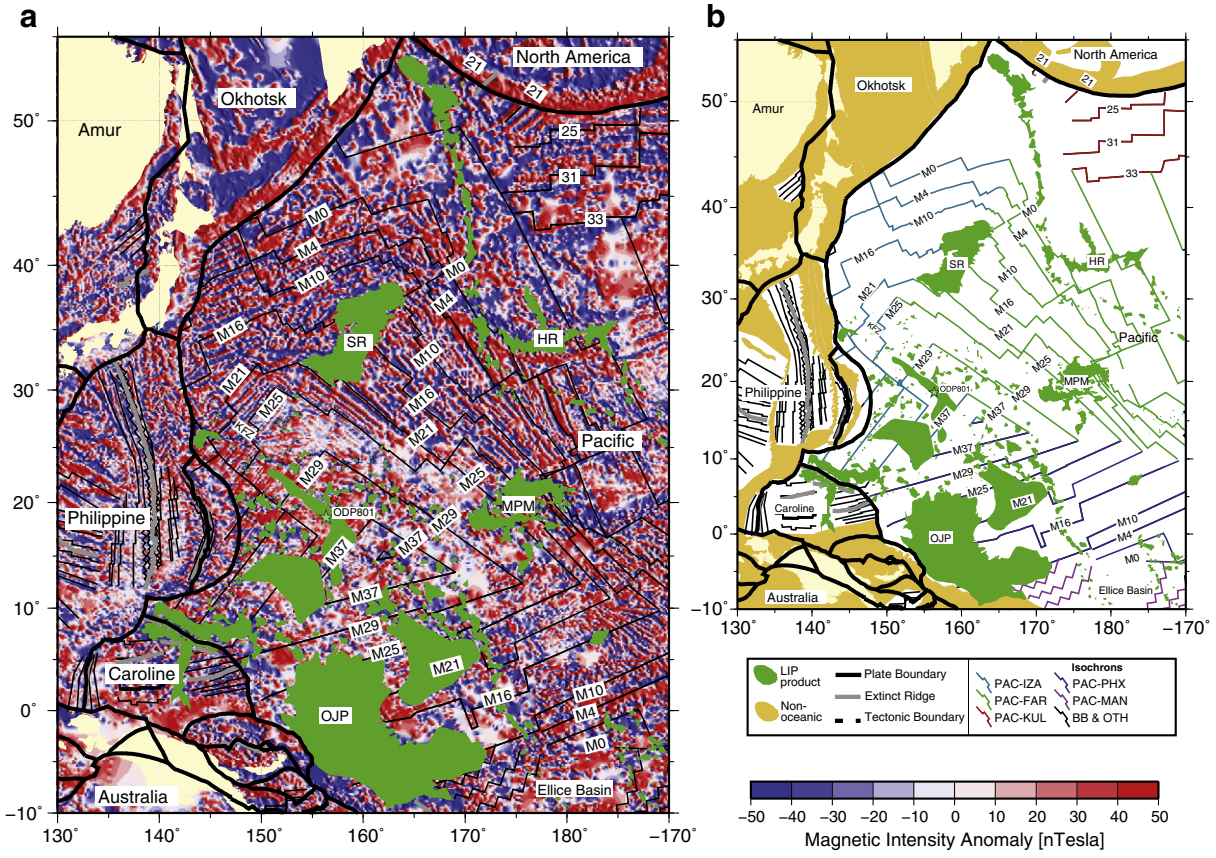

Fig. 6. (a) Gridded magnetic anomalies for the Western Pacific, based on isotropic gridding of a combination of public domain and in-house data. Seafloor spreading isochrons used in this study plotted as thin black lines. Numbers correspond to magnetic anomaly chron. HR = Hess Rise, OJP = Ontong Java Plateau, SR = Shatsky Rise. (b) Seafloor spreading isochron map colored by spreading system or plate pair. Legend abbreviations are: BB = Back-arc Basins, FAR = Farallon, IZA = Izanagi, KUL = Kula, MAN = Manihiki, OTH = Other spreading systems outside area of interest, PAC = Pacific, PHX = Phoenix.

interpolation to the center of the Pacific triangle, but this age appears to be inconsistent with the recent dating of magnetic anomalies and the dating from ODP site 801C, which is located ~750 km from the inferred center of the Pacific triangle. After the initiation of spreading between the Pacific and Izanagi plates, the ridge underwent some instability with one or more proposed ridge jumps postulated to explain the anomalously large distance between the adjacent isochrons along a spreading corridor between M33 and 29 (~158–156 Ma) (Sager et al., 1998). Analysis of the magnetic anomalies and seafloor fabric flanking this proposed ridge jump has not found an abandoned spreading center. Spreading continued with relatively high seafloor spreading rates between M29 and 25 (~156-154 Ma) (Nakanishi et al., 1992) before decreasing to average rates until M21 (~147 Ma).

The fracture zone pattern observed in the satellite gravity data and mapped via ship track data (Sager et al., 1988; Nakanishi and Winterer, 1998; Sager et al., 1998) indicates a large 24° clockwise rotation of the Izanagi plate relative to the Pacific at M21 (~147 Ma) (Sager et al., 1999), particularly evident along the Kashima Fracture Zone near the Izu-Bonin–Mariana trench (Fig. 6). The change in spreading direction from NW–SE to NNW–SSE coincides with the eruption of the Shatsky Rise at the Izanagi–Farallon–Pacific triple junction (Nakanishi et al., 1999; Sager et al., 1999) followed by the progressive reorganization and migration of the triple junction center for a period of about 2 million years. The period between Anomalies M21 and 20 (~147–145 Ma) also corresponds to changes in spreading rate and direction in the Pacific, Atlantic and Indian Oceans (Sager et al., 1988; Nakanishi et al., 1999). The youngest identified Japanese lineation corresponds to M0 (~120 Ma) (Nakanishi et al., 1999; Sager et al., 1999; Tominaga and Sager, 2010) trending similar to the post-M20 (~145 Ma) lineations (Fig. 6). This would suggest no measured change in spreading direction between at least 145–120 Ma. The oceanic crust to the north of M0 (~120 Ma) is inferred to have formed during the CNS and represents the youngest preserved oceanic lithosphere associated with Izanagi–Pacific spreading.

Previous interpretations have tied the cessation of spreading between the Pacific and Izanagi plates to the onset of spreading between the Kula and Pacific plates (Engebretson et al., 1985), sometime between 83.5 and 70 Ma (Lonsdale, 1988; Atwater, 1989) (see Section 3.2.2.1: Kula plate). In these models, the orientation of the Izanagi–Pacific ridge is depicted as a side-stepping E–W oriented ridge perpendicular to the East Asian margin. As the oldest discernable Japanese magnetic lineation is oriented NE–SW, an E–W oriented mid-ocean ridge requires a major change in spreading direction post-M0 (~120 Ma). However, there are no fracture zones present in the post-Mesozoic crust of the NW Pacific to suggest a major change in spreading direction during the CNS (Fig. 1).

An alternative approach to constrain the orientation and cessation of the Izanagi–Pacific ridge is through an analysis of the onshore geological record in east Asia together with the preserved seafloor spreading record in the NW Pacific (Whittaker et al., 2007; Seton et al., in preparation). The younging northwestward sequence of magnetic lineations and the presence of Indian-type mantle geochemical signatures in various volcanic arcs of the northwest Pacific (Straub et al., 2009) indicate a ridge subducted under east Asia at some time in the past. Whittaker et al. (2007) assumed no change in spreading direction of the Pacific–Izanagi from M0 (~120 Ma) onwards as there is no evidence for a major change in spreading direction post-M0 (~120 Ma) resulting in the mid ocean ridge intersecting the east Asian margin in a subparallel fashion. The timing for the intersection of the ridge with the

margin forming a slab window can be constrained through a number of geological observations from Japan and Korea. The geology in southern and central Japan records a pulse of volcanism and anomalous heatflow measurements (Agar et al., 1989; DiTullio, 1993; Sakaguchi, 1996; Lewis and Byrne, 2001) indicative of the presence of a slab window in the late Cretaceous-early Cenozoic. The cessation of granitic plutonism in Korea suggests that subduction was terminated along east Asia around 60–50 Ma (Sagong et al., 2005). In addition, seismic tomography profiles across east Asia reveal a break in the continuity of slab material in the mid-mantle (Seton et al., in preparation) possibility indicating the subduction of a mid-ocean ridge and slab break-off event. Based on this model, the cessation of spreading between the Izanagi and Pacific plates (i.e. the death of the Izanagi plate) occurred around 55–50 Ma followed by the complete subduction of the Izanagi plate along the East Asian margin by 40 Ma. In this model, the cessation of spreading between the Izanagi and Pacific plate is not correlated with the initiation of spreading in the Kula plate, as suggested by previous studies.

We model the Mesozoic–early Cenozoic evolution of the Izanagi plate using constraints still preserved on the Pacific plate. We define the onset of spreading between the Pacific and Izanagi plates to 190 Ma, 15–20 million years earlier than previous interpretations. We base our age estimation, which is a maximum age, on the following:

(1) The location of the oldest identified magnetic anomaly, M44 (~170 Ma) (Tivey et al., 2006) is over 750 km from the inferred center of the Pacific triangle
(2) ODP site 801C, which lies within M42 (~168 Ma) is consistent with the dating of microfossils overlying pillow basalts (Lancelot et al., 1990; Tivey et al., 2006)
(3) An extrapolation of intermediate seafloor spreading rates (~30–40 mm/yr) from the location of M44 to the center of the Pacific triangle suggests an approximate age to be closer to around 190 Ma.
(4) A younger age for the initiation of seafloor spreading between the Izanagi–Pacific, Farallon–Pacific and Phoenix–Pacific would require anomalously high spreading rates or substantial spreading asymmetry. This cannot be discounted as Tominaga et al. (2008) suggest a rapid spreading rate of ~75 mm/yr. Therefore, we believe an age of 190 Ma for the birth of the Pacific plate is a maximum age.

We have incorporated the Japanese magnetic lineations and fracture zones of Sager et al. (1988) and Nakanishi et al. (1999) together with fracture zone traces based on satellite gravity anomaly data (Sandwell and Smith, 2009) to define the seafloor spreading history between the Izanagi and Pacific plates. Our resultant seafloor spreading isochrons match well with the magnetic lineations seen in our magnetic anomaly grid from M25 (~154 Ma) onwards when the magnetic anomaly signature is strongest (Fig. 6). Magnetic lineations prior to M25 (~154 Ma) have larger variability (Tominaga and Sager, 2010) and are not observed in our magnetic anomaly grid (Fig. 6) (see Tominaga and Sager, 2010 for details). The ridge jump prior to M26 (~155 Ma) postulated by Sager et al. (1998) has not been incorporated as we were unable to identify magnetic lineations or an abandoned ridge. In addition, the conjugate ridge flank is absent.

We incorporate the major 24° clockwise change in spreading direction at M21 (~147 Ma) (Sager et al., 1988) primarily constrained via the Kashima Fracture Zone which shows continuity from at least M28–M10 (~156–130 Ma) (Fig. 6). This major change in spreading direction is coincident with the eruption of the southern-end of the Shatsky Rise at the Farallon–Izanagi–Pacific triple junction followed by triple junction instability. According to the model of Sager et al. (1988) two simultaneous triple junctions and at least nine small, short-lived ridge jumps occurred at the Pacific–Farallon–Izanagi junction. This led to an 800 km northeast jump in the triple junction center clearly observed in the gridded magnetic anomaly dataset between M21 (~147 Ma) and M16 (~138 Ma) (Fig. 6). Due to the complexity of the triple junction solutions and the lack of preserved data between the Izanagi and Farallon plates, we incorporate a simple model whereby the Pacific–Izanagi–Farallon triple junction remains in a ridge–ridge–ridge configuration during its entire history. As the instability of this triple junction is believed to have existed for only 2 million years (Sager et al., 1999), we believe that our assumption is reasonable and follows the broad scale development of the area.

The fracture zones in the westernmost Pacific do not show a major change in trend after M20 (~146 Ma) (Fig. 6). No discernable fracture zone trends after M0 indicate the direction of motion during the CNS hence we assume that no change in the direction of motion occurred from M20 to the CNS and use a fixed stage rotation pole for this entire period. As much of the evidence for the late Cretaceous–early Cenozoic history of the Izanagi plate has been lost due to subduction along the east Asian margin, we assume no major change in spreading rate, direction and accretion from M0 (last dated anomaly, ~120 Ma) to the cessation of spreading along the Izanagi–Pacific ridge.

Finite rotations were computed for Izanagi–Pacific spreading using the half-stage pole method and assuming spreading symmetry and rely heavily on fracture zone traces for direction of motion. For younger times when no preserved crust exists, we assume an intermediate full spreading rate of ~80 mm/yr (similar to the spreading rate in the late Cretaceous), spreading symmetry and a consistent spreading direction to model the position of the mid-ocean ridge. We find that this results in the Pacific–Izanagi ridge intersecting the east Asian margin around 55–50 Ma in a sub-parallel orientation and is consistent with geological and seismic tomography observations, as explained in Seton et al. (in preparation). Our model suggests that spreading continued along the Pacific–Izanagi ridge after the establishment of the Kula–Pacific ridge to the east, contrary to most previous models. The preserved seafloor spreading record in the regions adjacent to the Pacific–Izanagi ridge preserves no evidence to suggest a readjustment of the plate driving forces due to the merging of two major plates (i.e. the death of the Izanagi plate) prior to 55 Ma. Instead, we find that spreading between the Kula and Pacific plates underwent a major change in spreading rate and direction at Anomaly 24 (~55–53 Ma), which resulted in a dramatic doubling of the spreading rate of the Kula plate and a counter-clockwise change in spreading direction from largely N–S to NW–SE. Our model is in stark contrast to the prevailing models for the Izanagi–Pacific and Kula–Pacific ridges, but our interpretation is kinematically self-consistent, matches geological observations and can be linked to the subduction history as seen in seismic tomography (Seton et al., in preparation).

The birth of the Izanagi plate is far more uncertain. The Izanagi plate must have existed prior to the birth of the Pacific plate as part of a three-plate ridge–ridge–ridge triple junction with the Farallon and Phoenix plates, based on the rules of triple junction closure. However, there is no crust preserved in the seafloor spreading record reflecting this early history as it has been progressively subducted under the east Asian margin. We model a simple geometry whereby the spreading direction between the Izanagi–Farallon plates is constrained by the oldest Pacific–Izanagi and Pacific–Farallon isochrons via triple junction closure, intermediate spreading rates and spreading symmetry. We constructed the positions of the spreading ridges by computing small circle arcs between Izanagi–Pacific, Farallon–Pacific and Phoenix–Pacific spreading. The spreading direction between the Izanagi and Phoenix plates is similarly constrained using triple junction closure between the Pacific–Izanagi and Pacific–Phoenix plates and the length of the spreading ridges determined by intersection with the Pacific margins.

3.2.2. Farallon plate

Early mapping of magnetic lineations in the western Pacific identified a set of NW–SE trending Mesozoic magnetic lineations loosely

bounded by the Shatsky and Hess Rises and the Mid Pacific Mountains (Figs. 6 and 7). These lineations, termed the Hawaiian lineations, formed during NE–SW directed spreading between the Pacific and now extinct Farallon plate between at least M29–M0 (~156–120 Ma) (Larson et al., 1972; Atwater and Severinghaus, 1990). The Mesozoic oceanic crust on the Farallon plate subducted under North America beginning in the late Mesozoic (Bunge and Grand, 2000) and clearly imaged as seismically fast material under central and eastern North America (Bunge and Grand, 2000; Liu et al., 2010). The Hawaiian lineations show a clockwise change in spreading direction at M11 (~133 Ma) (Sager et al., 1988; Atwater and Severinghaus, 1990) with no major change in spreading direction during the early history of Pacific–Farallon spreading due to the uniformity of the magnetic lineations (Fig. 6) even though fracture zone traces prior to M25 (~154 Ma) are absent (Fig. 1). The pole of rotation to describe Mesozoic spreading was likely located in the south or equatorial Pacific due to the slightly fan-shaped nature of the lineations (Figs. 6 and 7).

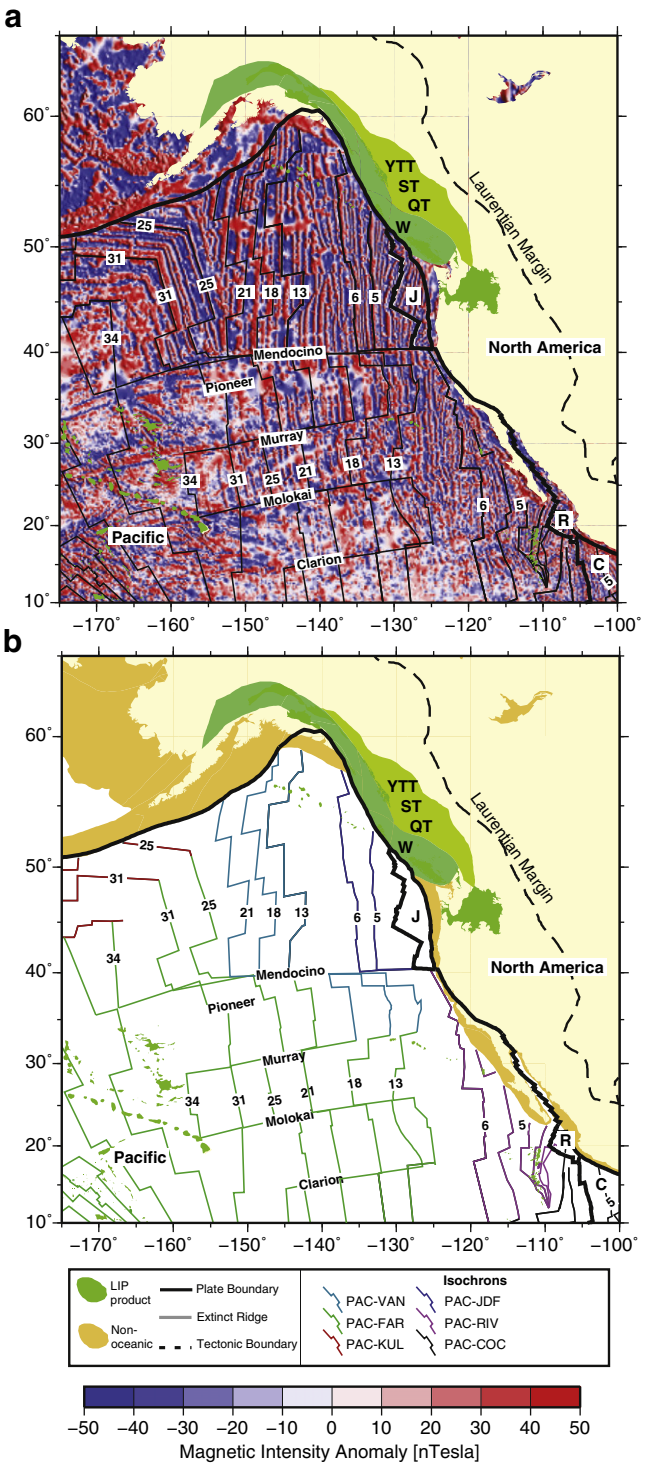

Fig. 7. (a) Gridded magnetic anomalies for the northeast Pacific. Seafloor spreading isochrons used in this study plotted as thin black lines. Numbers correspond to magnetic anomaly chron. QT = Quesnellia Terrane, ST = Stikinia Arc, W = Wrangellia, YTT = Yukon/Tanana Terrane. (b) Seafloor spreading isochron map colored by spreading system or plate pair. Map abbreviations are same as a. Legend abbreviations are: COC = Cocos, FAR = Farallon, JDF = Juan De Fuca, KUL = Kula, PAC = Pacific, R = Rivera/Guadalope, VAN = Vancouver.

The Hawaiian lineations form a magnetic bight with the Japanese lineation set in the north and trace the Pacific–Farallon–Izanagi triple junction (Fig. 6). The Shatsky Rise erupted along the triple junction center between M21 and 19 (~147–143 Ma), as confirmed by ODP leg 198 (Mahoney et al., 2005) either as a result of a mantle plume head reaching the surface or decompression melting at a mid-ocean ridge (Mahoney et al., 2005; Sager, 2005). The eruption of the Shatsky Rise was coincident with an 800 km, nine-stage jump in the location of the triple junction during which time the triple junction switched between ridge–ridge–ridge and ridge–ridge–transform configurations (Nakanishi et al., 1999). The triple junction regained its stability after the initial eruptive phase followed by waning volcanism forming the Papanin Ridge along the triple junction center until M1 (~121–124 Ma) (Nakanishi et al., 1999).

In the south, the Hawaiian lineations disappear beneath the Mid-Pacific Mountains obscuring the trace of the Pacific–Farallon–Phoenix triple junction. Further east, the Hawaiian lineations form a complex junction with several discrete fan-shaped lineation sets (e.g. Magellan and Mid-Pacific Mountain lineation sets) (Tamaki and Larson, 1988) characteristic of crust that formed during microplate formation at fast-spreading triple junction centers. These fan-shaped lineations were active between M15 and M1 (~138–121 Ma). In addition, a set of short ENE–WSW trending lineations south of the Mid-Pacific Mountains has been identified as M21 (~147 Ma) to M14 (~136 Ma) (Nakanishi and Winterer, 1998) and is suggested to have formed between the Phoenix plate and the postulated Trinidad plate.

East of the M-anomalies is a wide zone of crust which formed during the CNS. Indicators of spreading direction are observed in the prominent Mendocino, Pioneer, Murray, Molokai and Clarion fracture zones (Figs. 1 and 7). The Mendocino, Molokai and Clarion fracture zones record two clear changes in spreading direction: one between M0 and the middle of the CNS (Granot et al., 2009) and another clockwise change to almost E–W trending sometime towards the end of the CNS (Atwater, 1989; Searle et al., 1993b). No clearer indication of timing has been established. The isochrons that bound the beginning and end of the CNS in this region cannot be restored without significant misfit along length. Atwater et al. (1993), therefore proposed that spreading asymmetry and/or a series of ridge jumps must have occurred during the CNS between smaller segment of the ocean floor bounding the two isochrons. The Hess, Liliuokalani and Sculpin ridges were suggested as possible remnants of this early spreading history, whereas others suggest that they were instead related to the formation of the Hess Rise (Hillier, 2007). Oceanic crust that formed by Pacific–Farallon spreading during the CNS has also been identified in the central–south Pacific, east of the Manihiki Rise suggesting that the Pacific–Farallon ridge propagated southward after the Mesozoic (Fig. 8).

The Cenozoic lineations record five major episodes of break-up of the Farallon plate including the formation of the Kula, Vancouver, Cocos, Nazca and Juan De Fuca plates (Fig. 8) and extend almost the entire length of the eastern Pacific Ocean. In the northeast Pacific, the lineations are some of the best-mapped in the world, as observed in the magnetic grid compilation (Fig. 7). Spreading appears simple for the early Cenozoic with progressive complexity approaching the

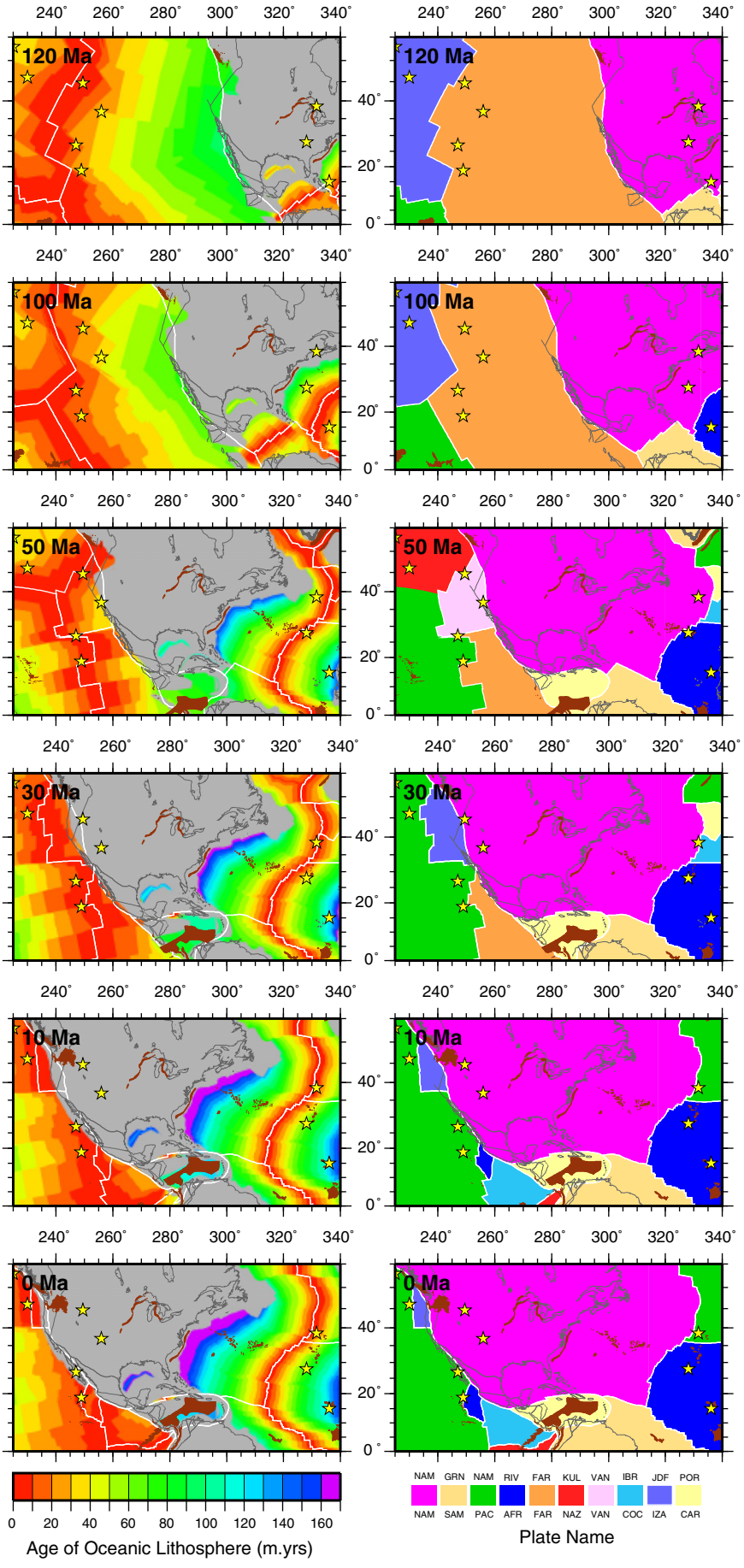
120 Ma
100 Ma
50 Ma
30 Ma
10 Ma
0 Ma
240° 260° 280° 300° 320° 340°
40° 20° 0°
0 20 40 60 80 100 120 140 160
Age of Oceanic Lithosphere (m.yrs)
NAM GRN NAM RIV FAR KUL VAN IBR JDF POR
NAM SAM PAC AFR FAR NAZ VAN COC IZA CAR
Plate Name

trench. The most prominent bend observed in all fracture zones in the northeast Pacific occurred just prior to Chron 33 (~79 Ma) where spreading changed from roughly E–W to ENE–WSW (Atwater et al., 1993). Atwater et al. (1993) suggested that the inferred continuity of the spreading system provides evidence of a simple two-plate system during this time, negating the need for microplate formation (e.g. Chinook plate). Anomaly 33 (~79 Ma) corresponds to the oldest clearly identified magnetic anomaly related to Pacific–Kula spreading (Lonsdale, 1988; Atwater, 1989) (see Section 3.2.2.1: Kula plate), marking the minimum timing for the initial break-up of the Farallon plate. Spreading was reasonably steady between Chrons 32–24 (~71–53 Ma), connecting with spreading along the Kula–Pacific ridge to the north at the Great Magnetic Bight (Fig. 7). Anomaly 24 (~55–53 Ma; late Paleocene–early Eocene) corresponds to a major hemisphere-wide plate reorganization event and is manifested in a 20° clockwise change in spreading direction between the Pacific and Farallon plates from WSW–ENE to E–W (Atwater, 1989), a change in spreading direction between Pacific–Kula plates (Lonsdale, 1988) and the break-up of the Farallon plate into the Vancouver plate at either Chron 24 (~55–53 Ma) (Atwater, 1989) or 23 (~51–52 Ma) (Menard, 1978; Rosa and Molnar, 1988) (Fig. 8). The break-up of the Farallon plate occurred in between the Pioneer and Murray fracture zones (Atwater, 1989) (Fig. 7) with oblique compression and slow relative motion (Rosa and Molnar, 1988). At this time, the mid-ocean ridge was located proximal to the subduction zone and was followed by a period of complex spreading and/or spreading instability forming a “disturbed zone” between Anomalies 19–12 (~41–31 Ma) (Atwater, 1989). Another major change in spreading direction is evident in the seafloor spreading record between the Murray and Pioneer fracture zones at Anomaly 10 (~28 Ma), forming the Monterey and Arguello plates (Atwater, 1989). South of the Murray fracture zone, the Guadalupe plate formed between Anomalies 7 and 5 (~25-10 Ma) (Mammerickx and Klitgord, 1982; Atwater, 1989). These plates formed progressively as transform faults intersected with the Farallon subduction zone. After Chron 10 (~28 Ma), the Vancouver plate is often referred to as the Juan De Fuca plate, coinciding with the establishment of the San Andreas fault no earlier than 30 Ma (Atwater, 1970) (Fig. 8).

Spreading between the Pacific and Farallon plates during the Mesozoic occurred in the region conjugate to the North American margin. However, starting in the CNS, the Pacific–Farallon spreading extended southward as far south as the Eltanin fracture zone in the South Pacific (Figs. 7 and 9). Magnetic anomalies 34 (~84 Ma) to 6 (~20 Ma) on the Pacific plate associated with Pacific–Farallon spreading conjugate to the South American margin have been identified (Herron, 1972; Cande et al., 1982; Mayes et al., 1990). This is restricted to Anomalies 23–6 (~52–20 Ma) on the Nazca plate (Cande and Haxby, 1991). Seafloor spreading between Anomalies 34–21 (~84–47 Ma) was reasonably stable until a major reorganization of the spreading system at Chron 21 (~47 Ma), observed in fracture zone trends in the South Pacific (Mayes et al., 1990). The cessation of spreading between the Pacific and Farallon plates occurred during break up into the Cocos and Nazca plates at 23 Ma (see Section 3.2.2.3: Nazca and Cocos plates).

Our model for spreading between the Pacific and Farallon plates incorporates spreading initiation at 190 Ma, based on the evidence presented earlier in the manuscript (see Section 3.2.1: Izanagi plate), even though the oldest Hawaiian lineation identified is M29 (~156 Ma). The model we have implemented closely follows that of Atwater and Severinghaus (1990). We use their seafloor spreading isochrons, with adjustments based on Nakanishi et al. (1992), for the Mesozoic lineations. Our resultant seafloor spreading isochrons match well with our magnetic anomaly grid (Figs. 6 and 7) in the north and central sections of the Mesozoic lineations but fail to account for the fan-shaped lineations in the south. This is a direct consequence of our decision to exclude the reconstruction of numerous microplates at the Pacific–Farallon–Phoenix triple junction (e.g. Magellan, Mid-Pacific Mountains and Trinidad lineation sets) and instead focus our model the broad-scale development of the area. To the north, the Hawaiian Mesozoic lineations show a clear magnetic bight with the Japanese lineations (Figs. 6 and 7), highlighting the geometric stability of the Pacific–Izanagi–Farallon triple junction from M29 to M22 (~156–148 Ma). A major clockwise change in spreading direction is recorded in the Japanese lineations and fracture zones at M21 (~147 Ma) leading to a period of instability of the Pacific–Izanagi–Farallon triple junction (see Section 3.2.1: Izanagi plate). Interestingly, this does not correspond to an adjustment of the Pacific–Farallon relative plate motion suggesting that the adjustment was related to the Shatsky Rise rather than a regional or global plate reorganization.

Finite rotations for the Pacific–Farallon ridge were derived using the half-stage pole method with an assumption of spreading symmetry and average spreading rates. Reconstruction of the Pacific–Izanagi–Farallon, Pacific–Phoenix–Farallon and Pacific–Kula–Farallon triple junctions additionally followed the principles of triple junction closure. Although ridge jumps have been proposed for early CNS spreading (Atwater et al., 1993), we have followed a simple model of seafloor spreading throughout the CNS as we cannot identify remnant features describing the proposed ridge jumps without access to high-resolution multibeam bathymetry data. Towards the end of the CNS, constraining the precise timing of the change in spreading direction observed in the Mendocino, Molokai and Clarion fracture zones is difficult. We extrapolate using the Müller et al. (2008a) model and suggest that a change in spreading direction between the Pacific and Farallon plates occurred at 103 Ma, closely corresponding with the observed bend in Pacific hotspots at ~99 Ma, implied by Veevers (2000) and Wessel and Kroenke (2008), based on an updated seamount dataset.

The Shatsky Rise formed at the Izanagi–Farallon–Pacific triple junction and as a consequence, part of the Shatsky Rise must have erupted onto the Farallon and Izanagi plates. We have modeled the conjugate Shatsky Rise (Farallon) and find that it intersects the North American margin at 90 Ma, correlating well with the onset of the Laramide Orogeny in western North America and a shallow seismically fast region underlying western North America (Liu et al., 2010). As the geological evidence and seismic tomography images are independent of the plate reconstructions used, our assumption of largely symmetrical seafloor spreading and average spreading rates between Pacific–Farallon appears to be reasonable.

After the CNS, we model seafloor spreading based on Atwater and Severinghaus (1990) for the northeast Pacific but without small-scale ridge adjustments associated with plate break-up events (Fig. 8). We concur with the interpretation of Atwater et al. (1993) that the most notable change in spreading direction observed in all northeast Pacific fracture zones occurred at Chron 33 (~79 Ma). This timing corresponds to our initiation of seafloor spreading between the Kula and Pacific plates and establishment of the Pacific–Kula–Farallon triple junction (see Section 3.2.2.1: Kula plate) (Fig. 8). Further southward, the

Fig. 8. (a) Agegrid reconstructions of the northeast Pacific at 120, 100, 50, 30, 10, 0 Ma highlighting the age–area distribution of oceanic lithosphere at the time of formation and the extent of continental crust (gray polygons). Plate boundaries from our continuously closing plate polygon dataset are denoted as thick white lines, hotspot locations as yellow stars, large igneous provinces and flood basalts as brown polygons and coastlines as thin black lines. (b) Reconstructions showing the outlines of the plates in the northeast Pacific for each reconstruction time listed above. Feature descriptions as in panel (a). Abbreviations are: AFR = African plate, CAR = Caribbean plate, COC = Cocos plate, EUR = Eurasian plate, FAR = Farallon plate, GRN = Greenland plate, IBR = Iberian plate, IZA = Izanagi plate, JDF = Juan de Fuca plate, KUL = Kula plate, NAM = North American plate, NAZ = Nazca plate, PAC = Pacific plate, POR = Porcupine plate, RIV = Rivera plate, SAM = South American plate, VAN = Vancouver plate. (For interpretation of the references to color in this figure legend, the reader is referred to the web version of this article.)

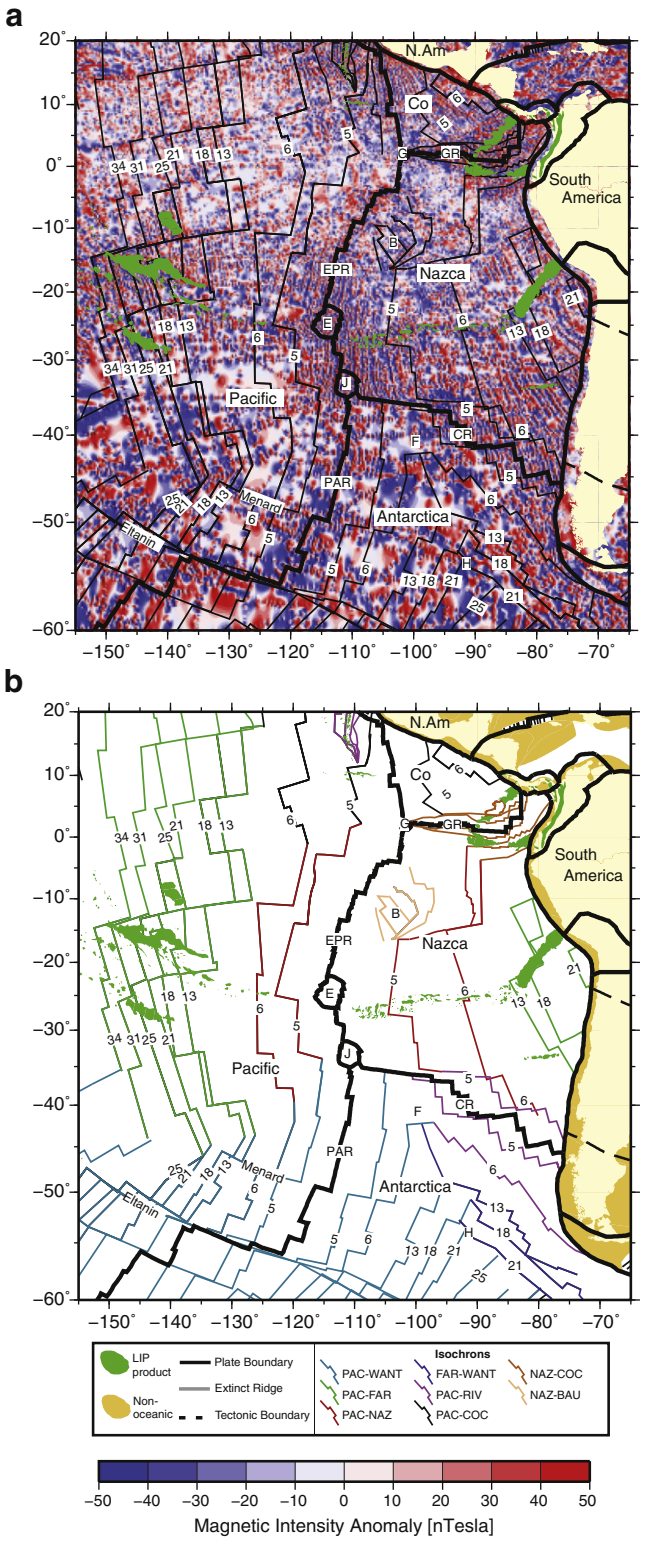

Fig. 9. (a) Gridded magnetic anomalies for the southeast Pacific. Seafloor spreading isochrons used in this study plotted as thin black lines. Numbers correspond to magnetic anomaly chron. B = Bauer Microplate, CR = Chile Ridge, E = Easter Microplate, EPR = East Pacific Rise, F = Friday Microplate, G = Galapagos Microplate, GR = Galapagos Ridge, J = Juan Fernandez Microplate, PAR = Pacific–Antarctic Ridge. (b) Seafloor spreading isochron map colored by spreading system or plate pair. Map abbreviations are same as a. Legend abbreviations are: BAU = Bauer, COC = Cocos, FAR = Farallon, NAZ = Nazca, PAC = Pacific, RIV = Rivera/Guadalope, WANT = West Antarctica/Antarctica.

Pacific–Farallon ridge extended to the Eltanin fracture zone and Pacific–Farallon–Antarctic triple junction. Spreading along the Pacific–Antarctic and Farallon–Antarctic ridges initiated at Chron 34 (~83.5 Ma) (see Section 3.2.3.1: Pacific–Antarctic spreading). Our model for the southeast Pacific is similar to that of Mayes et al. (1990) with no major change in spreading rate between Anomalies 33 and 21 (~79–47 Ma) followed by a change in spreading direction after Chron 21 (~47 Ma), recorded in the fracture zones in the South Pacific particularly along the Eltanin fracture zone. At this time, the Pacific–Farallon spreading ridge extended further southward, connecting up with spreading associated with the Aluk Plate.

The break-up of the Farallon plate into the Vancouver plate at Chron 24 (~53 Ma) (Atwater, 1989) resulted in minor relative motion along the Pioneer fracture zone (Figs. 7 and 8). Our finite rotations to describe Pacific–Vancouver spreading are taken from Müller et al. (1997). As the Pacific–Farallon ridge approached the North American subduction zone, spreading became more complex with the formation of numerous microplates, ridge jump and propagation events. Our model incorporates the Vancouver and Juan De Fuca plates (Fig. 8) but excludes the other proposed microplates, such as the Monterey, Arguello and Guadalupe plates, as no published poles of rotation to describe their history are available. Spreading between the Pacific and Farallon plates ceased in the area to the west of South and Central America at 23 Ma (Chron 6B) as the plate separated into the Cocos and Nazca plates.

3.2.2.1. Kula plate. The existence of the Kula plate during the late Cretaceous to the Paleocene/Eocene has been known since the early identification of northward younging, E–W trending magnetic anomalies in the northern Pacific (Rea and Dixon, 1983; Lonsdale, 1988; Mammerickx and Sharman, 1988; Atwater, 1990) (Fig. 7). These magnetic anomalies, located north of the Chinook Trough, represent only the southern (Pacific) flank of Kula–Pacific spreading, the remainder having been subducted beneath the Aleutian trench. The initiation of the Pacific–Kula ridge occurred within the Farallon plate and marks the first stage of Farallon plate break-up. Additionally, prevailing models of the Pacific (e.g. Engebretson et al., 1985) imply that cessation of spreading along the Izanagi–Pacific ridge preceded the establishment of the Pacific–Kula Ridge, therefore suggesting that Pacific–Izanagi and Pacific–Kula spreading was not simultaneous. This assumption has implications for the formation of the northern Pacific and plate driving forces in the area.

The oldest well recognized magnetic anomaly associated with Kula–Pacific spreading is either Anomaly 31 (~68 Ma) or possibly 32 (~71 Ma) (Rea and Dixon, 1983; Lonsdale, 1988) although some authors interpret Anomaly 33 (~79 Ma) (Mammerickx and Sharman, 1988) and tentatively Anomaly 34 (~83.5 Ma) (Atwater, 1990; Norton, 2007). The conventional view is that after the death of the Izanagi plate, the locus of rifting and spreading jumped eastward to the Chinook Trough where E–W trending magnetic lineations formed via simple Kula–Pacific spreading. However, Rea and Dixon (1983) postulated that two spreading ridges formed along existing Pacific–Farallon fracture zones after a change in spreading direction at ~83.5 Ma forming a second plate, the Chinook plate, south of the Chinook Trough.

The Stalemate Fracture Zone delineates the western extent of the Kula plate (Fig. 6) and tracks the motion of the Kula plate from N–S adjacent to Anomalies 34/31 (83.5–71 Ma) to 25 (~56 Ma) to NW from Anomalies 24 (~55–53 Ma) to 20/19 (~44–41 Ma). Additionally, Lonsdale (1988) interpreted an extinct spreading ridge adjacent to Anomalies 20/19 (~44–41 Ma) as well as a short sequence of Anomalies 21–20 (47–44 Ma) on the western side of this extinct ridge. The study of Lonsdale (1988) therefore suggests a spreading history for the Kula plate involving N–S spreading from 32 to 25 (~71–56 Ma) followed by a major change in plate motion by 20–25° at Chron 24 (~55–53 Ma). The cessation of spreading along the Pacific–

Kula ridge was initially believed to have occurred at Chron 25 (~56 Ma) (Byrne, 1979) and later to 43–47 Ma corresponding to the major Pacific plate reorganization event (Engebretson et al., 1985). The identification of an extinct spreading ridge in the far northwest corner of the plate by Lonsdale (1988) further refined the cessation of spreading to around Chron 18 (~40 Ma). However, the identification of this ridge was based on a small number of ship tracks and seismic profiles.

To the east, the Kula plate is delineated by the Great Magnetic Bight, which traces the Pacific–Kula-Farallon triple junction in a ridge–ridge–ridge configuration from Chron 34/31 (~84–71 Ma) to 25 (~56 Ma) (Fig. 7). This is followed by a "T" anomaly corresponding to Chron 24 (55–53 Ma), which likely formed during a reorganization of the Pacific–Kula–Farallon triple junction (Lonsdale, 1988; Atwater, 1990).

The Great Magnetic Bight traces the location of the Kula–Farallon–Pacific triple junction (Figs. 7 and 8). Previous models have predicted the location and orientation of the resultant Kula–Farallon ridge (for which there is no preserved evidence in the seafloor spreading record) based on triple junction closure and tracking evidence of a slab window beneath western North American margin (e.g. Engebretson et al., 1985; Atwater, 1990; Breitsprecher et al., 2003; Madsen et al., 2006). Most models lead to a reasonably consistent result of a NE–SW trending spreading ridge intersecting the North American margin and forming a slab window somewhere near the present-day Pacific Northwest (Engebretson et al., 1985; Atwater, 1990; Breitsprecher et al., 2003; Madsen et al., 2006).

Our interpretation for the Kula plate closely follows the model of Lonsdale (1988). However, we have interpreted Anomaly 33 (~79 Ma) north of the Chinook Trough as the oldest identified magnetic anomaly based on the interpretation in Atwater (1990) and our own analysis of the magnetic anomalies in the area. Most authors have only been able to interpret anomalies back to 32 (~71 Ma) as it is the last clearly identified magnetic anomaly, however the new gridded magnetic anomaly datasets such as WDMAM, EMAG2 and our own gridded compilation (Figs. 6–7) show E–W trending magnetic lineations south of Anomaly 32 (~71 Ma). There is space south of our interpreted Anomaly 33 (~79 Ma) to accommodate a very small portion of older crust (possibly back to Anomaly 34 (~84 Ma)), but we believe that the establishment of the stable Pacific–Kula–Farallon triple junction in a ridge–ridge–ridge configuration must have occurred at 33 (~79 Ma) and not earlier. Importantly, our model has contemporaneous Pacific–Izanagi and Pacific–Kula spreading (see Section 3.2.1: Izanagi plate) joined by a NNW–SSE transform. In our model, we have continuing N–S directed Pacific–Kula spreading until Anomaly 25 (~56 Ma) followed by an anticlockwise change in spreading direction starting at Anomaly 24 (~55–53 Ma), as suggested by Lonsdale (1988) and expressed in the Stalemate Fracture Zone. The magnetic anomaly grids clearly show the NE–SW trending magnetic lineations corresponding to the youngest part of Pacific–Kula spreading (Fig. 6). We follow the interpretation of Lonsdale (1988) for the cessation of Pacific–Kula spreading to be around 41–40 Ma. We compute finite rotations based on the half-stage pole method between Chrons 33–22 (~79–49 Ma) as only the Pacific flank of the spreading system is preserved. We use the magnetic lineations of Lonsdale (1988) and the Stalemate Fracture Zone to compute finite rotations between Chrons 21–20 (~47–44 Ma) using the traditional method.

The factor leading to the abrupt change in plate motion between the Kula and Pacific plates was suggested to be a result of the temporary elimination of northward slab pull when subduction shifted from the Siberian margin to the Aleutian Trench (Lonsdale, 1988). In our model, we argue that the subduction of the Izanagi–Pacific ridge at 55–50 Ma resulted in the temporary cessation of subduction and slab break-off along the east Asian margin leading to a change in motion of the Kula plate to the northwest. The intersection of the Pacific–Izanagi ridge with subduction under East Asia eliminated the ridge push force thus enabling the Kula plate to move to the west. The change in spreading direction in the Kula plate identified by Lonsdale (1988) matches with the change in the Pacific plate driven by the subduction of the Izanagi ridge (see Section 3.2.1: Izanagi plate) and changes that were occurring along the Pacific–Farallon spreading system (see Section 3.2.2: Farallon plate).

To the east, we model the Kula–Farallon ridge based on triple junction closure and the finite difference method resulting in a stable NE–SW orientation of the Kula–Farallon ridge, consistent with previous studies. The Yellowstone hotspot located offshore the North American margin in the Paleocene/Eocene (Fig. 8) was used as a further constraint to guide the position of the NE–SW trending Kula–Farallon ridge, as mid-ocean ridges are known to preferentially evolve near hotspots (Müller et al., 1998b). As a result our modeled position of the Kula–Farallon ridge with respect to the North American margin correlates with onshore geological and geochemical evidence of a northward migrating slab window near the northern US/Canadian margin (Atwater, 1990; Breitsprecher et al., 2003; Madsen et al., 2006). Additionally, our position of the Kula–Farallon ridge is supported by seismic tomography (Bunge and Grand, 2000).

3.2.2.2. Vancouver/Juan De Fuca plate. The recognition of a difference in trend by about 11° between the fracture zones north of the Murray fracture zone in the northeast Pacific and those to the south (Fig. 1), led Menard (1978) to suggest that the Farallon plate broke into two plates around 47–49 Ma Ma (Chrons 22–21). Menard (1978) termed the new plate north of the Murray Fracture Zone, the Vancouver plate. Differential motion between the Vancouver and Farallon plate was confirmed and dated to Chron 21 (~47 Ma) with the spacing of magnetic anomalies in the area between the Murray and Pioneer fracture zone possibly indicating either asymmetric spreading or a ridge jump between Anomalies 21 (~47 Ma) and 13 (~33 Ma) (Rosa and Molnar, 1988). The model of Rosa and Molnar (1988) implies slow transpressional motion across the plate boundary, which lies between the Murray and Pioneer fracture zones as a "set of curving, tooth-like disjunctures" (Atwater, 1990) clearly seen between Anomalies 19 and 13 (~41–33 Ma) (Fig. 7) possibly indicative of diffuse deformation.

The intersection of the Murray transform fault with the North American subduction zone around 30 Ma led to the establishment of the San Andreas Fault and corresponds to the establishment of the Juan De Fuca plate at the expense of the Vancouver plate. The spreading history of the Juan De Fuca plate is very complex (Wilson et al., 1984; Wilson, 1988) most likely due to its proximity to the Cascadia subduction zone. Spreading involved counter-clockwise motion followed by progressive clockwise rotation starting at Chron 5D (~17 Ma) (Atwater, 1990) and a series of propagating rifts and microplate formation (Wilson et al., 1984; Wilson, 1988). Currently, the Juan De Fuca plate is limited at its southern end by the Mendocino Fracture Zone and is subducting slowly along the Cascadia subduction zone (Fig. 7).

Our reconstructions of the Vancouver/Juan De Fuca plates are largely based on the detailed tectonic maps of Atwater and Severinghaus (1990) unchanged from the model used by Müller et al. (1997). We implement the break-up of the Farallon plate into the Farallon and Vancouver plates along the Pioneer Fracture Zone at Chron 22 (~50–49 Ma) (Fig. 8). We use the finite rotations from Müller et al. (1997) for the Vancouver plate and the rotations in this study for the Farallon plate. Our rotations result in transpressional motion along the transform fault connecting the Farallon and Vancouver plates. The Juan de Fuca plate is modeled as a simple two-plate system and we do not include the detailed interpretation of Wilson (1988) as there are no rotations associated with the isochrons making it difficult to incorporate into our tectonic model. On the broad scale, our seafloor spreading isochrons match well with the magnetic lineations from our magnetic grid compilation (Fig. 7),

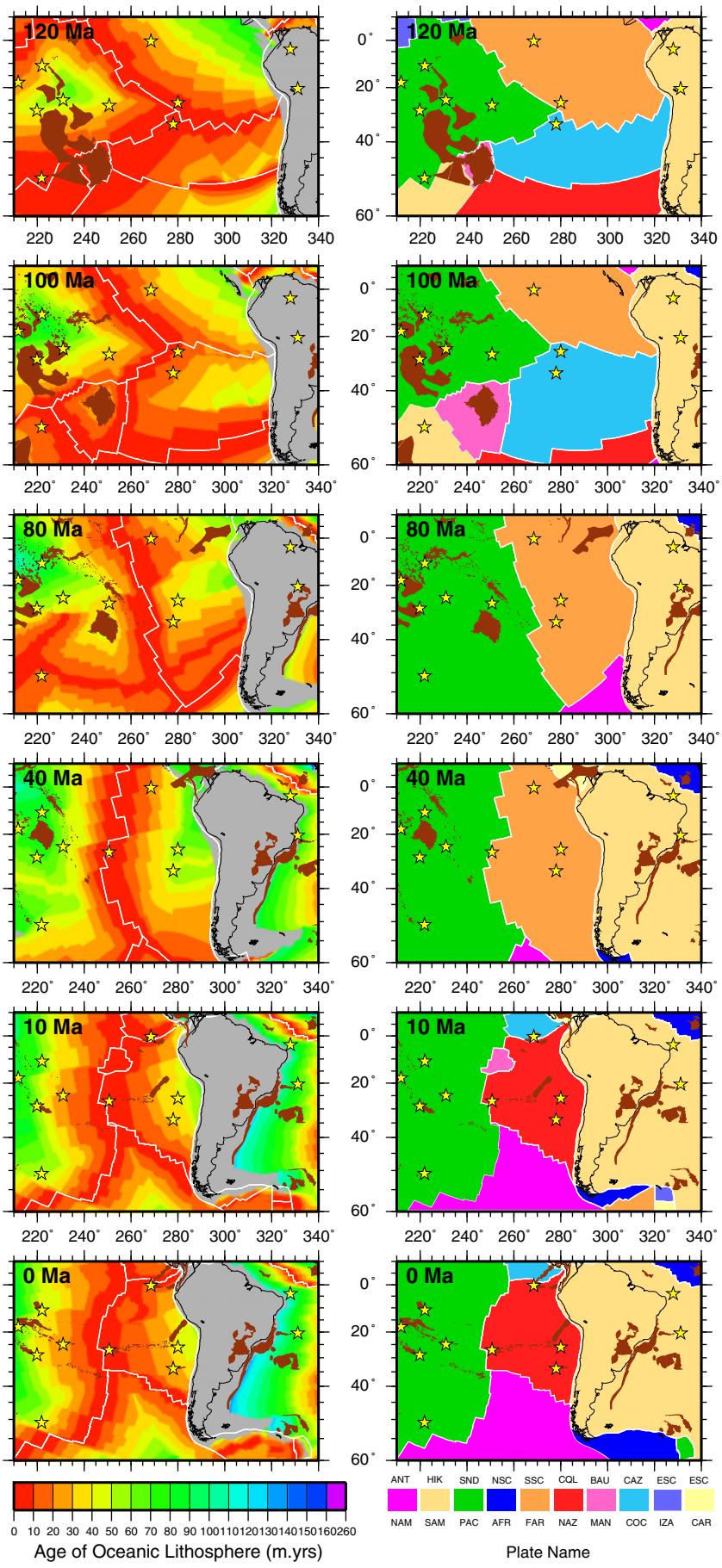
120 Ma
100 Ma
80 Ma
40 Ma
10 Ma
0 Ma
220 240 260 280 300 320 340
0 20 40 60
0 10 20 30 40 50 60 70 80 90 100 110 120 130 140 150 160 260
Age of Oceanic Lithosphere (m.yrs)
ANT HIK SND NSC SSC CQL BAU CAZ ESC ESC
NAM SAM PAC AFR FAR NAZ MAN COC IZA CAR
Plate Name

however there are some inconsistencies, particularly approaching the trench as we do not include small scale block rotations.

3.2.2.3. Nazca and Cocos plates. The East Pacific Rise is currently the site of very fast seafloor spreading between the Pacific and Nazca and Cocos plates and dominates the seafloor of the SE Pacific (Fig. 9). Other active seafloor spreading ridges are the Chile Ridge (active spreading between the Nazca and Antarctic plates) and the Galapagos Spreading Centre Nazca–Cocos spreading) (Fig. 9). The Nazca plate incorporates oceanic crust that formed as a result of Pacific–Nazca, Pacific–Farallon, Nazca–Cocos and Nazca–Antarctic spreading as well as the Bauer microplate (Fig. 9). The Cocos plate includes oceanic crust that formed as a result of Cocos–Pacific and Cocos–Nazca as well as spreading in the Rivera and Mathematician microplates.

Both the Nazca and Cocos plates formed as a result of the break-up of the southern part of the Farallon plate at approximately 23 Ma (Hey, 1977; Lonsdale, 2005) or Chron 6By (~23 Ma) (Barckhausen et al., 2008). The break-up of the Farallon plate is believed to have been driven by a combination of increased northward pull after the earlier break-up of the Farallon plate to the north (Lonsdale, 2005), an increase in slab pull at the Middle America subduction zone due to an increase in its length (Lonsdale, 2005) and/or the weakening of the plate along the point of break-up due to the influence of the Galapagos hotspot (Hey, 1977; Lonsdale, 2005; Barckhausen et al., 2008). In addition, plate break-up was preceded by a major plate reorganization in the Southeast Pacific at 24 Ma leading to a change in motion of the Farallon plate 1–2 million years before break-up (Tebbens and Cande, 1997; Lonsdale, 2005; Barckhausen et al., 2008). Although the Nazca and Cocos plates are now independent plates, an interpretation of their history must consider the evolution of the Farallon plate (see Section 3.2.2: Farallon plate) to understand the nature of the oceanic lithosphere in this region older than 23 Ma.

The oldest portion of the Nazca plate, adjacent to the South American margin includes the crust that formed due to Farallon–Pacific spreading. Magnetic anomalies up to Anomaly 23 (~51 Ma) have been tentatively identified on the Nazca plate (Cande and Haxby, 1991) but most models confidently identify magnetic anomalies only back to Anomaly 13 (~33 Ma) (Handschumacher, 1976; Pardo-Casas and Molnar, 1987; Tebbens and Cande, 1997). Pardo-Cassas and Molnar (1987) and Rosa and Molnar (1988) computed finite rotations and their uncertainties to describe the motion of Pacific–Farallon spreading by assuming symmetrical spreading where both flanks were not presently preserved. These rotations were used as a basis for the rotation model of Tebbens and Cande (1997) for the Nazca–Pacific–Antarctic triple junction. A South Pacific-wide study by Mayes et al. (1990) computed rotations for the Pacific–Farallon and Pacific–Nazca ridges.

The crust that formed between the Pacific–Nazca plates subsequent to plate break-up at 23 Ma has a complex spreading history. Spreading occurred as a northward "step-wise triple junction migration" (see Tebbens and Cande, 1997 for a description of this process) between the Pacific–Nazca–Antarctic ridges, leaving behind a record of ridge jumps and microcontinent formation particularly at Anomalies 6 (~20 Ma) and 5A (~12 Ma) (Tebbens and Cande, 1997) including the Friday microplate south of the Chile Fracture Zone (Fig. 9). This complexity in the spreading pattern has hindered the interpretation of magnetic anomalies post-Oligocene. Although most of the crust created during this spreading phase is preserved in the present day record, it has been suggested that isolated sections of Nazca–Pacific spreading have been captured by the Cocos plate to the north and subsequently subducted under the Middle America trench (Tebbens and Cande, 1997). Finite rotations and their uncertainties to describe the post break-up phase of Nazca–Pacific and Nazca–Antarctic motion were computed using a combination of the Hellinger technique (Tebbens and Cande, 1997), existing rotations (Pardo-Casas and Molnar, 1987) and the interpretation of South Pacific magnetic anomalies (Mayes et al. 1990).

A major component of the seafloor spreading history of the Nazca plate involves the formation of the Bauer Microplate (Fig. 9). The Bauer microplate formed along the northern East Pacific Rise and grew by crustal accretion and counter-clockwise rotation between Pacific and Nazca spreading (Goff and Cochran, 1996; Eakins and Lonsdale, 2003) shortly after a major plate reorganization event at 20 Ma (Fig. 9). The formation of the Bauer microplate is unlike the step-wise triple junction migration models used to explain the formation of the microplates associated with the Pacific–Nazca–Antarctic triple junction. Spreading is believed to have initiated at 17 Ma via northward propagation of the East Pacific Rise and southward propagation of the Galapagos Rise during counter clockwise rotation of the spreading axes (Eakins and Lonsdale, 2003). Rotation and spreading continued about a pole proximal to the spreading axis creating fan-shaped anomalies until 6 Ma when the spreading ridge realigned with the dominant East Pacific Rise spreading ridge and the Bauer microplate was captured by the Nazca plate (Eakins and Lonsdale, 2003) (Fig. 10).

The other smaller microplates within the Nazca/Cocos/Pacific realm are the presently active Easter and Juan Fernandez microplates, which form small pseudo-circular plates along the actively spreading East Pacific Rise. These plates are believed to have become active at around Chron 3o (~5 Ma) during a major plate reorganization event in the SE Pacific (Tebbens and Cande, 1997) and have rotated about an axis close to the center of the plate by between 80 and 90° (Searle et al., 1993a). The mechanism for the formation of these plates is believed to be the same process responsible for the development of the Hudson and Friday microplates related to the northward migrating Nazca–Pacific–Antarctic ridge (Bird et al., 1998).

To the north, the Cocos–Pacific spreading ridge was only established in its present form from Chron 2A (~3 Ma) (Atwater, 1990). Between 23 Ma and Chron 2A (~3 Ma), spreading was being accommodated along the Mathematician and Rivera Ridges to the north and the Cocos–Pacific to the south (Atwater, 1990; Eakins and Lonsdale, 2003). Spreading in this area included many block rotations and ridge jumps possibly due to the proximity of the Cocos–Pacific spreading center to the Middle America trench and Galapagos hotspot. The magnetic lineations that formed due to Cocos–Pacific spreading are fan-shaped with strongly curved fracture zones observed in the satellite gravity anomalies indicating a pole of rotation close to the northern end of the plate (Figs. 1 and 9).

The present day Cocos–Nazca ridge strides the Galapagos hotspot and intersects the Middle America convergent margin at the Bulboa Fracture Zone (Fig. 9). This E–W directed spreading ridge was established around 23 Ma, coinciding with the break-up of the Farallon plate. The early spreading history is quite complex, requiring several ridge jumps during its formation (Barckhausen et al., 2008), the most significant of which is the Malpelo Ridge, which became extinct around 15–10 Ma (Meschede et al., 1998a). In addition, numerous

Fig. 10. (left) Agegrid reconstructions of the southeast Pacific at 120, 100, 80, 40, 10, 0 Ma highlighting the age–area distribution of oceanic lithosphere at the time of formation and the extent of continental crust (gray polygons). Plate boundaries from our continuously closing plate polygon dataset are denoted as thick white lines, hotspot locations as yellow stars, large igneous provinces and flood basalts as brown polygons and coastlines as thin black lines. (right) Reconstructions showing the outlines of the plates in the southeast Pacific for each reconstruction time listed above. Feature descriptions as in panel (left). Abbreviations are: AFR = African plate, ANT = Antarctic plate, BAU = Bauer plate, CAR = Caribbean plate, CAZ = Chasca plate, COC = Cocos plate, CQL = Catquil plate, ESC = East Scotia Sea plate, FAR = Farallon plate, HIK = Hikurangi plate, IZA = Izanagi plate, MAN = Manihiki plate, NAM = North American plate, NAZ = Nazca plate, NSC = North Scotia Sea plate, PAC = Pacific plate, SAM = South American plate, SND = Sandwich plate, SSC = South Scotia Sea plate. (For interpretation of the references to color in this figure legend, the reader is referred to the web version of this article.)

pseudo-faults indicating rift propagation to the east have been identified in the seafloor fabric, the majority in the vicinity of the Galapagos hotspot (Atwater, 1990). Further complications occur close to the Middle America trench where several ridge jumps have isolated spreading systems, particularly in the Panama Basin (Lonsdale and Klitgord, 1978).

We incorporate the magnetic anomaly identifications from Munschy et al. (1996) to derive a set of finite rotations and seafloor spreading isochrons between the Pacific and Nazca plates and also extend our analysis to include the parts of Pacific–Farallon spreading that are currently preserved on the Nazca plate. The magnetic anomaly identifications of Munschy et al. (1996) do not extend to the easternmost Nazca plate where we would expect to find the oldest preserved oceanic lithosphere corresponding to Pacific–Farallon spreading, mainly due to a lack of data and signal intensity. Instead, we predict the age of the oceanic lithosphere in this area by reconstructing the conjugate Pacific–Nazca isochrons. We find that the resultant location of isochrons closely corresponds to the interpretation of magnetic anomalies from Cande and Haxby (1991) and matches well with the magnetic lineations observed on our magnetic anomaly grid (Fig. 9). Thus, our model predicts that the oldest ocean floor off South America corresponds to Anomaly 23 (~51 Ma) (Fig. 10). We derive a new set of finite rotations to describe Pacific–Nazca spreading largely based on the rotations of Mayes et al. (1990) to be consistent with our magnetic pick compilation. We do not incorporate the detailed triple junction migration model of Tebbens and Cande (1997).

The seafloor spreading model we implement for the Bauer microplate and its relationship to Pacific–Nazca spreading incorporate the finite rotations of Eakins and Lonsdale (2003). We implement spreading in the fan-like pattern whereby the pole of rotation is located close to the ridge axis (Fig. 10). Although magnetic anomalies cannot be clearly discerned, we have implemented the timing of Eakins and Lonsdale (2003) with spreading initiating at 17 Ma and continuing until 6 Ma. The locus of spreading then jumps back to the Pacific–Nazca ridge (Fig. 10).

The model for the Cocos and Mathematician/Rivera plates incorporates the magnetic anomaly identification of Munschy et al. (1996) together with the finite rotations derived from Eakins and Lonsdale (2003) between 17.3 and 11.9 Ma and newly derived finite rotation for 23 Ma and 10.9 Ma. We reconstruct the shape and location of the Cocos Ridge from Meschede et al. (1998b). We model spreading along the Galapagos Spreading Centre (Cocos–Nazca) based on the finite difference method. We do not include the small-scale ridge jumps that occurred along the Cocos–Nazca Ridge, instead we model a simple two plate system with an eastward propagating ridge (Figs. 9–10).

3.2.3. Phoenix plate

Until recently, the prevailing view for the evolution of the Phoenix plate was that the Phoenix–Pacific spreading ridge was active since the birth of the Pacific plate to at least the mid–late Cretaceous as a simple two-plate system with N–S directed spreading (Larson and Chase, 1972). The E–W trending Phoenix lineations (so named due to their proximity to the Phoenix Islands) form the southern arm of the Pacific triangle (Fig. 6) with magnetic anomalies ranging from M29 (~156 Ma) to M1 (~123 Ma) (Larson, 1976; Cande et al., 1978; Atwater, 1990) and possibly M0 (~120 Ma) (Larson, 1997; Nakanishi and Winterer, 1998). Undated, presumably older magnetic lineations can be traced north of M29 (~156 Ma) (Nakanishi et al., 1992; Nakanishi and Winterer, 1998) close to the inferred center of the Pacific triangle. The lineations disappear under the Ontong Java Plateau to the west and abut against a complex set of fan-shaped lineations (Magellan lineations) and NE–SW directed lineations (M21–14; ~147–136 Ma) south of the Mid-Pacific Mountains (Nakanishi and Winterer, 1998) to the east. The complex Magellan and Mid-Pacific lineations suggest the existence of several microplates (e.g. Trinidad and Magellan) at the Phoenix–Pacific–Farallon triple junction (Atwater, 1990) with patterns similar to the fast spreading migrating microplates of the East Pacific Rise (Tebbens and Cande, 1997).

The ocean floor within the Ellice Basin and directly east of the Tonga–Kermadec subduction zone is intrinsically linked to the evolution of the Pacific–Phoenix ridge after M0 (~120 Ma) (Figs. 6 and 11).

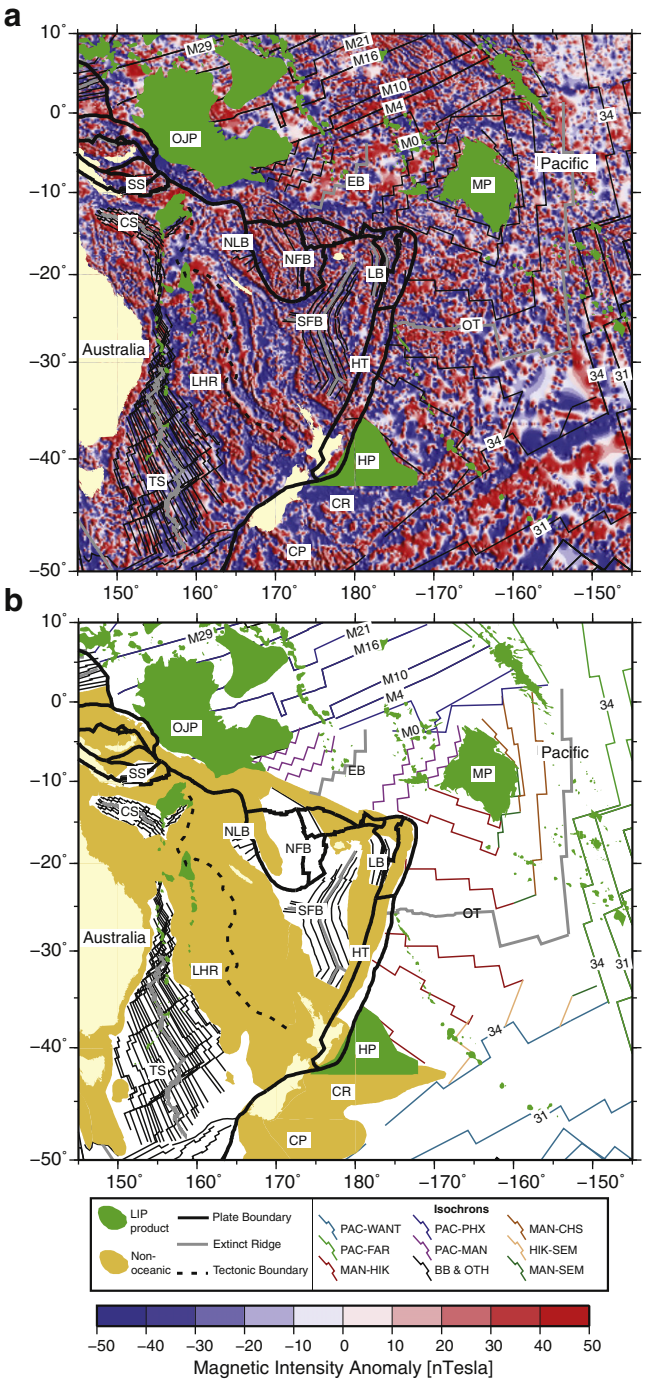

Fig. 11. (a) Gridded magnetic anomalies for the southwest Pacific. Seafloor spreading isochrons used in this study plotted as thin black lines. Numbers correspond to magnetic anomaly chron. CP = Campbell Plateau, CR = Chatham Rise, CS = Coral Sea, EB = Ellice Basin, HP = Hikurangi Plateau, HT = Havre Trough, LB = Lau Basin, LHR = Lord Howe Rise, MP = Manihiki Plateau, NFB = North Fiji Basin, NLB = North Loyalty Basin, OJP = Ontong Java Plateau, OT = Osbourn Trough, SFB = South Fiji Basin, SS = Solomon Sea. (b) Seafloor spreading isochron map colored by spreading system or plate pair. Map abbreviations are same as a. Legend abbreviations are: BB = Back arc Basins, CHS = Chasca, FAR = Farallon, HIK = Hikurangi, MAN = Manihiki, OTH = Other, PAC = Pacific, PHX = Phoenix, SEM = Southeast Manihiki, WANT = West Antarctica/Antarctica.

Early models predicted that the area formed as part of a simple, continuous N–S directed spreading system until the end on the CNS (Larson and Chase, 1972). However, the anomalously fast seafloor spreading rates required to populate the region with crust formed during the CNS (Atwater, 1990) as well as the identification of tectonic structures and seafloor fabric such as the E–W trending Nova Canton Trough, the E–W trending Osbourn Trough and the N–S directed seafloor fabric and side-stepping fracture zones in the Ellice Basin suggest a more complex history for the area. Based on the interpretation of the seafloor spreading structures, two distinct models have been developed to explain the evolution of the Pacific–Phoenix ridge after M1/M0 (~123–120 Ma): a successive southward ridge jump model (Winterer, 1976; Larson, 1997; Billen and Stock, 2000; Müller et al., 2008b) and a plateau break-up model (Taylor, 2006).

In the successive ridge jump model the Nova Canton Trough, an E–W gravity low located south and parallel to the Mesozoic lineations (Figs. 6 and 11), is interpreted as an abandoned spreading center associated with Pacific–Phoenix spreading (Rosendahl et al., 1975; Winterer, 1976; Müller et al., 2008b). A zone of disrupted seafloor fabric bounded by two prominent E–W trending gravity lows in the northern Ellice Basin observed in satellite gravity data led to the idea of a rift zone associated with N–S directed spreading along the Pacific–Phoenix ridge (Larson, 1997). The abandoned ridge/rift zone model implies that the Pacific–Phoenix ridge either became extinct shortly after M0 (~120 Ma) or that the spreading ridge jumped to another location, likely to the south subsequent to M0 (~120 Ma), during a regional plate reorganization. The timing is constrained by the identification of magnetic anomaly M0 (~120 Ma) just north of the Nova-Canton Trough (Larson, 1997; Nakanishi and Winterer, 1998). The southern ridge jump model is supported by the identification of the E–W trending Osbourn Trough (located to the east of the Tonga–Kermadec Trench and north of the Louisville Seamount Chain) as an extinct spreading ridge of Cretaceous age (Lonsdale, 1997; Billen and Stock, 2000) (Fig. 11) rather than a late stage crack in the Pacific plate (Small and Abbott, 1998).

The seafloor spreading morphology in the vicinity of the Osbourn Trough confirms roughly north–south spreading along a slow-intermediate spreading center (Worthington et al., 2006; Downey et al., 2007) whereas the early motion appears to be parallel to the Wishbone Ridge (Figs. 1 and 2g). Spreading along the Osbourn Trough is believed to have initiated right after M0 (~120 Ma) (Davy et al., 2008) leading to the separation of the Manihiki and Hikurangi Plateaus. The timing cannot be constrained from the seafloor spreading record as the early crust would have formed during the CNS. Instead, the timing for the initiation of spreading is constrained from the dating of rift-related structures on the southern side of the Manihiki Plateau (e.g. Nassau-Suwarrow Scarp) and the northern side of the Hikurangi Plateau (e.g. Rapuhia Scarp) (Lonsdale, 1997; Billen and Stock, 2000; Sutherland and Hollis, 2001; Davy et al., 2008). The cessation of spreading is poorly constrained but most authors tie the termination of spreading along the Osbourn Trough with the docking of the Hikurangi Plateau to the Chatham Rise. Unfortunately, the timing of collision between the Hikurangi Plateau and Chatham Rise is also ill constrained. Some authors favor collision at 105–100 Ma (Lonsdale, 1997; Sutherland and Hollis, 2001; Davy et al., 2008) based on geological observations and the onset of extension in New Zealand whereas others favor collision around 80–86 Ma (Billen and Stock, 2000; Worthington et al., 2006). The youngest magnetic anomalies associated with the Osbourn Trough are as young as Anomalies 33 (~79 Ma) or 32 (~71 Ma) (Billen and Stock, 2000) or Anomaly 34 (~84 Ma) but prior to ~87 Ma (Downey et al., 2007). Based on the age range allowed from the magnetic anomaly interpretation and the age constraints on the initiation of spreading between the Pacific and Antarctic plate to the south, Müller et al. (2008b) suggested that the spreading along the Osbourn Trough ceased at 85 Ma, leading to a final jump in the plate boundary to the south along the present day Pacific–Antarctic ridge.

The plateau break-up model (Taylor, 2006) suggests that the Ontong Java Plateau, Manihiki and Hikurangi Plateaus were joined at the time of their eruption. This mega-LIP erupted around Aptian time based on the dating of sediment overlying pillow basalts (Winterer et al., 1974) and Ar/Ar dating (Mahoney et al., 1993). Taylor (2006) based his interpretation on recently collected marine geophysical data from the Ellice Basin, which he believes was formed during the separation of the Ontong Java and Manihiki Plateau and confirmed by Chandler et al. (in press). In the Taylor (2006) model, the Nova-Canton Trough is interpreted as an extension of the Clipperton Fracture Zone (Larson et al., 1972; Joseph et al., 1990; Taylor, 2006) based on side-scan sonar data (Joseph et al., 1992) and not an abandoned spreading ridge. The disturbed "rift zone" identified by Larson (1997) is instead interpreted as the northern part of an E–W directed spreading system with stair-stepped, large offset E–W trending fracture zones and N–S abyssal hill fabric (Taylor, 2006) separating the Ontong Java and Manihiki Plateaus. This model suggests that after M0 (~120 Ma), the tectonic regime changed from N–S directed Pacific–Phoenix spreading to E–W directed spreading between the Pacific plate and a new Manihiki plate. Coincidently, N–S directed spreading was occurring between the Manihiki and Hikurangi plateaus, as suggested in the previous model. The differential motion between the two spreading systems requires a triple junction between the Pacific, Manihiki and Hikurangi plates (Taylor, 2006). The timing of plateau break-up is unconstrained from the seafloor spreading record as no magnetic anomalies can be interpreted. However, rift structures on the eastern side of the Ontong Java plateau and western margin of the Manihiki plateau suggest that this occurred around 120 Ma, matching well with the dated break-up of the Manihiki and Hikurangi plateaus. Further supporting the common origin of the Ontong Java, Manihiki and Hikurangi Plateaus is similar geochemical compositions between the three plateaus suggesting a related source (Mahoney et al., 1993; Hoernle et al., 2010).

The other main feature on the seafloor attributed to Pacific–Phoenix spreading is the Tongareva triple junction trace in the SW Pacific (Larson et al., 2002; Pockalny et al., 2002; Viso et al., 2005). The Tongareva triple junction trace is a roughly NNW–SSE linear feature which starts at the northeastern corner of the Manihiki Plateau in the Pernyn Basin and extends to west of the Cook Islands before it changes trend to NW–SE until it reaches spreading associated with Pacific–Antarctic Ridge (Fig. 11). The western side of the triple junction trace consists of ENE trending abyssal hill topography and directly east, the morphology is NNW–SSE trending (Larson et al., 2002; Pockalny et al., 2002). This lineament is believed to record the migration of a ridge–ridge–ridge triple junction between the Pacific–Farallon–Phoenix plates (Larson et al., 2002) whereas more detailed analysis revealed that the triple junction likely flipped between ridge–ridge–ridge and ridge–ridge–transform configurations throughout its evolution (Pockalny et al., 2002). Sutherland and Hollis (2001) suggested that this lineament was a rift but this has been refuted by subsequent studies (e.g. (Larson et al., 2002). The eastern margin of the Manihiki Plateau comprises a dramatic transtensional scarp (Winterer et al., 1974; Stock et al., 1998) suggesting that the easternmost portion of a presumably larger Manihiki Plateau was rifted off the margin and was controlled by the plate motions related to the triple junction. Larson et al. (2002) hypothesized that a piece traveled across Panthalassa on the Farallon plate and another piece rifted to the south with the Phoenix plate. The timing for activity along the triple junction is poorly constrained. Spreading is believed to have initiated around 120 Ma, based on the dating of carbonate sedimentation on the Manihiki Plateau (Larson et al., 2002) with termination around 84 Ma (Larson et al., 2002).

Our model for the evolution of the Phoenix plate incorporates simple N–S directed spreading in the Mesozoic followed by a major plate reorganization at ~120 Ma (M0) coincident with the eruption of the Ontong Java–Manihiki–Hikurangi plateau as one mega-LIP, as suggested by Taylor (2006) and Chandler et al. (in press) (Fig. 10). This spreading system shuts down at 86 Ma, after which spreading

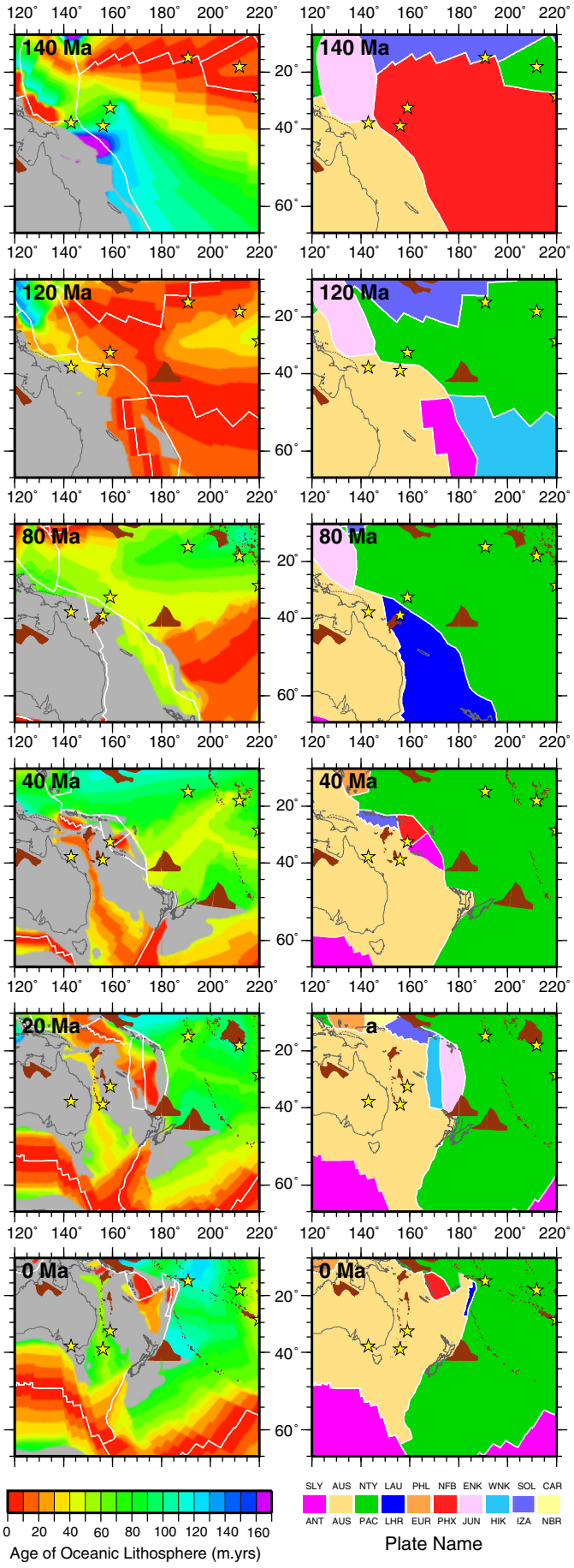

was accommodated along the Pacific–Farallon and Pacific–Antarctic Ridges (Figs. 10 and 12).

The Mesozoic lineations are constrained by magnetic anomaly identification from Munschy et al. (1996), with geophysical data (including satellite derived gravity data) constraining the location of the Osbourn Trough, Nova Canton Trough and Tongareva triple junction trace. Our seafloor spreading isochrons match the magnetic anomaly grid quite well for the central and western part of the Mesozoic lineations but there is a poor match to the east corresponding to the fan-shaped Magellan and Mid-Pacific Mountain lineations (Figs. 6 and 11). We do not reconstruct these complex lineation sets due to a lack of age constrains on initiation and cessation of the microplates at the Pacific–Phoenix–Farallon triple junction that would have formed these lineations. In addition, our aim is to model the broad scale development and the evolution of the larger plates in the area rather than the smaller scale microplates. Finite rotations are derived for the E–W trending M-series anomalies by using the half-stage pole methodology and following the fracture zones traced from satellite gravity data (Sandwell and Smith 2009).

Our reconstructions are based on the model of Taylor (2006) and Chandler et al. (in press) with roughly E–W directed spreading forming the crust underlying the Ellice Basin between the Ontong Java and Manihiki Plateaus and simultaneous rifting of the Manihiki and Hikurangi plateaus from a N–S directed spreading system along the Osbourn Trough. We initiate this spreading system at 120 Ma, corresponding to the timing of the LIP eruption and the dating of rift-related sequences along the margin. The oceanic crust between these plateaus formed during the CNS so no correlations can be observed in the magnetic anomaly grids (Fig. 11). However, the satellite derived gravity data indicates fracture zone trends and limited abyssal hill fabric. We derive our own finite rotations for the opening of the Osbourn Trough region by following fracture zone traces. The separation of the mega-LIP requires that a triple junction was active accommodating motion between the Ontong Java and Hikurangi Plateaus during its formation. We reconstruct the arm of the triple junction based on the finite difference method.

We suggest a further two triple junctions were located to the east of the Manihiki Plateau, one of which formed the Tongareva triple junction trace. However, unlike previous interpretations (Larson et al., 2002; Viso et al., 2005), we suggest that the triple junction represented spreading between the Manihiki, Hikurangi and a new plate we term the Chasca plate to the east of the Manihiki and Hikurangi plates (Fig. 10). The Chasca plate, which was located off the South American margin, is named after the Incan goddess of dawn and twilight. Our finite rotations were derived by using a combination of fracture zone and triple junction traces and the finite difference method. A second triple junction between the Hikurangi, Manihiki and a new plate we term the Catequil plate was required to account for the trends in the seafloor fabric to the west of the Tongareva triple junction trace. The Catequil plate is named after the Incan god of thunder and lightning.

The fracture zone traces between the Manihiki and Hikurangi Plateau show a change in direction but this change has never been

Fig. 12. (left) Agegrid reconstructions of the southwest Pacific at 140, 120, 80, 40, 20, 0 Ma highlighting the age–area distribution of oceanic lithosphere at the time of formation and the extent of continental crust (gray polygons). Plate boundaries from our continuously closing plate polygon dataset are denoted as thick white lines, hotspot locations as yellow stars, large igneous provinces and flood basalts as brown polygons and coastlines as thin black lines. (right) Reconstructions showing the outlines of the plates in the southwest Pacific for each reconstruction time listed above. Feature descriptions as in panel (left). Abbreviations are: ANT = Antarctic plate, AUS = Australian plate, CAR = Caroline plate, ENK = East Norfolk Basin plate, EUR = Eurasian plate, HIK = Hikurangi plate, IZA = Izanagi plate, JUN = Junction plate, LAU = Lau Basin plate, LHR = Lord Howe Rise plate, NBR = New Britain plate, NFB = North Fiji Basin plate, NTY = Neo-Tethys plate, PAC = Pacific plate, PHL = Philippine Sea plate, PHX = Phoenix plate, SLY = South Loyalty Basin plate, SOL = Solomon Sea plate, WNK = West Norfolk Basin plate. (For interpretation of the references to color in this figure legend, the reader is referred to the web version of this article.)

dated. We hypothesize that the date of the change in spreading direction occurred at 100 Ma as this corresponds to a time when the fracture zones in other parts of the Pacific change direction as well as a change in the bend of Pacific hotspots. In addition, a clockwise change in spreading direction between the Manihiki and Hikurangi plates at 100 Ma leads to a change in the plate boundary east of Australia from convergence to strike-slip, coincident with a change from subduction related tectonics to passive margin formation and extension. A further refinement of the plate kinematic model for the plateau break-up using improved gravity and vertical gravity gradient grids is presented in Chandler et al. (in press).

The cessation of spreading along all arms of our triple junctions has been dated based on the timing of collision between the Hikurangi Plateau and the Chatham Rise. As stated previously, there are two competing models for the timing of collision. We implement the docking of the Hikurangi Plateau to the Chatham Rise at 86 Ma based on the evidence presented in Worthington et al. (2006) related to a major episode of metamorphism and garnet growth in the Alpine Schist (Vry et al., 2004) and the seafloor spreading constraints presented in Billen and Stock (2000). The docking led to the shut-down of the seafloor spreading system in the South Pacific and a change in the east Australian margin from strike-slip to convergence (Fig. 12). After the cessation of spreading, the spreading ridge jumped to the south to initiate rifting and seafloor spreading between the Pacific and Antarctic plates. An earlier timing for docking of the Hikurangi Plateau requires that rifting and seafloor spreading between the Pacific and Antarctic plates started earlier than observed or that there were two contemporaneous spreading ridges located in close proximity in the South Pacific. It would also require fast seafloor-spreading rates between the Manihiki and Hikurangi plateaus not supported by the seafloor morphology. To the east, the Pacific–Farallon Ridge extended to the south connecting up with the Pacific–Antarctic Ridge at the Pacific–Antarctic–Farallon triple junction.

3.2.3.1. Pacific–Antarctic spreading. The Pacific–Antarctic Ridge and associated ocean floor dominate the South Pacific (Fig. 13) and form a crucial link in the global plate circuit. Early reconstructions of the South Pacific recognized that spreading between the Pacific and the Antarctic/Marie Byrd Land margin involved at least a three-plate system, this third plate was named the Bellinghausen plate and located east of the Marie Byrd Land seamounts (Stock and Molnar, 1987; Eagles et al., 2004a,b). Rifting between the Chatham Rise and Antarctica/Marie Byrd Land is believed to have occurred at 90 Ma (Larter et al., 2002; Eagles et al., 2004a) with the initiation of spreading between the Pacific and Bellinghausen plates at Anomaly 33r (83.0–79.1 Ma) (Stock and Molnar, 1987; Larter et al., 2002) contemporaneous with Pacific–Antarctic/Marie Byrd Land spreading (Molnar et al., 1975; Cande et al., 1982; Stock and Molnar, 1987; Mayes et al., 1990; Cande et al., 1995; Larter et al., 2002; Croon et al., 2008) or 80 Ma for Bellinghausen spreading (Eagles et al., 2004a, b). Spreading between the Campbell Plateau and Marie Byrd Land occurred from Anomaly 33r (83.0–79.1 Ma) (Larter et al., 2002; Eagles et al., 2004a). The cessation of the Bellinghausen plate as an independent plate and its accretion onto the Pacific plate was initially believed to have occurred at Anomaly 25 (~56 Ma) (Stock and Molnar, 1987), but this was revised to Anomaly 27 (~61 Ma) during a time of major plate reorganization (Cande et al., 1995). Cande et al. (1995) also found that any relative motion between the Bellinghausen and Antarctic plates was much smaller than previously thought.

New finite rotations based on the improved South Pacific dataset were computed for spreading between the Pacific and Antarctic plates from Anomaly 27 (~61 Ma) to the present day (Cande et al., 1995) and were used in the detailed model of Eagles et al. (2004a,b). Spreading between the Pacific and Antarctic plates occurred as a two-plate system with major changes in spreading direction recorded between Chron 27 (~61 Ma) and 20 (~43 Ma), between Chrons 13 (~33 Ma)

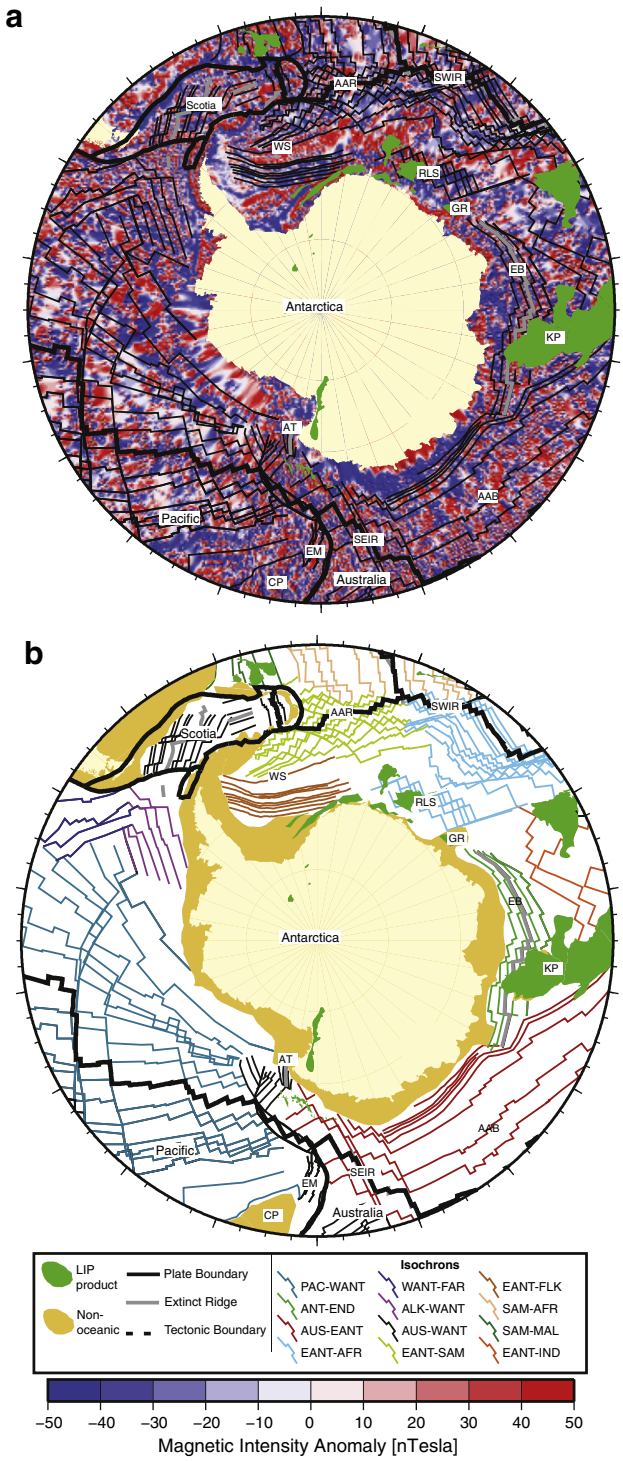

Fig. 13. (a) Gridded magnetic anomalies for the circum-Antarctic. Seafloor spreading isochrons used in this study plotted as thin black lines. AAB = Australia–Antarctic Basin, AAR = American–Antarctic Ridge, AT = Adare Trough, CP = Campbell Plateau, EB = Enderby Basin, EM = Emerald Basin, GR = Gunnerus Ridge, KP = Kerguelan Plateau, RLS = Riiser-Larson Sea, SEIR = Southeast Indian Ridge, SWIR = Southwest Indian Ridge, WS = Weddell Sea. (b) Seafloor spreading isochron map colored by spreading system or plate pair. Map abbreviations are same as a. Legend abbreviations are: AFR = Africa, ALK = Aluk, AUS = Australia/Lord Howe Rise, BB = Back arc Basins, EANT = East Antarctica/Antarctica, END = Enderby, FAR = Farallon, FLK = Falkland, IND = India, MAL = Malvinas, OTH = Other (Adare Trough and Emerald Basin), PAC = Pacific, SAM = South America, WANT = West Antarctica/Antarctica.

and 6C (~24 Ma) and at Chron 3a (~6 Ma) (Cande et al., 1995; Croon et al., 2008). A recent update of the seafloor spreading history between the Pacific and Antarctic plates (Croon et al., 2008) is in general agreement with the model of Cande et al. (1995) for times 61 Ma to 12.3 Ma, but the model and rotations differ slightly for younger times.

To construct our seafloor spreading isochrons between the Pacific and Antarctic plates, we used the magnetic anomaly pick identifications and finite rotations of Cande et al. (1995) for times from 61 Ma to the present day, which are also used in the model of Eagles et al. (2004a,b). Croon et al. (2008) provide updated rotations for times younger than 12.3 Ma but they are not incorporated into our model. As noted by Croon et al. (2008) the effect of using these rotations on motion between the Pacific and western North America is small and hence will not significantly alter Pacific plate motion. We anticipate that these rotations will be included in the next generation of our global plate tectonic model. For times between 61 Ma and 83.5 Ma, we followed the magnetic anomaly interpretation and finite rotations of Larter et al. (2002) for Pacific–Antarctic/Marie Byrd Land spreading and Pacific–Bellinghausen spreading. We assigned an age of 90 Ma for the Antarctic margin conjugate to the Chatham Plateau to reflect the initiation of rifting and an age of 80 Ma for the onset of spreading between the Campbell Plateau and Antarctic margins. Validating the shape and location of our seafloor spreading isochrons in this region using the magnetic grid compilation is difficult due to the paucity of data available in this region (Fig. 13). Some magnetic lineations can be identified adjacent to the Campbell Plateau and clearly reflect a clockwise change in spreading direction between Anomalies 31 (~68 Ma) and 25 (~56 Ma) consistent with our isochrons.

3.3. Tethys/Indian Ocean

The present day Indian Ocean comprises five main plates: the Indo-Australian, Antarctic, African, Somali and Arabian plates (Figs. 1 and 14). In addition, the Indo-Australian plate is often subdivided into three plates: the Australian, Indian and Capricorn plates along a zone of diffuse deformation in the East Indian Ocean (Demets et al., 1994; Royer and Gordon, 1997; Weissel et al., 1980) (Figs. 1 and 14). Several smaller plates exist along the East African margin associated with continental rifting and diffuse deformation, including the proposed Nubian and Lake Victoria plates (Lemaux et al., 2002; Bird, 2003). Prior to Gondwana break-up and the opening of the Indian Ocean, a now entirely vanished ocean basin, the Tethys Ocean, existed between Gondwana and Laurasia. The evidence for this ocean basin is primarily preserved in the terranes and ophiolite complexes along southern Eurasia and the Mediterranean. The Indian Ocean preserves a record of the early break-up history of Gondwana along the East African, Antarctic and West Australian passive margins. An extensive mid ocean ridge network developed separating India, Antarctica, Australia, Madagascar and Africa. In addition, a long-lived subduction zone to the north consumed oceanic lithosphere from the Tethys Ocean eventually leading to the uplift of the Himalayas resulting from the collision of the Indian continent with southern Eurasia.

Detailed reconstructions of the Indian Ocean as they currently stand are problematic, leading to gaps and overlaps in full-fit reconstructions, motions of continental blocks that are inconsistent with independently modeled motions of neighboring plates and not strongly constrained by geological observations. A concerted international collaborative effort is currently underway to update reconstructions for the entire Indian Ocean with completion expected by early 2013. Our current model is an amalgamation of a number of published models for different portions of the Indian Ocean. We will begin by describing the early break-up history of Gondwana and formation of the Indian Ocean followed by the Cenozoic–recent opening. Lastly we will discuss our current model for the inferred opening and closure history of the Tethys Ocean.

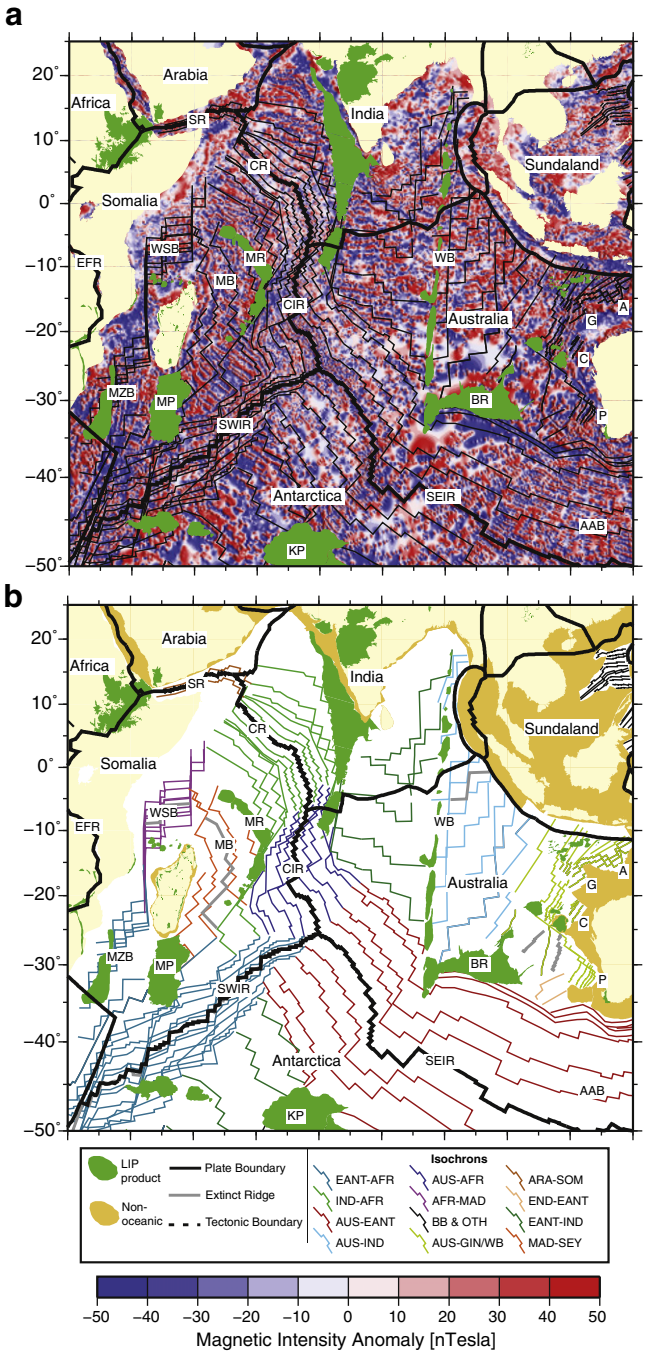

Fig. 14. (a) Gridded magnetic anomalies for the Indian Ocean. Seafloor spreading isochrons used in this study plotted as thin black lines. A = Argo Abyssal Plain, AAB = Australia–Antarctic Basin, BR = Broken Ridge, C = Cuvier Abyssal Plain, CIR = Central Indian Ridge, CR = Carlsberg Ridge, EFR = East Africa Rift, G = Gascoyne Abyssal Plain, KP = Kerguelan Plateau, MB = Mascarene Basin, MP = Madagascar Plateau, MR = Mascarene Ridge, MZB = Mozambique Basin, P = Perth Abyssal Plain, SEIR = Southeast Indian Ridge, SR = Sheba Ridge, SWIR = Southwest Indian Ridge, WB = Wharton Basin. (b) Seafloor spreading isochron map colored by spreading system or plate pair. Map abbreviations are same as a. Legend abbreviations are: AFR = Africa, ALK = Aluk, AUS = Australia/Lord Howe Rise, BB = Back arc Basins, EANT = East Antarctica/Antarctica, END = Enderby, FAR = Farallon, FLK = Falkland, IND = India, MAL = Malvinas, OTH = Other (Adare Trough and Emerald Basin), PAC = Pacific, SAM = South America, WANT = West Antarctica/Antarctica.

3.3.1. East African margins

The break-up of Gondwana initiated in the early Jurassic between West Antarctica, Africa and Madagascar following a long period of rifting along the Permo-Triassic Karoo Rift and eruption of the

Karoo Volcanics during the early Jurassic (around 185–180 Ma) (Cox, 1992; Forster, 1975; Jourdan et al., 2005; Reeves, 2000; Storey et al., 2001) (Fig. 14). The cessation of volcanism along the Karoo Rift led to a seaward jump in the locus of rifting, initiating contemporaneously between Africa and Antarctica in the Mozambique Basin and Riiser-Larson Sea (Simpson et al., 1979; Marks and Tikku, 2001; Eagles and König, 2008) and Africa and Madagascar in the West Somali Basin (Smith and Hallam, 1970; Hankel, 1994) and either contemporaneously or earlier between Africa and West Antarctica in the Weddell Sea (Livermore and Hunter, 1996; König and Jokat, 2006).

Separation between Africa and Antarctica/Madagascar forming the Mozambique Basin, Riiser-Larson Sea and West Somali Basin is believed to have initiated in the early–mid Jurassic supported by the stratigraphy and pre-rift structures along the conjugate margins (Smith and Hallam, 1970; Bunce and Molnar, 1977; Norton and Sclater, 1979; Ségoufin and Patriat, 1980; Scrutton et al., 1981; Coffin and Rabinowitz, 1987; Lawver and Scotese, 1987; Reeves, 2000; Müller et al., 2008b). The transition from continental rifting to seafloor spreading is believed to have occurred either at 183–177 Ma based on Eagles and Konig (2008) full-fit reconstruction, 170 Ma (Müller et al., 1997; Reeves and De Wit, 2000), 167 Ma (König and Jokat, 2006) or 165 Ma based on matching tectonic sequences in Africa and East Antarctica (Coffin and Rabinowitz, 1987; Livermore and Hunter, 1996; Marks and Tikku, 2001). Early full-fit reconstructions place Madagascar west of the Gunnerus Ridge (Royer and Coffin, 1992) whereas most recent studies place Madagascar to the east (Marks and Tikku, 2001; Eagles and König, 2008) thereby eliminating overlap issues between Antarctica and Madagascar.

The oldest identified magnetic anomalies interpreted in the Mozambique and West Somali Basins and Riiser-Larson Sea are Anomalies M25–M24 (~154–152 Ma) (Ségoufin and Patriat, 1980; Rabinowitz et al., 1983; Coffin and Rabinowitz, 1987; Roeser et al., 1996; Marks and Tikku, 2001; Jokat et al., 2003). However, some have inferred Jurassic Quiet Zone crust between the oldest magnetic anomalies and the continental slope (Coffin and Rabinowitz, 1987) possibly as old as M40 (~166 Ma) (Gaina et al., 2010). Spreading in all basins was directed N–S for most of the opening history, confirmed through the interpretation of fracture zones (Heirtzler and Burroughs, 1971), but a NNE–SSW direction can also be seen in the older oceanic crust fabric. Paleomagnetic (McElhinny et al., 1976), seismic and gravity anomaly data (e.g. (Rabinowitz, 1971; Bunce and Molnar, 1977; Coffin and Rabinowitz, 1987, 1988; Storey et al., 1995) support the southward motion of Madagascar relative to Africa during the Jurassic and Early Cretaceous.

The spreading histories of the Mozambique/Riiser-Larson Sea and the West Somali Basin diverge at about M10 (~130–132 Ma). Spreading in the West Somali Basin ceased either at M10 (~130–132 Ma) (Rabinowitz et al., 1983; Coffin and Rabinowitz, 1987; Eagles and König, 2008) or M0 (~120 Ma) (Ségoufin and Patriat, 1980; Cochran, 1988; Müller et al., 1997; Marks and Tikku, 2001; Müller et al., 2008a) depending on the magnetic anomaly identification used. After the cessation of spreading, the mid-ocean ridge jumped southward initiating spreading in between Madagascar and Antarctica. The timing of the southern ridge jump and seafloor spreading history in the surrounding Enderby Basin and Weddell Sea has major implications for the plate boundary configurations in the Mesozoic Indian Ocean. For example, the model of Eagles and Konig (2008) infers a southward ridge jump from the West Somali Basin at M10 (~130–132 Ma) transferred Madagascar to the African plate and initiated spreading in the Enderby Basin. In this model Madagascar did not act as an independent plate throughout any of its Mesozoic–Cenozoic history. Other models propose that Madagascar must have acted independently, at least for part of its history (e.g. Marks and Tikku, 2001). The mid-ocean ridge which formed the Mesozoic magnetic lineations in the Mozambique Basin/Riiser-Larson Sea continued throughout the Cenozoic eventually becoming the Southwest Indian Ridge where highly oblique, ultra-slow seafloor spreading is occurring (Patriat and Ségoufin, 1988; Royer et al., 1988).

The final break-up of Gondwana continental blocks occurred with the separation of Madagascar and India forming the Mascarene Basin. Previous interpretations of the area suggest that rifting initiated in the late Cretaceous (Norton and Sclater 1979; Masson 1984; (Bernard and Munschy, 2000) with the oldest magnetic anomaly identified being Anomaly 34 (~84 Ma) or 33 (~79 Ma). A major change to NE–SW spreading is recorded in the fracture zones and magnetic lineations around Anomaly 31 (~68 Ma) (Bernard and Munschy, 2000). Part of the Mascarene Ridge jumped northward isolating the Seychelles microcontinent (Masson, 1984). The model of Bernard and Munschy (2000) suggests contemporaneous spreading between the easternmost part of the Mascarene Basin and spreading to the north between the Seychelles and Laxmi Ridge, implying a cessation of spreading in the Mascarene Basin as late as Anomaly 27 (~61 Ma). The oldest identified magnetic lineation between the Seychelles and Laxmi Ridge in the East Somali and West Arabian Basin is Anomaly 28 (~63 Ma) (Masson, 1984; Collier et al., 2008) based on the dating of syn-rift volcanics offshore from the Seychelles (Collier et al., 2008) or Anomaly 27 (~61 Ma) (Chaubey et al., 1998) defining the initiation of spreading along the Carlsberg Ridge.

We have adopted a model for East Africa whereby pre-breakup margin extension was initiated at 180 Ma as a response to thermal weakening by the eruption of the Karoo flood basalts. We initiate seafloor spreading at 160 Ma along the entire East Africa margin after the cessation of rifting in the Karoo Rift, about 5 million years before the last confidently dated magnetic anomaly, M25 (~154 Ma) (Fig. 15). We connect the rift to the mid-ocean ridge that developed between Patagonia and Southern Africa (Torsvik et al., 2009) and Weddell Sea to the southwest and to a transform in the Tethys to the northeast (Figs. 14 and 15). The identification of magnetic anomalies and fracture zone trends is difficult in the area due to thick sediment cover and volcanic overprinting. Weakly trending magnetic lineations observed in the magnetic anomaly grid confirm the N–S directed spreading direction (Fig. 14). We adopt the model for the cessation of spreading in the West Somali Basin shortly after M0 (~120 Ma) and not at M10 (~131 Ma) as suggested by Eagles and Konig (2008). The cessation of spreading at M10 (~131 Ma) results in the position of Africa relative to Madagascar and Antarctica that is incompatible with newly interpreted aeromagnetic data in the area (König and Jokat, 2010). After the cessation of spreading, we implement a southward ridge jump towards the site of Madagascar Ridge and Conrad Rise eruption. Our model implies that Madagascar operated as an independent plate from 144 to 115 Ma, based on our interpretation of the West Somali Basin. Spreading in the Mozambique/Riiser-Larson Sea continued unabated throughout the Mesozoic and along the Southwest Indian Ridge to the present day.

Our model for the separation of Madagascar and India is similar to that presented in Masson (1984) and Müller et al. (1997). Although the oldest magnetic anomaly identified is Anomaly 34 (~84 Ma), we initiate rifting at 87 Ma, preceded by a period of strike-slip motion between India and Madagascar. A major change in spreading direction occurred at Anomaly 31 (~68 Ma) to NE–SW spreading based on an interpretation of the fracture zone trends in the basin. Spreading in the Mascarene Basin ceased at 64 Ma resulting in a northward ridge jump and initiation of spreading between India and the Seychelles microcontinent forming the crust in the East Somali and West Arabian Basins. However, spreading may have continued to at least Anomaly 27 (~61 Ma) in the eastern Mascarene Basin (Bernard and Munschy, 2000). The spreading ridge between the Seychelles to the south and Laxmi ridge to the north (Carlsberg Ridge) is modeled based on triple junction closure with India and Arabia. The Carlsberg Ridge connected with the Central Indian Ridge to the southeast and the Sheba Ridge via a series of large offset transform faults to the northwest. The Sheba Ridge separates Arabia from Africa/Somalia, which we initiate at 20 Ma to coincide with the initiation of the East African Rift. The Sheba Ridge propagated into the Red Sea at 15 Ma.

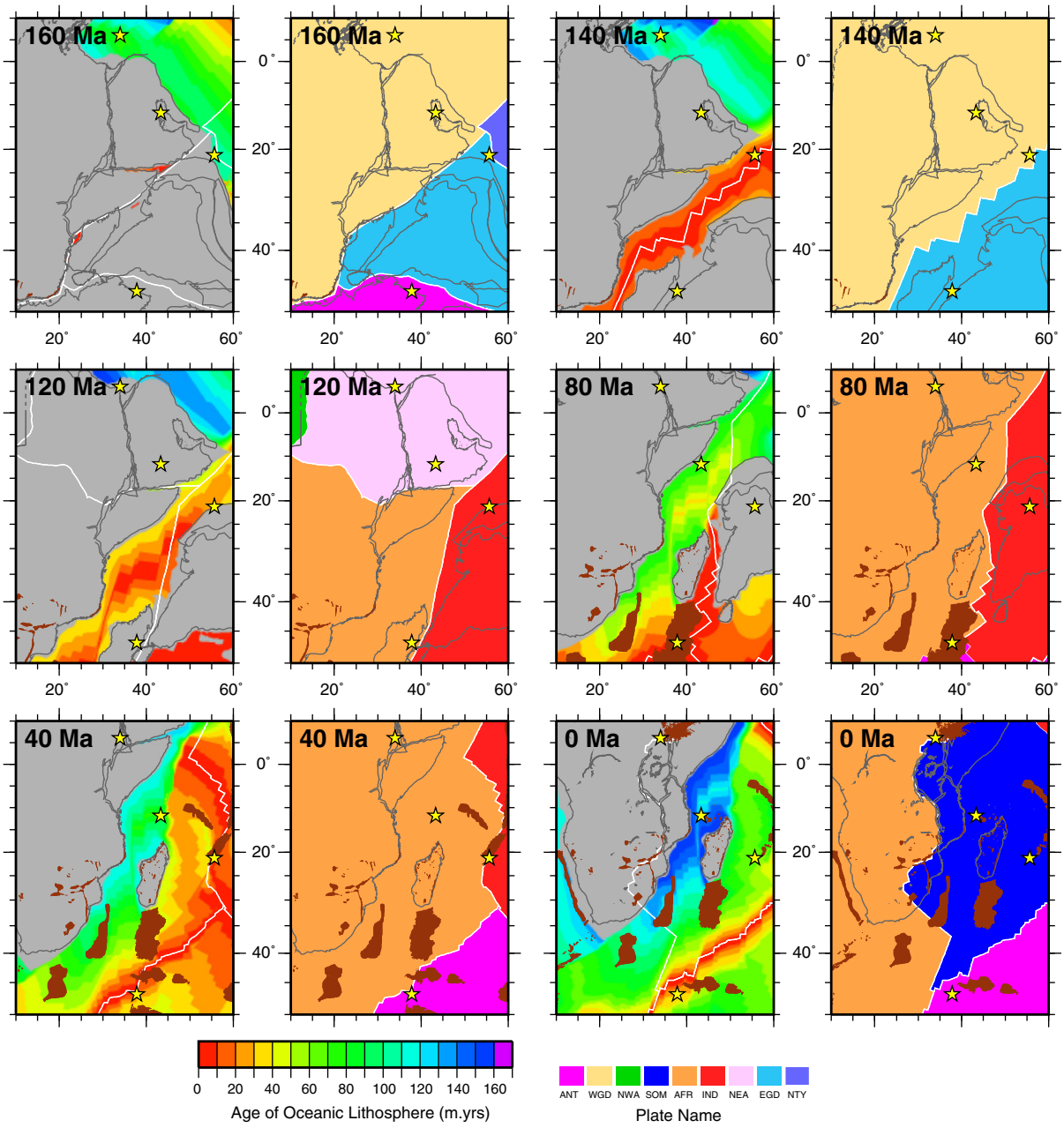

Fig. 15. Agegrid reconstructions of the east African basins at 160, 140, 120, 80, 40, 0 Ma highlighting the age–area distribution of oceanic lithosphere at the time of formation and the extent of continental crust (grey polygons) and reconstructions showing the outlines of the plates in the east African basins for each reconstruction time listed above. Plate boundaries from our continuously closing plate polygon dataset are denoted as thick white lines, hotspot locations as yellow stars, large igneous provinces and flood basalts as brown polygons and coastlines as thin black lines. Abbreviations are: AFR = African plate, ANT = Antarctic plate, EGD = east Gondwana plate, IND = Indian plate, NEA = northeast African plate, NTY = Neo-Tethys plate, NWA = northwest African plate, SOM = Somali plate, WGD = west Gondwana plate.

3.3.2. Antarctic margin

The Antarctic margin bordering the Indian Ocean involves at least four distinct spreading phases, including (from west to east): the Weddell Sea opening between West Antarctica and South America, the Riiser-Larson Sea between Antarctica and Africa (conjugate to the Mozambique Basin), the Enderby Basin between Antarctica and India/Elan Bank and the Southern Ocean between Antarctica and Australia (Figs. 13 and 14).

The opening of the Weddell Sea is believed to have initiated as a three-plate system between Antarctica, South America and Africa (Marks and Tikku, 2001), or initially as a two-plate system with N–S directed spreading between South America and Antarctica (Kovacs et al., 2002). The transition from seafloor spreading to incipient spreading is believed to have occurred at ~167 Ma (König and Jokat, 2006), 165 Ma (Livermore and Hunter, 1996; Marks and Tikku, 2001) and 160 Ma (Ghidella et al., 2002; Müller et al., 2008a). The M-series magnetic anomalies are difficult to identify but a recent study by Konig and Jokat (2006) identified magnetic anomalies as old as M17 (~140 Ma) with seafloor spreading believed to have initiated around M20 (~146 Ma), suggesting 15–20 Ma of rifting and continental stretching before the establishment of seafloor spreading. Seafloor spreading was initially very slow, directed north–south (König and Jokat, 2006). The Cenozoic magnetic anomalies are well-identified (LaBrecque and Barker, 1981; Kovacs et al., 2002) eventually leading to the establishment of the American–Antarctic Ridge (Fig. 13). Due to subduction starting in the Cretaceous, the entire northern plate involved in

Weddell Sea spreading has been subducted including parts of the Cenozoic crust from the Antarctic (southern) plate.

Spreading in the Riiser-Larson Sea (conjugate to Mozambique Basin, west of the Gunnerus Ridge), has been dated with a well-defined sequence from at least M24 (~152–153 Ma) (Roeser et al., 1996; Jokat et al., 2003), although a recent reinterpretation of magnetic anomalies suggests that magnetic anomalies as old as M40 (~166 Ma) exist in both the Riiser-Larson and Mozambique Basins (Gaina et al., 2010). The spreading system here continued into the Cenozoic to the west and north of the Conrad Rise where Anomalies 34 (~83.5 Ma) to 28 (~63 Ma) have been identified (Goslin and Schlich, 1976; Royer and Coffin, 1992). This spreading ridge developed into the ultra-slow Southwest Indian Ridge (Patriat and Ségoufin, 1988).

East of the Gunnerus Ridge and west of the Bruce Rise lies the Enderby Basin (Fig. 13) recording the opening and seafloor spreading history between Antarctica and India. The paucity of data in the area and the identification of magnetic anomaly sequences on the conjugate Indian side in the Bay of Bengal and south of Sri Lanka have led to two alternative theories for the break-up of Antarctica and India: (1) Break up and seafloor spreading during the CNS (Royer and Coffin, 1992; Banerjee et al., 1995; Müller et al., 2000; Jokat et al., 2010), or (2) Break-up and seafloor spreading in the Mesozoic at 135 Ma with the oldest identified magnetic anomaly being M11 (~132 Ma) (Ramana et al., 1994, 2001; Desa et al., 2006) or M9 (~129 Ma) (Gaina et al., 2007). The model of Marks and Tikku (2001) tentatively identified anomalies M10Ny–M1 (~132–121 Ma) in the West Enderby Basin, whereas the most recent model of Jokat et al. (2010) for the West Enderby Basin suggests break-up between India and Antarctica during the CNS (~90–118 Ma).

The Mesozoic spreading model implies contemporaneous opening with the well-documented M-sequence anomalies (M10–M0; ~132–120 Ma) off the Perth Abyssal Plain (Powell et al., 1988; Müller et al., 1998a). The model of Gaina et al. (2007) further incorporates microcontinent formation (Elan Bank) due to one or several ridge jumps associated with the Kerguelen Plume (Müller et al., 2000; Gaina et al., 2003).

The area east of the Bruce Rise and Vincennes Fracture Zone and south of Australia involves rifting, break-up and seafloor spreading between Antarctica and Australia forming the Southern Ocean (Figs. 13 and 14). The conjugate Australia and Antarctic margins consist of a wide zone of highly extended continental crust adjacent to a narrow zone of incipient oceanic crust formed by slow to ultra-slow seafloor spreading. Continental rifting is believed to have initiated at 165 Ma based on the dating of syn-rift sedimentary sequences within the Australian rift basins and increased tectonic subsidence rates (Totterdell et al., 2000) or 160 Ma (Powell et al., 1988). However, the nature of break-up and transition to true seafloor spreading along the margin remains controversial (Tikku and Cande, 1999; Sayers et al., 2001). The timing of break-up is inferred to be around 100 Ma based on the identification of seafloor spreading magnetic anomalies adjacent to the margin (Cande and Mutter, 1982) or by extrapolation of the spreading rate (Veevers et al., 1990), 135–125 Ma based on the relationship between continental margin sequences and the oceanic crust from seismic data (Stagg and Willcox, 1992) or 83.5 Ma based on the dating of the oldest magnetic anomaly (Tikku and Cande, 1999; Whittaker et al., 2007), depending on how the crust in the transition zone is defined. The oldest magnetic anomaly that can be identified is Anomaly 34 (~84 Ma) (Cande and Mutter, 1982; Tikku and Cande, 1999; Whittaker et al., 2007) but Anomalies 34 (~84 Ma) and 33 (~79 Ma) are located in a zone of transitional crust (i.e. morphology not typical of abyssal hill fabric), therefore Anomaly 32 (71 Ma) is often quoted as the oldest magnetic anomaly to indicate true seafloor spreading. The direction of spreading has previously been modeled as N–S, however a recent reanalysis of gravity and magnetic anomaly profiles (Whittaker et al., 2007) suggests early seafloor spreading (Anomalies 34–27; ~84-61 Ma) via NW–SE directed spreading. Spreading developed into a N–S configuration and has continued to the present day with a dramatic increase in spreading rate from Anomaly 13 (~33 Ma) (Tikku and Cande, 1999).

We adopt a model for the Antarctic margins, which suggests contemporaneous rifting in the Weddell Sea, Riiser-Larson Sea and the East African margins starting in the late Jurassic, at 180 Ma, after the cessation of Karoo volcanism and seaward jump in the locus of rifting. We model the opening of the Weddell Sea based on Konig and Jokat (2006), with M20 (~146 Ma) corresponding to the oldest oceanic crust in the area. Comparison of our seafloor spreading isochrons with our magnetic anomaly compilation is difficult (Figs. 13 and 14) due to the lack of data coverage and weak magnetic anomaly signatures. Spreading continued until the end of the CNS (83.5 Ma) when there was a reorganization of the spreading ridge system leading to the establishment of spreading along the American–Antarctic Ridge. This ultra-slow spreading system is currently intersecting the Sandwich subduction zone, one of the few regions of the world where an active mid ocean ridge is intersecting a subduction zone. The Mesozoic Weddell spreading center connected with spreading in the Riiser-Larson Sea/Mozambique Basin in a triple junction configuration.

Further east, we initiate rifting between Antarctica and India in the Enderby Basin (central and eastern parts) at 160 Ma to coincide with the initiation of rifting between Australia and Antarctic, which has been well dated. We adopt the Mesozoic seafloor spreading model in Gaina et al. (2007) using the finite rotations that describe motion between Antarctica and the Elan Bank from Gaina et al. (2003) for the central and eastern Enderby Basin. Here, seafloor spreading initiated at 132 Ma with M9 (~129 Ma) corresponding to the oldest identified magnetic anomaly. The initiation of spreading in the Enderby Basin results in strike-slip motion between India and Madagascar of over 1000 km. A ridge jump isolating the Elan Bank microcontinent occurred at 120 Ma coincident with the eruption of the Kerguelen Plateau. For the Western Enderby Basin, we initiate break-up during the CNS at around 118 Ma, consistent with the model of Jokat et al. (2010).

We model a simple scenario for the rifting, break-up and seafloor spreading history between Australia and Antarctica with rifting initiating at 165 Ma based on the evidence presented in Totterdell et al. (2000) and break-up at 99 Ma (Müller et al., 2000; Müller et al., 2008a). The rift boundary extended into the Enderby Basin from 165 Ma and extended eastward to connect with the Western Panthalassic subduction zone along eastern Australia. We incorporate the oldest magnetic anomaly as Anomaly 34 (~83.5 Ma) based on the model of Tikku and Cande (2000) with a N–S direction of spreading. We do not incorporate the NW–SE early separation motion of Australia and Antarctica (Whittaker et al., 2007) but anticipate that this will be incorporated in a future model. We use the rotations and magnetic anomaly identifications of Müller et al. (1997) for Anomalies 31–18 (~68–40 Ma) and Royer and Chang (1991) from Anomaly 18 (~40 Ma) to the present day. Our resultant seafloor spreading isochrons match very well with the trends observed in our magnetic anomaly grid (Figs. 13 and 14).

3.3.3. West Australian margins

The West Australian continental margin is an old, sediment-starved volcanic continental margin, which formed as a result of multistage rifting and seafloor-spreading during a late Paleozoic and early Mesozoic phase of East Gondwana break-up (Baillie and Jacobson, 1995; Bradshaw et al., 1988; Veevers, 1988). The area can be separated into four distinct zones: the Argo Abyssal Plain, alongside the Browse and Roebuck (former offshore Canning Basin) basins, the Gascoyne Abyssal Plain, alongside the Exmouth Plateau and the Northern Carnarvon Basin, the Cuvier Abyssal Plain delimited by the Cape Range Fracture Zone (CRFZ) and Wallaby-Zenith Fracture Zones (WZFZ), and includes the Southern Carnarvon Basin, the Exmouth Sub-basin and the Wallaby

and Zenith plateaus and the Perth Abyssal Plain extending from the WZFZ to the Naturaliste Plateau in the south (Fig. 14).

Rifting in the Argo Abyssal Plain started around 230 Ma (e.g. Müller et al., 2005) eventually leading to the separation of the West Burma block/Argoland from the Australian continental margin. The transition from rifting to seafloor spreading has been constrained by the dating of magnetic anomalies in the Argo Abyssal Plain and through tectonic subsidence analysis along the margin. The interpretation of magnetic lineations resolves that seafloor spreading initiated immediately prior to Anomaly M26 (~155 Ma) (Fullerton et al., 1989; Sager et al., 1992; Müller et al., 1998a; Heine and Müller, 2005) with NW–SE directed spreading. Previous models have invoked a southward propagating ridge along the Western Australian margin, which started in the Argo Abyssal Plain progressing southward. Spreading in the Gascoyne and Cuvier Abyssal Plains initiated at M10 (~132 Ma) (Johnson et al., 1976, 1980; Larson, 1977; Falvey and Mutter, 1981; Powell et al., 1988; Fullerton et al., 1989; Sager et al., 1992; Müller et al., 1998a) and marked the break-up between Australia and Greater India. The model for the opening of the Argo Abyssal Plain presented in Heine and Müller (2005) differs from previous models and that of Robb et al. (2005) in that spreading between the Argo and Gascoyne Abyssal Plains initiated almost simultaneously with the same orientation. The model also invoked a landward ridge jump at M13 (~136 Ma). Further southward, spreading in the Perth Abyssal Plain which records break-up between Australia and India occurred around 132 Ma based on the mapping of magnetic anomalies (Veevers et al., 1985; Müller et al., 1998a) and involved several seaward ridge jumps towards the Kerguelan plume (Müller et al., 2000). However, the majority of the crust may have formed during the CNS.

We adopt the model for the formation of the Argo and Gascoyne Abyssal Plains following Heine and Müller (2005) which involves NW–SE oriented rifting of West Burma from the northwestern margin of Australia at around 156 Ma (Fig. 16). The continent–ocean boundary along Australia's western margin is from Heine and Müller (2005). Spreading continued until a landward ridge jump at M13 (~136 Ma). We infer that the plate boundary connected with a Tethyan spreading ridge located to the north of India/Greater India to the west and a transform fault to the north (Fig. 16). Our model invokes a southward propagating ridge into the Cuvier and Perth Abyssal Plain at 132 Ma following the models presented in Müller et al. (1998a) and Müller et al. (2000). The mid-ocean ridge associated with spreading in the Perth Abyssal Plain formed a triple junction with mid-ocean ridge opening the Enderby Basin (between East Antarctica and India) (e.g. Gaina et al., 2007) and the Australia–Antarctic mid-ocean ridge (Fig. 16). The NW-–SE directed spreading along the Western Australian margin persisted until around 99 Ma. The fracture zones record a dramatic change in trend from NW–SE to roughly N–S at around 99 Ma (Müller et al., 1998a). The change to N–S spreading forms the oldest crust associated with the Wharton Ridge/Wharton Basin. Seafloor spreading in the Wharton Basin ceased at 43 Ma (Singh et al., 2010).

3.3.4. Tethys Ocean

The Tethys Ocean represents a now largely subducted ocean basin that existed between Gondwanaland and Laurasia and involves a history of successive continental rifting events along the northern Gondwana margin, oceanic basin formation and accretion of Gondwana-derived continental blocks onto the southern Laurasian margin and Indochina/SE Asia. The majority of Tethyan oceanic crust no longer exists due to long-lived subduction along the southern Eurasian margin, except in the Argo Abyssal Plain off NW Australia where a fragment of in-situ oceanic crust recording the youngest Tethyan spreading system is preserved (Fullerton et al., 1989; Heine and Müller, 2005). In addition, the Ionian Sea and several basins in the eastern Mediterranean (e.g. Levant Basin) may be floored by Mesozoic Tethyan oceanic crust (Stampfli and

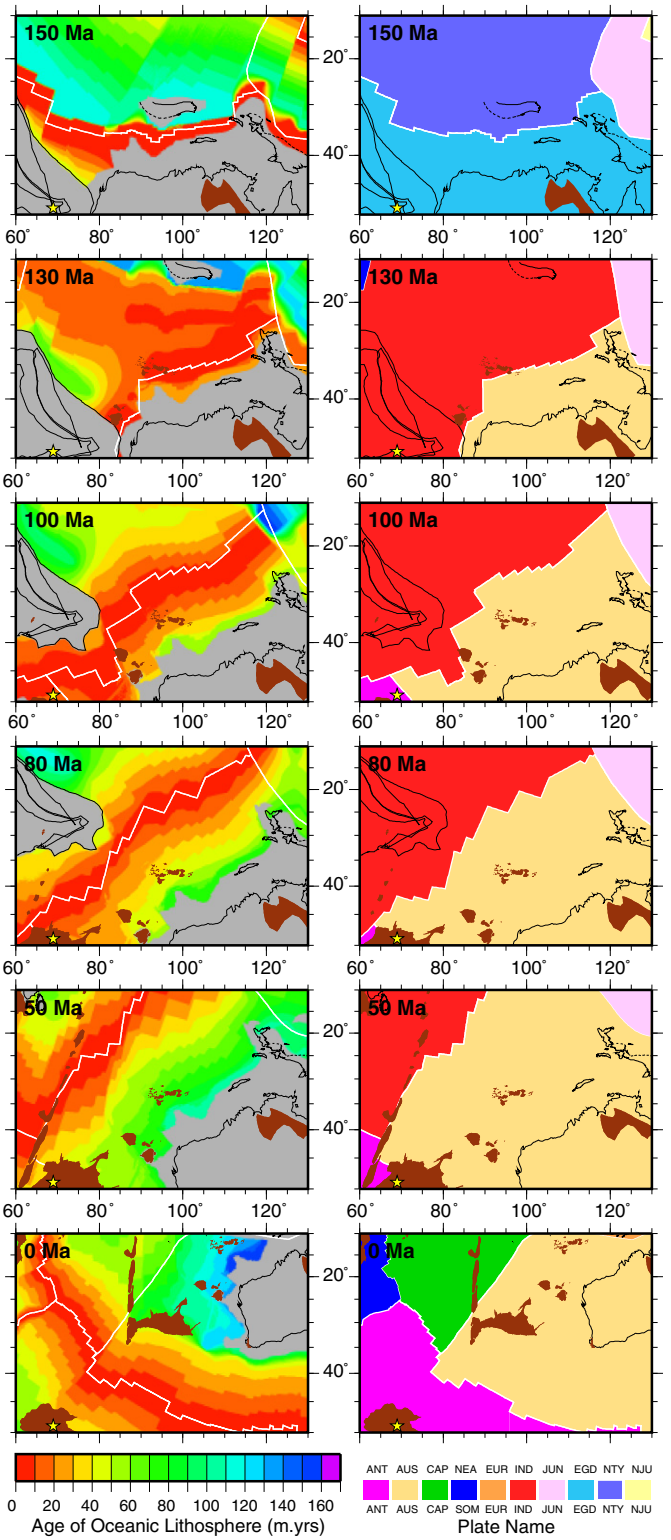

Fig. 16. (left) Agegrid reconstructions of the west Australian margin at 150, 130, 100, 80, 50, 0 Ma highlighting the age–area distribution of oceanic lithosphere at the time of formation and the extent of continental crust (gray polygons). Plate boundaries from our continuously closing plate polygon dataset are denoted as thick white lines, hotspot locations as yellow stars, large igneous provinces and flood basalts as brown polygons and coastlines as thin black lines. (right) Reconstructions showing the outlines of the plates in the west Australian margins for each reconstruction time listed above. Feature descriptions as in panel (left). Abbreviations are: ANT = Antarctic plate, AUS = Australian plate, CAP = Capricorn plate, EGD = east Gondwana plate, EUR = Eurasian plate, IND = Indian plate, JUN = Junction plate, NEA = northeast African plate, NJU = north Junction plate, NTY = Neo-Tethys plate, NWA = northwest African plate, SOM = Somali plate. (For interpretation of the references to color in this figure legend, the reader is referred to the web version of this article.)

Borel, 2002; Müller et al., 2008b), however identification of magnetic anomalies is difficult. The limited amount of preserved in-situ oceanic crust of Tethyan origin hampers our knowledge and understanding of the evolution and structure of the Tethys Ocean. Instead we primarily rely on the accreted terranes and sutures in SE Asia, southern Eurasia, Arabia and throughout the Mediterranean and southern and central Europe (e.g. Sengor, 1987; Metcalfe, 1996; Stampfli and Borel, 2002) as they record the timing of continental block collision, ophiolite emplacement, back-arc basin development and provide paleo-latitudinal estimates of continental material derived from the northern Gondwana margin.

Successive rifting events from the Gondwana margin have led to the subdivision of the Tethys Ocean into several oceanic domains: the paleo- and neo-Tethys (e.g. Stampfli and Borel, 2002) or the paleo-, meso- and neo-Tethys (Metcalfe, 1996; Heine et al., 2004) (Fig. 3a–d). The additional subdivision by Metcalfe (1996) and Heine et al. (2004) stems from an alternative rift history for crust that formed after the paleo-Tethys, which affects whether the Argo Abyssal Plain is classified as part of the Tethys or Indian Ocean domains.

The paleo-Tethys formed after the initiation of rifting and seafloor spreading between the European and Asian Hunic superterrane (e.g. North China, Indochina, Tarim, Serindia, Bohemia) and the northern Gondwana margin (Metcalfe, 1996; Stampfli and Borel, 2002; Blakely, 2008). The timing of passive margin formation is dependent on the margin segment and ranges from Ordovician/Silurian based on subsidence analysis in the western Tethys (Stampfli, 2000; Stampfli and Borel, 2002) or the late/early Devonian based on the Gondwana affinity of Devonian vertebrate faunas in the Hun superterrane (Metcalfe, 1996), Devonian to Triassic passive margin sequences along the southern margin of South China (Metcalfe, 1996) and the dating of oceanic deep-marine ribbon bedded cherts in the Chang-Rai region of Thailand (Sashida et al., 1993; Metcalfe, 1996). The direction of spreading is uncertain due to the lack of in-situ preserved crust, however the seafloor spreading model of Stampfli and Borel (2002) invokes NE–SW directed spreading orthogonal to the inferred margin. The passage of the Hunic superterrane from south to north was facilitated by northward-dipping subduction along the southern Eurasian margin. The Hunic superterrane accreted to the southern Laurasian margin diachronously in the Carboniferous–Permian (Stampfli and Borel, 2002). The cessation of spreading in the paleo-Tethys is difficult to establish, however most modelers agree the paleo-Tethys spreading ridge jumped southward along the northern Gondwana margin and initiated the rifting of a new continental sliver from the Gondwana margin (e.g. Metcalfe, 1996; Stampfli and Borel, 2002; Blakely, 2008) after the accretion of the Hunic superterrane.

The second main phase of rifting isolated the Cimmerian terrane from the Gondwana margin some time in the Pennsylvanian–early Permian (Metcalfe, 1996; Stampfli and Borel, 2002), constrained by changes in biota (Shi and Archbold, 1998) and evidence of rifting on the northwest shelf of Australia (Falvey and Mutter, 1981; Müller et al., 2005), northern Pakistan and Afghanistan (Boulin, 1988; Pogue et al., 1992) and Iran (Stocklin, 1974). The Cimmerian terrane comprises elements including Sibumasu (Sino-Burma-Malaya-Sumatra continental sliver), Qiangtang (North Tibet), Helmand (Afghanistan), Iran and possibly Lhasa/South Tibet (Fig. 18a). The ocean basin that formed between the Gondwana margin to the south and the Cimmerian terrane is labeled as the meso-Tethys in the models of Metcalfe (1996) and Heine et al. (2004) but the neo-Tethys for most other models. Continued northward-dipping subduction of paleo-Tethys oceanic lithosphere along southern Laurasia carried the Cimmerian terrane northward, leading to its accretion and closure of the paleo-Tethys ocean starting in the late Triassic (Metcalfe, 1996; Stampfli and Borel, 2002; Golonka et al., 2006; Blakely, 2008). Accretion is constrained by the Cimmerian orogeny in present-day Iran, which initiated in the late Triassic (Sengor, 1987; Stampfli and Borel, 2002; Hassanzadeh et al., 2008), the collision of Sibumasu/Malaya to Indochina by 250–220 Ma (Metcalfe, 1999; Stampfli and Borel, 2002; Golonka, 2007) and 200–160 Ma for other elements including Qiangtang (North Tibet) and Helmand (Stampfli and Borel, 2002). The accretion of South Tibet varies from 200 to 160 Ma (Stampfli and Borel, 2002), 150 Ma (Golonka et al., 2006) and 120 Ma related to a separate episode of accretion (Metcalfe, 1996).

Following closure of the paleo-Tethys and accretion of the Cimmerian terrane, several back-arc basins opened as a response to slab-pull forces along the Tethyan subduction zone. The major back-arc complexes include the Pindos, Maliac, Meliata, Küre, Sangpan, Kudi, Vardar (Stampfli and Borel, 2002) and the early Cretaceous Taurus, Troodos, Hatay and Baer-Bassit ophiolite complexes (Whitechurch et al., 1984). The closure of these back-arc basins varied along the margin from Triassic to Cenozoic (Stampfli and Borel, 2002), with a date of ~70–65 Ma for the obduction of the Taurus, Troodos, Hatay and Baer-Bassit ophiolite complexes (Whitechurch et al., 1984) and an early Cenozoic age of obduction for the Pindos and Vardar back-arc basins (Stampfli and Borel, 2002). As these back-arc basins opened and closed, inferred NE–SW directed spreading continued in the meso-Tethys (or neo-Tethys ocean) orthogonal to the Gondwana rifted margin (Stampfli and Borel, 2002). The cessation of spreading in the meso- or neo-Tethys is difficult to ascertain. However, Stampfli and Borel (2002) postulate that the subduction of the mid-ocean ridge diachronously across the margin can be tied to the initiation of rifting of the Argoland Block/West Burma from the northwest shelf of Australia, thus timing the cessation of spreading in the meso-/neo-Tethys ocean.

A third phase of rifting along the northern Gondwana margin in the northwest Australian shelf initiated in the late Triassic (Müller et al., 2005). The models of Metcalfe (1996) and Heine et al. (2004) label the resultant ocean basin as the neo-Tethys as their models extend the Argo Abyssal Plain mid-ocean ridge north of Greater India. Hence, this ocean basin forms part of the Tethys ocean domain. However, most other studies associate the Argo Abyssal Plain with the Indian Ocean because they follow the Argo spreading ridge southward between India and Australia, thus representing earliest Indian Ocean spreading. The preserved seafloor spreading record in the Argo Abyssal Plain confirms that spreading initiated around 156 Ma leading to the separation of the West Burma Block from the northwest Australian margin (Heine and Müller, 2005). The model of Metcalfe (1996) suggests that Lhasa (South Tibet) also rifted off the northern margin of Greater India at the time. Spreading in the Argo Abyssal Plain is described in the Indian Ocean section of this paper. The West Burma Block was carried northward due to continuing subduction along the northern Tethyan margin and sutured to Sibumasu in the Cretaceous around 80 Ma (Lee and Lawver, 1995; Metcalfe, 1996; Heine and Müller, 2005).

The termination of spreading in the Tethys Ocean is controversial. The model of Stampfli and Borel (2002) suggests cessation of spreading in the early Cretaceous when the meso- or neo-Tethys spreading ridge intersected the Tethyan subduction zone. However, other models (Metcalfe, 1996; Heine et al., 2004; Heine and Müller, 2005) suggest that neo-Tethyan spreading continued through the Cretaceous, merging into the Wharton Basin spreading ridge from the end of the CNS to 43 Ma (Heine et al., 2004). The final closure of the Tethys Ocean started with the collision of Greater India to the southern Eurasian margin either around 55 Ma (Lee and Lawver, 1995) or 35 Ma (Van der Voo et al., 1999b; Hafkenscheid et al., 2001; Aitchison et al., 2007) marked by the Indus-Tsangpo Suture zone and ended with the closure of the Tethyan seaway between Arabia and Iran forming the Zagros Mountains (Hessami et al., 2001). Several fragments of Tethyan ocean floor are postulated to underlay some of the basins in the eastern Mediterranean (see Müller et al., 2008a).

In the Mediterranean region, several Cenozoic back-arc basins formed due to the convergence between Eurasia and Africa (Rosenbaum et al., 2002). The Liguro–Provençal basin opened from around early Oligocene (~35 Ma) due to the eastward rollback of Apennines subduction (e.g.

Carminati et al., 2004) and the rotation of Corscia and Sardinia (Speranza et al., 2002) and the accretion of the Kabylies blocks to the African margin (e.g. Rosenbaum et al., 2002). Additional extensional basins such as the Pannonian basin were associated with Africa–Eurasia collision and associated with the Carpathian, Ionian and Hellenic subduction zones (Faccenna et al., 2001).

Our model for the evolution of the Tethys Ocean closely follows that of Heine et al. (2004), which is largely based on Stampfli and Borel (2002) except in the Jurassic–Cretaceous. We agree with the separation of the Tethys into three oceanic domains, as first suggested by Metcalfe (1996) and adopted by Heine et al. (2004). We define the paleo-Tethys as the ocean basin that formed after the separation of the Hunic superterrane from the northern Gondwana margin, the meso-Tethys as the ocean basin that formed after the separation of the Cimmerian terrane from the northern Gondwana margin and the neo-Tethys as the ocean basin that formed when West Burma/Argoland separated from northwest Australia. Finite rotations describing the opening of all three basins as well as associated seafloor spreading isochrons are mostly derived by following the model of Stampfli and Borel (2002) and Heine et al. (2004).

We follow a Devonian opening model for the paleo-Tethys (Metcalfe, 1996) but do not discount that opening may have been diachronous and occurred as early as the Silurian (Stampfli and Borel, 2002) in the western Tethys. As the reconstructions presented in this paper do not extend beyond 200 Ma, we will not describe the accretionary history of the Hunic superterrane. We agree with Stampfli and Borel (2002) that the cessation of spreading in the paleo-Tethys led to southern ridge jump, initiating opening of the meso-Tethys around 280 Ma, coincident with the collision of the Hunic terrane to the southern Laurasian margin and the initiation of rifting of the Cimmerian terrane from the northern Gondwana margin in the early–mid Permian (Metcalfe, 1996). We invoke NE–SW directed spreading for the meso-Tethys consistent with Stampfli and Borel (2002). The accretion of the Cimmerian terrane to the southern Laurasian margin also marks the closure of the paleo-Tethys ocean. We broadly follow the timing of accretion based on Golonka et al. (2006) and Golonka (2007). The uncertainty in the southern extent of the Laurasian margin means that the timing of accretion may change significantly depending on the southern extent of the Laurasian continental margin. Following the closure of the paleo-Tethys, a margin-wide episode of back-arc opening occurred along the southern Eurasian margin—from China to western Europe. This back-arc system was responsible for the crust that now forms part of the Cretaceous aged ophiolite complexes through southern Europe, Cyprus (Troodos), Iran and Oman. Although these basins are known to have existed after the closure of the paleo-Tethys, we do not include their formation (e.g. Whitechurch et al., 1984; Robertson, 2000; Stampfli and Borel, 2002) as we focused on the broad-scale development of the Tethys Ocean. However, these back-arc basins have played a vital role in the development of the region and we anticipate that a thorough review of ophiolite complexes and back-arc basin correlatives will be included in the next generation of the plate motion model.

Our model invokes continuous seafloor spreading in the meso-Tethys from 280 Ma to 145–140 Ma. The neo-Tethys ocean forms with rifting and seafloor spreading in the Argo Abyssal Plain, following the model of Heine and Müller (2005), isolating the West Burma Block from the Gondwana margin. We initiate seafloor spreading at 156 Ma and extend the mid-ocean ridge westward, north of Greater India where it intersects with a Tethyan transform fault. The accretion of West Burma to Sibumasu occurred at 80 Ma, following Heine and Müller (2005). Seafloor spreading in the neo-Tethyan ocean continued unabated eventually transforming into the Wharton basin spreading ridge system in the eastern Indian Ocean until 43 Ma (Singh et al., 2010).

In the western Mediterranean, we reconstruct the continental blocks that comprise southern Europe and the Middle East in the same manner as in Müller et al. (2008a). The basins floored by oceanic crust in the Mediterranean fall into two types. The Mesozoic basins in the eastern Mediterranean (e.g. Levant basin and Ionian Sea) represent the oldest preserved in-situ ocean floor, ranging in age from about 270 Ma (Late Permian) to 230 Ma (Middle Triassic) according to our model. The Cenozoic basins in the western Mediterranean (e.g. Liguro–Provençal Basin) are reconstructed based on the tectonic model and rotations from Speranza et al. (2002), describing a Miocene counter-clockwise rotation of Corsica–Sardinia relative to Iberia and France, thereby creating accommodation space for back-arc opening.

3.4. Marginal and back-arc basins

The present day distribution of the continents and oceans includes many smaller ocean basins that formed either in a back-arc setting behind a retreating subduction zone (Karig, 1971; Sleep and Toksoz, 1971; Uyeda and Kanamori, 1979; Taylor and Karner, 1983; Faccenna et al., 2001; Sdrolias and Müller, 2006) or as a result of continental rifting without the influence of a subduction zone forming marginal seas. The presence of ophiolites embedded within accreted terranes provides evidence for the opening and closing of marginal seas and back-arc basins in the past, most notably along the Tethyan margin and in the western North American margin. We have modeled some of the major marginal and back-arc basins observed in the seafloor spreading record today. We have also modeled the opening of three critical marginal and back-arc basins that existed in the past but have been subsequently destroyed. These include the Mongol–Okhotsk Ocean in Central Asia, the marginal basins that formed in the Caribbean, off the coast of western North America and the proto-South China Sea. We also model the opening of the Caribbean, which includes a combination of marginal seas and back-arc basins.

3.4.1. Caribbean

The Caribbean resides between the North American and South American plates and contains Jurassic–Cretaceous ocean floor in the Gulf of Mexico and Venezuela Basin, Cenozoic ocean basins such as the Cayman Trough, Gernada and Yucatan Basins, numerous continental blocks, accreted terranes, volcanic arcs and the Caribbean Large Igneous Province (CLIP) (Figs. 3 and 9). The sedimentary basins surrounding the Gulf of Mexico are some of the world's most productive hydrocarbon bearing basins, prompting quite detailed studies of the tectonic evolution of the region (Pindell, 1987; Burke, 1988; Ross and Scotese, 1988; Pindell and Kennan, 2009). The development of the Caribbean is tied to break-up of Pangea and rifting in the Central Atlantic, which extended into the Caribbean during the Triassic to earliest Cretaceous. This early phase formed rift basins, stretched continental crust and salt basins in areas such as the South Florida Basin, Great Bank of the Bahamas, Yucatan and along northern South America (Pindell and Kennan, 2009). To the west, a continuous subduction zone along the eastern margin on Panthalassa was consuming oceanic lithosphere beneath the western margin of the proto-Caribbean/trans-American region.

The Gulf of Mexico is bounded by predominately Triassic–Jurassic syn-rift structures and salt bearing basins and is partly floored by Jurassic–Cretaceous oceanic crust. The timing of seafloor spreading in the Gulf of Mexico is not well constrained with ages ranging from 158 to 170 Ma based on the timing of salt deposition and regional changes in structural trend and block rotations (Buffler and Sawyer, 1983; Ross and Scotese, 1988; Pindell and Kennan, 2009). The cessation of extensional faulting in the SE Gulf of Mexico and the dating of a post-rift unconformity (Ross and Scotese, 1988; Marton and Buffler, 1999; Pindell and Kennan, 2009), places the cessation of seafloor spreading in the latest Jurassic-earliest Cretaceous between 145 and 135 Ma. The opening of the Gulf of Mexico led to a two-stage anti-clockwise rotation of the Yucatan Block away from North America into its present day location (Pindell and Kennan, 2009).

The existence of a proto-Caribbean Basin has been hypothesized based on the accommodation space created by the relative motion

between the North and South American plates. The development of this basin (its orientation and timing) is therefore purely dependent on the chosen plate tectonic model. Opening of the basin was either coincident with spreading in the Gulf of Mexico (Meschede and Frisch, 1998; Pindell and Kennan, 2009) or initiated only after a southward ridge jump in the early Cretaceous (Ross and Scotese, 1988). Models that propose the encroachment of proto-Pacific oceanic lithosphere into the Caribbean (e.g. Ross and Scotese, 1988; Pindell and Kennan, 2009) imply that all evidence of the proto-Caribbean Basin was subducted by the late-Cretaceous–early Cenozoic, whereas models that do not invoke an advancing trench relate NE–SW trending magnetic lineations in the Venezuela Basin (Ghosh et al., 1984) to the proto-Caribbean Basin (Meschede and Frisch, 1998).

One of the major features that controlled the broad-scale development of the Caribbean is the nature of the plate boundary between the Caribbean and Panthalassa/Pacific Ocean. Most models agree that east-dipping trans-America subduction was consuming proto-Pacific oceanic lithosphere during the Triassic–Cretaceous (Ross and Scotese, 1988; Meschede and Frisch, 1998; Pindell and Kennan, 2009). However, models subsequently diverge into either "Pacific origin" (Malfait and Dinkelman, 1972; Burke, 1988; Ross and Scotese, 1988; Pindell and Kennan, 2009) or "intra-American origin" scenarios (Meschede and Frisch, 1998; James, 2006). "Pacific-origin" scenarios propose a switch in the polarity of the trans-American plate boundary from east-dipping to southwest-dipping in the late Cretaceous along the Caribbean/Greater Antilles Arc, causing the subduction of the proto-Caribbean Basin and encroachment of oceanic lithosphere from the Pacific domain into the Caribbean. The timing of this polarity flip is believed to be around 100–90 Ma (Ross and Scotese, 1988; Pindell and Kennan, 2009) and constrained to 90 Ma in the south on Aruba and within the Bonaire Block (van der Lelij et al., 2010). Continued northeastward rollback of the subduction hinge eventually caused collision with Yucatan and accretion of the arc along the Bahamas Platform. In the model of Ross and Scotese (1988) this accretion led to a jump in the locus of subduction westward, initiating subduction along the Panama–Costa Rica Arc around 60 Ma. However, other models place the initiation of Panama–Costa Rica Arc to 80–88 Ma (Pindell and Kennan, 2009) before the accretion of the Caribbean Arc to the Bahamas Platform. Recent tectonostratigraphic and geochemical data from exposed rocks in southern Costa Rica and western Panama indicate protoarc initiation on top of CLIP basement occurred between 75 and 73 Ma (Buchs et al., 2010). Irrespective of timing, in the "Pacific origin" model, the initiation of the Panama–Costa Rica Arc trapped Pacific-derived oceanic lithosphere (now underlying the Venezuela Basin) as well as the CLIP onto the Caribbean plate. "Intra-American origin" models assume a continuous trans-America east-dipping subduction zone, which provided a permanent barrier between the Pacific/Panthalassa and Caribbean. Concurrently, southwest-dipping subduction to the east of the proto-Caribbean Basin led to the docking of tectonic elements along the Bahaman Platform. In the "intra-American" model, the origin of the oceanic lithosphere underlying the Venezuela Basin and the CLIP are both derived in-situ. This model implies that the Panama–Costa Rica Arc was built upon a much older arc sequence.

After ~60 Ma, most models for the Caribbean are largely similar on a broad scale. After the establishment of subduction along the Panama–Costa Rica Arc, the Caribbean plate became a stationary feature influenced only by the relative motions between the North and South American plates (Ross and Scotese, 1988). The southern margin of the Bahaman platform changed from convergence to sinistral strike-slip after the accretion of arc terranes with E–W transform faults dominating the region. To the east, west-dipping subduction and arc volcanism along the Aves Ridge were still occurring. To the south, thermochronological and sedimentological analyses suggest that the Bonaire Block collided with the South American margin at ~50 Ma thereby constraining the change from convergence to strike-slip along South America (van der Lelij et al., 2010). The new tectonic regime led to opening of the Yucatan and Grenada–Tobago Basins in the Paleogene, Cayman Trough since the Eocene (Ross and Scotese, 1988; Pindell and Kennan, 2009) and the Puerto Rico Basin in the Oligocene (Ross and Scotese, 1988).

The Yucatan Basin currently resides between Cuba and the Cayman Ridge and is believed to have formed prior to the collision of the Caribbean Arc as a passive response to the northwestward rollback of the trench (Pindell et al., 2006). The cessation of spreading is correlated with the docking of the arc terranes along Cuba and the Bahaman Platform. The Grenada–Tobago Basin formed as a back-arc between the Aves Ridge and Lesser Antilles Ridge due to the eastward rollback of the Lesser Antilles Trench. The timing of spreading is unconstrained by magnetic anomaly interpretations but initiation is believed to have occurred sometime in the Paleogene based on the cessation of plutonism on the Aves Ridge (Pindell et al., 1988) and from seismic stratigraphy and heatflow measurements within the basin (Speed, 1985; Pindell and Kennan, 2009). Spreading is believed to have ceased in the Oligocene coincident with the collision of the Lesser Antilles forearc with the Venezuelan margin (Pindell and Kennan, 2009). The Cayman Trough formed as a left-lateral pull-apart basin between two major transform faults starting at Chron 19 (~41 Ma) (Rosencrantz et al., 1988; Ross and Scotese, 1988) based on the interpretation of magnetic anomalies. The Puerto Rico Basin opened in the Oligocene–early Miocene as a result of relative motion between Hispaniola and the Caribbean plate (Ross and Scotese, 1988).

Our model largely follows the hierarchical model of Ross and Scotese (1988) (with an updated timescale) and elements of Pindell and Kennan (2009), with minor adjustments based on recent geological information and an updated spreading model in the Central and Equatorial Atlantic. Rifting in the Caribbean since the Triassic connected to the Central Atlantic rift zone through Florida and Gulf of Mexico and extended westward to the trans-America subduction zone, which was actively consuming Panthalassic ocean floor. In our model, we follow the initiation of spreading in the Gulf of Mexico at 170 Ma based on Ross and Scotese (1988) coincident with accelerated seafloor spreading rates in the Central Atlantic (Labails et al., 2010) (Fig. 8). We update the cessation of spreading to 145 Ma based on evidence presented in Pindell and Kennan (2009). After the cessation of spreading in the Gulf of Mexico, we model a ridge jump to the south initiating the opening of the proto-Caribbean Basin within the accomodation space created by the relative motion between the North and South American plates (Fig. 8). Spreading was NW–SE directed and initiated around 145 Ma forming a triple junction to the east between the mid ocean ridge of the Central Atlantic and rift axis of the Equatorial/South Atlantic. To the west, the mid ocean ridge of the proto-Caribbean Basin formed a ridge–ridge–transform triple junction with the spreading ridge of the Andean back-arc basin and the trans-American subduction zone.

We favor the "Pacific-origin" model for the formation of the Caribbean plate with a subduction polarity flip of the trans-America subduction zone to west-dipping along the eastern boundary of the Caribbean Arc at 100 Ma (Fig. 8). The rollback of this subduction zone led to the consumption of the actively spreading proto-Caribbean ocean floor and encroachment of the Farallon plate into the Caribbean domain. Our model predicts that the oceanic lithosphere intruding into the Caribbean (and currently underlying the Venezuela Basin) formed along the Pacific–Farallon ridge between Chrons M16-M4 (~139–127 Ma) at a latitude of around 10–15°S, agreeing well with paleomagnetic constraints, which suggest an equatorial formation for the oceanic crust of the Nicoya Complex (Duncan and Hargraves, 1984). The continued roll-back of the Caribbean Arc subduction zone led to the formation of the Yucatan Basin as a back-arc in the late Cretaceous with cessation of spreading occurring at 70 Ma when the Caribbean Arc accreted to the Bahaman

Platform. The accretion led to a jump in the locus of subduction westward along the newly developed Panama–Costa Rica to accommodate the continued eastward motion of the Farallon plate, trapping Farallon oceanic lithosphere onto the Caribbean plate in the process. The eruption of the Caribbean flood basalt province occurred around 90 Ma on top of the oceanic lithosphere that now underlies much of the Caribbean ocean floor (Sinton et al., 1998). The Caribbean flood basalt province (or CLIP) has been suggested to be the product of the Galapagos hotspot (Pindell and Kennan, 2009), however in our model the CLIP erupted on Farallon oceanic lithosphere over 2000 km away from the present day position of the Galapagos hotspot precluding this as a source, even assuming the motion of hotspots relative to each other (Fig. 10).

Coincident with subduction along the proto-middle America trench was west-dipping subduction to the east along the Aves/Lesser Antilles Ridge, consuming Atlantic Ocean floor (Fig. 8). The rollback of this subduction zone led to the formation of the Grenada Basin between the Aves and Lesser Antilles Arcs in the Paleogene. In the middle Eocene (41 Ma), relative motion between North America and Caribbean began to form the Cayman Trough along sinistral faults that later merge with the Lesser Antilles trench. In the early Miocene (20 Ma), the Cayman Trough continued to expand and develop, and the Chortis Block moved over the Yucatan promontory. Westward motion of the North American plate relative to the slow moving Caribbean plate was accommodating the opening of the Cayman Trough. The Puerto Rico Basin formed in the Oligocene–early Miocene due to a similar process. Currently, opening is continuing within the Cayman Trough accommodated by the motion along the bounding transforms. Active subduction of Atlantic oceanic lithosphere is occurring along the Lesser Antilles Trench, which connects up to the Mid-Atlantic Ridge along the Researcher Ridge and Royal Trough (Müller et al., 1999).

3.4.2. Mongol–Okhotsk Basin

The Mongol–Okhotsk Basin is a Mesozoic ocean basin that existed between the Siberian craton to the north and the Amuria/Mongolia block to the south. The Mongol–Okhotsk suture zone defines basin closure (Apel et al., 2006; Golonka et al., 2006; Cocks and Torsvik, 2007). Evidence for the existence of the Mongol–Okhotsk Basin is found in a series of remnant island arc volcanics and ophiolites adjacent to the suture zone as well as a large area of seismically fast material in the lower mantle underlying Siberia imaged in seismic tomography (Van der Voo et al., 1999a).

The opening of the Mongol–Okhotsk Basin is not well constrained, ages range from 610 to 570 Ma (Sengör et al., 1993), Ordovician (Cocks and Torsvik, 2007), Cambrian (Harland et al., 1990) and Permian (Zorin, 1999; Kravchinsky et al., 2002). The large age range stems from the associations made between geological units in the Siberia, Mongolia and North China realm and the definition of the ocean basins that existed between these geological units. A zircon age of 325 Ma from a leucogabbro pegmatite has been associated with oceanic crust from the Mongol–Okhotsk Ocean (Tomurtogoo et al., 2005) indicating that seafloor spreading was active from at least the late Carboniferous. In addition, paleomagnetic data suggests that Siberia and Mongolia were separated by 10–15° (Zorin, 1999) by the Permian. The presence of continental volcano-sedimentary sequences and granitoid magmatism proximal to the suture zone indicates that the basin was being subducted northward during the Permian (Zorin, 1999), Triassic and Jurassic (Stampfli and Borel, 2002; Golonka et al., 2006). It is difficult to ascertain when seafloor spreading ceased in the Mongol–Okhotsk Basin. Triassic MORB basalts in the eastern part of the Mongol–Okhotsk belt (Golonka et al., 2006) provide a minimum age for seafloor spreading. Continued subduction along the Siberian margin led to initial closure of the Mongol–Okhotsk Ocean sometime in the Jurassic (Van der Voo et al., 1999a; Zorin, 1999; Kravchinsky et al., 2002; Stampfli and Borel, 2002; Golonka et al., 2006; Golonka, 2007) based on collision followed by folding and intrusion of granitic batholiths in Mongolia and the trans-Baikal area (Golonka et al., 2006) and the formation of the Mongol–Okhotsk Suture (Tomurtogoo et al., 2005). Complete closure may have ended as late as the early Cretaceous (Zorin, 1999) based on the cessation of compression in the area (Zorin, 1999). Alternative models exist that predict an older initial closure age of late Carboniferous (Badarch et al., 2002; Cocks and Torsvik, 2007), but again, this may be due to a difference in the definition of the Mongol–Okhotsk Ocean.

We have modeled the opening of the Mongol–Okhotsk Basin in the late Carboniferous to account for the zircon data of Tomurtogoo et al. (2005), followed by the onset of subduction along the Siberian margin in the late Permian. We continue seafloor spreading in the Mongol–Okhotsk Basin until the Permo-Triassic boundary (250 Ma). Based on our initiation and termination of spreading, we suggest that the Mongol–Okhotsk Ocean had a maximum width of about 4000 km. We model the closure of the Mongol–Okhotsk Basin to 150 Ma (late Jurassic) based on the overwhelming evidence in the literature for the dating of the Mongol–Okhotsk Suture.

3.4.3. North American margins

The western North American margin is characterized by the accretion of native and exotic terranes throughout the late Paleozoic and Mesozoic. The timing of formation of the numerous terranes with island arc affinities, their accretion onto the continental margin and other subduction-related structures provide constraints for the age, orientation and tectonics associated with the oceanic basins that formed adjacent to the margin. The Laurentian peri-continental margin was a passive Atlantic-style margin until the early Mesozoic (Nokleberg et al., 2001). Many accretion events have been recorded along this margin but we simplify them into three main sectors: the Yukon-Tanana/Quesnellia/Stikina terrane, the East Klamath terrane and the Wrangellia superterrane separated by major fault systems. There are many alternative interpretations for the source of the terranes, their age of formation, timing and location of accretion and their field relationships. Our model relies heavily on the reconstructions represented in Nokleberg et al. (2001) and Colpron et al. (2007) but note that other alternative scenarios exist.

Arc magmatism occurred along the western Laurentian margin ~390–380 Ma forming many of the rocks of the Yukon-Tanana Terrane (YTT) and western Kootenay terranes (Nokleberg et al., 2001) currently located in Yukon and southern Alaska (Fig. 7). The base of the YTT has isotopic, geochemical characteristics indicating a Laurentian source for the terrane (Nokleberg et al., 2001). Following a period of arc magmatism was a period with coeval rift-related magmatism leading to the rifting of the YTT from the Laurentian margin around 360–320 Ma (Mortensen, 1992; Nokleberg et al., 2001; Colpron et al., 2002; Nelson et al., 2006). The separation of the YTT was driven by N–NE dipping subduction and led to the opening of the Slide Mountain Ocean. The Slide Mountain ophiolite, which is currently emplaced onto the YTT and Cassier Terranes (Nokleberg et al., 2001) preserves evidence of this paleo-ocean basin. The Slide Mountain Ocean is less commonly referred to as the Anvil Ocean (Hansen, 1990). Some of the rocks related to arc magmatism were left on the margin (in the parautochthonous rocks of east–central Alaska and the Kootenay terrane) before the opening of the Slide Mountain Ocean while the majority of the YTT formed the base of the frontal arc (Nokleberg et al., 2001).

The Slide Mountain Ocean opened due to west–southwest slab roll-back, reaching a maximum width in the early Permian (Nelson et al., 2006) of around 1300 km (Nokleberg et al., 2001). Spreading in the back-arc basin ceased at around 280–260 Ma coincident with a subduction polarity reversal (Mortensen, 1992; Nokleberg et al., 2001) recorded in west-facing coveal calc-alkalic and alkalic plutons (Nokleberg et al., 2001). The subduction polarity reversal led to the formation of two adjacent arcs, the Stikinia and Quesnellia Arcs, overlying the YTT via a southwest-dipping subduction zone along the

eastern side of the YTT. This subduction led to the closure of the Slide Mountain Ocean and the accretion of the YTT/Quesnellia Arc to the Laurentian margin by the middle Triassic (240–230 Ma) (Hansen, 1990; Nokleberg et al., 2001; Nelson et al., 2006). The Stikinia Arc was still intraoceanic when the YTT/Quesnellia Arc accreted to the margin as it trends outboard of the Cache Creek Terrane (Fig. 7). The Cache Creek Terrane is a mid-Paleozoic to mid Jurassic oceanic terrane with exotic Permian Tethyan faunas in limestone blocks and long-lived island edifices (Nelson and Mihalynuk, 1993; Mihalynuk et al., 1994). The Cache Creek Terrane, which is very distinct from the Slide Mountain Terrane implies that another ocean basin, the Cache Creek Ocean, formed in between the Stikinia Arc to the west and the rapidly retreating YTT/Quesnellia Arc to the east. Based on trend-surface analysis of the distribution of Permian coral genera, taxonomic diversity and paleomagnetic data, Belasky and Runnegar (1994) predict that the Stikinia Arc was located up to 6700 km from the Laurentian margin in the early Permian and that the Eastern Klamath terrane was located proximal to the Stikinia Arc.

To address the field relationships of the YTT, Quesnellia Arc, Cache Creek Terrane and Stikinia Arc, Colpron et al. (2007) invoke an "oroclinal" model whereby the Stikinia Arc segment rotated counterclockwise consuming the Cache Creek Ocean along a west–southwest-dipping subduction zone. The rotation of the Stikinia Arc may have initiated as early as ~230 Ma. The timing of accretion of the Stikinia Arc to the North American margin and therefore the closure of the Cache Creek Ocean is tightly constrained to around 172–174 Ma (Colpron et al., 2007 and references therein). However, collision may have started in the early Jurassic coincident with a phase of cooling (Nokleberg et al., 2001).

The next major event to affect the margin was the accretion of the exotic Wrangellia superterrane. The basement of the Wrangellia superterrane consists of Triassic flood basalts (285–297 Ma) that formed at equatorial latitudes and overlain by a carbonate platform (Richards et al., 1991; Greene et al., 2008). Although recent data suggests initial collision with the North American margin at about 175 Ma (Gehrels, 2001, 2002; Colpron et al., 2007), the main accretion event occurred at 145–130 Ma (Nokleberg et al., 2001; Trop et al., 2002). There is controversy over whether the allochthonous terranes (including Wrangellia) of southern Alaska and western Canada were originally accreted (1) ≤1000 km of their existing location, offshore present day British Columbia, Oregon, and Washington, during the late Mesozoic and early Cenozoic or (2) were located 1000–5000 km along the western coast of the North American Craton and subsequently transported northwards during the Late Cretaceous and Cenozoic (Keppie and Dostal, 2001; Stamatakos et al., 2001). After collision, the Wrangellia terrane underwent margin-parallel dextral motion but the amount of dextral motion is a matter of debate.

We model the evolution of the marginal and back-arc basins that formed along the western North American margin as described above. We create a set of synthetic seafloor spreading isochrons to depict the opening of the Slide Mountain Ocean starting at 340 Ma based on a margin parallel opening and a maximum opening width of 1300 km, suggested by Nokleberg et al. (2001). Break-up may have been at least partially driven by a mantle plume as our reconstructions show that the plume associated with the present day Azores hotspot closely corresponds to the break-up location. Osmium isotopes suggest that Azores has a deep origin (Schaefer et al., 2002) suggesting that this plume may have been long-lived but whether hotspots are active and can be traced as far back as 340 Ma remains open to debate. We terminate spreading in the Slide Mountain Ocean at 280 Ma followed by a subduction polarity flip along the YTT and the establishment of an eastward retreating subduction zone. Subduction led to the consumption of the Slide Mountain Ocean along this southwest–west dipping subduction zone.

We form the Cache Creek Ocean in between the retreating YTT and the Stikinia Arc and East Klamath at 280 Ma with a cessation of spreading in the Cache Creek Ocean simultaneous with the accretion of the YTT along the Laurentian margin at 230 Ma. This is followed by the subduction of the Cache Creek Ocean behind a rapidly retreating west-dipping subduction zone along the eastern side of the Stikinia Arc and East Klamath (Fig. 17). The Stikinia Arc and East Klamath accrete to the North American margin at 172 Ma (Fig. 17), resulting in the emplacement of the Cache Creek ophiolite between the Stikinia Arc and the Quesnellia Arc. We accrete the Wrangellia superterrane to the margin at 140 Ma following the northern accretion model. The accretion of the Wrangellia Terrane marks the true establishment of the boundary between North America and the Pacific.

3.4.4. Proto-South China Sea

A Mesozoic–Cenozoic back-arc basin situated adjacent to the Eurasian passive margin, named the proto-South China Sea, is incorporated into many regional models of SE Asia (Hamilton, 1979; Holloway, 1982; Williams et al., 1988; Hutchison, 1989; Lee and Lawver, 1994; Hall, 2002). Rifting is believed to have initiated along the South China margin in the late Cretaceous (Ru and Pigott, 1986; Lee and Lawver, 1994) although a rift-related unconformity is dated to the early Cretaceous (Lee and Lawver, 1994). This rift event led to the separation of northern Borneo from the South China margin resulting in the formation of NE–SW trending structures and sedimentary basins (Lee and Lawver, 1994). The provenance of ophiolitic igneous rocks in northwest Borneo from late Jurassic–late Cretaceous (based on the dating of sediments overlying pillow basalts) is tied to the proto-South China Sea (Hutchison, 2005), further constraining the timing of formation of the basin.

The cessation of spreading in the proto-South China Sea and its lateral extent is unknown. Most models invoke the initiation of closure in the early Cenozoic/early Neogene beneath Kalimantan/northern Borneo and Palawan (Ludwig et al., 1979; Williams et al., 1988; Lee and Lawver, 1994; Hall, 2002). The closure is believed to have been triggered either by the counterclockwise rotation of Borneo (Hall, 2002) or by the southeast extrusion of Indochina (Lee and Lawver, 1994).

We model the opening of the proto-South China Sea during rifting between the stable Eurasian margin and northern Borneo during the late Cretaceous (~90 Ma) with spreading orthogonal to the Eurasian margin. The cessation of spreading occurred at 50 Ma coincident with the clockwise rotation of the neighboring Philippine Sea plate. The dramatic change in motion of the Philippine Sea plate reorganized the plate boundaries in the area leading to the establishment of a subduction zone between Palawan and the proto-South China Sea, which began actively consuming the proto-South China Sea since 50 Ma with an increase in convergence rate from 25 Ma. We model complete closure of the proto-South China Sea at around 10 Ma behind a subduction zone located along Palawan and the north Borneo/Kalimantan margin.

3.4.5. Western Pacific and SE Asian back-arc basins

The continental blocks and basins in SE Asia comprise one of the most complex regions in the world. Most models focus on the Cenozoic interpretation of onshore geology, including: Rangin et al. (1990), Lee and Lawver (1995), and Hall (2002). Other models couple the seafloor spreading history in the back-arc basins of both SE Asia and the Western Pacific for a continent and ocean basin evolution (Gaina and Müller, 2007). The model we use in our reconstructions is based on Gaina and Müller (2007) and additionally incorporate the rotation of the Philippine Sea plate based on Hall et al. (1995) and the seafloor spreading model of Sdrolias et al. (2003b) for spreading in the Parece Vela and Shikoku Basins. For further details of the model, we refer to Sdrolias et al. (2003b) and Gaina and Müller (2007).

3.4.6. SW Pacific Back-arc basins and marginal seas

The SW Pacific is characterized by a series of marginal basins (Tasman and Coral Seas), submerged continental slivers (Lord Howe

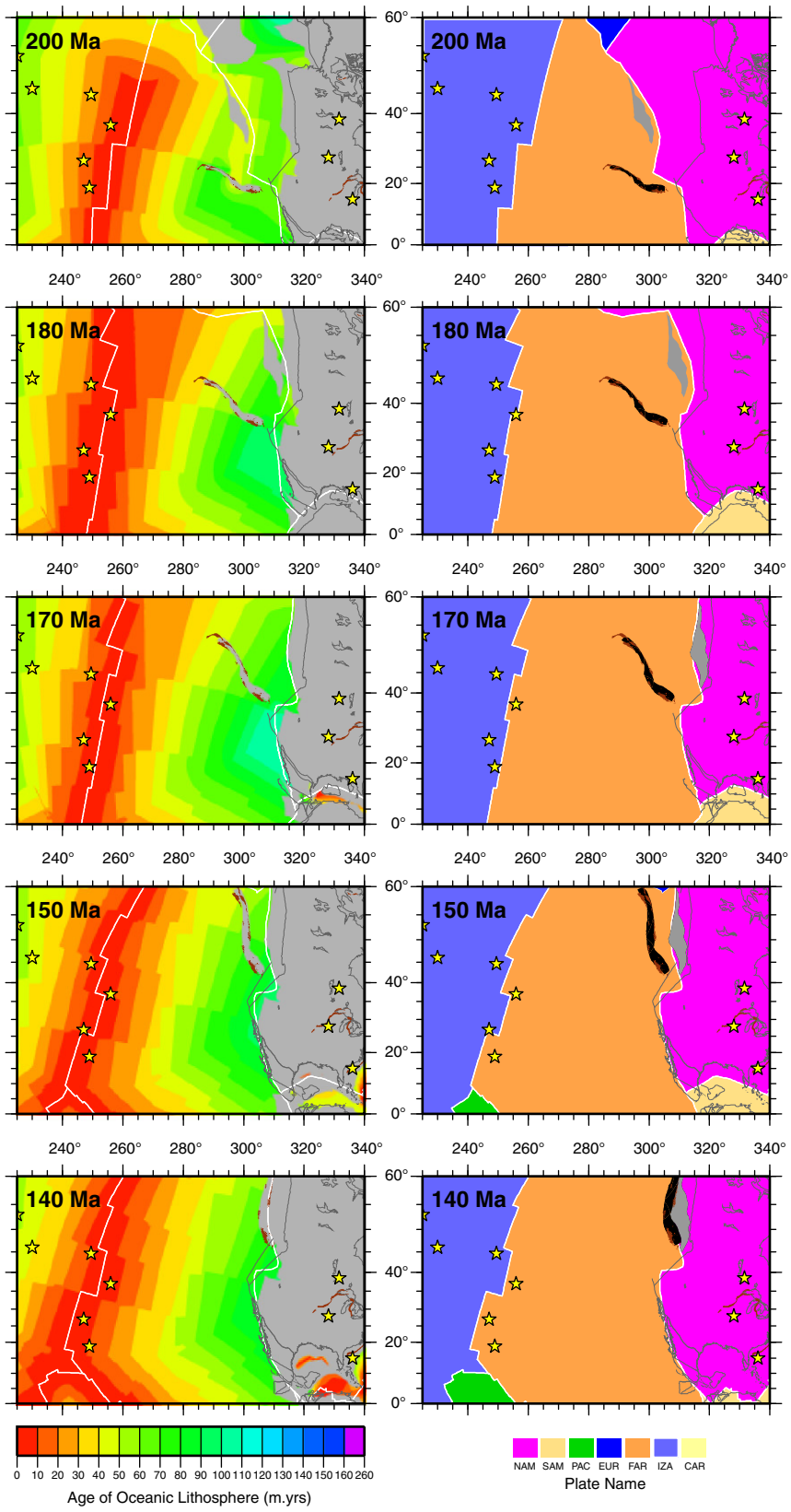

Fig. 17. (left) Agegrid reconstructions of Mesozoic North America at 200, 180, 170, 150, 140 Ma highlighting the age–area distribution of oceanic lithosphere at the time of formation and the extent of continental crust (gray polygons). Plate boundaries from our continuously closing plate polygon dataset are denoted as thick white lines, hotspot locations as yellow stars, large igneous provinces and flood basalts as brown polygons and coastlines as thin black lines. (right) Reconstructions showing the outlines of the plates around Mesozoic North America for each reconstruction time listed above. Feature descriptions as in panel (left). Abbreviations are: CAR = Caribbean plate, EUR = Eurasian plate, FAR = Farallon plate, IZA = Izanagi plate, NAM = North American plate, PAC = Pacific plate, SAM = South American plate. (For interpretation of the references to color in this figure legend, the reader is referred to the web version of this article.)

Rise, Mellish Rise, Louisiade, Papuan, Kenn, Dampier and Chesterfield Plateaus), island arcs (Norfolk, Three-Kings, Loyalty, New Hebrides, Vitiaz and Lau-Colville Ridges), back-arc basins (South Loyalty, North Loyalty, Norfolk, South Fiji, North Fiji and Lau Basins and Havre Trough) as well as numerous features with an uncertain origin (e.g. D'Entrecasteaux Zone and Basin and Rennell Trough and Basin) (Fig. 11). In a broad sense, these features developed behind the eastward migrating Australia–Pacific plate boundary from the late Mesozoic to the present day (Karig, 1971; Symonds et al., 1996; Müller et al., 2000; Crawford et al., 2002; Sdrolias et al., 2003a). Our plate motion model incorporates the opening model for the Tasman and Coral Seas based on Gaina et al. (1998) and Gaina et al. (1999). We incorporate the model of Sdrolias et al. (2003a) and Sdrolias et al. (2004) for the formation of the back-arc basin and island arc systems seaward of the Lord Howe Rise. For further details, we refer to the abovementioned publications.

4. Global plate reconstructions

Our regional kinematic models fit within a hierarchical global plate circuit tied to a hybrid moving hotspot/true polar wander corrected absolute reference frame through Africa. We create a set of dynamic plate polygons since the time of Pangea break-up with the assumption that the plates themselves are rigid. The birth of a plate (the establishment of relative motion after a break in the lithosphere), can be defined in two ways: either the initiation of rifting due to weakening of the lithosphere by basal heating forming a series of faults and rift-related structures (sometimes called incipient spreading), or the initiation of seafloor spreading, when there is a complete break of the lithosphere and extrusion of the mantle. Our plate boundary set distinguishes between the two modes via a continental/oceanic rift or mid-ocean ridge coding of the plate boundaries, which allows for the construction of a plate polygon dataset using either mode. The plate polygons presented in this study follow the former definition but an ancillary set can be produced to follow the later definition. Below we describe tectonic events every 20 million years with accompanying maps (Figs. 18–28) and also provide the plate polygon and plate boundary files. These files can be directly loaded into *GPlates* software for reconstructions in one million year time intervals.

4.1. 200–180 Ma (Figs. 18 and 19)

Prior to the Mesozoic, the continents were amalgamated into one big supercontinent, Pangea, surrounded by two ancient oceans, Panthalassa and the smaller Tethys Ocean. By the early–mid Mesozoic, Pangea was undergoing slow continental break-up centered along a rift zone extending from the Arctic, North Atlantic (adjacent to the Norwegian shelf and Iberia–Newfoundland margins), Central Atlantic and along the Jacksonville Fracture Zone through Florida and the Gulf of Mexico in the Caribbean region. The Caribbean rift zone, defined by a series of Mesozoic rift basins, connected with east-dipping trans-America subduction, which was consuming oceanic lithosphere from Panthalassa. At 190 Ma, there was a change from rift to drift along the early Atlantic rift, restricted to the Central Atlantic. Contemporaneously, dextral motion was occurring along the early Atlas Rift, isolating Morocco.

The Panthalassic Ocean was entirely surrounded by subduction during the mid–early Mesozoic. We model seafloor spreading as a simple three-plate system between the Izanagi, Farallon and Phoenix plates. The three arms of the triple junction extended outward intersecting with the circum-Panthalassic margins with minor margin migration: east of Australia (Izanagi–Phoenix ridge), along the Amurian margin (Izanagi–Farallon ridge) and southern North America (Farallon–Phoenix ridge). At 190 Ma, the birth of the Pacific plate established a more complex spreading ridge system involving three triple junctions and six spreading centers (Izanagi–Farallon, Izanagi–Phoenix, Izanagi–Pacific, Phoenix–Farallon, Phoenix–Pacific, Farallon–Pacific). Initially spreading along the Pacific ridges was slow/moderate (70–80 mm/yr) with a progressive increase in spreading rates to a peak in the mid Cretaceous. In northeast Panthalassa, closure of the Cache Creek Ocean (back-arc basin which formed between the Yukun-Tanana Terrane and the Stikinia Arc) was occurring along a southwest dipping subduction zone on the eastern side of the Stikinia Arc. In northwestern Panthalassa, the Mongol–Okhotsk Ocean (an ancient ocean basin which formed between Amuria and Siberia) continued its closure via northeast directed subduction along the southern Siberia margin. This Mongol–Okhotsk subduction zone connected with the landward-facing northern Panthalassic subduction zone to its northeast and the Tethyan subduction zone to its southwest.

In the Tethys Ocean, the remnant paleo-Tethys was separated from the actively spreading meso-Tethys ocean by the continental blocks of the Cimmerian terrane (e.g. Iran, Afghanistan, Pakistan, South Tibet, Sibumasu). The Tethyan subduction zone located along the southern Laurasian margin was driving the opening of the Meso-Tethys and consumption of the paleo-Tethys ocean. Active rifting was occurring along the Argo Abyssal Plain (NW Australia) that we suggest extended to the north of Greater India and westward to the East Africa/Karoo Rift, marking the break-up of Gondwanaland into West Gondwana (including South America, most of Africa and Arabia) and East Gondwana (including Antarctica, Australia, India, eastern Africa, Madagascar). We continue the Karoo Rift southward to connect with extension along the Agulhas-Falkland transform. This plate boundary between West Gondwana and Patagonia connected with east-dipping subduction along the South American/Panthalassa margin.

An extensive seaway between the Tethys Ocean and Panthalassa existed in the mid-Mesozoic. We envisage that the confluence of these two oceanic domains occurred north of Australia at the so-called Junction region/plate (Seton and Müller, 2008). The differential motion between the meso-Tethys and Izanagi plates results in convergence and we model the subduction of Izanagi lithosphere beneath a westward verging subduction zone.

4.2. 180–160 Ma (Figs. 19 and 20)

At 180 Ma, early opening by ultra-slow seafloor spreading continued in the Central Atlantic with ongoing rifting in the northern Atlantic and Caribbean. A readjustment of the plate-mantle system occurred at 170 Ma, coincident with a doubling of seafloor spreading rates in the Central Atlantic (Labails et al., 2010) and the establishment of seafloor spreading in the Gulf of Mexico. Evidence for changes in plate motion and accretion events in the Tethys Ocean and Panthalassa at 170 Ma (see below) may indicate a global plate reorganization event at this time.

This time period saw the accelerated growth of the Pacific plate at the expense of the Izanagi, Farallon and Phoenix plates. In northeast Panthalassa, closure of the Cache Creek Ocean, obduction of the Cache Creek Terrane and accretion of the Stikinia Arc occurred along the Laurentian margin between 175 and 172 Ma. The accretion of the Stikinia Arc forced a jump in the locus of subduction and reversal of subduction polarity from southwest to northeast along the new Laurentian margin, establishing the Farallon subduction zone. The northwest Panthalassa margin interacted with the Mongol–Okhotsk Ocean, which continued its closure along the southern Siberia subduction zone.

Rifting continued along the southern Tethyan margin, adjacent to Argoland/West Burma and northern Greater India to the east African rifts. In the western Tethys, volcanism ceased along the Karoo Rift at 180 Ma leading to a jump in the locus of rifting from the Karoo Rift to the area between Africa and Madagascar/Antarctica, later forming the Weddell and Riiser-Larson Sea and Mozambique and West Somali Basins. Incipient spreading in the Mozambique and West Somali

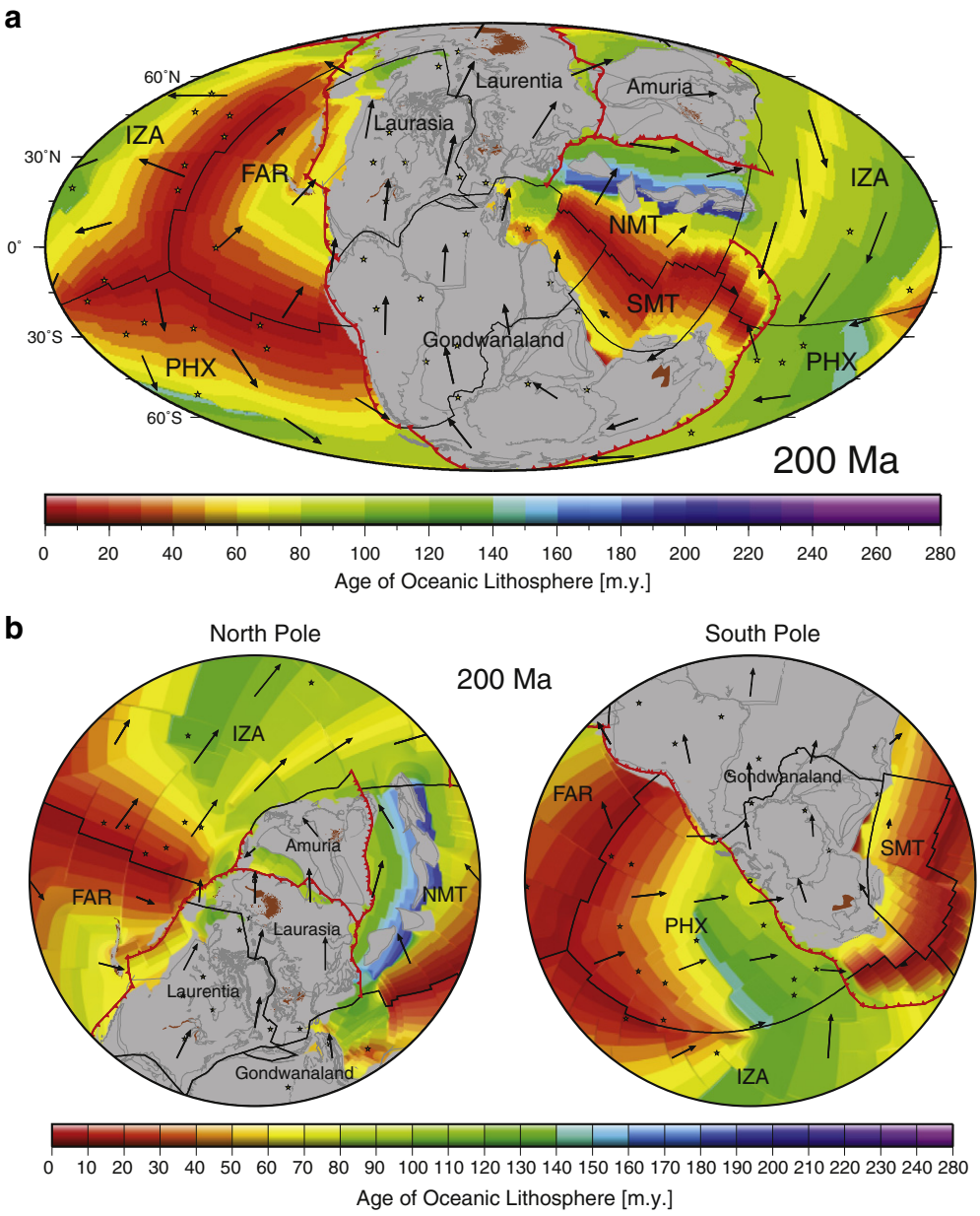

Fig. 18. Global plate reconstructions from 200 Ma to the present day in 20 million year time intervals. Basemap shows the age–area distribution of oceanic lithosphere at the time of formation. Red lines denote subduction zones, black lines denote mid-ocean ridges and transform faults. Brown polygons indicate products of plume-related excessive volcanism. Yellow stars are present day hotspot locations. Absolute plate velocity vectors are denoted as black arrows. Abbreviations for the plates are the same as in previous figures. Additional abbreviations include: ALA = Alaska, CA = Central Atlantic, CAP = Capricorn, CAR = Caribbean, CAT = Catequil, CCO = Cache Creek Ocean, COL = Colorado, CS = Caroline Sea, JUN = Junction, MOO = Mongol–Okhotsk Ocean, NL = North Loyalty Basin, NMT = North Meso-Tethys, NNT = North Neo-Tethys, PAR = Parana, PAT = Patagonia, PS = Philippine Sea, PSC = Proto-South China Sea, SCO = Scotia Sea, SLB = South Loyalty Basin, SMT = South Meso-Tethys, TS = Tasman Sea.

Basins connected with both the Weddell Sea rift and the Agulhas-Falkland transform in the south. In the northern Tethys, closure of the paleo-Tethys and accretion of the Cimmerian terrane occurred along the southern Laurasian margin at 170 Ma. Spreading in the meso-Tethys continued with an acceleration in spreading rate after the complete accretion of the Cimmerian terrane at 170 Ma. At 165 Ma, rifting extended southward from Argoland to the area between Australia and India (adjacent to the Gascoyne, Cuvier and Perth Abyssal Plains) thereby initiating a plate boundary between India and Australia. This connected with the newly established rift margin between Australia and Antarctica at 165 Ma and extended into the Enderby Basin from 165 Ma to the west connected with the Western Panthalassic subduction zone along eastern Australia to the east.

4.3. 160–140 Ma (Figs. 20 and 21)

The Central Atlantic continued spreading between 160 and 140 Ma, connecting with the Gulf of Mexico ridge system to the south. After the cessation of spreading in the Gulf of Mexico, the mid-ocean ridge jumped southward initiating the opening of the proto-Caribbean Basin through the accommodation space created due to the relative motion between the North and South American plates. Spreading was NW–SE directed and initiated around 145 Ma forming a triple junction to the east between the mid ocean ridge of the Central Atlantic and rift axis of the Equatorial/South Atlantic. To the west, the spreading ridge of the proto-Caribbean Basin formed a ridge–ridge–transform triple junction with the spreading ridge of the Andean back-arc basin and the trans-American subduction zone.

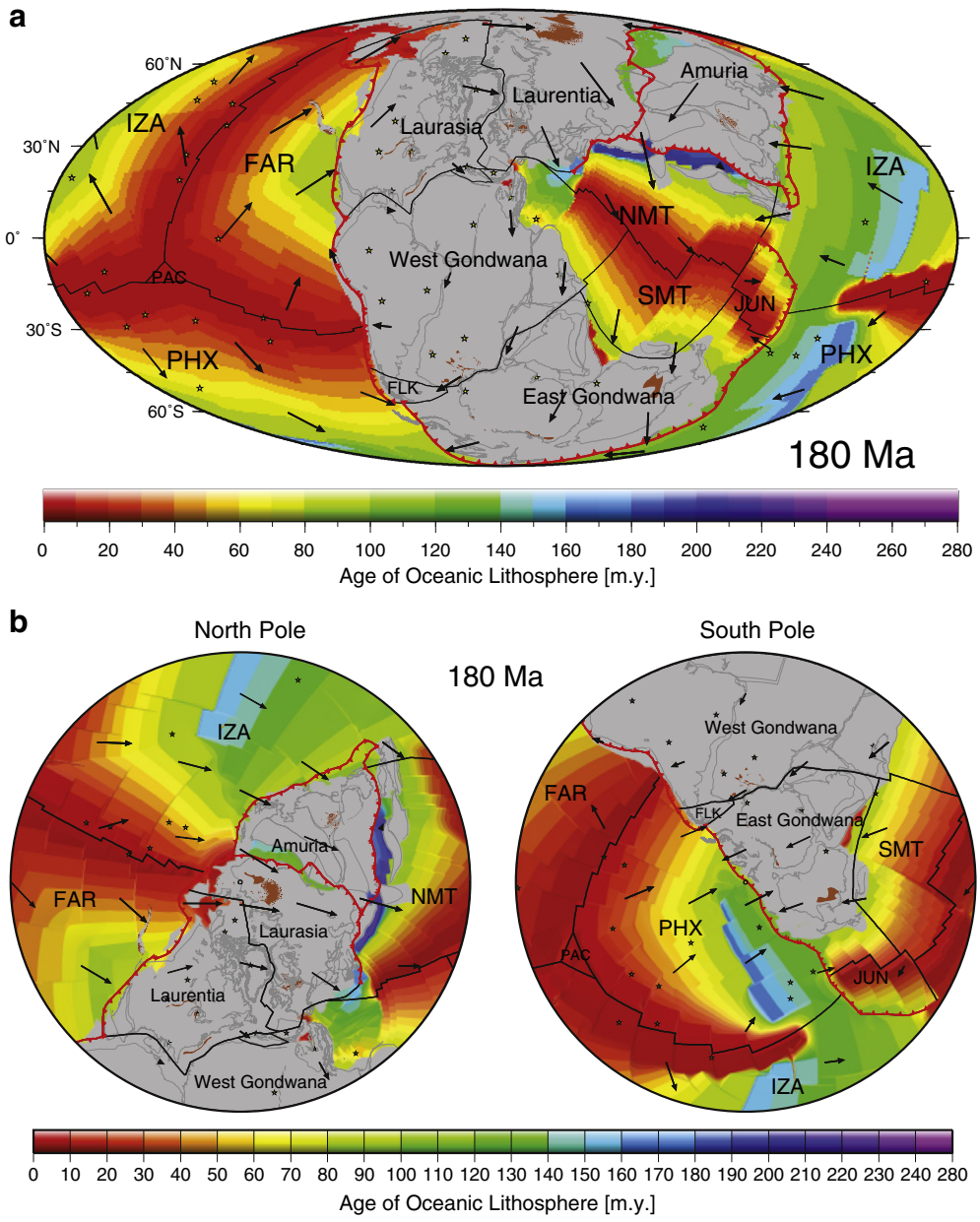

Fig. 19. Description same as Fig. 18.

In the South Atlantic, extension began within continental South America at 150 Ma, partitioning the southern part of the continent into the Parana and Colorado subplates and inducing a rift zone between South America and Africa, which connected to the Agulhas-Falkland transform to the south.

The Agulhas-Falkland transform extended eastward connecting to the mid-ocean ridge in the Weddell Sea, which was established at 160 Ma. The Weddell Sea ridge joined with mid-ocean ridges along East Africa, including between Africa and Antarctica in the Mozambique Basin/Riiser-Larson Sea and Africa and Madagascar in the West Somali Basin. This newly established ridge system led to an acceleration of break-up between East and West Gondwana. From 144 Ma onwards, Madagascar operated as an independent plate. In the eastern Tethys, rifting extended along the Argo Gascoyne, Cuvier and Perth Abyssal Plains forming a triple junction between the Australia/Antarctic rift margin and the Enderby rift. By 156 Ma, NW–SE oriented seafloor spreading begun in the Argo Abyssal Plain, rifting West Burma/Argoland and establishing the mid-ocean ridge system that resulted in the formation of the neo-Tethys ocean. Spreading in the meso-Tethys continued the meso-Tethys ridge intersected the Tethyan subduction zone around 140–145 Ma resulting in a southern ridge jump and continuation of seafloor spreading in the meso-Tethys.

Spreading and growth of the Pacific plate continued in Panthalassa, with a gradual increase in spreading rate. The eruption of the Shatsky Rise at the Pacific–Izanagi–Farallon triple junction led to a major readjustment of the triple junction center and was coincident with a major clockwise change in spreading direction, by 24°, between the Pacific and Izanagi plates at M21 (~147 Ma). This resulted in an increased clockwise rotation and a change in configuration of the Pacific–Izanagi, Izanagi–Phoenix and Izanagi–Farallon ridges. The Mongol–Okhotsk Ocean closed at 150 Ma forming the Mongol–Okhotsk Suture.

In the Arctic Ocean, the Canada Basin initiated opening at 145 Ma via counterclockwise rotation of North Slope of Alaska with seafloor spreading starting at 142 Ma. The Canada Basin spreading ridge connected with the North Atlantic rift zone, which extended as far south as the Kings Trough adjacent to the Newfoundland/Iberia margin. The

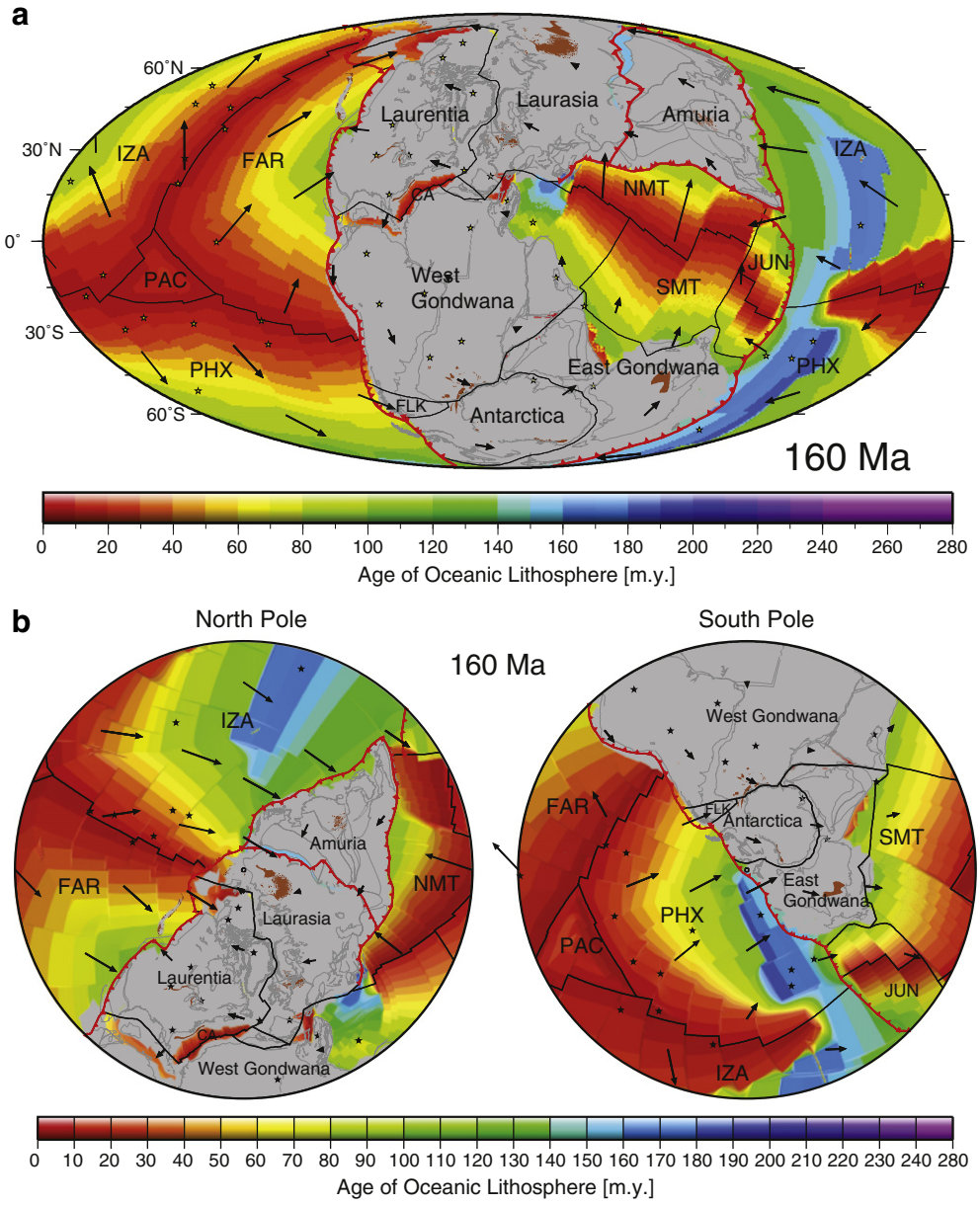

Fig. 20. Description same as Fig. 18.

plate boundary follows the Kings Trough through the Pyrenees connecting with the northern Tethyan subduction zone and to the south connects with the Central Atlantic mid-ocean ridge.

4.4. 140–120 Ma (Figs. 21 and 22)

The Central Atlantic and Iberia–Newfoundland spreading ridge continued and connected via a series of rift zones to the Canada Basin in the Arctic and to the South Atlantic spreading center to the south. In addition, rifting between North America and Greenland initiated around 135 Ma, establishing Greenland as an independent plate and marking the end of the Laurentian continental landmass. The proto-Caribbean Sea continued its growth via differential motion between South and North America. Seafloor spreading initiated in the southern South Atlantic by 132 Ma coinciding with a peak in magmatism (Parana–Etendeka Large Igneous Province) and the initiation of rifting in the African continental interior via the West and Central African rift zones. At this time, we break the African continent into three discrete plates: South, NW and NE Africa. Seafloor spreading between Madagascar and the East African margin ceased around 120 Ma. In the South Atlantic, seafloor spreading propagated northward to the central segment of this ocean by 125 Ma.

The early–mid Cretaceous marks a significant increase in seafloor spreading rates in Panthalassa corresponding to the mid-Cretaceous seafloor spreading pulse. Spreading was occurring between the Pacific, Farallon, Izanagi and Phoenix plates. In northern Panthalassa, North Slope of Alaska was continuing its counterclockwise rotation and opening of the Canada Basin.

The southwest Panthalassic margin, along eastern Australia involved the opening of the South Loyalty Basin, due to roll-back of the southwest Panthalassic subduction zone from 140 Ma. The South Loyalty Basin was actively opening until 120 Ma until a major change in the plate configurations in the SW Panthalassic Ocean.

Seafloor spreading in the meso-Tethys continued after its southern ridge jump at 140 Ma. Coincidently, spreading along the neo-Tethys

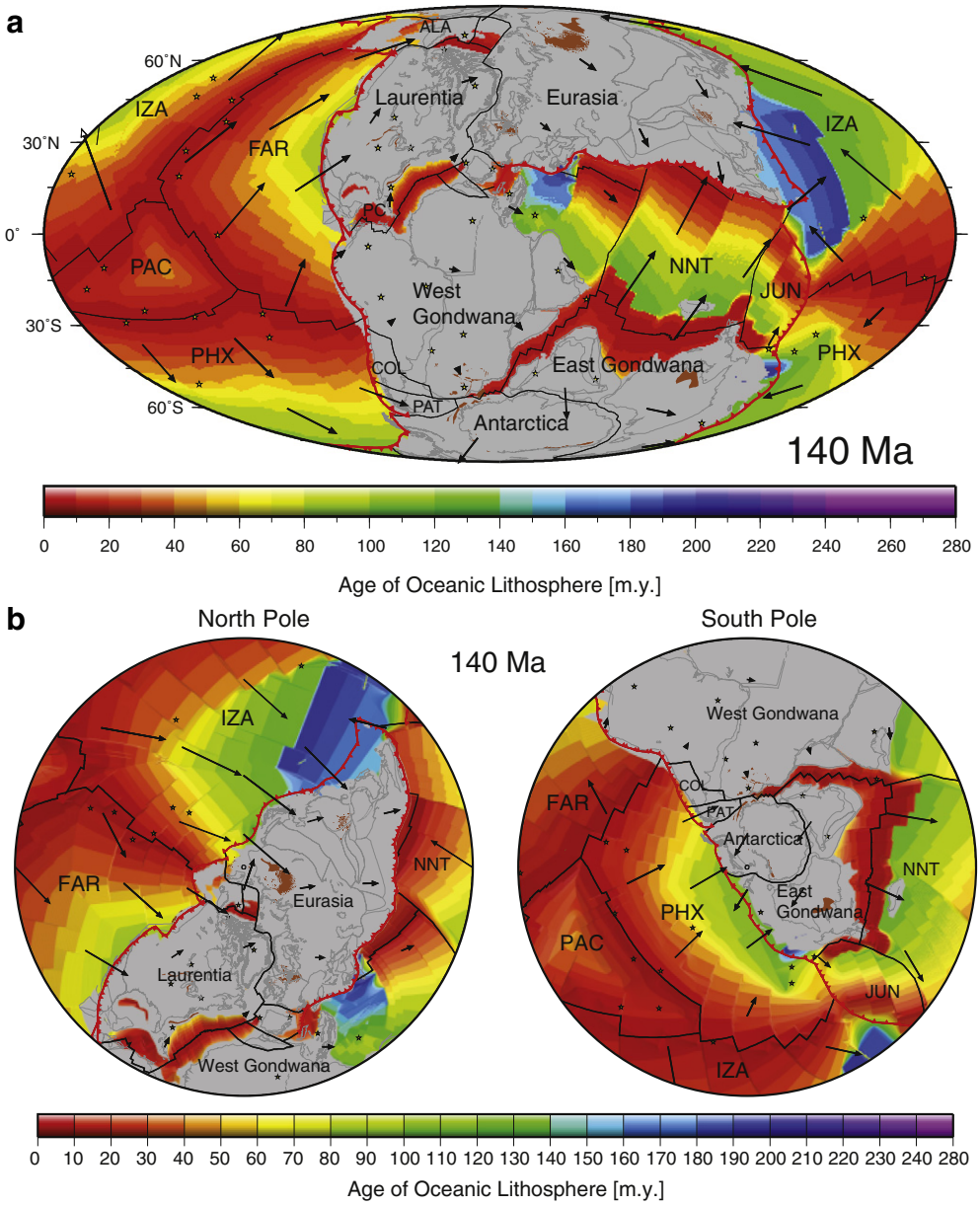

Fig. 21. Description same as Fig. 18.

ridge extending from the Argo Abyssal Plain to north of Greater India. After a landward ridge jump of the neo-Tethys ridge at 135 Ma, the mid-ocean ridge propagated southward to open the Gascoyne, Cuvier and Perth Abyssal Plains between India and Australia. The West Australian spreading ridge system joined with the Enderby Basin spreading ridge, separating Antarctica from the Elan Bank/India, to the west and to the rift between Australia and Antarctica to the east. The initiation of seafloor spreading in the Enderby Basin accommodated strike-slip motion between India and Madagascar of over 1000 km and connected to the West Somali Basin spreading ridge. The East African and Weddell Sea spreading ridges were active during this time period and connected to the South Atlantic via the Agulhas-Falkland transform.

4.5. 120–100 Ma (Figs. 22 and 23)

Spreading along the Central Atlantic ridge continued into the proto-Caribbean Sea until 100 Ma. Spreading extended southward along the South Atlantic ridge with a northward propagation leading to seafloor spreading in the "Central" segment by 120 Ma and in the "Equatorial" segment by 110 Ma. Extension along the West and Central African rifts, including the Benue Trough continued during this time period. Further north, spreading between Iberia and Newfoundland connected to a rift zone adjacent to the Rockall and Porcupine Plateaus and continued to the Labrador Sea/Baffin Bay (between Greenland and North America) and between Greenland and Eurasia. Break-up between Porcupine and North America occurred from 110 Ma. These North Atlantic rift zones connected with the Canada Basin spreading center until about 118 Ma when spreading ceased in the Canada Basin. Spreading terminated when the rotation of North Slope Alaska ceased, coincident with a change in the southern North Slope margin from largely strike-slip to convergence due to a change in spreading direction in Panthalassa.

Ultra fast seafloor spreading rates were occurring in Panthalassa together with the eruption of a suite of Large Igneous Provinces, most

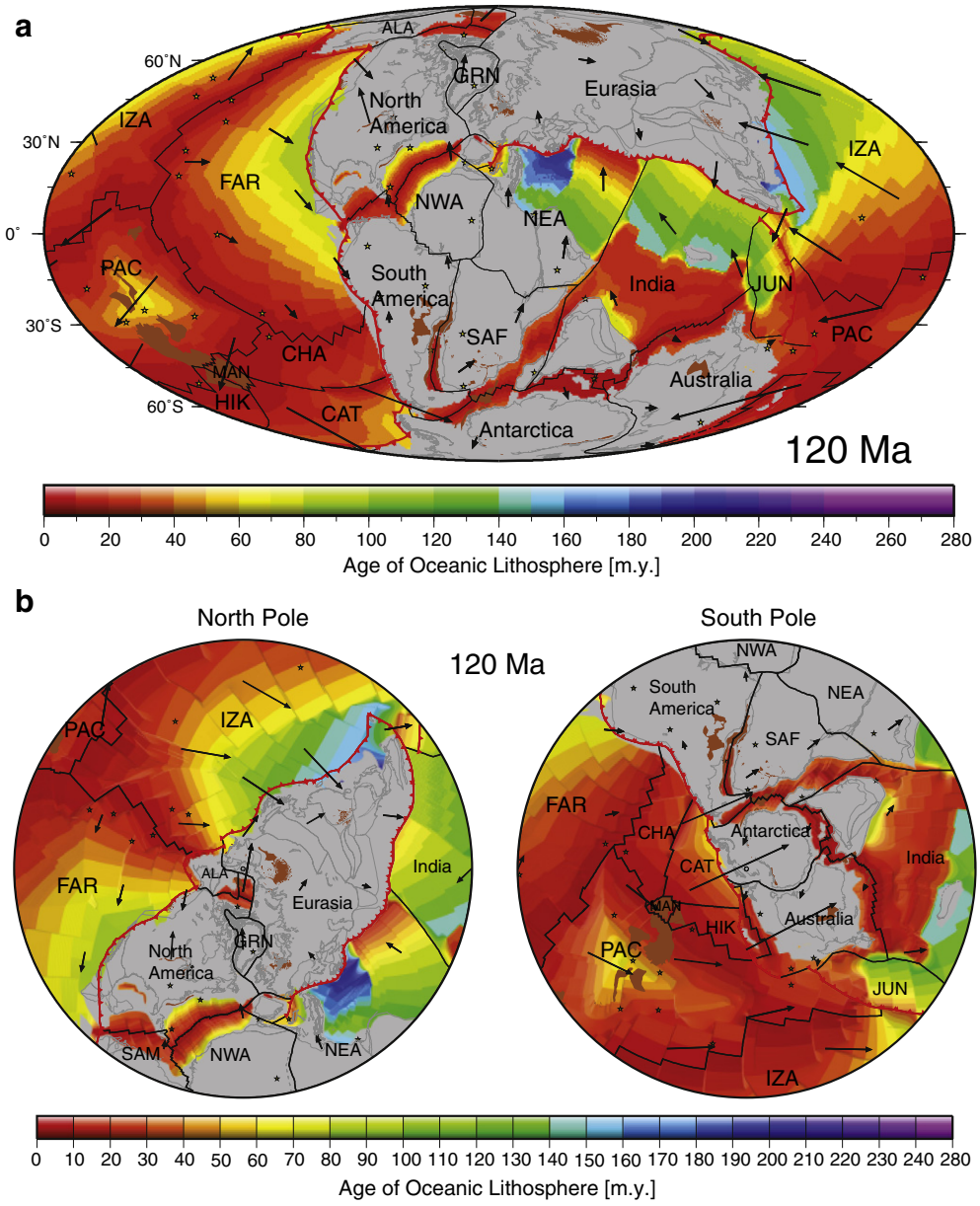

Fig. 22. Description same as Fig. 18.

notably the eruption of the Ontong-Java, Manihiki and Hikurangi Plateaus at 120 Ma. The eruption of this mega-LIP led directly to the break-up of the Phoenix plate into four plates: the Hikurangi, Manihiki, Chasca and Catequil plates. The separation occurred at 120 Ma in an E–W direction in the Ellice Basin between the Ontong Java and Manihiki Plateaus with simultaneous rifting of the Manihiki and Hikurangi plateaus from a N–S directed spreading system along the Osbourn Trough. An additional two triple junctions were active in the region leading to the break-up of the Eastern Manihiki Plateau and the development of the Tongareva triple junction. The eastern triple junction represented spreading between the Manihiki, Phoenix and Chasca plate and the southern triple junction represented spreading between the Hikurangi, Catequil and Manihiki plates. The initiation of the Pacific–Manihiki–Hikurangi triple junction led to change in the tectonic regime along eastern Australia. Prior to 120 Ma, the Phoenix plate was subducting beneath the east Australia margin, which changed to the Hikurangi plate and a small portion of the Catequil plate but with a decreased rate of convergence after 120 Ma.

In the Tethys Ocean, spreading was continuing along the western Australian margin, connecting to spreading in the Enderby Basin and rifting between Australia and Antarctica. A ridge jump at 120 Ma isolated the Elan Bank microcontinent, roughly coincident with the eruption of the Kerguelen Plateau. A strike-slip margin between India and Madagascar joined to a transform in the Tethys Ocean and not to the West Somali Basin spreading ridge which had become extinct at 120 Ma. Spreading continued in the Mozambique Basin/Riiser Larson Sea and continued to the Weddell Sea and north to the South Atlantic spreading ridge.

4.6. 100–80 Ma (Figs. 23 and 24)

The Mid and South Atlantic Ridges were well established from 100 Ma. As spreading occurred, rifting in the interior of Africa ceased at about 85 Ma. The Mid-Atlantic ridge propagated northward to between the Porcupine margin and between North America and the Rockall margin at 50 Ma. Rifts were still active surrounding Greenland.

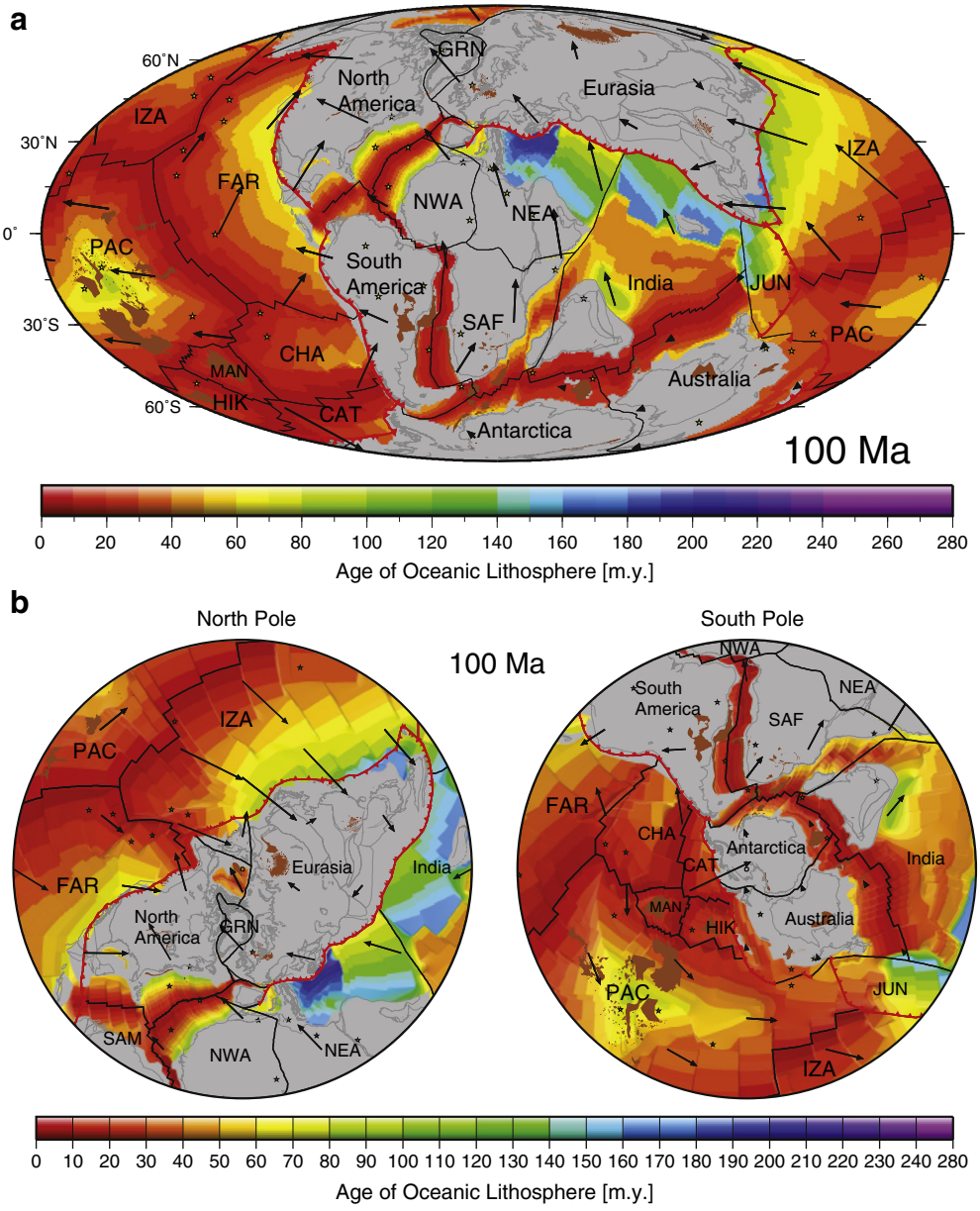

Fig. 23. Description same as Fig. 18.

The south of the Mid Atlantic Ridge connected to the actively opening proto-Caribbean Sea along a major transform fault. The western margin of the Caribbean plate underwent a change in subduction polarity from east-dipping to west-dipping at 100 Ma. The rollback of this subduction zone along the Caribbean Arc led to the consumption of the actively spreading proto-Caribbean ocean floor and encroachment of the Farallon plate into the Caribbean domain (Fig. 9). The continued rollback of the Caribbean Arc subduction zone led to the formation of the Yucatan Basin as a back-arc in the late Cretaceous. The eruption of the Caribbean flood basalt province occurred around 90 Ma overlying oceanic lithosphere that formed on the Farallon plate and later migrated to the Caribbean region.

In Panthalassa, spreading was occurring along the Pacific–Izanagi, Pacific–Farallon, Farallon–Izanagi and along the ridges associated with the plateau break-up region. A change in spreading direction is recorded in the Mendocino, Molokai and Clarion fracture zones (associated with Pacific–Farallon spreading), which we date to 103–100 Ma coincident with an observed bend in the hotspot trails on the Pacific plate, suggesting a plate reorganization at this time. In addition, we model a clockwise change in spreading direction in the Osbourn Trough region based on our age estimate for a bend in observed fracture zones between the Manihiki and Hikurangi plateaus. The change in spreading direction modified the nature of the boundary east of Australia from convergence to dominantly strike-slip. At 86 Ma, we model the docking of the Hikurangi Plateau with the Chatham Rise triggering a cessation in spreading associated the Ontong-Java, Manihiki and Hikurangi plateaus. After the cessation of spreading along these ridges axes, the locus of extension jumped southward between Antarctica and the Chatham Rise, establishing the Pacific–Antarctic spreading ridge. To the east, the Pacific–Farallon Ridge extended to the south connecting with the Pacific–Antarctic Ridge at the Pacific–Antarctic–Farallon triple junction.

After the cessation of the spreading centers associated with the LIP break-up, the Pacific plate became the dominant plate in Panthalassa and it is at this time that we switch to the Pacific Ocean. In the

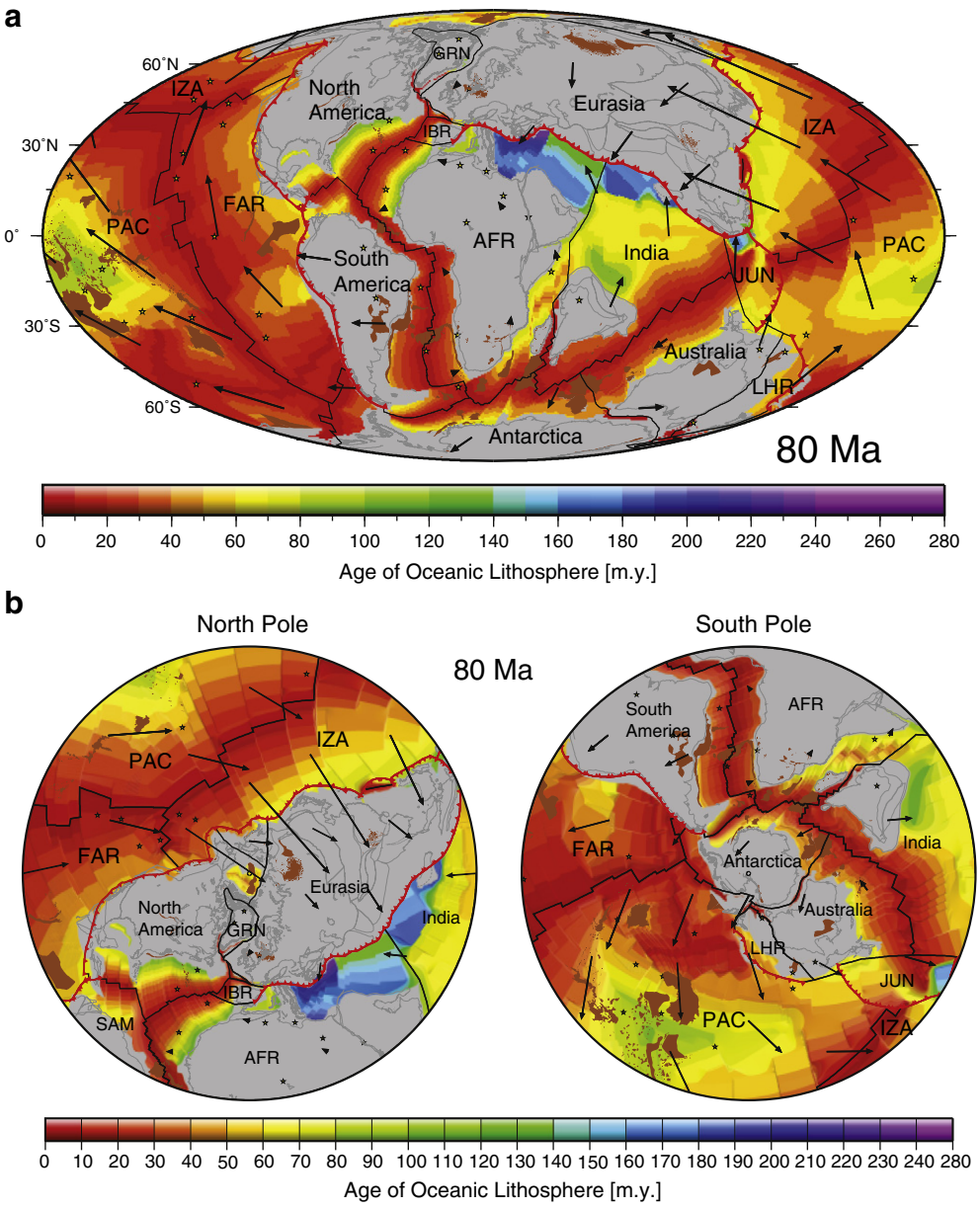

Fig. 24. Description same as Fig. 18.

western Pacific, the Tasman Sea was opening from 84 Ma leading to the establishment of the Lord Howe Rise plate. Further north, the proto-South China Sea initiated its opening between the South China margin and Borneo/Kalimantan.

In the Tethys/Indian Ocean, spreading was occurring along the West Australian margins continuing the separation of India and West Burma from Australia. A major change direction is recorded in the fracture zone trends at 99 Ma, led to a change in the motion of the Indian plate. Spreading became dominantly N–S directed establishing spreading in the Wharton Basin. The West Australian mid ocean ridge system formed a triple junction with the Australian–Antarctic ridge at 99 Ma (initiation of ultra-slow seafloor spreading) and spreading between India and Antarctica north of Elan Bank. The Indian–Antarctic ridge (or Southeast Indian Ridge) connected with the African–Antarctic ridge (or Southwest Indian Ridge) from 100 Ma. Rifting between India and Madagascar in the Mascarene Basin initiated at 87 Ma. The Southwest Indian Ridge connected with spreading in the Malvinas plate in the southernmost Atlantic at 83.5 Ma and the American–Antarctic ridge (established after the cessation of spreading in the Weddell Sea). The West Burma continental sliver reached the Eurasian margin and accreted starting at 87 Ma and sutured to Sibumasu at 73 Ma.

4.7. 80–60 Ma (Figs. 24 and 25)

The South and Mid-Atlantic ridges continued spreading. The Mid-Atlantic Ridge propagated northward into the North Atlantic with the initiation of seafloor spreading in the Labrador Sea (between North America and Greenland) and between Rockall and Greenland at 79 Ma. Spreading propagated from the Labrador Sea to Baffin Bay by 63 Ma across the Davis Straits via left-lateral transform faults and connected to the Arctic via the Nares Strait. In the Caribbean, spreading in the proto-Caribbean Sea ceased at 80 Ma whereas the Caribbean Arc subduction zone continued its northeastward rollback. The Yucatan Basin opened as a back-arc in the late Cretaceous with cessation

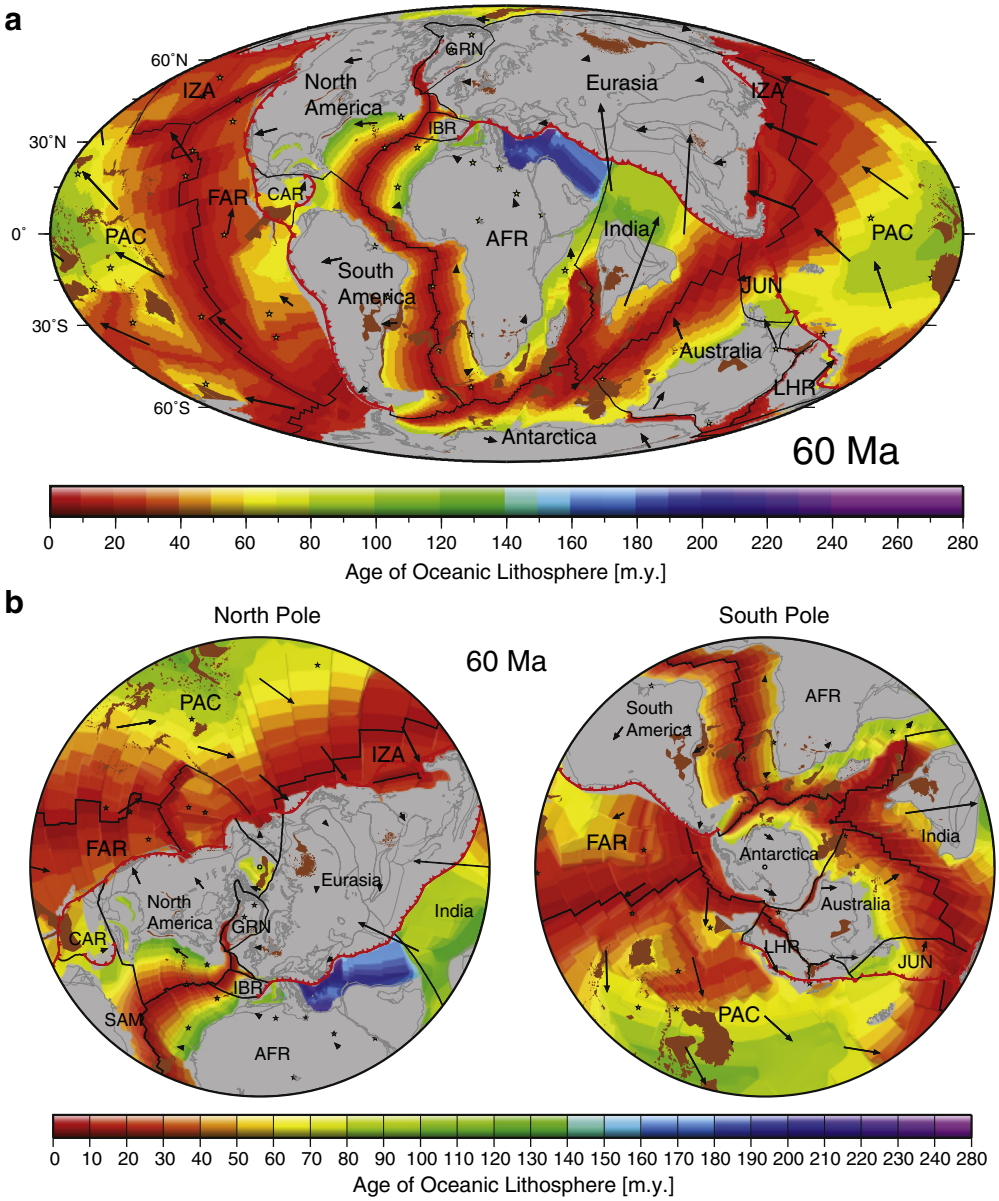

Fig. 25. Description same as Fig. 18.

occurring at 70 Ma when the Caribbean Arc accreted to the Bahaman Platform. The accretion led to a jump in the locus of subduction westward along the newly developed Panama–Costa Rica to accommodate the continued eastward motion of the Farallon plate, trapping Farallon oceanic lithosphere onto the Caribbean plate.

The Pacific was dominated by the break-up of the Farallon plate into the Kula plate at 79 Ma initiating spreading along the E–W trending Kula–Pacific ridge and the NE–SW trending Kula–Farallon ridge. The Kula–Farallon Ridge follows the location of the Yellowstone hotspot and intersects the North American margin in Washington/British Columbia before migrating northward along the margin. The break up of the Farallon plate into the Kula plate coincides with a major change in spreading direction observed in all northeast Pacific fracture zones. In our model spreading continued along the Pacific–Izanagi ridge after the establishment of the Kula–Pacific ridge to the east connected via a large offset transform fault. The Pacific–Izanagi ridge was rapidly approaching the East Asian margin and was proximal by 60 Ma. In the southern Pacific, spreading was occurring along the Pacific–Antarctic ridge, extending eastward to connect with the Pacific–Farallon and Farallon–Antarctic spreading ridges. At 67 Ma, a change in spreading direction is recorded in the fracture zones of the South Pacific.

In the Indian Ocean, spreading was occurring along the Wharton Ridge, Southeast Indian Ridge, Southwest Indian Ridge and in the Mascarene Basin. Spreading in the Mascarene Basin ceased at 64 Ma jumping northward, isolating the Seychelles microcontinent and initiating spreading between India and the Seychelles along the Carlsberg Ridge. The Southwest Indian Ridge connected with spreading in the Malvinas plate until 66 Ma. After this, the Southwest Indian Ridge connected directly with the American–Antarctic and South Atlantic Ridge.

4.8. 60–40 Ma (Figs. 25 and 26)

Seafloor spreading propagated into the Eurasia–Greenland margin along the Reykjanes Ridge by 58 Ma, forming a triple junction between North America, Greenland and Eurasia. The Jan Mayen microcontinent rifted off the margin forming the fan-shaped Norway

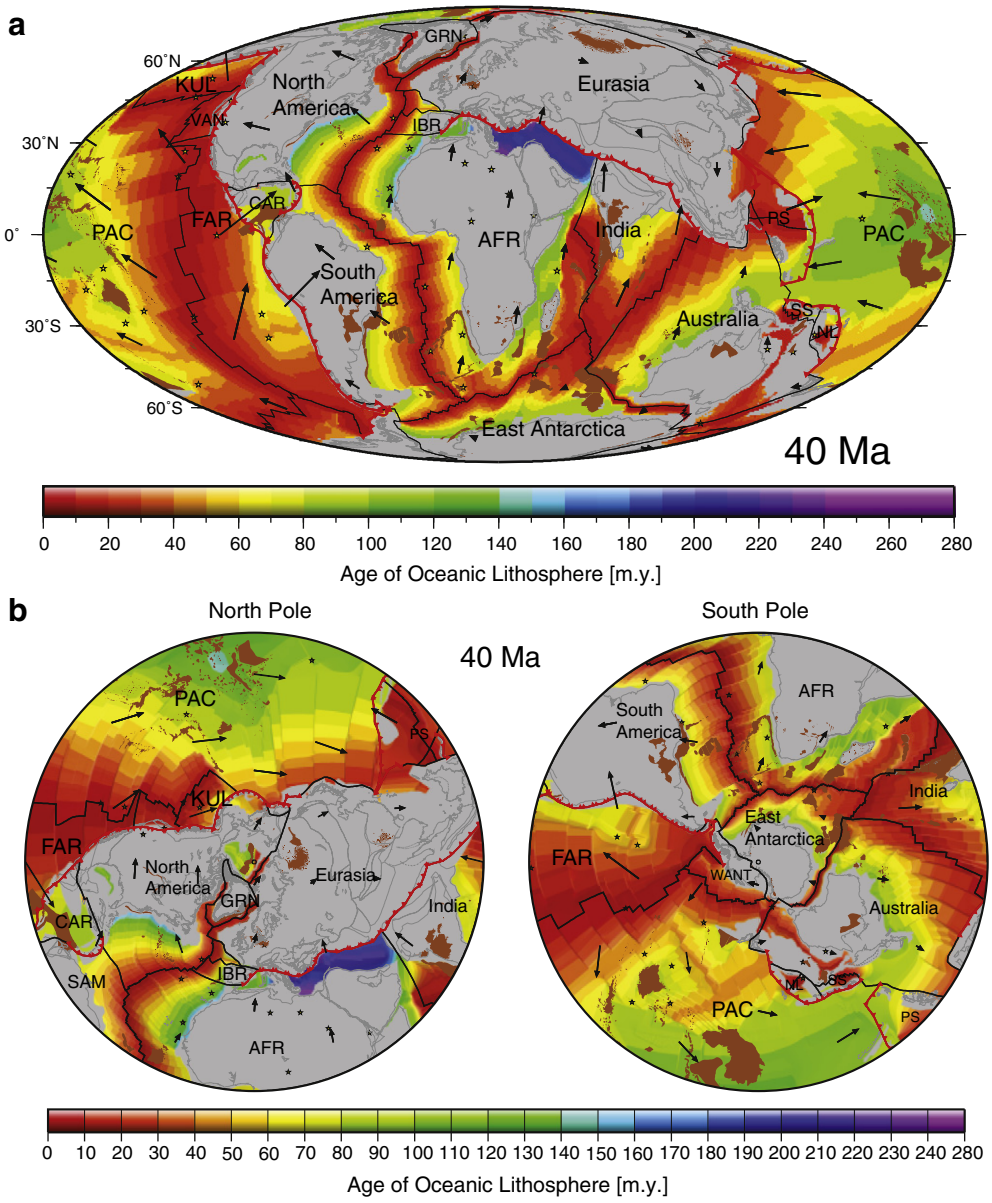

Fig. 26. Description same as Fig. 18.

Basin along the Aegir Ridge. The Aegir Ridge connected to the Mohns Ridge to the north and Reykjanes Ridge to the south via a series of transform faults. Spreading in the Eurasian Basin to the north initiated around 55 Ma along the Gakkel/Nansen Ridge. This ridge connected to the Baffin Bay ridge axis through the Nares Strait and the Mohns Ridge to the south via major strike-slip faults with minor compression between Greenland and Svalbard. In our model the Lomonosov Ridge is coupled to North America. The initiation of spreading in the Eurasian Basin also coincides with the initiation of independent motion of the Porcupine Plate, resulting in a small clockwise rotation of Eurasia and counter-clockwise rotation of Iberia relative to the Porcupine Plate. A change in spreading direction is also observed in the Labrador Sea.

The Mid-Atlantic Ridge connects with the west-dipping subduction zone bordering the Caribbean via a transform fault. By the middle Eocene, relative motion between North America and the Caribbean began to form the Cayman Trough along sinistral faults that later merge with the Lesser Antilles trench. East-dipping subduction was still occurring along the Middle America margin bordering the Pacific.

In the Pacific, the Pacific–Izanagi ridge started to subduct under the East Asian margin between 55 and 50 Ma, signaling the death of the Izanagi plate coincident with a dramatic change in spreading direction from N–S to NW–SE between Kula–Pacific spreading. The Kula–Pacific Ridge connected with the Pacific–Farallon Ridge and Kula–Farallon Ridge from 60 to 55 Ma. After 55 Ma, the eastern Pacific was dominated by the rupture of the Farallon plate close to the Pioneer Fracture Zone, forming the Vancouver plate. The break-up resulted in minor relative motion along the Pioneer fracture zone. Further south, spreading was continuing along the Pacific–Farallon, Pacific–Antarctic, Farallon–Antarctic and Pacific–Aluk Ridges. The fracture zones associated with the Pacific–Antarctic Ridge close to the Campbell Plateau record a change in spreading direction at 55 Ma, coincident with other events that occurred in the Pacific at this time.

In the western Pacific, spreading in the proto-South China Sea ceased at 50 Ma coincident with the clockwise rotation of the neighboring Philippine Sea plate. The dramatic change in motion of the Philippine Sea plate reorganized the plate boundaries in the area leading to the establishment of a subduction zone between Palawan and the proto-

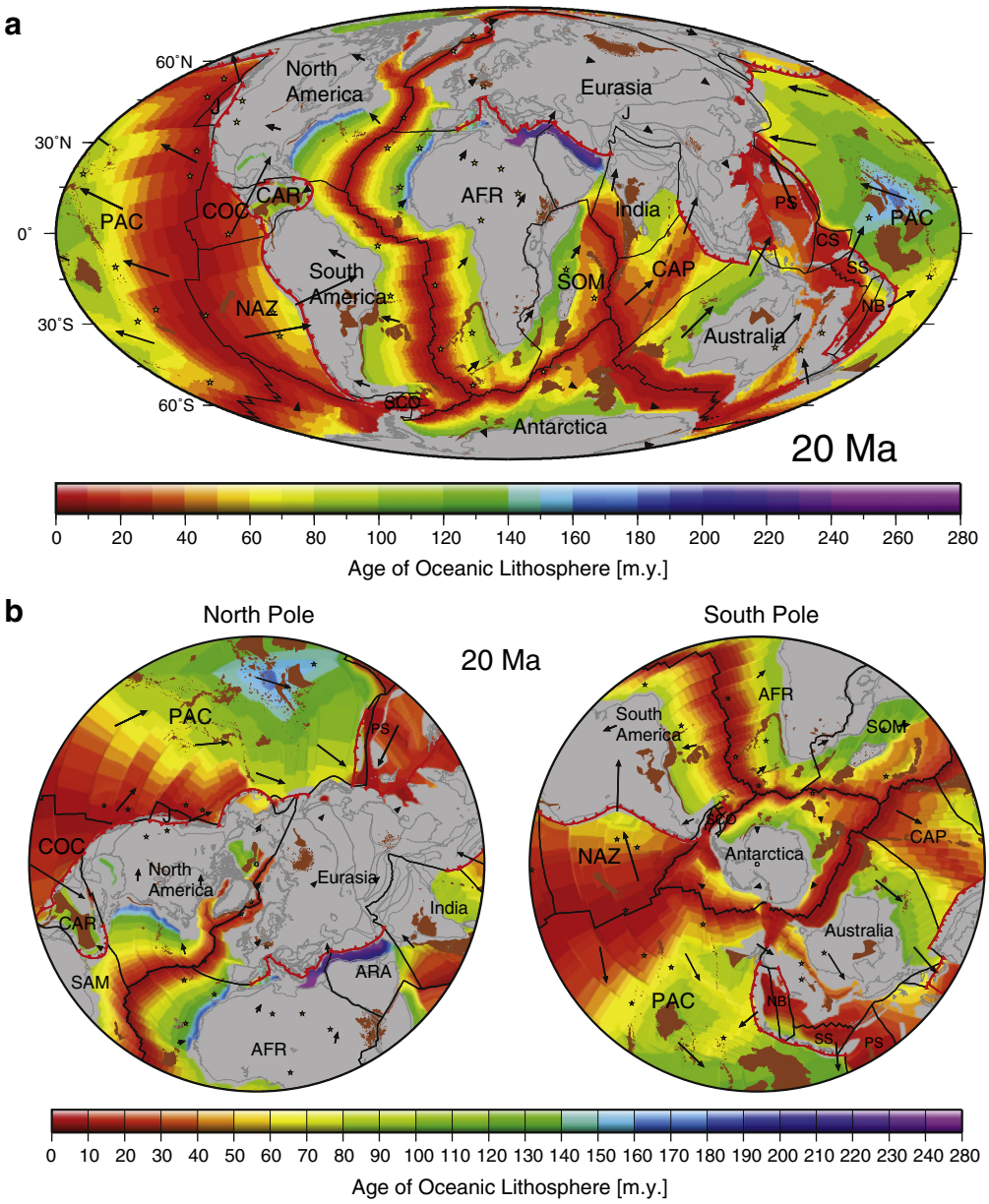

Fig. 27. Description same as Fig. 18.

South China Sea, which led to the subduction of the proto-South China Sea after 50 Ma. Spreading was occurring in the West Philippine Basin and Celebes Sea. Further south, spreading initiated in the North Loyalty Basin behind the proto-Tonga–Kermadec Trench.

The Indian Ocean was dominated by a series of mid ocean ridges such as the Wharton Ridge, Southeast Indian Ridge, Southwest Indian Ridge and Carlsberg Ridge. Prior to 55 Ma, subduction was occurring along the Tethyan subduction zone, consuming crust that formed during meso and neo Tethys spreading. At 55 Ma, the northern tip of Greater India marks the start of collision between India and Eurasia and the uplift of the Himalayas. Closure of the Tethys Ocean in this area occurred by about 43 Ma. Full closure of the neo-Tethys between India and Eurasia also corresponds to the cessation of spreading in the Wharton Basin, which describes Australia–India motion.

4.9. 40–20 Ma (Figs. 26 and 27)

At 40 Ma, the Atlantic Ocean consisted of a continuous mid-ocean ridge system that extended from the South America–Antarctica–Africa triple junction to the Eurasian Basin in the north. The cessation of independent Porcupine motion occurred at 33 Ma coinciding with the cessation of seafloor spreading in the neighboring Labrador Sea and Baffin Bay and the establishment of a simple two-plate system to describe the plate motions in the North Atlantic. From 33 Ma onwards, Greenland and North America have been fused into one plate. At about 30 Ma, spreading jumped from the Aegir Ridge in the Norway Basin to the Kolbeinsey Ridge connecting up with the Mohns Ridge via a series of transform faults. Further south, adjacent to the Iberian margin, a southern jump of the plate boundary at 28 Ma from the Kings Tough to the Azores transform fault and along the Straits of Gibraltar led to the capture of Iberia by the Eurasian plate.

In the Pacific, spreading between the Kula–Pacific and Kula–Farallon ceased at 40 Ma, leading to the Pacific plate consisting of the Pacific, Vancouver, Farallon, Aluk and Antarctic plates. The intersection of the Murray transform fault with the North American subduction zone around 30 Ma led to the establishment of the San Andreas Fault and corresponds to the establishment of the Juan De Fuca plate at the expense of the Vancouver plate. A further rupture of the Farallon plate

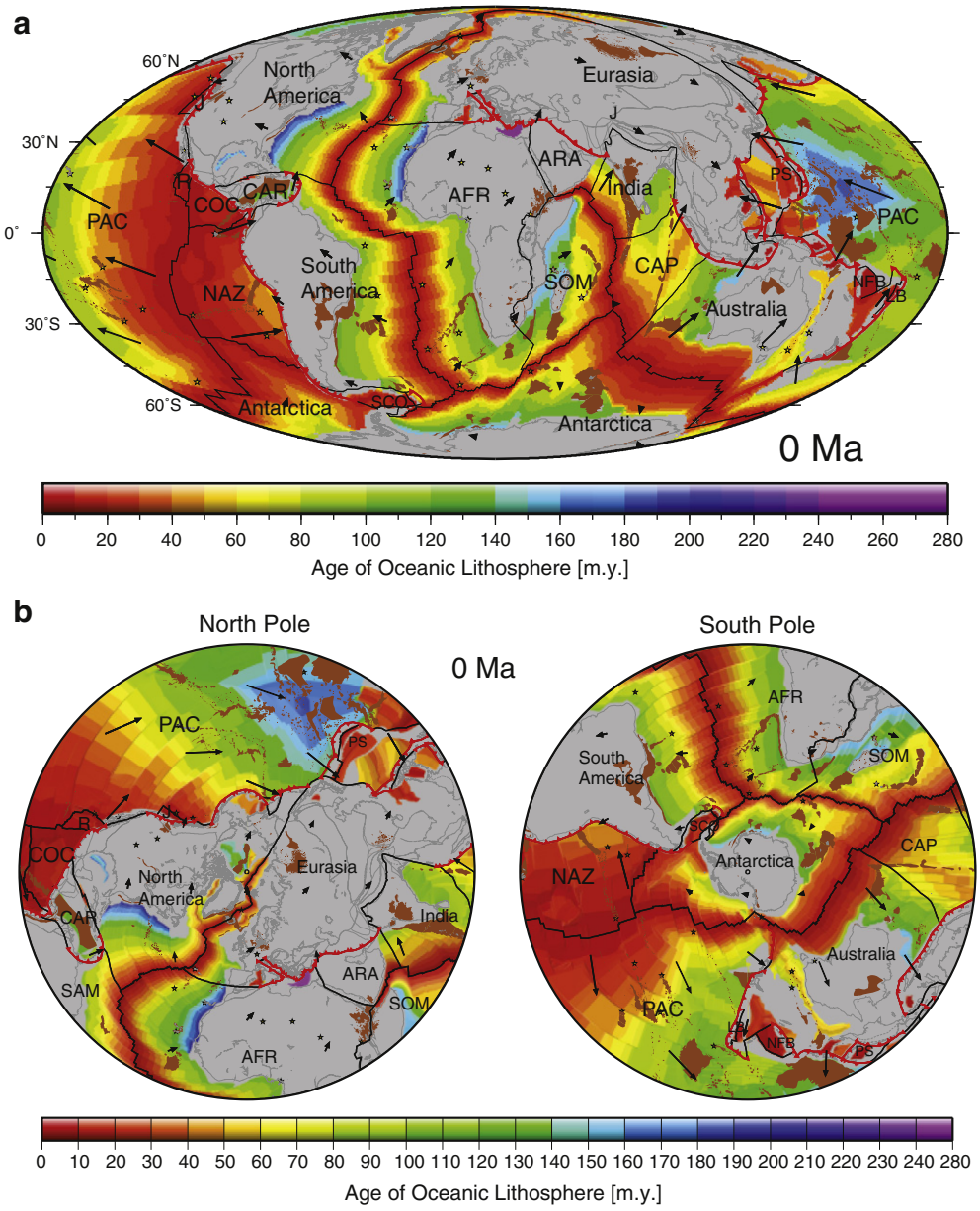

Fig. 28. Description same as Fig. 18.

occurred at 23 Ma leading to the establishment of the Cocos and Nazca plates and initiation of the East Pacific Rise, Galapagos Spreading Centre and Chile Ridge.

In the Western Pacific, spreading in the West Philippine Basin ceased at 38 Ma whereas spreading continued in the Celebes Sea. The formation of the Caroline Sea occurred behind a rapidly southward migrating subduction zone. By 30 Ma, spreading initiated in the Shikoku and Parece Vela Basins behind the west-dipping Izu-Bonin–Mariana Arc. Spreading terminated in the Celebes Sea. In the SW Pacific, spreading initiated in the Solomon Sea at 40 Ma and in the South Fiji Basin at 35 Ma. Cessation of spreading in the South Fiji Basin occurred at 25 Ma.

In the Indian Ocean, spreading continued along the Southwest Indian Ridge, Southeast Indian Ridge, Central Indian Ridge and Carlsberg Ridge. Extension along the East Africa rifts was established at 30 Ma leading to the break-up of Africa into Somalia plate. Rifting along the Sheba Ridge, separating Arabia from Africa/Somalia initiated at 30 Ma.

4.10. 20–0 Ma (Figs. 27 and 28)

Spreading in the South, Central and North Atlantic continued unabated for the last 20 million years. In the Caribbean, the Cayman Trough continued to expand and develop, and the Chortis Block moved over the Yucatan promontory. Westward motion of the North American plate relative to the slow moving Caribbean plate was accommodating the opening of the Cayman Trough. Active subduction of Atlantic oceanic lithosphere has been occurring along the Lesser Antilles Trench, which connects to the Mid-Atlantic Ridge along the Researcher Ridge and Royal Trough.

In the Pacific, spreading was occurring along the Pacific–Juan De Fuca, Pacific–Nazca, Pacific–Cocos, Cocos–Nazca, Pacific–Antarctic and Nazca–Antarctic ridges. The Bauer microplate formed along the East Pacific Rise at 17 Ma and continued until 6 Ma. The locus of spreading then jumped back to the East Pacific Rise (between the Pacific and Nazca plates). The East Pacific Rise is the fastest spreading

ridge system (excluding back-arc opening) and currently encompasses microplate formation at the Easter, Juan Fernandez and Galapagos plates. Currently, the Juan De Fuca plate is limited at its southern end by the Mendocino Fracture Zone and is subducting slowly along the Cascadia subduction zone.

The western Pacific is dominated by the opening of a series of back-arc basins due to the roll-back of the subduction hinge of the Tonga–Kermadec and Izu-Bonin–Mariana trenches. Spreading in the Shikoku and Parece Vela Basins and South China Sea ceased at 15 Ma. By 9 Ma, spreading initiated in the Mariana Trough. We model complete closure of the proto-South China Sea at around 10 Ma behind a subduction zone located along Palawan and the north Borneo/Kalimantan margin. In the SW Pacific, spreading in the Lau Basin initiated by 7 Ma with back-arc extension occurring in the Havre Trough.

In the Indian Ocean, diffuse deformation occurring in the middle of the Indo-Australian plate led to the development of the Capricorn plate in the central–east Indian Ocean at 20 Ma. Further west, we initiate spreading along the Sheba Ridge at 20 Ma. The Sheba Ridge propagated into the Red Sea at 15 Ma.

5. Discussion

5.1. Comparison with other models

Our plate motion model offers an alternative approach to traditional global plate reconstructions. Tectonic features that reside on the surface of the Earth are not modeled as discrete features but rather the plates themselves are modeled as dynamically evolving features. The nature of the plate boundaries that combine to form a plate will necessarily change based on the magnitude and direction of motion of each plate. Therefore, one of the supplementary outcomes of this approach is the ability to directly compare competing tectonic models, most easily expressed through plate velocity vectors for a common set of points on the surface of the Earth. We directly compare the plate motion model presented in Gurnis et al. (2012) to the model presented in this study (Fig. 29).

In this study we have adopted a new absolute plate motion model for Africa for times prior to 100 Ma based on a true-polar wander corrected paleomagnetic reference frame (Steinberger and Torsvik, 2008). This new reference frame allows us to extend our plate reconstructions back to 200 Ma, the time of Pangea break-up, with the potential to model processes occurring during supercontinent break-up and dispersal. The Gurnis et al. (2012) dataset was restricted to the past 140 million years. Adjusting the absolute reference frame causes a global shift in the absolute positioning of the continents but in theory, should not affect the relative motion and therefore the nature of the plate boundary between plates. However prior to 83.5 Ma, the Pacific plate can no longer link to the African plate circuit via seafloor spreading (see Section 2: Methodology) requiring a distinct absolute reference frame for the Pacific realm. As a result, a change in the absolute reference frame for either the African or Pacific realms will change the nature of the plate boundaries that border the Pacific/Panthalassic Ocean (Fig. 29).

Relative motions between most of the plates in Panthalassa have been updated compared to the Gurnis et al. (2012) model. We reinterpreted the M-series Japanese magnetic lineations leading to a dramatic change in spreading direction by about 24° and an updated orientation of the Izanagi–Farallon and Izanagi–Phoenix ridges. The change in the Izanagi plate motion results in an increase in the convergence rate and more orthogonal convergence in northern Panthalassa bordering eastern Laurasia but more oblique convergence in the area further south adjacent to the Junction plate (Fig. 29).

Another major addition to the model presented in this study is the implementation of the plateau break-up model of Taylor (2006) for the Ontong-Java, Manihiki and Hikurangi plateaus (Fig. 29). Incorporating the plateau break-up has consequences for the evolution of the Phoenix plate and the eastern Gondwana margin. Most Mesozoic models for eastern Gondwana propose a long-lived convergent plate margin along the eastern edge of Australia (Veevers, 2006; Cluzel et al., 2010; Matthews et al., 2011), expressed through andesitic volcanism that occurred along the Queensland margin north to Papua New Guinea (Jones and Veevers, 1983) and Aptian–Albian andesitic volcanogenic detritus in east Australian continental basins (e.g. Eromanga and Surat Basins) (Hawlader, 1990; Veevers, 2006). Plate velocity vectors using either Gurnis et al. (2012) or this study, predict a convergent margin between the Phoenix plate and eastern Gondwana during this time (Fig. 29). There is ambiguity as to whether the margin continued as a convergent margin or whether there was a major tectonic regime change after ~120 Ma, coincident with the eruption of the Ontong-Java, Manihiki and Hikurangi plateaus and subsequent change in the mid ocean ridge configuration in southern Panthalassa. Extensive magmatism recorded in the Whitsunday Volcanic Province is attributed to continental margin break-up rather than from a convergent margin setting (Bryan et al., 1997) while others invoke a rift-related volcanics associated with west-dipping subduction (Veevers, 2006). New Caledonia and parts of New Zealand, which were located at the easternmost boundary of the Australian continent record subduction related magmatism until at least 99 Ma (Veevers, 2006) or 95 Ma (Cluzel et al. 2010) suggesting convergence was occurring along eastern Gondwana. Although the plate motion model of Gurnis et al. (2012) does not include the rotations associated with the plateau break-up, both models predict continuing convergence until 100 Ma (Fig. 29).

At 100–99 Ma, a major tectonic regime change is recorded in eastern Australia (Veevers, 2006). Sedimentation in the east Australian basins changed from volcanogenic dominated to quartzose sandstone (Veevers, 2006), the basins themselves changed from a prolonged period of subsidence to uplift (Matthews et al., 2011) and volcanism became alkalitic (Veevers, 2006). In addition, the eastern margin changed to a period of extension and passive margin formation (e.g. extension in the Lord Howe Rise and New Caledonia Basins), which are believed to have formed adjacent to a strike-slip margin defining the boundary between Panthalassa and eastern Gondwana (Jones and Veevers, 1983; Veevers, 2006). A hiatus in subduction-related volcanism in Eastern Australia, New Caledonia and New Zealand is recorded between 95 and 83 Ma (Cluzel et al., 2010). This major tectonic regime change is coincident with a change in spreading direction in the plates associated with the plateau break-up and bordering the eastern Gondwana margin at this time. The result is that the eastern Gondwana margin changes from convergent to strike-slip, as predicted by geological observations. This is in contrast to the model of Gurnis et al. (2012) which suggests oblique convergence after 100–99 Ma (Fig. 29). In our current plate motion model, a strike-slip dominated margin is predicted from 100 to 86 Ma, which marks the timing of Hikurangi plateau collision with the Chatham Rise and the cessation of mid ocean ridge subduction related to the plateau break-up. The plate adjacent to eastern Australia became the Pacific plate and all subsequent motions have been between the Pacific and Australian or Lord Howe Rise plates.

Additional differences between the relative plate motions presented in Gurnis et al. (2012) and this study include an updated northern Atlantic based on Gaina et al. (2009) and the Arctic based on Alvey et al. (2008). The changes here are minor adjustments and do not substantially change plate motion directions or the nature of the plate boundaries in the area.

5.2. Future directions

Our global plate motion model presents the development of the continents and oceans on a global scale within a rigid plate framework, underpinned by a combination of marine geophysical data, onshore geological data and plate tectonic principles. Although we have presented our preferred interpretations for each region based on

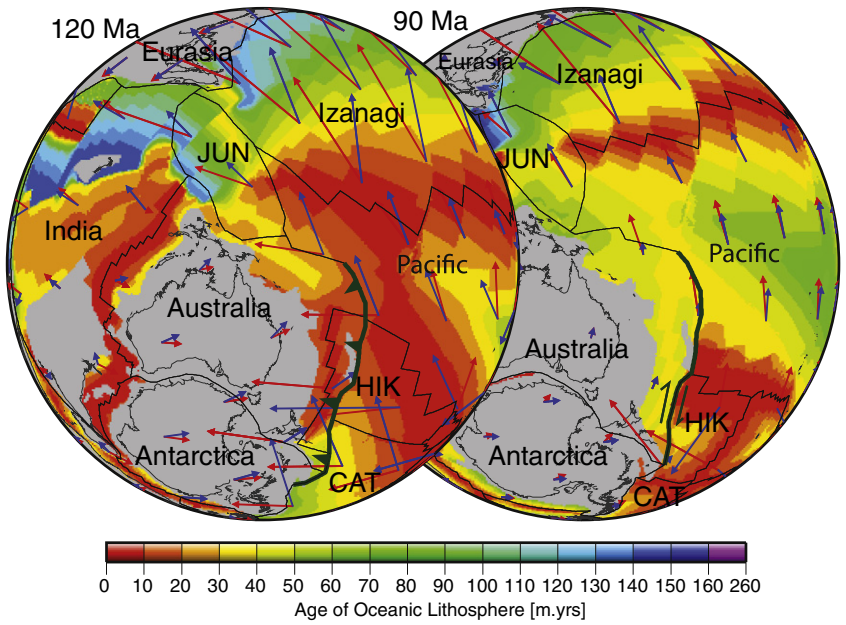

Fig. 29. Global comparison between the Gurnis et al. (2012) plate motion model and the one presented in this study, centered on Australia and the western Panthalassic margin. Reconstructions are shown at 120 and 90 Ma with red plate velocity vectors denoting the Gurnis et al. (2012) model and blue plate velocity vectors from this study. Dark green line indicates the east Australian margin.

available data, there are regions that could benefit from re-analysis of the seafloor spreading and break-up history, which will have a significant flow-on effect further down the global plate circuit. These include:

(1) The early break-up history between Africa and South America to account for significant overlaps and gaps between the two margins. Refining the history between these two plates will lead to a revision of the Mesozoic history of the Caribbean region (i.e. the accommodation space created to form the proto-Caribbean Sea and the rift basins associated with hydrocarbon-bearing basins in the Gulf of Mexico), a more tightly constrained equatorial Atlantic and also the plate boundaries surrounding the Weddell Sea, which are very ill-constrained due to a paucity of data.
(2) The early break-up history and Mesozoic spreading between Africa and Antarctica. A further refinement of the opening history of this area will affect the motions of Antarctica, India and Australia and the interaction (plate boundary processes) along the eastern Gondwana margin bordering Panthalassa.
(3) The break-up history of the Pacific–Marie Byrd Land margin (~100–83 Ma), which has consequences for the motion of the Pacific plate and associated plates, such as the Izanagi, Phoenix, Farallon, Hikurangi, Manihiki, Catequil and Chasca plates. The Pacific plate can only be linked to the plate circuit, through Africa, when there is a mid-ocean ridge (or rift) between the Pacific and Antarctica/Marie Byrd Land. Greater constraints on the timing of break-up between the Campbell Plateau and Antarctica and a revised set of finite rotations to describe the opening will potentially mean we can confidently extend the Pacific plate's link to the plate circuit further back in time and decrease the uncertainty in Pacific plate motion during this time interval.

A major improvement that is essential for global plate motion models that extend into the Mesozoic is a more robust Pacific absolute plate motion model. The latest models available with associated published rotation poles for Pacific hotspots (Wessel et al. 2006; Wessel and Kroenke 2008) result in major shifts and rotations of the Pacific plate, which are inconsistent with geological observations; for example their Pacific hotpot models, combined with a relative plate motion model for motion between the Farallon and Pacific plates, result in transform motion between the Farallon and North American plates, while geological observations indicate subduction being active (DeCelles, 2004). This model also leads to an anomalous amount of material entering the mantle in the southern hemisphere (Shephard et al., 2012). This inconsistency may result from the assumption of Pacific hotspot fixity and poor sampling of Pacific seamount chains due to a paucity of available data. A new approach using a combination of methods, for example moving hotspot models, paleomagnetics and coupled geodynamic-plate motion models, may result in a more robust model for the Pacific plate prior to ~83 Ma and may potentially extend the Pacific absolute reference frame to the earliest Mesozoic.

A further limitation of the present model is that the entire surface of the earth is represented as rigid blocks, which is clearly not true for some plate interiors and plate boundaries (Gordon and Stein, 1992; Bird, 2003). Deforming regions within plate interiors or straddling plate boundaries will clearly be required for reconstructions beyond those presented here. For future models, deforming regions can now be encompassed within the domain of an evolving, closed polygon and consequently incorporated as an extension of the CCP algorithm (see Gurnis et al., 2012). We expect that such deforming regions will be represented as deforming meshes within continuously closing polygons as the lowest level of a global hierarchy. Such functionality has now been incorporated in experimental versions of *GPlates* and will be a part of a new generation of global plate reconstructions. The first region to be addressed within a deforming plate network is the opening of the rift basins within the interior of Africa as the accounting of this extension will have flow-on effects for all the plates that hang-off the African-centered plate circuit.

6. Conclusions

There are currently three main types of plate motion models that enable us to place features on the surface of the earth into their spatio-temporal context. Geologically-current plate motion models are ideal because they provide a set of plate velocity vectors and delineate the boundaries between tectonic plates in a self-consistent

way (i.e. the combined area of the plates equals the area of the Earth). However, they are restricted to the Pliocene, making analysis of supercontinent break-up and accretion, the linkages between the deep earth and surface processes and larger-scale tectonic cycles unrealistic. Traditional plate motion models do not treat plates in a self-consistent way but rather reconstruct discrete features on the surface of the Earth without regard to the evolving nature of plate boundaries. Coupled geodynamic models are prone to large uncertainties and have not been successful at replicating past plate motions consistently in deep time.

In this paper, we have presented a new type of global plate motion model, which extends into deep time and involves a continuously evolving and self-consistent set of plate polygons and plate boundaries from the time of Pangea break-up. Our model is underpinned by a detailed analysis of the seafloor spreading record for the major tectonic plates. Our regional models are built within a hierarchical plate circuit framework linked to a hybrid absolute reference frame that includes moving Indian/Atlantic hotspots and a true polar wander corrected paleomagnetic-based model.

The plate motion model presented in this study will be of particular use to geodynamicists who require surface boundary conditions for the motions of the plates through time to link to models of the convecting mantle. However, our hope is that it can also be used as a framework for further detailed work so that we may converge towards an ever-improved set of global plate reconstructions. We provide all data freely in digital form, welcome feedback to improve our models and anticipate that refinements to the plate model will be published in the future. The plate polygon data files with associated rotation file and an accompanying coastline and continent–ocean boundary file can be downloaded from the following location: ftp://ftp.earthbyte.org/papers/Seton_etal_Global_ESR/Seton_etal_Data.zip.

Acknowledgments

We thank Roi Granot and an anonymous reviewer for agreeing to review such a lengthy manuscript and for their thoughtful and careful review, which greatly improved the manuscript. We would also like to thank members of the EarthByte Group and the group at Caltech led by Michael Gurnis who have contributed over many years towards the continuous improvement of the global plate motion model and associated files. This project was funded through Australian Research Council grants FL0992245 and DP0987713.

References

Agar, S., Cliff, R., Duddy, I., Rex, D., 1989. Short Paper: Accretion and uplift in the Shimanto Belt, SW Japan. Journal of the Geological Society 146, 893.
Aitchison, J.C., Ali, J.R., Davis, A.M., 2007. When and where did India and Asia collide. Journal of Geophysical Research 112, B05423.
Alvey, A., Gaina, C., Kusznir, N., Torsvik, T., 2008. Integrated crustal thickness mapping and plate reconstructions for the high Arctic. Earth and Planetary Science Letters 274, 310–321.
Apel, E., B¸Rgmann, R., Steblov, G., Vasilenko, N., King, R., Prytkov, A., 2006. Independent active microplate tectonics of northeast Asia from GPS velocities and block modeling. Geophysical Research Letters 33, L11303.
Argus, D.F., Heflin, M.B., 1995. Plate motion and crustal deformation estimated with geodetic data from the Global Positioning System. Geophysical Research Letters 22, 1973–1976.
Argus, D.F., Gordon, R.G., Heflin, M.B., Ma, C., Eanes, R.J., Willis, P., Peltier, W.R., Owen, S.E., 2010. The angular velocities of the plates and the velocity of Earth's centre from space geodesy. Geophysical Journal International 180, 913–960.
Atwater, T., 1970. Implications of plate tectonics for the Cenozoic tectonic evolution of Western North America. Geological Society of America Bulletin 81, 3513–3536.
Atwater, T., 1990. Plate tectonic history of the northeast Pacific and western North America. In: Winterer, E.L., Hussong, D.M., Decker, R.W. (Eds.), The Eastern Pacific Ocean and Hawaii, Volume N: The Geology of North America. Geological Society of America, Boulder, Colorado, pp. 21–72.
Atwater, T., 1989. Magnetic Anomalies in the North Pacific. Geological Society of America: Geology of North America.
Atwater, T., Severinghaus, J., 1989. Magnetic Anomalies in the North Pacific: Geological Society of America, v. Geology of North America.
Atwater, T., Severinghaus, J., 1990. Tectonic maps of the northeast Pacific. In: Winterer, E.L., Hussong, D.M., Decker, R.W. (Eds.), The Eastern Pacific Ocean and Hawaii, Volume N: The Geology of North America. Geological Society of America, Boulder, Colorado, pp. 15–20.
Atwater, T., Sclater, J., Sandwell, D., 1993. Fracture zone traces across the North Pacific Cretaceous Quiet Zone and their tectonic implications. In: Pringle, M.S., et al. (Ed.), Mesozoic Pacific: Geology, Tectonics, and Volcanism. Geophysical Monograph Series, vol. 77. AGU, Washington, D.C., pp. 137–154.
Badarch, G., Dickson Cunningham, W., Windley, B.F., 2002. A new terrane subdivision for Mongolia: implications for the Phanerozoic crustal growth of Central Asia. Journal of Asian Earth Sciences 21, 87–110.
Baillie, P.W., Jacobson, E., 1995. Structural evolution of the Carnarvon Terrace, Western Australia. The APEA Journal 35, 321–332.
Banerjee, B., Sengupta, B., Banerjee, P., 1995. Signals of Barremian (116 Ma) or younger oceanic crust beneath the Bay of Bengal along 14 N latitude between 81 E and 93 E. Marine Geology 128, 17–23.
Banks, N., Bardwell, K., Musiwa, S., 1995. Karoo rift basins of the Luangwa Valley, Zambia. Geological Society London Special Publications 80, 285.
Barckhausen, U., Ranero, C.R., Cande, S.C., Engels, M., Weinrebe, W., 2008. Birth of an intraoceanic spreading center. Geology 36, 767.
Beauchamp, W.H., 1998. Tectonic evolution of the Atlas Mountains, North Africa.
Belasky, P., Runnegar, B., 1994. Permian longitudes of Wrangellia, Stikinia, and Eastern Klamath terranes based on coral biogeography. Geology 22, 1095–1098.
Bernard, A., Munschy, M., 2000. Were the Mascarene and Laxmi Basins (western Indian Ocean) formed at the same spreading centre? Comptes Rendus de l'Academie des Sciences Series IIA Earth and Planetary Science 330, 777–783.
Binks, R., Fairhead, J., 1992. A plate tectonic setting for Mesozoic rifts of West and Central Africa. Tectonophysics 213, 141–151.
Billen, M.I., Stock, J., 2000. Morphology and origin of the Osbourn Trough. Journal of Geophysical Research-Solid Earth 105, 13481–13489.
Bird, P., 2003. An updated digital model of plate boundaries. Geochemistry, Geophysics, Geosystems 4, 1027. doi:10.1029/2001GC000252.
Bird, R.T., Naar, D.F., 1994. Intrafransform origins of mid-ocean ridge microplates. Geology 22, 987–990.
Bird, R.T., Naar, D.F., Larson, R.L., Searle, R.C., Scotese, C.R., 1998. Plate tectonic reconstructions of the Juan Fernandez microplate: transformation from internal shear to rigid rotation. Journal of Geophysical Research-Solid Earth 103, 7049–7067.
Bird, D., Hall, S., Burke, K., Casey, J., Sawyer, D., 2007. Early Central Atlantic Ocean seafloor spreading history. Geosphere 3, 282.
Blakely, R., 2008. Gondwana paleogeography from assembly to breakup: A 500 my odyssey. Resolving the late Paleozoic ice age in time and space, p. 1.
Boillot, G., Girardeau, J., Kornprobst, J., 1988. Rifting of the Galicia margin: crustal thinning and emplacement of mantle rocks on the seafloor. In: Goillot, G., Winterer, E.L. (Eds.), Proceedings of the Ocean Drilling Program, Scientific Results 103, 741–756.
Boillot, G., Winterer, E., 1988. Drilling on the Galicia margin: retrospect and prospect. Proceedings of the Ocean Drilling Program, Scientific Results 103, 809–828.
Boulin, J., 1988. Hercynian and Eocimmerian events in Afghanistan and adjoining regions. Tectonophysics 148, 253–278.
Boyden, J.A., Müller, R.D., Gurnis, M., Torsvik, T.H., Clark, J.A., Turner, M., Ivey-Law, H., Watson, R.J., Cannon, J.S., 2011. Next-generation plate-tectonic reconstructions using GPlates. In: Keller, G.R., Baru, C. (Eds.), Geoinformatics: Cyberinfrastructure for the Solid Earth Sciences. Cambridge University Press, pp. 95–114.
Bradley, D.C., Haeussler, P.J., Kusky, T.M., 1993. Timing of early Tertiary ridge subduction in southern Alaska. US Geological Survey Bulletin 2068, 163–177.
Bradley, D., 2008. Passive margins through Earth history. Earth-Science Reviews 91, 1–26.
Bradshaw, M.T., Yeates, A.N., Beynon, R.M., Brakel, A.T., Langford, R.P., Totterdell, J.M., Yeung, M., 1988. Paleogeographic evolution of the North West Shelf region. In: Purcell, P.G., Purcell, R.R. (Eds.), The North West Shelf of Australia: Petroleum Exploration Society of Australia Symposium: Perth, pp. 29–53.
Breitsprecher, K., Thorkelson, D., Groome, W., Dostal, J., 2003. Geochemical confirmation of the Kula-Farallon slab window beneath the Pacific Northwest in Eocene time. Geology 31, 351.
Brekke, H., 2000. The tectonic evolution of the Norwegian Sea continental margin with emphasis on the Voring and More basins. Geological Society London Special Publications, v. 167, p. 327.
Brozena, J., Childers, V., Lawver, L., Gahagan, L., Forsberg, R., Faleide, J., Eldholm, O., 2003. New aerogeophysical study of the Eurasia Basin and Lomonosov Ridge: implications for basin development. Geology, 31, p. 825.
Bryan, S.E., Constantine, A.E., Stephens, C.J., Ewart, A., Schon, R.W., Parianos, J., 1997. Early Cretaceous volcano-sedimentary successions along the Eastern Australian continental margin — implications for the break-up of Eastern Gondwana. Earth and Planetary Science Letters 153, 85–102.
Buchs, D.M., Arculus, R.J., Baumgartner, P.O., Baumgartner-Mora, C., Ulianov, A., 2010. Late Cretaceous arc development on the SW margin of the Caribbean Plate: insights from the Golfito, Costa Rica, and Azuero, Panama, complexes. Geochemistry, Geophysics, Geosystems 11, Q07S24.
Buffler, R.T., Sawyer, D.S., 1983. Distribution of crust and early history, Gulf of Mexico basin. Gulf Coast Association Geological Society Transcripts 35, 334–344.
Bunce, E.T., Molnar, P., 1977. Seismic reflection profiling and basement topography in the Somali Basin: possible fracture zones between Madagascar and Africa. Journal of Geophysical Research 82, 5305–5311.
Bunge, H., Grand, S., 2000. Mesozoic plate-motion history below the northeast Pacific Ocean from seismic images of the subducted Farallon slab. Nature 405, 337–340.
Burke, K., 1988. Tectonic evolution of the Caribbean. Annual Review of Earth and Planetary Sciences 16, 201–230.
Byrne, T., 1979. Late Paleocene demise of the Kula–Pacific spreading center. Geology 7, 341.

Cande, S.C., Haxby, W.F., 1991. Eocene propagating rifts in the Southwest Pacific and their conjugate features on the Nazca Plate. Journal of Geophysical Research 96, 19609.
Cande, S.C., Herron, E.M., Hall, B.R., 1982. The early Cenozoic tectonic history of the southeast Pacific. Earth and Planetary Science Letters 57, 63–74.
Cande, S.C., Kent, D.V., 1992. A new geomagnetic polarity time scale for Late Cretaceous and Cenozoic. Journal of Geophysical Research 97, 13917–13951.
Cande, S.C., Kent, D.V., 1995. Revised calibration of the geomagnetic polarity timescale for the Late Cretaceous and Cenozoic. Journal of Geophysical Research 100, 6093–6095.
Cande, S.C., Larson, R.L., LaBrecque, J.L., 1978. Magnetic lineations in the Pacific Jurassic Quiet Zone. Earth and Planetary Science Letters 41, 434–440.
Cande, S.C., Mutter, J.C., 1982. A revised identification of the oldest sea-floor spreading anomalies between Australia and Antarctica. Earth and Planetary Science Letters 58, 151–160.
Cande, S., Labrecque, J., Haxby, W., 1988. Plate kinematics of the South Atlantic: Chron C34 to present. Journal of Geophysical Research 93, 13479–13492.
Cande, S.C., Raymond, C.A., Stock, J., Haxby, W.F., 1995. Geophysics of the Pitman fracture zone and Pacific–Antarctic plate motions during the Cenozoic. Science 270, 947–953.
Cande, S., Stock, J., Raymond, C., Müller, R.D., 1998. New constraints on an old plate tectonic puzzle of the Southwest Pacific. Eos 79, 81–82.
Caress, D.W., Menard, H.W., Hey, R.N., 1988. Eocene reorganization of the Pacific-Farallon Spreading Center north of the Mendocino Fracture Zone. Journal of Geophysical Research 93, 2813–2838.
Carey, S.W., 1955. The orocline concept in geotectonics. Royal Society of Tasmania Proceedings 89, 255–288.
Carminati, E., Doglioni, C., Scrocca, D., 2004. Alps vs Apennines. Special volume of the Italian Geological Society for the IGC, vol. 32, pp. 141–151.
Catuneanu, O., Wopfner, H., Eriksson, P., Cairncross, B., Rubidge, B., Smith, R., Hancox, P., 2005. The Karoo basins of south-central Africa. Journal of African Earth Sciences 43, 211–253.
Chalmers, J.A., 1991. New evidence on the structure of the Labrador Sea/Greenland continental margin. Journal of the Geological Society of London 148, 899–908.
Chalmers, J.A., Laursen, K.H., 1995. Labrador Sea: the extent of continental and oceanic crust and the timing of the onset of seafloor spreading. Marine and Petroleum Geology 12, 205–217.
Chalmers, J., Pulvertaft, T., 2001. Development of the continental margins of the Labrador Sea: a review. Geological Society London Special Publications 187, 77.
Chandler, M., Wessel, P., Seton, M., Taylor, B., Hyeong, K., Kim, S., in press. Reconstructing Ontong Java Nui: Implications for Pacific absolute plate motion, hotspot drift and true polar wander. Earth and Planetary Science Letters.
Channell, J.E.T., 1995. Recalibration of the geomagnetic polarity timescale. Reviews of Geophysics 33, 161–168.
Chaubey, A.K., Bhattacharya, G.C., Murty, G.P.S., Srinivas, K., Ramprasad, T., Rao, D.G., 1998. Early Tertiary seafloor spreading magnetic anomalies and paleo-propagators in the Northern Arabian Sea. Earth and Planetary Science Letters 154, 41–52.
Churkin, M., Trexler, J.H., 1980. Circum-Arctic plate accretion-isolating part of a Pacific plate to form the nucleus of the Arctic Basin. Earth and Planetary Science Letters 49, 356–362.
Cluzel, D., Adams, C., Meffre, S., Campbell, H., Maurizot, P., 2010. Discovery of Early Cretaceous rocks in New Caledonia; new geochemical and U–Pb zircon age constraints on the transition from subduction to marginal breakup in the Southwest Pacific.
Cocks, L.R.M., Torsvik, T.H., 2007. Siberia, the wandering northern terrane, and its changing geography through the Palaeozoic. Earth-Science Reviews 82, 29–74.
Cochran, J.R., 1988. The Somali Basin, Chain Ridge and the origin of the northern Somali Basin gravity and geoid low. Journal of Geophysical Research 93, 11985–12008.
Coffin, M.F., Rabinowitz, P.D., 1987. Reconstruction of Madagascar and Africa: evidence from the Davie Fracture Zone and western Somali Basin. Journal of Geophysical Research 92, 9385–9406.
Coffin, M.F., Rabinowitz, P.D., 1988. Evolution of the East African continental margin and the Western Somali Basin. 78 pp.
Cole, J., Peachey, J., 1999. Evidence for Pre-Cretaceous Rifting in the Rockall Trough: An Analysis using Quantitative Plate Tectonic Modelling. Geological Society Pub House, p. 359.
Collier, J., Sansom, V., Ishizuka, O., Taylor, R., Minshull, T., Whitmarsh, R., 2008. Age of Seychelles–India break-up. Earth and Planetary Science Letters 272, 264–277.
Colpron, M., Logan, J.M., Mortensen, J.K., 2002. U–Pb zircon age constraint for late Neoproterozoic rifting and initiation of the lower Paleozoic passive margin of western Laurentia. Canadian Journal of Earth Sciences 39, 133–143.
Colpron, M., Nelson, J.A.L., Murphy, D.C., 2007. Northern Cordilleran terranes and their interactions through time. GSA Today 17, 4–10.
Conrad, C., Lithgow-Bertelloni, C., 2002. How mantle slabs drive plate tectoncs. Science 298, 207–209.
Cox, K.G., 1992. Karoo igneous activity, and the early stages of the break-up of Gondwanaland. In: Storey, B.C., Alabaster, T., Pankhurst, R.J. (Eds.), Magmatism and the causes of continental break-up. : Geological Society Special Publication, 68. Geological Society, London, pp. 137–148.
Crawford, T., Meffre, S., Symonds, P.A., 2002. Tectonic Evolution of the SW Pacific: lessons for the geological evolution of the Tasman fold belt system in eastern Australia from 600 to 220 Ma. In: Hillis, R., Müller, R.D. (Eds.), Evolution and Dynamics of the Australian Plate.
Croon, M.B., Cande, S.C., Stock, J.M., 2008. Revised Pacific–Antarctic plate motions and geophysics of the Menard Fracture Zone. Geochemistry, Geophysics, Geosystems 9, 7.
Daly, M., Chorowicz, J., Fairhead, J., 1989. Rift basin evolution in Africa: the influence of reactivated steep basement shear zones. Geological Society London Special Publications 44, 309.
Davy, B., Hoernle, K., Werner, R., 2008. Hikurangi Plateau: Crustal structure, rifted formation, and Gondwana subduction history. Geochemistry, Geophysics, Geosystems 9, Q07004.
De Graciansky, P., Poag, C., Cunningham Jr., R., Loubere, P., Masson, D., Mazzullo, J., Montadert, L., Muller, C., Otsuka, K., Reynolds, L., 1985. The Goban Spur transect: geologic evolution of a sediment-starved passive continental margin. Bulletin of the Geological Society of America 96, 58.
Decelles, P., 2004. Late Jurassic to Eocene evolution of the Cordilleran thrust belt and foreland basin system, western USA. American Journal of Science 304, 105.
Demets, C., Gordon, R.G., Argus, D.F., Stein, S., 1990. Current plate motions. Geophysical Journal International 101, 425–478.
Demets, C., Gordon, R.G., Argus, D.F., 2010. Geologically current plate motions. Geophysical Journal International 181, 1–80.
Demets, C., Gordon, R., Vogt, P., 1994. Location of the Africa-Australia-India triple junction and motion between the Australian and Indian plates: Results from an aeromagnetic investigation of the Central Indian and Carlsberg ridges. Geophysical Journal International 119, 893–930.
Desa, M., Ramana, M., Ramprasad, T., 2006. Seafloor spreading magnetic anomalies south off Sri Lanka. Marine Geology 229, 227–240.
DiTullio, L., 1993. Geologic summary and conceptual framework for the study of thermal maturity within the Eocene-Miocene Shimanto Belt, Shikoku, Japan. Thermal evolution of the Tertiary Shimanto Belt, southwest Japan: an example of ridge-trench interaction, p. 1.
Dore, A., Lundin, E., Jensen, L., Birkeland, ÿ, Eliassen, P., Fichler, C., 1999. Principal tectonic events in the evolution of the northwest European Atlantic margin. Geological Society of London 5, 41.
Downey, N.J., Stock, J.M., Clayton, R.W., Cande, S.C., 2007. History of the Cretaceous Osbourn spreading center. Journal of Geophysical Research 112, B04102.
Dove, D., Coakley, B., Hopper, J., Kristoffersen, Y., 2010. Bathymetry, controlled source seismic and gravity observations of the Mendeleev ridge; implications for ridge structure, origin, and regional tectonics. Geophysical Journal International 1, 348.
Dunbar, J., Sawyer, D., 1989. Patterns of continental extension along the conjugate margins of the central and North Atlantic Ocean and Labrador Sea. Tectonics 8.
Duncan, R., Hargraves, R., 1984. Plate tectonic evolution of the Caribbean region in the mantle reference frame. The Caribbean-South American Plate Boundary and Regional Tectonics, p. 81ñ93.
Eagles, G., 2007. New angles on South Atlantic opening. Geophysical Journal International 168, 353–361.
Eagles, G., König, M., 2008. A model of plate kinematics in Gondwana breakup. Geophysical Journal International 173, 703–717.
Eagles, G., Gohl, K., Larter, R.D., 2004a. High-resolution animated tectonic reconstruction of the South Pacific and West Antarctic margin — art. no. Q07002. Geochemistry, Geophysics, Geosystems 5 7002-7002.
Eagles, G., Gohl, K., Larter, R.D., 2004b. Life of the Bellingshausen plate. Geophysical Research Letters 31 7603-7603.
Eakins, B.W., Lonsdale, P.F., 2003. Structural patterns and tectonic history of the Bauer microplate, Eastern Tropical Pacific. Marine Geophysical Researches 24, 171–205.
Engebretson, D.C., Cox, A., Gordon, R.G., 1985. Relative Motions between Oceanic and Continental Plates in the Pacific Basin. Geol. Soc. of Am.
Faccenna, C., Becker, T.W., Lucente, F.P., Jolivet, L., Rossetti, F., 2001. History of subduction and back arc extension in the Central Mediterranean. Geophysical Journal International 145, 809–820.
Falvey, D.A., Mutter, J.C., 1981. Regional plate tectonics and the evolution of Australia's passive margins. Journal of Australian Geology and Geophysics 6, 1–29.
Forster, R., 1975. The geological history of the sedimentary basins of southern Mozambique, and some aspects of the origin of the Mozambique Channel. Palaeogeography, Palaeoclimatology, Palaeoecology 17, 267–287.
Forsyth, D.A., Asudeh, I., Green, A.G., Jackson, H.R., 1986. Crustal structure of the northern Alpha Ridge beneath the Arctic Ocean. Nature 322, 349–352.
Fullerton, L.G., Sager, W.W., Handschumacher, D.W., 1989. Late Jurassic–Early Cretaceous evolution of the eastern Indian Ocean adjacent to northwest Australia. Journal of Geophysical Research 94, 2937–2953.
Gaina, C., Müller, R.D., 2007. Cenozoic tectonic and depth/age evolution of the Indonesian gateway and associated back-arc basins. Earth-Science Reviews 83, 177–203.
Gaina, C., Müller, D.R., Royer, J.Y., Stock, J., Hardebeck, J., Symonds, P., 1998. The tectonic history of the Tasman Sea: a puzzle with 13 pieces. Journal of Geophysical Research 103, 12413–12433.
Gaina, C., Müller, R.D., Royer, J.-Y., Symonds, P., 1999. The tectonic evolution of the Louisiade Triple Junction. Journal of Geophysical Research 104, 12927–12939.
Gaina, C., Roest, W.R., Müller, R.D., 2002. Late Cretaceous–Cenozoic deformation of northeast Asia. Earth and Planetary Science Letters 197, 273–286.
Gaina, C., Müller, R.D., Brown, B., Ishihara, T., 2003. Micro-continent formation around Australia. In: Hillis, R., Müller, R.D. (Eds.), The Evolution and Dynamics of the Australian Plate, vol. 22. Geol. Soc. Aust. Spec. Publ., Geological Society of Australia.
Gaina, C., Müller, R.D., Brown, B., Ishihara, T., Ivanov, S., 2007. Breakup and early seafloor spreading between India and Antarctica. Geophysical Journal International 170, 151–169.
Gaina, C., Gernigon, L., Ball, P., 2009. Palaeocene–Recent plate boundaries in the NE Atlantic and the formation of the Jan Mayen microcontinent. Journal of the Geological Society 166, 601.
Gaina, C., Labails, C., Reeves, C., 2010. The Early Opening of the Indian Ocean: An African Perspective, 2010 Fall Meeting, Volume Abstract T13C-2222. AGU, San Francisco, California. 13–17 Dec.
Gee, J., Kent, D., 2007. Source of Oceanic magnetic anomalies and the geomagnetic polarity timescale. Treatise on Geophysics 5, 455ñ507.

Gehrels, G.E., 2001. Geology of the Chatham Sound region, southeast Alaska and coastal British Columbia. Canadian Journal of Earth Sciences 38, 1579–1599.
Gehrels, G.E., 2002. Detrital zircon geochronology of the Taku terrane, southeast Alaska. Canadian Journal of Earth Sciences 39, 921–931.
Genik, G., 1992. Regional framework, structural and petroleum aspects of rift basins in Niger, Chad and the Central African Republic (CAR). Tectonophysics 213, 169–185.
Gerstell, M., Stock, J., 1994. Testing the porcupine plate hypothesis. Marine Geophysical Researches 16, 315–323.
Ghidella, M.E., Yanez, G., LaBrecque, J.L., 2002. Revised tectonic implications for the magnetic anomalies of the western Weddell Sea. Tectonophysics 347, 65–86.
Ghosh, N., Hall, S., Casey, J., 1984. Seafloor spreading magnetic anomalies in the Venezuelan Basin. The Caribbean–South American Plate Boundary and Regional Tectonics, pp. 65–80.
Goff, J.A., Cochran, J.R., 1996. The Bauer scarp ridge jump: a complex tectonic sequence revealed in satellite altimetry. Earth and Planetary Science Letters 141, 21–33.
Golonka, J., 2007. Late Triassic and Early Jurassic palaeogeography of the world. Palaeogeography, Palaeoclimatology, Palaeoecology 244, 297–307.
Golonka, J., Ford, D., 2000. Pangean (Late Carboniferous–Middle Jurassic) paleoenvironment and lithofacies. Palaeogeography, Palaeoclimatology, Palaeoecology 161, 1–34.
Golonka, J., Gahagan, L., Krobicki, M., Marko, F., Oszczypko, N., Slaczka, A., 2006. Plate-tectonic evolution and paleogeography of the circum-Carpathian region: the Carpathians and their foreland: geology and hydrocarbon resources. AAPG Memoir 84, 11-46.
Gordon, R.G., Stein, S., 1992. Global tectonics and space geodesy. Science 256, 333.
Goslin, J., Schlich, R., 1976. Structural limits of the South Crozet Basin; relations to Enderby Basin and the Kerguelen-Heard Plateau. International Geological Congress, Abstracts, vol. 25 (3), pp. 884–885.
Guiraud, R., Maurin, J.C., 1992. Early Cretaceous rifts of Western and Central Africa: an overview. Tectonophysics 213, 153–168.
Gradstein, F.M., Agterberg, F.P., Ogg, J.G., Hardenbol, S., Vanveen, P., Thierry, J., Huang, Z.H., 1994. A Mesozoic time scale. Journal of Geophysical Research-Solid Earth 99, 24051–24074.
Gradstein, F., Ogg, J., Smith, A., Agterberg, F., Bleeker, W., Cooper, R., Davydov, V., Gibbard, P., Hinnov, L., House, M., 2004. A Geologic Time Scale 2004. Cambridge University Press.
Granot, R., Cande, S.C., Gee, J.S., 2009. The implications of long-lived asymmetry of remanent magnetization across the North Pacific fracture zones. Earth and Planetary Science Letters 288, 551–563.
Grantz, A., Clark, D., Phillips, R., Srivastava, S., Blome, C., Gray, L., Haga, H., Mamet, B., McIntyre, D., Mcneil, D., 1998. Phanerozoic stratigraphy of Northwind Ridge, magnetic anomalies in the Canada basin, and the geometry and timing of rifting in the Amerasia basin, Arctic Ocean. Geological Society of America Bulletin 110, 801.
Greene, A.R., Scoates, J.S., Weis, D., 2008. Wrangellia flood basalts in Alaska: a record of plume–lithosphere interaction in a Late Triassic accreted oceanic plateau. Geochemistry, Geophysics, Geosystems 9, 12004.
Gurnis, M., Turner, M., Zahirovic, S., Dicaprio, L., Spasojevic, S., Müller, R.D., Boyden, J., Seton, M., Manea, V., Bower, D., 2012. Plate tectonic reconstructions with continuously closing plates. Computers and Geosciences 38, 35–42.
Haeussler, P.J., Bradley, D., Goldfarb, R., Snee, L., Taylor, C., 1995. Link between ridge subduction and gold mineralization in southern Alaska. Geology 23, 995.
Hafkenscheid, E., Buiter, S.J.H., Wortel, M.J.R., Spakman, W., Bijwaard, H., 2001. Modelling the seismic velocity structure beneath Indonesia: a comparison with tomography. Tectonophysics 333, 35–46.
Hager, B.H., O'Connell, R.J., 1981. A simple global model of plate dynamics and mantle convection. Journal of Geophysical Research 86, 4843–4867.
Halgedahl, S., Jarrard, R., 1987. Paleomagnetism of the Kuparuk River formation from oriented drill core: evidence for rotation of the North Slope block. In: Tailleur, I.L., Weimer, P. (Eds.), Alaskan North Slope Geology. Soc. Econ. Paleont. and Min., Pacific Section, Los Angeles, pp. 581–617.
Hall, R., 2002. Cenozoic geological and plate tectonic evolution of Southeast Asia and the SW Pacific: computer-based reconstructions, models and animations. Journal of Asian Earth Sciences 20, 353–431.
Hall, R., Fuller, M., Ali, J.R., Anderson, C.D., 1995. The Philippine Sea plate: magnetism and reconstructions. In: Taylor, B., Natland, J.H. (Eds.), A Synthesis of Western Pacific Drilling Results, vol. 88. American Geophysical Union, pp. 371–404.
Hamilton, W., 1979. Tectonics of the Indonesian Region. USGS Professional Paper 1078, 345.
Handschumacher, D.W., 1976. Post-Eocene Plate Tectonics of the Eastern Pacific. In: G.H.S., et al. (Ed.), The Geophysics of the Pacific Ocean Basin and its Margin: A Volume in Honour of George P. Woollard. American Geophysical Union, Washington D.C., pp. 177–202.
Handschumacher, D., Sager, W., Hilde, T., Bracey, D., 1988. Pre-Cretaceous tectonic evolution of the Pacific plate and extension of the geomagnetic polarity reversal time scale with implications for the origin of the Jurassic 'Quiet Zone'. Tectonophysics 155, 365–380.
Hankel, O., 1994. Early Permian to middle Jurassic rifting and sedimentation in East Africa and Madagascar. Geologische Rundschau 83, 703–710.
Hansen, V.L., 1990. Yukon-Tanana terrane: a partial acquittal. Geology 18, 365.
Harland, W.B., Armstrong, R.L., Cox, A.V., Craig, I.E., Smith, A.G., Smith, D.G., 1990. A Geologic Time Scale. Camibridge University Press, Cambridge.
Hassanzadeh, J., Stockli, D.F., Horton, B.K., Axen, G.J., Stockli, L.D., Grove, M., Schmitt, A.K., Walker, J.D., 2008. U–Pb zircon geochronology of late Neoproterozoic–Early Cambrian granitoids in Iran: implications for paleogeography, magmatism, and exhumation history of Iranian basement. Tectonophysics 451, 71–96.
Hawlader, H., 1990. Diagenesis and reservoir potential of volcanogenic sandstones—Cretaceous of the Surat Basin, Australia. Sedimentary Geology 66, 181–195.
Heine, C., Muller, R., 2005. Late Jurassic rifting along the Australian North West Shelf: margin geometry and spreading ridge configuration. Australian Journal of Earth Sciences 52 (1), 27–39.
Heine, C., Müller, R.D., Gaina, C., 2004. Reconstructing the lost Eastern Tethys Ocean Basin: constraints for the convergence history of the SE Asian margin and marine gateways. In: Clift, P., Hayes, D., Kuhnt, W., Wang, P. (Eds.), Continent–Ocean Interactions in Southeast Asia, Volume 1149: Geophys. Monogr. Ser. American Geophysical Union, Washington.
Heirtzler, J., Burroughs, R., 1971. Madagascar's paleoposition: new data from the Mozambique channel. Science (New York, N.Y.) 174, 488.
Heirtzler, J.R., Dickson, G.O., Herman, E.M., Pitman III, W.C., Lepichon, X., 1968. Marine magnetic anomalies, geomagnetic field reversals, and motions of the ocean floor and continents. Journal of Geophysical Research 73, 2119–2136.
Herron, E.M., 1972. Sea Floor Spreading and the Cenozoic History of the East-Central Pacific. Geological Society of America Bulletin 83, 1671–1692.
Hessami, K., Koyi, H.A., Talbot, C.J., Tabishi, H., Shabanian, E., 2001. Progressive unconformities within an evolving foreland fold–thrust belt, Zagros Mountains. Journal of the Geological Society 158, 969.
Hey, R., 1977. Tectonic evolution of the Cocos–Nazca spreading center. Geological Society of America Bulletin 88, 1404–1420.
Hillier, J., 2007. Pacific seamount volcanism in space and time. Geophysical Journal International 168, 877–889.
Hoernle, K., Hauff, F., Van Den Bogaard, P., Werner, R., Mortimer, N., Geldmacher, J., Garbe-Schˆ Nberg, D., Davy, B., 2010. Age and geochemistry of volcanic rocks from the Hikurangi and Manihiki oceanic plateaus. Geochimica et Cosmochimica Acta.
Holloway, N., 1982. North Palawan block, Philippines—its relation to Asian mainland and role in evolution of South China Sea. American Association of Petroleum Geologists Bulletin 66, 1355ñ1383.
Hopper, J., Funck, T., Tucholke, B., Larsen, H., Holbrook, W., Louden, K., Shillington, D., Lau, H., 2004. Continental breakup and the onset of ultraslow seafloor spreading off Flemish Cap on the Newfoundland rifted margin. Geology 32, 93.
Hutchison, C.S., 1989. Geological Evolution of South-east Asia, p. 368.
Hutchison, C.S., 2005. Geology of North-west Borneo. Elsevier Science Ltd., Sarawak, Brunei and Sabah.
Jackson, H., Gunnarsson, K., 1990. Reconstructions of the Arctic: Mesozoic to present. Tectonophysics 172, 303–322.
James, K., 2006. Arguments for and against the Pacific origin of the Caribbean Plate. Geologica Acta 4, 279.
Johnson, B.D., Powell, C.M., Veevers, J.J., 1976. Spreading history of the eastern Indian Ocean and Greater India's northward flight from Antarctica and Australia. Geological Society of America Bulletin 87, 1560–1566.
Johnson, B.D., Powell, C.M., Veevers, J.J., 1980. Early spreading history of the Indian Ocean between India and Australia. Earth and Planetary Science Letters 47, 131–143.
Jokat, W., Uenzelmann-Neben, G., Kristoffersen, Y., Rasmussen, T., 1992. Lomonosov Ridge—a double-sided continental margin. Geology 20, 887.
Jokat, W., Ritzmann, O., Schmidt-Aursch, M.C., Drachev, S.S., Gauger, S., Snow, J.H., 2003. Geophysical evidence for reduced melt production on the Arctic ultraslow Gakkel mid-ocean ridge. Nature 423, 962–965.
Jokat, W., Nogi, Y., Leinweber, V.T., 2010. New aeromagnetic data from the western Enderby Basin and consequences for Antarctic–India break-up. Geophysical Research Letters 37, L21311.
Jones, J.G., Veevers, J.J., 1983. Mesozoic origins and antecedents of Australia's Eastern Highlands. Journal of the Geological Society of Australia 30, 305–322.
Joseph, D., Shor, A., Hussong, D., Malikides, M., 1990. The origin of the Nova Canton Trough reexamined. Transactions, American Geophysical Union 71, 1640.
Joseph, D., Taylor, B., Shor, A.N., 1992. New sidescan sonar and gravity evidence that the Nova-Canton Trough is a fracture zone. Geology 20, 435–438.
Jourdan, F., FÈraud, G., Bertrand, H., Kampunzu, A.B., Tshoso, G., Watkeys, M.K., Le Gall, B., 2005. Karoo large igneous province: Brevity, origin, and relation to mass extinction questioned by new 40Ar/39Ar age data. Geology 33, 745.
Karig, D.E., 1971. Origin and development of marginal basins in the Western Pacific. Journal of Geophysical Research 76, 2542.
Keppie, J.D., Dostal, J., 2001. Evaluation of the Baja controversy using paleomagnetic and faunal data, plume magmatism, and piercing points. Tectonophysics 339, 427–442.
Kimbell, G., Ritchie, J., Johnson, H., Gatliff, R., 2005. Controls on the structure and evolution of the NE Atlantic margin revealed by regional potential field imaging and 3D modelling. Geological Society of London 6, 933.
Klitgord, K., Schouten, H., 1986. Plate kinematics of the central Atlantic. In: Vogt, P.R., Tucholke, B.E. (Eds.), The Western North Atlantic Region, DNAG, Volume M: The Geology of North America. Geol. Soc. Am., Boulder, CO, United States, pp. 351–378.
Knott, S., Burchell, M., Jolley, E., Fraser, A., 1993. Mesozoic to Cenozoic Plate Reconstructions of the North Atlantic and Hydrocarbon Plays of the Atlantic margins, Volume 4, Geological Society of London, p. 953.
König, M., Jokat, W., 2006. The Mesozoic breakup of the Weddell Sea. Journal of Geophysical Research 111, B12102.
König, M., Jokat, W., 2010. Advanced insights into magmatism and volcanism of the Mozambique Ridge and Mozambique Basin in the view of new potential field data. Geophysical Journal International 180, 158–180.
Kovacs, L.C., Morris, P., Brozena, J., Tikku, A., 2002. Seafloor spreading in the Weddell Sea from magnetic and gravity data. Tectonophysics 347, 43–64.
Kravchinsky, V.A., Cognè, J.P., Harbert, W.P., Kuzmin, M.I., 2002. Evolution of the Mongol–Okhotsk Ocean as constrained by new palaeomagnetic data from the Mongol-Okhotsk suture zone, Siberia. Geophysical Journal International 148, 34–57.

Kuzmichev, A.B., 2009. Where does the South Anyui suture go in the New Siberian islands and Laptev Sea?: implications for the Amerasia basin origin. Tectonophysics 463, 86–108.
Labails, C., Olivet, J., Aslanian, D., Roest, W., 2010. An alternative early opening scenario for the Central Atlantic Ocean. Earth and Planetary Science Letters.
Labrecque, J.L., Hayes, D.E., 1979. Seafloor spreading history of the Agulhas Basin. Earth and Planetary Science Letters 45, 411–428.
LaBrecque, J.L., Barker, P., 1981. The age of the Weddell Basin. Nature 290, 489–492.
LaBrecque, J.L., Rabinowitz, P.D., 1977. Magnetic anomalies bordering the continental margin of Argentina: Tulsa. Amer. Assoc. Petr. Geol. map series.
Lancelot, Y., Larson, R.L., et al., 1990. Proc. ODP Initial Reports 129. Ocean Drilling Program, College Station, TX.
Lane, L.S., 1997. Canada basin, Arctic Ocean — evidence against a rotational origin [Review]. Tectonics 16, 363–387.
Larson, R.L., 1995. The mid-Cretaceous superplume episode. Scientific American 272, 66–70.
Larson, R.L., 1997. Superplumes and ridge interactions between Ontong Java and Manihiki plateaus and the Nova-Canton trough. Geology 25, 779–782.
Larson, R.L., Chase, C.G., 1972. Late Mesozoic evolution of the Western Pacific. Geological Society of America Bulletin 83, 3627–3644.
Larson, R.L., Pitman, W.C.I., 1972. World-wide correlation of Mesozoic magnetic anomalies, and its implications. Geological Society of America Bulletin 83, 3645–3662.
Larson, R., Smith, S., Chase, C., 1972. Magnetic lineations of Early Cretaceous age in the western equatorial Pacific Ocean. Earth and Planetary Science Letters 15, 315–319.
Larson, R.L., Pockalny, R.A., Viso, R.F., Erba, E., Abrams, L.J., Luyendyk, B.P., Stock, J.M., Clayton, R.W., 2002. Mid-Cretaceous tectonic evolution of the Tongareva triple junction in the southwestern Pacific Basin. Geology 30, 67–70.
Larson, R.L., 1976. Late Jurassic and Early Cretaceous evolution of the Western Central Pacific Ocean. Journal of Geomagnetism and Geoelectricity 28, 219–236.
Larson, R.L., 1977. Early Cretaceous breakup of Gondwanaland off western Australia. Geology 5, 57–60.
Larter, R.D., Cunningham, A.P., Barker, P.F., Gohl, K., Nitsche, F.O., 2002. Tectonic evolution of the Pacific margin of Antarctica 1. Late Cretaceous tectonic reconstructions. Journal of Geophysical Research-Solid Earth 107, 2345.
Lawver, L.A., Müller, R.D., 1994. Iceland hotspot track. Geology 22, 311.
Lawver, L.A., Müller, R.D., Srivastava, S.P., Roest, W., 1990. Opening of the Arctic Ocean. In: Bleil, U., Thiede, J. (Eds.), Geological History of the Polar Oceans: Arctic Versus Antarctic, pp. 29–62.
Lawver, L.A., Scotese, C.R., 1987. A revised reconstruction of Gondwanaland. AGU Geophysical Monograph 40, 17–23.
Lawver, L., Grantz, A., Gahagan, L., 2002. Plate kinematic evolution of the present Arctic region since the Ordovician. Geological Society of America Special Papers 360, 333.
Lee, T.-Y., Lawver, L.A., 1994. Cenozoic plate reconstruction of the South China Sea region. Tectonophysics 235, 149–180.
Lee, T.-Y., Lawver, L.A., 1995. Cenozoic plate reconstruction of Southeast Asia. Tectonophysics 251, 85–138.
Lemaux, J., Gordon, R.G., Royer, J.Y., 2002. Location of the Nubia–Somalia boundary along the Southwest Indian Ridge. Geology 30, 339–342.
Lemoine, M., 1983. Rifting and early drifting: Mesozoic central Atlantic and Ligurian Tethys. Initial Reports of the Deep Sea Drilling Project 76, 885ñ895.
Lewis, J.C., Byrne, T.B., Pasteris, J.D., London, D., Morgan, G.B., 2000. Early Tertiary fluid flow and pressure-temperature conditions in the Shimanto accretionary complex of south-west Japan: constraints from fluid inclusions. Journal of Metamorphic Geology 18, 319–333.
Lithgow-Bertelloni, C., Richards, M., 1998. The Dynamics of Cenozoic and Mesozoic Plate Motions. Reviews of Geophysics 36, 27–78.
Liu, L., Gurnis, M., Seton, M., Saleeby, J., MļLler, R., Jackson, J., 2010. The role of oceanic plateau subduction in the Laramide orogeny. Nature Geoscience 3, 353–357.
Livermore, R., Hunter, R., 1996. Mesozoic seafloor spreading in the southern Weddell Sea. Geological Society London Special Publications 108, 227.
Lonsdale, P., 1988. Paleogene history of the Kula plate: offshore evidence and onshore implications. Geological Society of America Bulletin 100, 733.
Lonsdale, P., 1997. An incomplete geologic history of the southwest Pacific basin. GSA Abstracts with Programs, vol. 29, p. 25.
Lonsdale, P., 2005. Creation of the Cocos and Nazca plates by fission of the Farallon plate. Tectonophysics 404, 237–264.
Lonsdale, P., Klitgord, K.D., 1978. Structure and tectonic history of the eastern Panama Basin. Geological Society of America Bulletin 89, 981–999.
Lowrie, W., Kent, D., 2004. Geomagnetic polarity timescales and reversal frequency regimes: timescales of the Paleomagnetic Field. Geophysical Monograph Series 145, 117ñ129.
Ludwig, W.J., Kumar, N., Houtz, R.E., 1979. Profiler-Sonobuoy measurements in the South China Sea basin. Journal of Geophysical Research 84, 3505–3518.
Madsen, J.K., Thorkelson, D.J., Friedman, R.M., Marshall, D.D., 2006. Cenozoic to Recent plate configurations in the Pacific Basin: Ridge subduction and slab window magmatism in western North America. Geosphere 2, 11–34.
Mahoney, J.J., Storey, M., Duncan, R.A., Spencer, K.J., Pringle, M., 1993. Geochemistry and geochronology of Leg 130 basement lavas: nature and origin of the Ontong Java Plateau. In: Berger, W.H., Kroenke, L.W., Mayer, L.A. (Eds.), Proceedings of the Ocean Drilling Program, Scientific Results, vol. 130. Ocean Drilling Program, Texas A&M University, College Station, TX, pp. 3–22.
Mahoney, J., Duncan, R., Tejada, M., Sager, W., Bralower, T., 2005. Jurassic–Cretaceous boundary age and mid-ocean-ridge-type mantle source for Shatsky Rise. Geology 33, 185.
Malfait, B.T., Dinkelman, M.G., 1972. Circum-Caribbean Tectonic and Igneous Activity and the Evolution of the Caribbean Plate. Geological Society of America Bulletin 83, 251–272.
Mammerickx, J., Klitgord, K., 1982. Northern East Pacific rise: evolution from 25 my BP to the present. Journal of Geophysical Research 87, 6751–6759.
Mammerickx, J., Sharman, G.F., 1988. Tectonic evolution of the North Pacific during the Cretaceous quiet period. Journal of Geophysical Research 93, 3009–3024.
Marks, K.M., Stock, J.M., 2001. Evolution of the Malvinas Plate south of Africa. Marine Geophysical Researches 22, 289–302.
Marks, K.M., Tikku, A.A., 2001. Cretaceous reconstructions of East Antarctica, Africa and Madagascar. Earth and Planetary Science Letters 186, 479–495.
Marton, G., Buffler, R., 1999. Jurassic–early cretaceous tectono-paleogeographic evolution of the southeastern gulf of Mexico basin. Sedimentary Basins of the World 4, 63–91.
Masson, D.G., 1984. Evolution of the Mascarene basin, western Indian Ocean, and the significance of the Amirante arc. Marine Geophysical Researches 6, 365–382.
Matthews, K.J., et al., 2011. Dynamic subsidence of Eastern Australia during the Cretaceous. Gondwana Research 19, 372–383.
Maus, S., Sazonova, T., Hemant, K., Fairhead, J.D., Ravat, D., 2007. National geophysical data center candidate for the world digital magnetic anomaly map. Geochemistry, Geophysics, Geosystems 8, Q06017. doi:10.1029/2007GC001643.
Maus, S., Barckhausen, U., Berkenbosch, H., Bournas, N., Brozena, J., Childers, V., Dostaler, F., Fairhead, J., Finn, C., Von Frese, R., 2009. EMAG2: a 2-arc min resolution Earth Magnetic Anomaly Grid compiled from satellite, airborne, and marine magnetic measurements. Geochemistry, Geophysics, Geosystems 10, Q08005.
Mayes, C.L., Lawver, L.A., Sandwell, D.T., 1990. Tectonic history and new isochron chart of the South Pacific. Journal of Geophysical Research 95, 8543–8567.
Mcelhinny, M.W., Embleton, B.J.J., Daly, L., Pozzi, J.P., 1976. Paleomagnetic evidence for the location of Madagascar in Gondwanaland. Geology 4, 455–457.
McKenzie, D.P., Morgan, J., 1969. The evolution of triple junctions. Nature 224, 125–133.
Menard, H.W., 1978. Fragmentation of the Farallon plate by pivoting subduction. Journal of Geology 86, 99–110.
Meschede, M., Frisch, W., 1998. A plate-tectonic model for the Mesozoic and Early Cenozoic history of the Caribbean plate. Tectonophysics 296, 269–291.
Meschede, M., Barckhausen, U., Worm, H.U., 1998a. Extinct spreading on the Cocos Ridge. Terra Nova 10, 211–216.
Meschede, M., Barckhausen, U., Worm, H.U., 1998b. Extinct spreading on the Cocos Ridge: Terra Nova. The European Journal of Geosciences 10, 211–216.
Metcalfe, I., 1996. Gondwanaland dispersion, Asian accretion and evolution of Eastern Tethys. Australian Journal of Earth Sciences 43, 605–623.
Metcalfe, I., 1999. Gondwana dispersion and Asian accretion: an overview. In: Metcalfe, I. (Ed.), Gondwana Dispersion and Asian Accretion. A.A. Balkema, Rotterdam, pp. 9–29.
Mihalynuk, M.G., Nelson, J.A., Diakow, L.J., 1994. Cache Creek terrane entrapment: oroclinal paradox within the Canadian Cordillera. Tectonics 13, 575–595.
Molnar, P., Atwater, T., Mammerickx, J., Smith, S.M., 1975. Magnetic anomalies, bathymetry and the tectonic evolution of the South Pacific since the Late Cretaceous. Geophysical Journal of the Royal Astronomical Society 40, 383–420.
Moran, K., Backman, J., Brinkhuis, H., Clemens, S.C., Cronin, T., Dickens, G.R., Eynaud, F., Gattacceca, J., Jakobsson, M., Jordan, R.W., 2006. The Cenozoic palaeoenvironment of the Arctic Ocean. Nature 441, 601–605.
Morgan, W.J., 1972. Plate motions and deep mantle convection. GSA Memoir 132, 7–22.
Mortensen, J., 1992. Pre-mid-Mesozoic tectonic evolution of the Yukon-Tanana terrane, Yukon and Alaska. Tectonics 11, 836–853.
Moulin, M., Aslanian, D., Unternehr, P., 2010. A new starting point for the South and Equatorial Atlantic Ocean. Earth-Science Reviews 98, 1–37.
Müller, R.D., Roest, W.R., 1992. Fracture zones in the North Atlantic from combined Geosat and Seasat data. Journal of Geophysical Research 97, 3337–3350.
Müller, R.D., Roest, W.R., Royer, J.-Y., Gahagan, L.M., Sclater, J.G., 1997. Digital isochrons of the world's ocean floor. Journal of Geophysical Research 102, 3211–3214.
Müller, R.D., Mihut, D., Baldwin, S., 1998a. A new kinematic model for the formation and evolution of the Northwest and West Australian margin. In: Purcell, P.G., Purcell, R.R. (Eds.), The Sedimentary Basins of Western Australia, 2. Petroleum Exploration Society of Australia, Perth, pp. 55–72.
Müller, R.D., Roest, W.R., Royer, J.-Y., 1998b. Asymmetric seafloor spreading expresses ridge–plume interactions. Nature 396, 455–459.
Müller, R.D., Cande, S.C., Royer, J.-Y., Roest, W.R., Maschenkov, S., 1999. New constraints on the Late Cretaceous/Tertiary plate tectonic evolution of the Caribbean. In: Mann, P. (Ed.), Caribbean Basins, Volume 4: Sedimentary Basins of the World. Elsevier, Amsterdam, pp. 39–55.
Müller, R.D., Gaina, C., Tikku, A., Mihut, D., Cande, S., Stock, J.M., 2000. Mesozoic/Cenozoic tectonic events around Australia. In: Richards, M., Gordon, R. (Eds.), The History and Dynamics of Global Plate Motions, Volume 121: American Geophysical Union Monograph. American Geophysical Union, pp. 161–188.
Müller, R., Goncharov, A., Kritski, A., 2005. Geophysical evaluation of the enigmatic Bedout basement high, offshore northwestern Australia. Earth and Planetary Science Letters 237, 264–284.
Müller, R.D., Sdrolias, M., Gaina, C., Roest, W.R., 2008a. Age, spreading rates and spreading asymmetry of the world's ocean crust. Geochemistry, Geophysics, Geosystems 9.
Müller, R.D., Sdrolias, M., Gaina, C., Steinberger, B., Heine, C., 2008b. Long-term sea-level fluctuations driven by ocean basin dynamics. Science 319, 1357–1362.
Munschy, M., Antoine, C., Gachon, A., 1996. Tectonic evolution in the Tuamotu Islands Region, Central Pacific Ocean. Comptes Rendus de l'Academie des Sciences Series IIA Earth and Planetary Science 323, 941–948.
Nakanishi, M., Tamaki, K., Kobayashi, K., 1992. A new Mesozoic isochron chart of the northwestern Pacific Ocean: paleomagnetic and tectonic implications. Geophysical Research Letters 19, 693–696.
Nakanishi, M., Winterer, E.L., 1998. Tectonic history of the Pacific–Farallon–Phoenix triple junction from late Jurassic to early Cretaceous: an abandoned Mesozoic spreading system in the central Pacific basin. Journal of Geophysical Research-Solid Earth 103, 12453–12468.

Nakanishi, M., Sager, W.W., Klaus, A., 1999. Magnetic lineations within Shatsky Rise, northwest Pacific Ocean: implications for hot spot-triple junction interaction and oceanic plateau formation. Journal of Geophysical Research-Solid Earth 104, 7539–7556.
Nelson, J.A., Mihalynuk, M., 1993. Cache Creek ocean: closure or enclosure? Geology 21, 173.
Nelson, J.A.L., Colpron, M., Piercey, S.J., Dusel-Bacon, C., Murphy, D.C., Roots, C.F., 2006. Paleozoic tectonic and Metallogenetic Evolution of Pericratonic Terranes in Yukon, Northern British Columbia and Eastern Alaska 1: Paleozoic Evolution and Metallogeny of Pericratonic Terranes at the Ancient Pacific Margin of North America, Canadian and Alaskan Cordillera, p. 323.
Nokleberg, W., Parfenov, L., Monger, J., Norton, I., Chan Uk, A., Stone, D., Scotese, C., Scholl, D., Fujita, K., 2001. Phanerozoic Tectonic Evolution of the Circum-North Pacific. US Dept. of the Interior, US Geological Survey.
Norton, I.O., Sclater, J.G., 1979. A model for the evolution of the Indian Ocean and the breakup of Gondwanaland. Journal of Geophysical Research 84, 6803–6830.
Norton, I., 2007. Speculations on Cretaceous tectonic history of the northwest Pacific and a tectonic origin for the Hawaii hotspot. Geological Society of America Special Papers 430, 451.
Nunns, A.G., 1983. Plate tectonic evolution of the Greenland-Scotland Ridge and surrounding regions. In: Bott, M.H.P., Saxov, S., Talwani, M., Thiede, J. (Eds.), Structure and Development of the Greenland–Scotland Ridge. Plenum, New York, New York, pp. 11–30.
Nürnberg, D., Müller, R.D., 1991. The tectonic evolution of the South Atlantic from Late Jurassic to present. Tectonophysics 191, 27–53.
O'Neill, C., Müller, R.D., Steinberger, B., 2005. On the uncertainties in hotspot reconstructions, and the significance of moving hotspot reference frames. Geochemistry, Geophysics, Geosystems 6. doi:10.1029/2004GC000784.
Pardo-Casas, F., Molnar, P., 1987. Relative motion of the Nazca (Farallon) and South American plates since Late Cretaceous time. Tectonics 6, 215–232.
Patriat, P., Ségoufin, J., 1988. Reconstruction of the central Indian Ocean. Tectonophysics 155, 211–234.
Peron-Pinvidic, G., Manatschal, G., Minshull, T., Sawyer, D., 2007. Tectonosedimentary evolution of the deep Iberia-Newfoundland margins: evidence for a complex breakup history. Tectonics 26.
Pindell, J.L., B., S.F., 1987. Geological evolution of the Caribbean Region: A plate tectonic perspective. The Caribbean Region. : The Geology of North America, vol. 1. Geol. Soc. America, Boulder, Colorado.
Pindell, J., Kennan, L., 2009. Tectonic evolution of the Gulf of Mexico, Caribbean and northern South America in the mantle reference frame: an update. Geological Society London Special Publications 328, 1.
Pindell, J.L., Cande, S., Pitman III, W.C., Rowley, D.B., Dewey, J.F., Labrecque, J., Haxby, W., 1988. A plate-kinematic framework for models of Caribbean evolution. Tectonophysics 155, 121–138.
Pindell, J., Kennan, L.S., K-P, M., 2006. Foundations of Gulf of Mexico and Caribbean evolution: eight controversies resolved. Geologica Acta 4, 303ñ341.
Pockalny, R.A., Larson, R.L., Viso, R.F., Abrams, L.J., 2002. Bathymetry and gravity data across a mid-Cretaceous triple junction trace in the southwest Pacific basin. Geophysical Research Letters 29, 1007.
Pogue, K.R., Dipietro, J.A., Khan, S.R., Hughes, S.S., Dilles, J.H., Lawrence, R.D., 1992. Late Paleozoic rifting in northern Pakistan. Tectonics 11, 871–883.
Powell, C.M., Roots, S.R., Veevers, J.J., 1988. Pre-breakup continental extension in East Gondwanaland and the early opening of the eastern Indian Ocean. Tectonophysics 155, 261–283.
Rabinowitz, P.D., 1971. Gravity anomalies across the East African continental margin. Journal of Geophysical Research 76, 7107–7117.
Rabinowitz, P.D., Coffin, M.F., Falvey, D., 1983. The separation of Madagascar and Africa. Science 220, 67–69.
Ramana, M.V., Nair, R.R., Sarma, K.V.L.N.S., Ramprasad, T., Krishna, K.S., Subrahmanyam, V., D'Cruz, M., Subrahmanyam, C., Paul, J., Subrahmanyam, A.S., Sekhar, D.V.C., 1994. Mesozoic anomalies in the Bay of Bengal. Earth and Planetary Science Letters 121, 469–475.
Ramana, M.V., Krishna, K.S., Ramprasad, T., Desa, M., Subrahmanyam, V., Sarma, K., 2001. Structure and tectonic evolution of the northeastern Indian Ocean. Indian Ocean - a Perspective, vols. 1 and 2. A A Balkema Publishers, Rotterdam, pp. 731–816.
Rangin, C., Jolivet, L., Pubellier, M., 1990. A simple model for the tectonic evolution of southeast Asia and Indonesia region for the past 43 my. Bulletin de la Société Géologique de France 8, 889–905.
Rea, D.K., Dixon, J.M., 1983. Late Cretaceous and Paleogene tectonic evolution of the North Pacific Ocean. Earth and Planetary Science Letters 65, 145–166.
Reeves, C., 2000. The geophysical mapping of Mesozoic dyke swarms in southern Africa and their origin in the disruption of Gondwana. Journal of African Earth Sciences 30, 499–513.
Reeves, C., De Wit, M., 2000. Making ends meet in Gondwana: retracing the transforms of the Indian Ocean and reconnecting continental shear zones. Terra Nova 12, 272–280.
Richards, M.A., Jones, D.L., Duncan, R.A., Depaolo, D.J., 1991. A mantle plume initiation model for the formation of Wrangellia and other oceanic flood basalt plateaus. Science 254, 263–267.
Riisager, P., Hall, S., Antretter, M., Zhao, X., 2003. Paleomagnetic paleolatitude of Early Cretaceous Ontong Java Plateau basalts: implications for Pacific apparent and true polar wander. Earth and Planetary Science Letters 208, 235–252.
Robb, M.S., Taylor, B., Goodliffe, A.M., 2005. Re examination of the magnetic lineations of the Gascoyne and Cuvier Abyssal Plains, off NW Australia. Geophysical Journal International 163 (1), 42–55.
Robertson, A.H.F., 2000. Mesozoic–Tertiary tectonic–sedimentary evolution of a south Tethyan oceanic basin and its margins in southern Turkey. Geological Society, London, Special Publications 173, 97–138.
Roeser, H.A., Fritsch, J., Hinz, K., 1996. The development of the crust off Dronning Maud Land, East Antarctica. In: Storey, B.C., King, E.C., Livermore, R.A. (Eds.), Weddell Sea Tectonics and Gondwana Break-upGeological Society, London, Special Publications 108, 243–264.
Roeser, H., Steiner, C., Schreckenberger, B., Block, M., 2002. Structural development of the Jurassic Magnetic Quiet Zone off Morocco and identification of Middle Jurassic magnetic lineations. Journal of Geophysical Research 107, 2207.
Roest, W.R., Srivastava, S.P., 1989. Seafloor spreading in the Labrador Sea: a new reconstruction. Geology 17, 1000–1004.
Roest, W., Srivastava, S., 1991. Kinematics of the plate boundaries between Eurasia, Iberia, and Africa in the North Atlantic from the Late Cretaceous to the present. Geology 19, 613.
Rosa, J.W.C., Molnar, P., 1988. Uncertainties in reconstructions of the Pacific, Farallon, Vancouver, and Kula plates and constraints on the rigidity of the Pacific and Farallon (and Vancouver) plates between 72 and 35 Ma. Journal of Geophysical Research 93, 2997–3008.
Rosenbaum, G., Lister, G.S., Duboz, C., 2002. Relative motions of Africa, Iberia and Europe during Alpine orogeny. Tectonophysics 359, 117–129.
Rosenbaum, G., Giles, D., Saxon, M., Betts, P.G., Weinberg, R.F., Duboz, C., 2005. Subduction of the Nazca Ridge and the Inca Plateau: insights into the formation of ore deposits in Peru. Earth and Planetary Science Letters 239, 18–32.
Rosencrantz, E., Ross, M.I., Sclater, J.G., 1988. Age and spreading history of the Cayman Trough as determined from depth, heat flow and magnetic anomalies. Journal of Geophysical Research 93, 2141–2157.
Rosendahl, B.R., Moberly, R., Halunen, A.J., Rose, J.C., Kroenke, L.W., 1975. Geological and geophysical studies of the Canton Trough region. Journal of Geophysical Research 80, 2565–2574.
Ross, M., Scotese, C., 1988. A hierarchical tectonic model of the Gulf of Mexico and Caribbean region. Tectonophysics 155, 139–168.
Rowley, D.B., Lottes, A.L., 1988. Plate-kinematic reconstructions of the North Atlantic and Arctic: Late Jurassic to present. Tectonophysics 155, 73–120.
Royer, J.-Y., Chang, T., 1991. Evidence for relative motions between the Indian and Australian plates during the last 20 m.y. from plate tectonic reconstructions: implications for the deformation of the Indo-Australian plate. Journal of Geophysical Research 96, 11779–11802.
Royer, J.-Y., Coffin, M.F., 1992. Jurassic to Eocene plate tectonic reconstructions in the Kerguelen Plateau region. In: S.W., Wise, J., Julson, A.P., Schlich, R., Thomas, E. (Eds.), Proceedings of the Ocean Drilling Program, Scientific Results, vol. 120. Ocean Drilling Program, Texas A&M University, College Station, TX, pp. 917–930.
Royer, J.-Y., Patriat, P., Bergh, H., Scotese, C.R., 1988. Evolution of the Southwest Indian Ridge from the Late Cretaceous (anomaly 34) to the middle Eocene (anomaly 20). Tectonophysics 155, 235–260.
Royer, J.Y., Gordon, R.G., 1997. The motion and boundary between the Capricorn and Australian plates. Science 277, 1268–1274.
Ru, K., Pigott, J.D., 1986. Episodic rifting and subsidence in the South China Sea. American Association of Petroleum Geologists Bulletin 70, 1136–1155.
Russell, S.M., Whitmarsh, R.B., 2003. Magmatism at the west Iberia non-volcanic rifted continental margin: evidence from analyses of magnetic anomalies. Geophysical Journal International 154, 706–730.
Sager, W.S., Pringle, M.S., 1987. Tectonic evolution of the Central Pacific during the Cretaceous Quiet Period. EOS Transactions American Geophysical Union 68, 44–45.
Sager, W.W., Fullerton, L.G., Buffler, R.T., Handschumacher, D.W., 1992. Argo Abyssal Plain magnetic lineations revisited: implications for the onset of seafloor spreading and tectonic evolution of the eastern Indian Ocean. Proceedings of the Ocean Drilling Program, Scientific Results 123 (College Station, Texas, ODP).
Sager, W., 2005. What built Shatsky Rise, a mantle plume or ridge tectonics? Geological Society of America Special Papers 388, 721.
Sager, W., Handschumacher, D., Hilde, T., Bracey, D., 1988. Tectonic evolution of the northern Pacific plate and Pacific–Farallon Izanagi triple junction in the Late Jurassic and Early Cretaceous (M21–M10). Tectonophysics 155, 345–364.
Sager, W.W., Weiss, C.J., Tivey, M.A., Johnson, H.P., 1998. Geomagnetic polarity reversal model of deep-tow profiles from the Pacific Jurassic Quiet Zone. Journal of Geophysical Research-Solid Earth 103, 5269–5286.
Sager, W.W., Kim, J., Klaus, A., Nakanishi, M., Khankishieva, L.M., 1999. Bathymetry of Shatsky Rise, northwest Pacific Ocean: implications for ocean plateau development at a triple junction. Journal of Geophysical Research-Solid Earth 104, 7557–7576.
Sagong, H., Kwon, S., Ree, J., 2005. Mesozoic episodic magmatism in South Korea and its tectonic implication. Tectonics 24.
Sahabi, M., Aslanian, D., Olivet, J., 2004. A new starting point for the history of the central Atlantic. Comptes Rendus Geoscience 336, 1041–1052.
Sakaguchi, A., 1996. High paleogeothermal gradient with ridge subduction beneath the Cretaceous Shimanto accretionary prism, southwest Japan. Geology 24, 795.
Sandwell, D.T., Smith, W.H.F., 1997. Marine gravity anomaly from Geosat and ERS-1 satellite altimetry. Journal of Geophysical Research-Solid Earth 102, 10039–10054.
Sandwell, D.T., Smith, W.H.F., 2005. Retracking ERS-1 altimeter waveforms for optimal gravity field recovery. Geophysical Journal International 163, 79–89.
Sandwell, D., Smith, W., 2009. Global marine gravity from retracked Geosat and ERS-1 altimetry: ridge segmentation versus spreading rate. Journal of Geophysical Research 114.
Sashida, K., Igo, H., Hisafa, K.I., Nakornsri, N., Ampornmaha, A., 1993. Occurrence of Paleozoic and Early Mesozoic radiolaria in Thailand (preliminary report). Journal of Southeast Asian Earth Sciences 8, 97–108.
Sayers, J., Symonds, P.A., Direen, N.G., Bernadel, G., 2001. Nature of the continent–ocean transition on the non-volcanic rifted margin in the central Great Australian Bight. In: Wilson, R.C.L., Whitmarsh, R.B., Taylor, B., Froitzheim, N. (Eds.), Non-volcanic rifting of continental margins: a comparison of evidence from land and sea, Volume Special Publication, Geological Society of London, pp. 51–76.

Schaefer, B.F., Turner, S., Parkinson, I., Rogers, N., Hawkesworth, C., 2002. Evidence for recycled Archaean oceanic mantle lithosphere in the Azores plume. Nature 420, 304–307.
Schettino, A., Scotese, C.R., 2005. Apparent polar wander paths for the major continents (200 Ma to the present day): a palaeomagnetic reference frame for global plate tectonic reconstructions. Geophysical Journal International 163, 727–759.
Schettino, A., Turco, E., 2009. Breakup of Pangaea and plate kinematics of the central Atlantic and Atlas regions. Geophysical Journal International 178, 1078–1097.
Scotese, C.R., 1991. Jurassic and cretaceous plate tectonic reconstructions. Palaeogeography, Palaeoclimatology, Palaeoecology 87, 493–501.
Scotese, C.R., Gahagan, L.M., Larson, R.L., 1988. Plate tectonic reconstructions of the Cretaceous and Cenozoic ocean basins. Tectonophysics 155, 27–48.
Scrutton, R.A., Heptonstall, W.B., Peacock, J.H., 1981. Constraints on the motion of Madagascar with respect to Africa. Marine Geology 43, 1–20.
Sdrolias, M., Müller, R.D., 2006. The controls on back-arc basin formation. Geochemistry, Geophysics, Geosystems 7, Q04016. doi:10.1029/2005GC001090.
Sdrolias, M., Müller, R.D., Gaina, C., 2003a. Tectonic evolution of the SW Pacific using constraints from back-arc basins. In: Hillis, R., Müller, R.D. (Eds.), Evolution and Dynamics of the Australian Plate, Geological Society of Australia Special Publication 22 and Geological Society of America Special Paper.
Sdrolias, M., Müller, R.D., Gaina, C., 2003b. Tectonic evolution of the Southwest Pacific using constraints from backarc basins. In: Hills, R.R., Müller, R.D. (Eds.), Evolution and Dynamics of the Australian Plate. Geological Society of Australia Special Publication, vol. 22, pp. 343–359.
Sdrolias, M., Müller, R.D., Mauffret, A., Bernardel, G., 2004. Enigmatic formation of the Norfolk Basin, SW Pacific: a plume influence on back-arc extension. Geochemistry, Geophysics, Geosystems 5, Q06005.
Searle, R., Bird, R., Rusby, R., Naar, D., 1993a. The development of two oceanic microplates: Easter and Juan Fernandez microplates, East Pacific Rise. Journal of the Geological Society 150, 965.
Searle, R., Holcomb, R., Wilson, J., Holmes, M., Whittington, R., Kappel, E., Mcgregor, B., Shor, A., 1993b. The Molokai fracture zone near Hawaii, and the Late Cretaceous change in Pacific/Farallon spreading direction. The Mesozoic Pacific: Geology, Tectonics, and Volcanism: A Volume in Memory of Sy Schlanger, p. 155.
Segoufin, J., Patriat, P., 1980. Existence d'anomalies mesozoîques dans le bassin de Mozambique. Comptes Rendus de l'Academie des Sciences 287, 109–112.
Sengor, A., 1987. Tectonics of the Tethysides: orogenic collage development in a collisional setting. Annual Review of Earth and Planetary Sciences 15, 213–244.
Sengör, A.M.C., Cin, A., Rowley, D.B., S-Y, N., 1993. Space-time patterns of magmatism along the Tethysides: A Preliminary Study. Journal of Geology 101, 51–84.
Seton, M., Müller, R., 2008. Reconstructing the junction between Panthalassa and Tethys since the Early Cretaceous. Eastern Australasian Basins III, p. 263ñ266.
Seton, M., Gaina, C., Müller, R.D., Heine, C., 2009. Mid-Cretaceous seafloor spreading pulse: fact or fiction? Geology 37, 687.
Seton, M., Whittaker, J., Flament, N., Müller, R., Gurnis, M., in preparation. A case for a top-down plate reorganization at 50 Ma. Nature Geosciences, v.
Shaw, P., Cande, S.C., 1990. High-resolution inversion for South Atlantic plate kinematics using joint altimeter and magnetic anomaly data. Journal of Geophysical Research 95, 2625–2644.
Shephard, G.E., Bunge, H.P., Schuberth, B.S.A., Müller, R.D., Talsma, A.S., Moder, C., Landgrebe, T.C.W., 2012. Testing absolute plate reference frames and the implications for the generation of geodynamic mantle heterogeneity structure. Earth and Planetary Science Letters 317–318, 204–217.
Shi, G., Archbold, N., 1998. Permian marine biogeography of SE Asia. Biogeography and Geological Evolution of SE Asia. Backhuys, Leiden, p. 57ñ72.
Sibuet, J., Srivastava, S., Spakman, W., 2004. Pyrenean orogeny and plate kinematics. Journal of Geophysical Research 109, B08104.
Sibuet, J., Srivastava, S., Manatschal, G., 2007. Exhumed mantle-forming transitional crust in the Newfoundland–Iberia rift and associated magnetic anomalies. Journal of Geophysical Research 112, B06105.
Silva, E.A., Miranda, J., Luis, J., Galdeano, A., 2000. Correlation between the Palaeozoic structures from West Iberian and Grand Banks margins using inversion of magnetic anomalies. Tectonophysics 321, 57–71.
Simpson, E.S.W., Sclater, J.G., Parsons, B., Norton, I.O., Meinke, L., 1979. Mesozoic magnetic lineations in the Mozambique Basin. Earth and Planetary Science Letters 43, 260–264.
Singh, S.C., Carton, H., Chauhan, A.S., Androvandi, S., Davaille, A., Dyment, J., Cannat, M., Hananto, N.D., 2010. Extremely thin crust in the Indian Ocean possibly resulting from Plume–Ridge Interaction. Geophysical Journal International.
Sinton, C., Duncan, R., Storey, M., Lewis, J., Estrada, J., 1998. An oceanic flood basalt province within the Caribbean plate. Earth and Planetary Science Letters 155, 221–235.
Sisson, V.B., Pavlis, T.L., 1993. Geologic consequences of plate reorganization: An example from the Eocene southern Alaska fore arc. Geology 21, 913.
Skogseid, J., Planke, S., Faleide, J., Pedersen, T., Eldholm, O., Neverdal, F., 2000. NE Atlantic continental rifting and volcanic margin formation. Dynamics of the Norwegian Margin, vol. 167, p. 295ñ326.
Sleep, N.H., Toksoz, M.N., 1971. Evolution of marginal seas. Nature 233, 548–550.
Small, C., Abbott, D., 1998. Subduction obstruction and the crack-up of the Pacific plate. Geology 26, 795–798.
Smith, A.G., Hallam, A., 1970. The fit of the southern continents. Nature 225, 139–144.
Sokolov, S., Ye, B., Morozov, O., Shekhovtsov, V., Glotov, S., Ganelin, A., Kravchenko-Berezhnoy, I., 2002. South Anjui suture, northeast Arctic Russia. Tectonic Evolution of the Bering Shelf-Chukchi Sea-Arctic Margin and Adjacent Landmasses, pp. 209–223.
Speed, R.C., 1985. Cenozoic collision of the Lesser Antilles arc and continental South America and the origin of the El Pilar fault. Tectonics 4, 41–69.
Speranza, F., Villa, I., Sagnotti, L., Florindo, F., Cosentino, D., Cipollari, P., Mattei, M., 2002. Age of the Corsica–Sardinia rotation and Liguro–Provençal basin spreading: new paleomagnetic and Ar/Ar evidence. Tectonophysics 347, 231–251.
Srivastava, S.P., 1985. Evolution of the Eurasian Basin and its implication to the motion of Greenland along Nares Strait. Tectonophysics 114, 29–53.
Srivastava, S.P., Roest, W.R., 1989, Seafloor spreading history II–IV, in East Coast Basin Atlas Series: Labrador Sea, J.S. Bell (co-ordinator). Atlantic Geoscience Centre, Geologic Survey of Canada, Map sheets L17-2–L17-6.
Srivastava, S.P., Roest, W.R., 1996. Porcupine plate hypothesis — comment. Marine Geophysical Researches 18, 589–593.
Srivastava, S.P., Tapscott, C.R., 1986. Plate kinematics of the North Atlantic. In: Vogt, R.R., Tucholke, B.E. (Eds.), The Western North Atlantic Region, Volume M: The Geology of North America. Geol. Soc. Am., pp. 379–405.
Srivastava, S., Schouten, H., Roest, W., Klitgord, K., Kovacs, L., Verhoef, J., Macnab, R., 1990. Iberian plate kinematics: a jumping plate boundary between Eurasia and Africa.
Srivastava, S.P., Sibuet, J.C., Cande, S., Roest, W.R., Reid, I.D., 2000. Magnetic evidence for slow seafloor spreading during the formation of the Newfoundland and Iberian margins. Earth and Planetary Science Letters 182, 61–76.
Stadler, G., Gurnis, M., Burstedde, C., Wilcox, L., Alisic, L., Ghattas, O., 2010. The dynamics of plate tectonics and mantle flow: From local to global scales. Science 329, 1033.
Stagg, H.M.J., Willcox, J.B., 1992. A case for Australia–Antarctica separation in the Neocomian (c.a. 125 Ma). Tectonophysics 210, 21–32.
Stamatakos, J.A., Trop, J.M., Ridgway, K.D., 2001. Late Cretaceous paleogeography of Wrangellia: paleomagnetism of the MacColl Ridge Formation, southern Alaska, revisited. Geology 29, 947–950.
Stampfli, G.M., Borel, G.D., 2002. A plate tectonic model for the Paleozoic and Mesozoic constrained by dynamic plate boundaries and restored synthetic oceanic isochrons. Earth and Planetary Science Letters 196, 17–33.
Stampfli, G.M., 2000. Tethyan Oceans. In: Bozkurt, E., Winchester, J.A., Piper, J.D.A. (Eds.), Tectonics and Magmatism in Turkey and the Surroundings AreaGeological Society, London, Special Publications 173, 1–23.
Steinberger, B., Torsvik, T., 2008. Absolute plate motions and true polar wander in the absence of hotspot tracks. Nature 452, 620–623.
Stock, J., Molnar, P., 1987. Revised history of early Tertiary plate motion in the southwest Pacific. Nature 325, 495–499.
Stock, J., Molnar, P., 1988. Uncertainties and implications of the Late Cretaceous and Tertiary position of North America relative to the Farallon, Kula, and Pacific plates. Tectonics 7, 1339–1384.
Stock, J., Luyendyk, B., Clayton, R., Party, S.S., 1998. Tectonics and structure of the Manihiki Plateau, western Pacific Ocean. EOS Transactions of the American Geophysical Union 79.
Stocklin, J., 1974. Possible ancient continental margins in Iran. The Geology of Continental Margins, pp. 873–887.
Storey, M., Mahoney, J.J., Saunders, A.D., Duncan, R.A., Kelley, S.P., Coffin, M.F., 1995. Timing of hot spot-related volcanism and the breakup of Madagascar and India. Science 267, 852–855.
Storey, B.C., Leat, P.T., Ferris, J.K., 2001. The location of mantleplume centers during the initial stages of Gondwana breakup. Mantle Plumes: Their Identification Through Time, pp. 71–80.
Straub, S., Goldstein, S., Class, C., Schmidt, A., 2009. Mid-ocean-ridge basalt of Indian type in the northwest Pacific Ocean basin. Nature Geoscience 2, 286–289.
Sun, W., Ding, X., Hu, Y.-H., Li, X.-H., 2007. The golden transformation of the Cretcaous plate subduction in the west Pacific. Earth and Planetary Science Letters 262, 533–542.
Sutherland, R., Hollis, C., 2001. Cretaceous demise of the Moa Plate and strike-slip motion at the Gondwana margin. Geology 29, 279–282.
Symonds, P.A., Colwell, J.B., Struckmeyer, H.I.M., Willcox, J.B., Hill, P.J., 1996. Mesozoic rift basin development off eastern Australia. Mesozoic Geology of the Eastern Australia Plate, vol. 43. Geological Society of Australia, Brisbane, pp. 528–542.
Talwani, M., Eldholm, O., 1977. Evolution of the Norwegian–Greenland Sea. Geological Society of America Bulletin 88, 969–999.
Tamaki, K., Larson, R.L., 1988. The Mesozoic tectonic history of the Magellan microplate in the western Central Pacific. Journal of Geophysical Research 93, 2857–2874.
Tankard, A.J., Welsink, H.J., 1987. Extensional tectonics and stratigraphy of Hibernia Oil Field, Grand Banks, Newfoundland. American Association of Petroleum Geologists Bulletin 71, 1210–1232.
Taylor, B., 2006. The single largest oceanic plateau: Ontong Java-Manihiki-Hikurangi. Earth and Planetary Science Letters 241, 372–380.
Taylor, B., Karner, G., 1983. On the evolution of marginal basins. Reviews of Geophysics 21, 1727–1741.
Taylor, P.T., Kovacs, L.C., Vogt, P.R., Johnson, G.L., 1981. Detailed aeromagnetic investigation of the Arctic Basin. II. Journal of Geophysical Research 86, 6323–6333.
Tebbens, S.F., Cande, S.C., 1997. Southeast Pacific tectonic evolution from early Oligocene to Present. Journal of Geophysical Research-Solid Earth 102, 12061–12084.
Thorkelson, D.J., 1996. Subduction of diverging plates and the principles of slab window formation. Tectonophysics 255, 47–63.
Tikku, A.A., Cande, S.C., 1999. The oldest magnetic anomalies in the Australian–Antarctic Basin: are they isochrons? Journal of Geophysical Research 104, 661–677.
Tikku, A.A., Cande, S.C., 2000. On the fit of Broken Ridge and Kerguelen plateau. Earth and Planetary Science Letters 180, 117–132.
Tivey, M., Sager, W., Lee, S., Tominaga, M., 2006. Origin of the Pacific Jurassic quiet zone. Geology 34, 789.
Todd, B., Reid, I., Keen, C., 1988. Crustal structure across the southwest Newfoundland transform margin. Canadian Journal of Earth Sciences 25, 744–759.
Tominaga, M., Sager, W.W., 2010. Revised Pacific M-anomaly geomagnetic polarity timescale. Geophysical Journal International 182, 203–232.
Tominaga, M., Sager, W.W., Tivey, M.A., Lee, S.M., 2008. Deep-tow magnetic anomaly study of the Pacific Jurassic Quiet Zone and implications for the geomagnetic

polarity reversal timescale and geomagnetic field behavior. Journal of Geophysical Research 113, B07110.
Tomurtogoo, O., Windley, B., Kroner, A., Badarch, G., Liu, D., 2005. Zircon age and occurrence of the Adaatsag ophiolite and Muron shear zone, central Mongolia: constraints on the evolution of the Mongol–Okhotsk ocean, suture and orogen. Journal of the Geological Society 162, 125.
Torsvik, T., Steinberger, B., Cocks, L., Burke, K., 2008. Longitude: linking Earth's ancient surface to its deep interior. Earth and Planetary Science Letters 276, 273–282.
Torsvik, T., Rousse, S., Labails, C., Smethurst, M., 2009. A new scheme for the opening of the South Atlantic Ocean and the dissection of an Aptian salt basin. Geophysical Journal International 177, 1315–1333.
Totterdell, J., Blevin, J., Bradshaw, B., Colwell, J., Kennard, J., 2000. A new sequence framework for the Great Australian Bight: starting with a clean slate. The APPEA Journal 95.
Trop, J.M., Ridgway, K.D., Manuszak, J.D., Layer, P., 2002. Mesozoic sedimentary-basin development on the allochthonous Wrangellia composite terrane, Wrangell Mountains basin, Alaska: a long-term record of terrane migration and arc construction. Geological Society of America Bulletin 114, 693.
Tucholke, B., Whitmarsh, R., 2006. The Newfoundland–Iberia conjugate rifted margins. Principles of Phanerozoic Regional Geology.
Tucholke, B., Sawyer, D., Sibuet, J., 2007. Breakup of the Newfoundland Iberia rift. Geological Society London Special Publications 282, 9.
Umpleby, D., 1979. Geology of the Labrador shelf. Geological Survey of Canada Commission Gèologique du Canada.
Unternehr, P., Curie, D., Olivet, J.L., Goslin, J., Benzarty, P., 1988. South Atlantic fits and intraplate boundaries in Africa and South America. Tectonophysics 155, 169–179.
Uyeda, S., Kanamori, H., 1979. Back-arc opening and the mode of subduction. Journal of Geophysical Research 84, 1049–1061.
Van Der Lelij, R., Spikings, R., Kerr, A., Kounov, A., Cosca, M., Chew, D., Villagomez, D., 2010. Thermochronology and Tectonics of the Leeward Antilles: evolution of the Southern Caribbean Plate Boundary Zone and accretion of the Bonaire Block.
Van Der Voo, R., Spakman, W., Bijwaard, H., 1999a. Mesozoic subducted slabs under Siberia. Nature 397, 246–249.
Van Der Voo, R., Spakman, W., Bijwaard, H., 1999b. Tethyan subducted slabs under India. Earth and Planetary Science Letters 171, 7–20.
Veevers, J.J., 2000. Change of tectono-stratigraphic regime in the Australian plate during the 99 Ma (mid-Cretaceous) and 43 Ma (mid-Eocene) swerves of the Pacific. Geology 28, 47–50.
Veevers, J., 2006. Updated Gondwana (Permian–Cretaceous) earth history of Australia. Gondwana Research 9, 231–260.
Veevers, J.J., 1988. Morphotectonics of Australia's north-western margin - a review. In: Purcell, P.G., Purcell, R.R. (Eds.), The North West Shelf of Australia: Petroleum Exploration Society of Australia Symposium: Perth, pp. 19–27.
Veevers, J.J., Tayton, J.W., Johnson, B.D., 1985. Prominent magnetic anomaly along the continent–ocean boundary between the northwestern margin of Australia (Exmouth and Scott plateaus) and the Argo abyssal plain. Earth and Planetary Science Letters 72, 415–426.
Veevers, J.J., Stagg, H.M.J., Willcox, J.B., Davies, H.L., 1990. Pattern of slow seafloor spreading (<4 mm/year) from breakup (96 Ma) to A20 (44.5 Ma) off the southern margin of Australia. BMR Journal of Australian Geology and Geophysics 11, 499–507.
Viso, R.F., Larson, R.L., Pockalny, R.A., 2005. Tectonic evolution of the Pacific-Phoenix-Farallon triple junction in the South Pacific ocean. Earth and Planetary Science Letters 233, 179–194.
Vry, J., Baker, J., Maas, R., Little, T., Grapes, R., Dixon, M., 2004. Zoned (Cretaceous and Cenozoic) garnet and the timing of high grade metamorphism, Southern Alps: New Zealand. Journal of Metamorphic Geology 22, 137ñ157.
Weissel, J.K., Anderson, R.N., Geller, C.A., 1980. Deformation of the Indo-Australian Plate. Nature 287, 284–291.
Wessel, P., Kroenke, L., 2008. Pacific absolute plate motion since 145 Ma: an assessment of the fixed hot spot hypothesis. Journal of Geophysical Research 113, B06101.
Wessel, P., Harada, Y., Kroenke, L.W., 2006. Toward a self-consistent, high-resolution absolute plate motion model for the Pacific. Geochemistry, Geophysics, Geosystems 7, Q03L12.
Whitechurch, H., Juteau, T., Montigny, R., 1984. Role of the Eastern Mediterranean ophiolites (Turkey, Syria, Cyprus) in the history of the Neo-Tethys. Geological Society, London, Special Publications 17, 301–317.
Whitmarsh, R.B., Miles, P.R., 1995. Models of the development of the West Iberia rifted continental margin at 40-degrees-30′N deduced from surface and deep-tow magnetic anomalies. Journal of Geophysical Research-Solid Earth 100, 3789–3806.
Whittaker, J., Müller, R.D., Leitchenkov, G., Stagg, H., Sdrolias, M., Gaina, C., Goncharov, A., 2007. Major Australian–Antarctica plate reorganization at Hawaiian-Emperor bend time. Science 318, 83–86.
Williams, P., Johnston, C., Almond, R., Simamora, W., 1988. Late Cretaceous to early Tertiary structural elements of West Kalimantan. Tectonophysics 148, 279–297.
Wilson, D.S., 1988. Tectonic history of the Juan de Fuca Ridge over the last 40 million years. Journal of Geophysical Research 33, 11,863–11,876.
Wilson, D.S., 1996. Fastest known spreading on the Miocene Cocos-Pacific plate boundary. Geophysical Research Letters 23, 3003–3006.
Wilson, D.S., Hey, R.N., Nishimura, C., 1984. Propagation as a mechanism of reorientation of the Juan de Fuca Ridge. Journal of Geophysical Research 89, 9215–9225.
Winterer, E., 1976. Anomalies in the tectonic evolution of the Pacific. In: Sutton, G., Manghnani, M., Moberly, R. (Eds.), The Geophysics of the Pacific Ocean Basin and its Margins. AGU, Washington D.C., pp. 269–278.
Winterer, E., Lonsdale, P., Matthews, J., Rosendahl, B., 1974. Structure and acoustic stratigraphy of the Manihiki Plateau. Deep Sea Research 21, 793–814.
Withjack, M.O., Schlische, R.W., Olsen, P.E., 1998. Diachronous rifting, drifting, and inversion on the passive margin of central eastern North America — an analog for other passive margins. AAPG Bulletin-American Association of Petroleum Geologists 82, 817–835.
Woods, M.T., Davies, G.F., 1982. Late Cretaceous genesis of the Kula plate. Earth and Planetary Science Letters 58, 161–166.
Worthington, T.J., Hekinian, R., Stoffers, P., Kuhn, T., Hauff, F., 2006. Osbourn Trough: structure, geochemistry and implications of a mid-Cretaceous paleospreading ridge in the South Pacific. Earth and Planetary Science Letters 245, 685–701.
Zorin, Y.A., 1999. Geodynamics of the western part of the Mongolia-Okhotsk collisional belt, Trans-Baikal region (Russia) and Mongolia. Tectonophysics 306, 33–56.